NBS SPECIAL PUBLICATION 637
Volume 2

U.S. DEPARTMENT OF COMMERCE/National Bureau of Standards

Optical Fiber Characterization

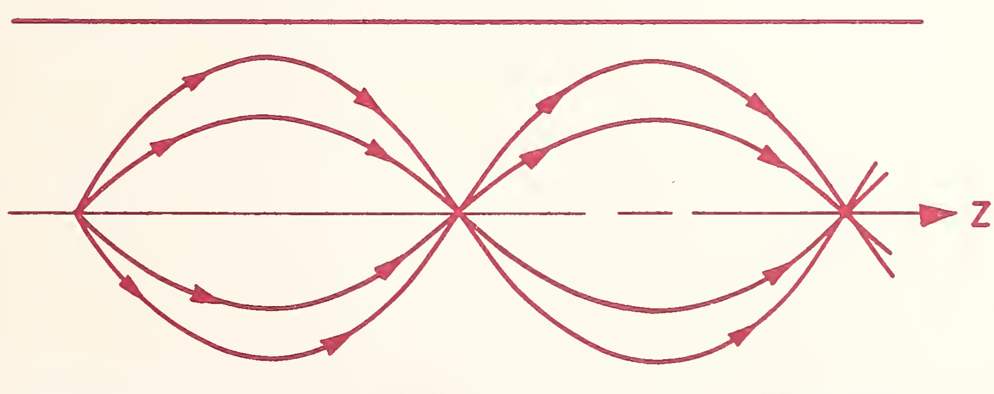

NATIONAL BUREAU OF STANDARDS

The National Bureau of Standards[1] was established by an act of Congress on March 3, 1901. The Bureau's overall goal is to strengthen and advance the Nation's science and technology and facilitate their effective application for public benefit. To this end, the Bureau conducts research and provides: (1) a basis for the Nation's physical measurement system, (2) scientific and technological services for industry and government, (3) a technical basis for equity in trade, and (4) technical services to promote public safety. The Bureau's technical work is performed by the National Measurement Laboratory, the National Engineering Laboratory, and the Institute for Computer Sciences and Technology.

THE NATIONAL MEASUREMENT LABORATORY provides the national system of physical and chemical and materials measurement; coordinates the system with measurement systems of other nations and furnishes essential services leading to accurate and uniform physical and chemical measurement throughout the Nation's scientific community, industry, and commerce; conducts materials research leading to improved methods of measurement, standards, and data on the properties of materials needed by industry, commerce, educational institutions, and Government; provides advisory and research services to other Government agencies; develops, produces, and distributes Standard Reference Materials; and provides calibration services. The Laboratory consists of the following centers:

Absolute Physical Quantities[2] — Radiation Research — Chemical Physics — Analytical Chemistry — Materials Science

THE NATIONAL ENGINEERING LABORATORY provides technology and technical services to the public and private sectors to address national needs and to solve national problems; conducts research in engineering and applied science in support of these efforts; builds and maintains competence in the necessary disciplines required to carry out this research and technical service; develops engineering data and measurement capabilities; provides engineering measurement traceability services; develops test methods and proposes engineering standards and code changes; develops and proposes new engineering practices; and develops and improves mechanisms to transfer results of its research to the ultimate user. The Laboratory consists of the following centers:

Applied Mathematics — Electronics and Electrical Engineering[2] — Manufacturing Engineering — Building Technology — Fire Research — Chemical Engineering[2]

THE INSTITUTE FOR COMPUTER SCIENCES AND TECHNOLOGY conducts research and provides scientific and technical services to aid Federal agencies in the selection, acquisition, application, and use of computer technology to improve effectiveness and economy in Government operations in accordance with Public Law 89-306 (40 U.S.C. 759), relevant Executive Orders, and other directives; carries out this mission by managing the Federal Information Processing Standards Program, developing Federal ADP standards guidelines, and managing Federal participation in ADP voluntary standardization activities; provides scientific and technological advisory services and assistance to Federal agencies; and provides the technical foundation for computer-related policies of the Federal Government. The Institute consists of the following centers:

Programming Science and Technology — Computer Systems Engineering.

[1]Headquarters and Laboratories at Gaithersburg, MD, unless otherwise noted;
mailing address Washington, DC 20234.
[2]Some divisions within the center are located at Boulder, CO 80303.

Optical Fiber Characterization

Attenuation, Frequency Domain Bandwidth, and Radiation Patterns

G.E. Chamberlain
G.W. Day
D.L. Franzen
R.L. Gallawa
E.M. Kim
M. Young

Electromagnetic Technology Division
Center for Electronics and Electrical Engineering
National Bureau of Standards
Boulder, CO 80303

Second of a series on optical fiber technology.

U.S. DEPARTMENT OF COMMERCE, Malcolm Baldrige, Secretary
NATIONAL BUREAU OF STANDARDS, Ernest Ambler, Director

Issued October 1983

Library of Congress Catalog Card Number: 82-600563

National Bureau of Standards Special Publication 637 Volume 2
Natl. Bur. Stand. (U.S.), Spec. Publ. 637, Vol. 2, 239 pages (Oct. 1983)
CODEN: XNBSAV

U.S. GOVERNMENT PRINTING OFFICE
WASHINGTON: 1983

CONTENTS

Page

Chapter 1. Measurement of Multimode Optical Fiber Attenuation
R. L. Gallawa, G. E. Chamberlain, G. W. Day,
D. L. Franzen, and M. Young 1

Chapter 2. Measurement of Optical Fiber Bandwidth in the Frequency Domain
G. W. Day 57

Chapter 3. Measurement of Near-Field Radiation Patterns from Optical Fibers
E. M. Kim and D. L. Franzen 101

Chapter 4. Measurement of Far-Field Radiation Patterns from Optical Fibers
E. M. Kim and D. L. Franzen 187

Appendix: Optical Waveguide Communications Glossary 207

PREFACE

During the past several years, a number of optical fiber measurement systems have been developed at the National Bureau of Standards. This book is the second volume of a series intended to describe the design and performance of these systems. Volume 1 includes a description of systems to measure backscatter, bandwidth (time domain), and index profile (refracted near field); Volume 2 covers attenuation, bandwidth (frequency domain), and radiation patterns. Chapters describing these systems are minor revisions of former NBS Technical Notes, many of which are now out of print. Each chapter contains a brief tutorial on the particular subject and a detailed description of the system. This level of engineering detail is not usually found in other books on the subject.

The appendix of this volume contains a glossary of optical fiber terms and is a reprint of NBS Handbook 140 (1982) which is now out of print. The following individuals were contributors to that handbook: A. G. Hanson, L. R. Bloom, A. H. Cherin, G. W. Day, R. L. Gallawa, E. M. Gray, C. Kao, F. P. Kapron, B. S. Kawasaki, P. Reitz, and M. Young. The reader should be cautioned that terminology continually evolves and this glossary will undoubtedly undergo change as new terms are added and others revised. However, the glossary does represent a several-year effort by many in the industry and is currently the best available.

The authors would like to thank M. E. DeWeese for preparing the manuscript and providing editorial assistance. Partial support for the work reported here was provided by the Department of Defense, Calibration Coordination Group (CCG).

Boulder, Colorado
1983

ABSTRACT

This is the second volume of a series intended to describe optical fiber measurement systems developed at the National Bureau of Standards. The topics covered in this volume are attenuation, bandwidth (frequency domain), and far-field near-field radiation patterns. Each chapter includes a tutorial section and a detailed description of the apparatus. The volume concludes with a glossary of optical communications terms.

Key words: attenuation; bandwidth; core diameter; far field; measurements; near field; optical fiber.

Chapter 1

Measurement of Multimode Optical Fiber Attenuation

R. L. Gallawa

G. E. Chamberlain

G. W. Day

D. L. Franzen

M. Young

This document is one of a series which describes optical fiber measurement capabilities at the National Bureau of Standards. We concentrate here on the measurement of attenuation of multimode, telecommunication-grade fibers for the wavelength range of 850 nm to 1300 nm. The document begins by discussing the need for restricted launch conditions, the most fundamental and crucial aspect of precise attenuation measurements. The limited phase space launch (also called the beam optics launch) and the mode filter launch are discussed. Attention then turns to the practical matter of ensuring that the conditions of the restricted launch are met. Discussions of system noise and system linearity are also included. The document describes measurement procedure and results obtained in the laboratory using three typical fibers. Results are presented for the two wavelengths of current interest: 850 nm and 1300 nm. The procedures are applicable to any wavelength, however. The document touches briefly on the matter of monomode fibers. Finally, a summary of the results from an interlaboratory comparison are presented to give perspective to the stability of a fiber subjected to handling and shipping.

CONTENTS

	Page
1. INTRODUCTION	3
2. LAUNCH CONDITIONS	7
2.1 Phase Space	8
2.1.1 A Summary of Phase Space Concepts	18
2.2 LPS Launch	20
2.3 Mode Filter Launch	22
3. COMPONENT AND SYSTEM VARIABILITIES	26
3.1 Spot Size and Launch Numerical Aperture	27
3.2 Mode Filter Qualification	34
3.3 Component Linearity	37
3.4 System Linearity	37
3.5 System Noise	38
3.6 Detector Uniformity	39
3.7 Measurement Procedure	40
3.8 Some Results	44
4. MEASUREMENT COMPARISONS AND RESULTS	44
4.1 Participants and Instructions	44
4.2 Comparison Results	46
4.3 Attenuation Measurements in High-DMA Fibers	50
4.4 Summary of Interlaboratory Comparisons	52
5. REFERENCES	53
APPENDIX A. MODE VOLUME AND LIMITED PHASE SPACE	55

1. INTRODUCTION

Two operational parameters are basic to the utility of any transmission line: attenuation and bandwidth. These two determine repeater spacing and ultimate cost of a telecommunication network. Both must be characterized because either attenuation or bandwidth may limit the range-bandwidth product of a communication link; the range-bandwidth product is the most frequently used measure of performance and cost. Full exploitation of system components depends on an understanding of which parameter (bandwidth or attenuation) is restricting system capability.

The techniques described in this document are applicable to all wavelengths of interest for telecommunications. The measurements reported on, however, were done at only 850 nm and 1300 nm. The system uses an incandescent strip filament light source in conjunction with interference filters for wavelength selection. Thus, it is amenable to measurement at discrete wavelengths.

We restrict attention to telecommunications-quality graded-index multimode fibers. Such fibers have a nominally 50 μm core diameter and the refractive index profile is carefully controlled. Usually the profile is nearly parabolic, yielding high bandwidth. The loss in telecommunication-grade fibers is as low as practical. Fibers used in short-distance applications or LAN (local area networks) are frequently large core fibers and often have a step index profile. The attenuation is less important than it is for long haul fibers. Even if the fibers used in the two applications (long and short distances) were identical, the philosophy behind the measurement technique would undoubtedly be different in the two cases. For long distance fibers, the measured value of attenuation should be indicative of the attenuation experienced in a long link. Likewise, the attenuation measured for a short distance fiber should be representative of the attenuation experienced in a typical short distance application. The modal power distribution at launch is important to the measured value of attenuation in each case.

The philosophy of improving measurement precision by restricting the launch is intimately related to the excitation of high-loss modes, including leaky modes. The concept is distinctly different in graded-index and step-index fibers. By uniformly illuminating the fiber core using a limited launch numerical aperture, one avoids the excitation of high-order and leaky modes of a step-index fiber. This is not true when the fiber has a graded refractive index because the local numerical aperture of the fiber is a function of radial position.

A launch condition that works well for step-index fibers may not work well for graded-index ones. The converse is also true: a launch condition that yields usable results for a graded-index fiber may not be the most suitable one for step-index fibers. The reported attenuation must be meaningful in the context of its application. Short-haul links using

LED (light-emitting diode) sources are not considered in this document. We are concerned here with the characterization of fibers in a way that will be useful in predicting the performance of a telecommunication link, which may include concatenated fibers.

Monomode fibers, though not considered in this document, are important in high capacity, long haul systems, where attenuation is more likely to be the limiting parameter in system design. Launch conditions are simpler for monomode fibers since only the fundamental mode will propagate. A mode filter or limited launch numerical aperture is therefore not necessary. The fiber will support two orthogonal polarization states and this may be a source of inaccuracy if the light is polarized. Coupling between the polarization states of the fiber may be difficult to control. Furthermore, the attenuation coefficient is different for the two states. The problems associated with the birefringence of the fiber are especially important in systems that are phase sensitive. A meaningful characterization of the monomode fiber is difficult in that case.

Fiber attenuation is the diminution of average optical power, measured in decibels. The rate of diminution, with respect to distance, is known as the attenuation coefficient for the fiber, usually denoted by α, and is specified in decibels/kilometer. If α is constant, the attenuation of a length L of fiber is

$$\alpha L(\mathrm{dB}) = -10 \log [P(L)/P(0)], \qquad (1)$$

where P(L) is the power at distance L from the reference position where the power is P(0) and log indicates the common logarithm. In practice, the attenuation coefficient varies with distance and operating wavelength, λ. The parameter of interest, then, is the average attenuation of the fiber, as found from eq (1), where

$$\frac{P(L,\lambda)}{P(0,\lambda)} = 10^{-\int_0^L \frac{\alpha(z,\lambda)dz}{10}} \qquad (2)$$

The obvious method of measuring attenuation, then, is as follows: power reaching a detector through two different lengths of fiber (L_0, L_1) is measured for the operating wavelength of interest. The average attenuation coefficient is

$$\alpha(\lambda) = \frac{10}{L_1 - L_0} \log \frac{P(L_0)}{P(L_1)} . \qquad (3)$$

In this form, attenuation is positive if $L_1 > L_0$.

For graded-index multimode fibers, the utility of such a measurement depends on how power was launched into the fiber. The transmitted power resides in a finite number of modes, and different modes have different attenuation coefficients. Thus, the measured average attenuation of a multimode fiber depends on the relative amount of power in each mode. At launch, the relative power depends on launch conditions. A small LD (laser diode)

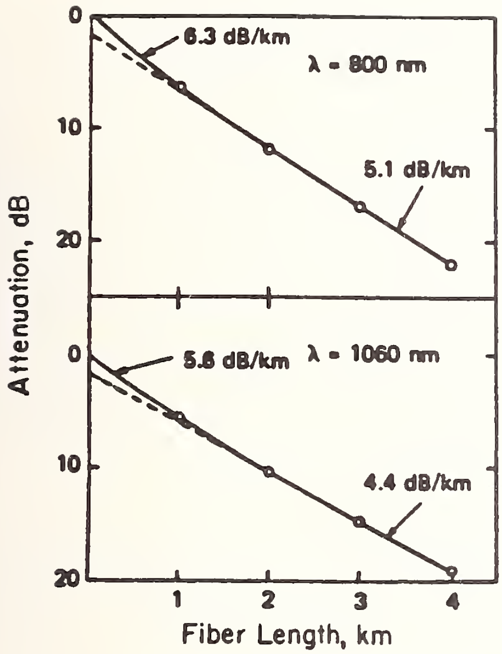

Figure 1. Loss in a 4 km length of parabolic profile fiber. Launch NA = 0.1 in each case (after ref. 1).

may launch its power into the center region of the fiber but overfill the fiber numerical aperture. An LED has a broad angular radiation pattern and large size so it excites all modes more or less uniformly. Clearly, the attenuation measured using an LED source is different from that measured using an LD. This difference in attenuation disappears after the fiber reaches the steady-state or condition of equilibrium modal power distribution, in which case the relative power in the various modes is independent of length. Thus, the modal power distribution at the output is independent of the modal power distribution at input. The equilibrium condition is achieved beyond a certain propagation distance called the equilibrium length. The condition is reached after the high-loss modes have been attenuated or coupled into modes which have less attenuation. In the steady-state condition, intermodal coupling is in equilibrium, so power coupled from one mode to the others is just compensated by differential attenuation and power coupled in the opposite direction. The effect of an equilibrium modal power distribution is shown in figure 1 (after ref. 1) which shows the result of length-dependent measurements on a 4 km length of parabolic profile fiber at 800 nm and 1060 nm. The launch numerical aperture is 0.10 in each case. Steady state appears to be reached after about 2 km. For shorter lengths, the attenuation coefficient is higher than the steady-state value; this can be attributed to the presence of high-loss modes. The slope of the curve at any point gives the local attenuation coefficient. The slope (attenuation coefficient) in the first kilometer of fiber is significantly higher than in the fourth kilometer of the same fiber. This figure illustrates, then, the need for launch conditions which create the desired power distribution and, hence, lead to attenuation values that are typical of long fibers.

More recent results show a similar trend but the distance required to reach steady state is considerably reduced [2]. Recent data confirm that differential mode attenuation is considerably less today than it was just a few years ago. Furthermore, differential mode attenuation is a function of operating wavelength, so the distance required to reach steady state changes with a change in operating wavelength.

The two launch conditions used in this report are the LPS (limited phase space) launch (also called the beam optics launch) and the mode filter launch. In the first, the launch spot size and the launch numerical aperture are adjusted to be, respectively, 70 percent of the fiber core size and 70 percent of the fiber numerical aperture. The condition is therefore also referred to as the 70/70 launch condition. The LPS launch apparatus is more complicated than the mode filter launch because the apparatus must allow for independent adjustment of launch spot size and launch angle. The product of launch spot size and launch angle is related to phase space volume, discussed in section 2.1.

The mode filter launch calls for launch spot size and launch angle larger than fiber core size and fiber numerical aperture. The launch optics can therefore be rather simple. The overfilled fiber is subjected to a filter, the purpose of which is to establish a modal power distribution that approximates the modal power distribution at the end of a long fiber without the filter. The mode filter is deemed appropriate if a short length of the test fiber which is subjected to the filter produces a far-field radiation pattern that is similar (within tolerance) to that of the long test fiber without the filter.

Details on the two launch conditions are given in section 2.

The problems discussed here are not applicable to monomode fibers, where the optical size of the fiber is so small that only a single mode can propagate.

Since the strength of intermodal coupling influences the attenuation of the fiber, the environment can affect the measured attenuation. The loss value assigned to an uncabled fiber may not be appropriate to the cabled fiber. Likewise, the loss of an uncabled fiber on a spool depends on how tightly the fiber is wrapped around the spool.

For purposes of fiber specification (i.e., for purposes of trade and commerce) it is important that the attenuation assigned to a fiber be of practical use. When fibers are concatenated, the attenuation of the resulting link should be predictable from the specified attenuation of individual fiber sections. That is the crux of the attenuation measurement problem.

In this report, we discuss specific details of a meaningful measurement technique. Before proceeding, however, we note that the mode coupling discussed above has a beneficial effect on fiber bandwidth as well. Different modes have different phase and group velocities, as well as different attenuations. The duration of a pulse increases as it propagates in a multimode fiber. The increased duration results from different group velocities of the

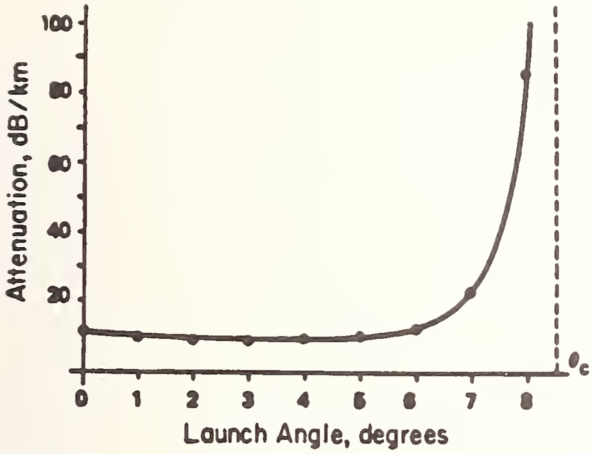

Figure 2. Attenuation coefficient as a function of input plane wave angle at 632.8 nm (after ref. 5).

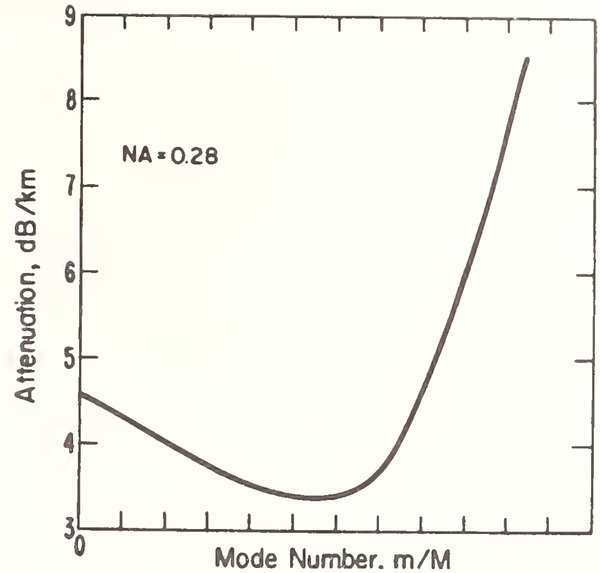

Figure 3. Symbolic representation of 0.28 NA fiber waveguide attenuation at 800 nm as a function of mode number. Mode number was altered by changing launch spot position but not launch angle. Launch angle is 0 (after ref. 6).

different modes. Initially, pulse duration usually increases linearly with distance, but for lengths exceeding the equilibrium length, the pulse duration may increase more slowly with distance, approaching $L^{1/2}$ variation in some cases [3,4].

2. LAUNCH CONDITIONS

That different modes have different attenuation coefficients is intuitive. Figures 2 and 3 [5,6] give experimental evidence to support the allegation. Figure 2 shows the attenuation coefficient as a function of input launch angle for a step-index fiber at 6328 nm. The high-order modes associated with the steep input angles show a very high attenuation per unit length. In contrast, the low-order rays have fairly uniform attenuation. Clearly then, the input launch condition plays an important role in the measured attenuation. Figure 3 is symbolic of the attenuation coefficient as a function of normalized mode number at 800 nm for a graded fiber having 0.28 NA. Both scattering and absorptive loss have been accounted for in this curve [6]. In the figure, M is the mode volume of the fiber or the total number of modes the fiber will support (cf. appendix A). m is the counting index that identifies the mode number.

A complete description of modal properties and how those properties influence fiber attenuation is beyond the scope of this manuscript. The reader is referred to the references for additional details [7]. For our purposes, we concentrate on the launch conditions and how those conditions influence the excitation of various modes. To that end, we digress briefly to discuss the concept of phase space. That concept is fundamental to one of the two launch conditions discussed in this document. Those conditions are discussed later in this section.

2.1 Phase Space

The concept of phase space is basic to the limited phase space launch condition. In this section, we give some basic definitions and connecting relationships that lend credence to the proposition that the LPS launch is a reasonable one to use. The reader who is not interested in these connecting relationships can skip directly to section 2.2 or he may pause to read the summary paragraphs in section 2.1.1.

Phase space and its relationship to the problem of coupling optical energy to and from a source is understood by noting first that a light ray has "momentum" which depends on its position and direction. If the optical axis is the z-axis of a rectangular (x,y,z) coordinate system, the momentum of the ray depends on x, y, dx/ds and dy/ds, where x,y is its location and ds is its incremental distance along the ray path. In particular, the momenta in the x and y directions are

$$p_x = n\, dx/ds, \tag{4a}$$

$$p_y = n\, dy/ds, \tag{4b}$$

where n is the refractive index at x, y and may be a function of position. Figure 4 shows a typical light ray and its angle with respect to the axial (z) direction. In this case,

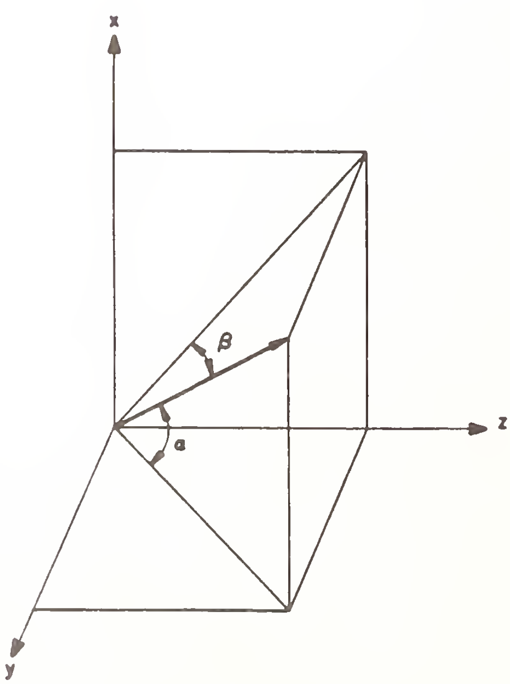

Figure 4. A typical light ray and angles in a rectangular coordinate system.

$$p_x = n \sin \alpha, \tag{5a}$$

$$p_y = n \sin \beta. \tag{5b}$$

The physical state of a ray is completely specified by the four variables x, y, p_x, p_y. These four variables define a four-dimensional space called the phase space. The position of a ray in phase space has a one-to-one relationship with its trajectory in physical space.

The power coupled into a fiber mode depends on the trajectory of the launch ray so it is not surprising that these concepts should be encountered in a discussion of restricted launch conditions. Indeed, the efficiency of coupling between fibers or between a fiber and a terminal device (e.g., a light source) is characterized by the phase space match. The conservation of radiance, for example, is a manifestation of this concept, as will be seen below. For the purpose of measuring fiber attenuation, we seek to establish a launch condition for which the phase space matches the phase space desired in the fiber.

Optical coupling depends on the density of points in phase space. Each ray in a bundle of rays is represented by a point in phase space, and the collection of rays in the bundle corresponds to a volume (denoted ψ) in phase space. As the ray bundle moves through physical space, the direction and location of the rays change; this corresponds to a change in location of the various points in phase space. The density of points ρ is the number of points per phase space volume. One form of Liouville's theorem [8] demands that neither the density of points in phase space nor the phase space volume can change with axial direction; i.e., $d\rho/dz = 0$, $d\psi/dz = 0$.

Normally, and not unexpectedly, the density is defined in terms of the incremental power, dP, in an increment of phase space volume $d\psi$.

$$\rho = dP/d\psi. \tag{6}$$

This equation shows that radiance is proportional to density, as will be seen. The total power (or, equivalently, the total number of rays) is found by integrating over phase space:

$$P = \int dP = \int \rho d\psi = \int \rho \; dx dy dp_x dp_y. \tag{7}$$

Figure 5 shows the relationship between the differential volume element in phase space and the product of differential area and differential solid angle in physical space. The area dxdy is normal to the z-axis and could represent a source radiating into the right-half plane. The figure shows that

$$p_x = n \sin \alpha, \tag{8a}$$

$$p_y = n \cos \alpha \sin \gamma = n \sin \beta, \tag{8b}$$

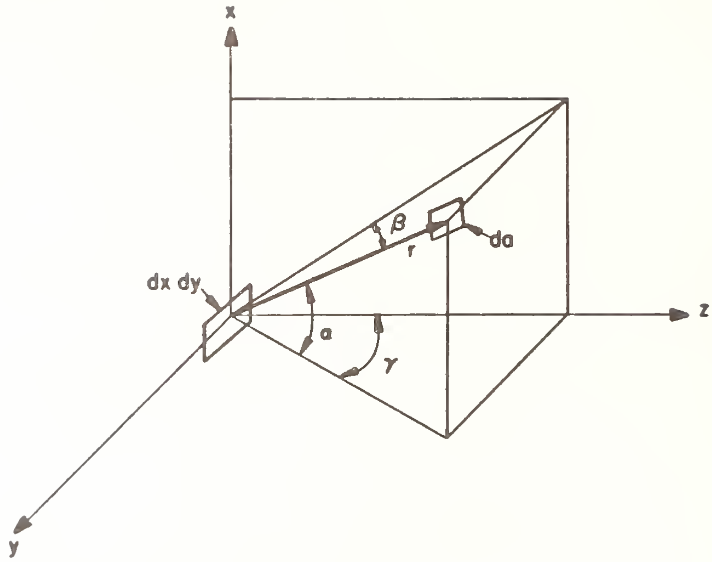

Figure 5. Illustrating angles and areas used to discuss phase space.

$$dp_x = n \cos \alpha \, d\alpha, \quad (8c)$$

$$dp_y = n \cos \alpha \cos \gamma \, d\gamma = n \cos \beta \, d\beta. \quad (8d)$$

The differential volume in the plane z = 0 is

$$d\psi = dxdy \; n^2 \cos^2 \alpha \cos\gamma \; d\alpha \; d\gamma. \quad (9)$$

The projection of the source normal to the ray is

$$da = dxdy \cos\alpha \cos\gamma = r d\alpha \; r \cos \alpha \; d\gamma. \quad (10)$$

The solid angle encompassed by da is therefore

$$d\Omega = da/r^2 = \cos \alpha \; d\alpha d\gamma. \quad (11)$$

Thus,

$$d\psi = n^2 \; dxdy \; d\Omega \cos\alpha \cos\gamma = n^2 \; da \; d\Omega, \quad (12)$$

where da is normal to the ray.

This important connecting relationship between phase space and the product of area and solid angle is fundamental to one of the launch conditions used to measure attenuation. The relationship is a manifestation of the conservation of radiance, since

$$\rho = \frac{dP}{d\psi} = \frac{dP}{n^2 da\ d\Omega} = \frac{L}{n^2}, \tag{13}$$

where radiance L is, by definition,

$$L = \frac{dP}{da\ d\Omega}. \tag{14}$$

The requirement $d\rho/dz = 0$ is equivalent, then, to the conservation of radiance:

$$\frac{d}{dz}\left(\frac{L}{n^2}\right) = 0. \tag{15}$$

The concept of a LPS (limited-phase space) launch is based on eq (12) and the requirement that only bound modes having "reasonable" loss values should be launched when measuring attenuation. This leads to measured values that are reproducible (precise) and more or less independent of the person who made the measurement. The LPS launch calls for a launch spot size equal to 70 percent (actually, $\sqrt{0.5}$) of the fiber core diameter and a launch numerical aperture equal to 70 percent (actually, $\sqrt{0.5}$) of the fiber numerical aperture [9]. The reason for this selection is related to the power-accepting properties of a fiber and the concept of fiber NA (numerical aperture). To examine the relationship between fiber NA and phase space, consider the following.

The concept of fiber NA becomes slightly complex when leaky rays are considered [10]. A leaky ray (or, correspondingly, a leaky mode) is one for which geometric optics would predict total internal reflection at the core-cladding boundary, but which suffers loss by virtue of the curved core boundary. Specifically, a leaky ray is a ray located at radial position r and having direction such that

$$n^2(r) - n^2(a) \leq \sin^2 \theta(r) \leq \frac{n^2(r) - n^2(a)}{1 - (r/a)^2 \cos^2\phi(r)}, \tag{16a}$$

where $\theta(r)$ is the angle the ray makes with the waveguide axis, $n(r)$ is the r-dependent refractive index, a is the core radius, and $\phi(r)$ is the azimuthal angle of the projection of the ray on the transverse plane [11]. A bound ray is one for which

$$0 \leq \sin^2(\theta) \leq n^2(r) - n^2(a). \tag{16b}$$

Figure 6 shows a ray in a fiber; the angles appearing in eq (16) are shown, as are other angles, as well as the radial, azimuthal, and axial components of the wave vector k (k_r, k_ϕ, $k_z = \beta$); k_0 is the wave number in free space. Skew rays correspond to $\phi < \pi/2$; meridional rays correspond to $\phi = \pi/2$. Meridional rays always traverse the fiber axis while skew rays never do.

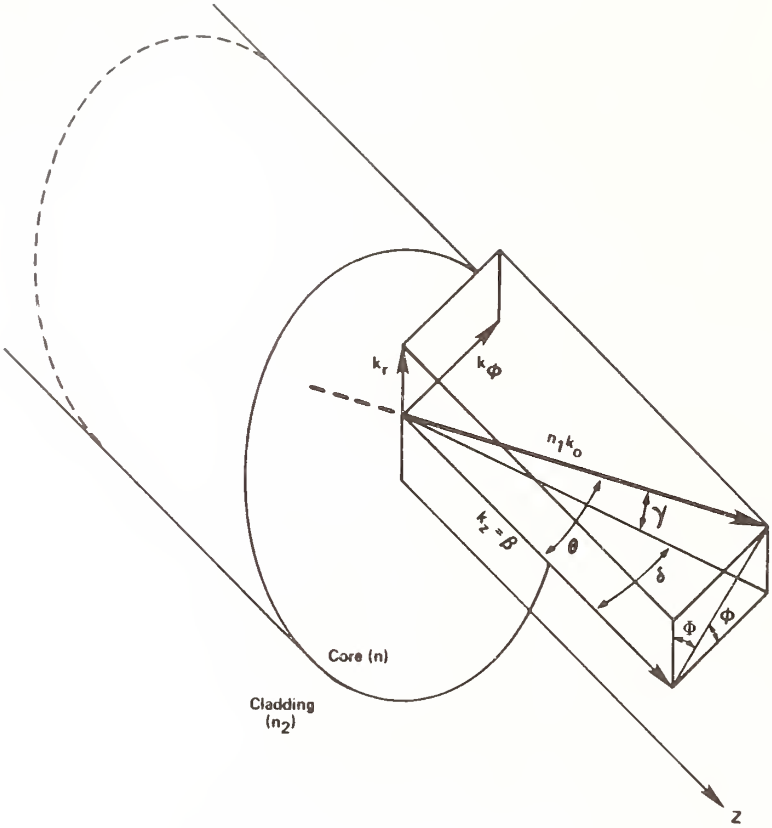

Figure 6. A typical light ray and angles in a fiber.

If leaky rays are included, the local numerical aperture of a fiber (which determines whether or not an incident ray is accepted) is defined as

$$NA = (NA)_o \left[\frac{1 - (r/a)^g}{1 - (r/a)^2 \cos^2\phi}\right]^{1/2} \tag{17}$$

where

$$(NA)_o = (n_1^2 - n_2^2)^{1/2} \tag{18}$$

and g is the power-law profile parameter; i.e., it is assumed that

$$n(r) = n_1[1 - 2\Delta(r/a)^g]^{1/2}, \tag{19}$$

where n_1 is the refractive index at $r = 0$; Δ is the contrast, specifying the difference between n(0) and $n(a) = n_2$. If $\phi = \pi/2$,

$$NA]_{\phi=\pi/2} = (NA)_o[1 - (r/a)^g]^{1/2}. \tag{20}$$

The power accepted by the fiber at any point on the core is proportional to the square of the numerical aperture. The equation for $(NA)^2$ is the equation of an ellipse, which degenerates to a circle at $r = 0$. The ellipse has semi-major axis

$$(NA)_o \left[\frac{1 - (r/a)^g}{1 - (r/a)^2}\right]^{1/2}, \tag{21}$$

and semi-minor axis

$$(NA)_o[1 - (r/a)^g]^{1/2}. \tag{22}$$

The area of the ellipse is proportional to the product of these two axes:

$$\text{Area} = \pi(NA)_o^2 \frac{1 - (r/a)^g}{[1 - (r/a)^2]^{1/2}}. \tag{23}$$

At $r = 0$, the circle that describes NA has area $\pi(NA)_o^2$. The ratio of the two areas is the ratio of power accepted by the fiber at radius r to that accepted at $r = 0$:

$$\frac{P(r)}{P(0)} = \frac{1 - (r/a)^g}{[1 - (r/a)^2]^{1/2}}. \tag{24}$$

This result can also be obtained from the phase space representation using the notation of figure 6. For the circular cylindrical system

$$d\psi = dA \sin\theta \cos\theta \, d\theta \, d\phi, \tag{25a}$$

where dA is the incremental area on the fiber core. The fiber near field, as given in eq (24), is obtained by integrating $d\psi/dA$ over all angles:

$$\frac{P(r)}{P(0)} = \frac{\int_0^{\pi/2} d\phi \int_0^{\theta_c(r,\phi)} \sin\theta \cos\theta \, d\theta}{\int_0^{\pi/2} d\phi \int_0^{\theta_c(0,\pi/2)} \sin\theta \cos\theta \, d\theta} \tag{25b}$$

where in the numerator,

$$\sin^2\theta_c(r,\phi) = \frac{n^2(r) - n^2(a)}{1 - (r/a)^2 \cos^2\phi}, \tag{25c}$$

and in the denominator,

$$\sin^2\theta_c(0,\pi/2) = n^2(0) - n^2(a) = n_1^2 - n_2^2. \tag{25d}$$

Telecommunication-grade multimode fibers have parabolic (or nearly parabolic) profiles, so $g \cong 2$. In that case, the near field becomes

$$\frac{P(r)}{P(0)} = \sqrt{1 - (r/a)^2}. \tag{26a}$$

If leaky rays are excluded,

$$\frac{P(r)}{P(0)} = 1 - (r/a)^2. \tag{26b}$$

The far field of the fiber can be obtained similarly from eq (25b) by again assuming all modes are equally excited and $g = 2$:

$$\frac{P(\theta)}{P(0)} = \int_0^{R(\theta,\phi)} \int_0^{\pi/2} R dR\, d\phi,$$

where $R = r/a$ and, for leaky and guided rays,

$$R^2(\theta,\phi) = \frac{1 - [\sin\theta/(NA)_o]^2}{1 - [\sin\theta/(NA)_o]^2 \cos^2\phi}. \tag{27a}$$

When leaky rays are excluded,

$$R^2(\theta,\phi) = 1 - [\sin\theta/(NA)_o]^2. \tag{27b}$$

For $g = 2$, the fiber far field is

$$\frac{P(\theta)}{P(0)} = 1 - \left(\frac{\sin\theta}{(NA)_o}\right)^2 \tag{28a}$$

for bound modes only and

$$\frac{P(\theta)}{P(0)} - \left[1 - \left(\frac{\sin\theta}{(NA)_o}\right)^2\right]^{1/2} \tag{28b}$$

when leaky rays are included.

The LPS launch calls for a uniform launch spot of specified size and specified launch angle. These conditions can be put into perspective by using the concepts discussed here. Consider a uniform spot of diameter r_o focused onto the end of a fiber core having diameter a. The launch angle with respect to the fiber axis is θ_o. The power that the spot launches into the fiber can be found using eqs (7), (12), and (13). The radial and azimuthal coordinate variables in the plane of the fiber end face (or spot) are taken to be r, ξ. Incremental area da is therefore r dr dξ. The total power coupled from the spot to the fiber is

$$P(r_0,\theta_0) = \int_0^{r_0} \int_0^{\theta_0} \int_0^{2\pi} \int_0^{2\pi} L\ r dr d\xi\ \sin\theta \cos\theta\ d\theta d\phi \tag{29a}$$

where L is the (uniform) radiance of the launch spot and $\sin\theta\ d\theta d\phi$ is the solid angle into which da launches power (cf. fig. 6, but r and ξ are not shown in that figure). da $\cos\theta$ is the component of da that is normal to the ray direction. We suppose that the launch spot radiance is independent of ξ, yielding

$$P(r_0,\theta_0) = L_0(\pi r_0)^2 \sin^2\theta_0. \tag{29b}$$

In deriving this equation, we have assumed that the fiber accepts all rays incident from the launch spot. The validity of this assumption depends on the refractive index profile of the fiber. If the fiber has a parabolic profile, the assumption will hold if r_0 and θ_0 are related thus:

$$(r_0/a)^2 + [\sin\theta_0/(NA)_0]^2 \leqslant 1, \tag{29c}$$

with $(NA)_0$ defined in eq (18).

Additional insight is had by normalizing eq (29b), using $R_0 = r_0/a$:

$$P(R_0,\theta_0) = KR_0^2\left[\frac{\sin\theta_0}{(NA)_0}\right]^2, \tag{29d}$$

where K is a constant that depends on the strength of source. The LPS launch is based on a meaningful choice of R_0 and θ_0. This is discussed further below.

Equation (29d) is a measure of how well the phase space of the spot matches that of the fiber. In this sense, it gives the expected coupling efficiency between the two but without including reflection loss. This will be seen in discussing figure 7c, which is a plot of eq (29d). Equation (29d) is fundamental to the LPS launch, since it contains only the launch spot parameters and the fiber parameters.

Figures 7a, b, c, and d are plots of eqs (16), (26), (28), and (29d) subject to eq (29c) for g = 2. They are included to help explain the LPS launch. Note first that the straight diagonal line between (0,1) and (1,0) in the figures is the line $y^2 = 1 - x^2$, where y^2 is the ordinate and x^2 is the abscissa. The region below that line represents the region of bound modes. Figure 7a shows that if the launch spot size is 70 percent of the fiber core size and the launch numerical aperture is 70 percent of the fiber numerical aperture, the phase space excited in the fiber is shown by the square in the lower left corner of the figure. The power launched is given by eq (29d) with $R_0^2 = 0.5$ and $[\sin\theta_0/(NA)_0]^2 = 0.5$. No leaky modes are excited.

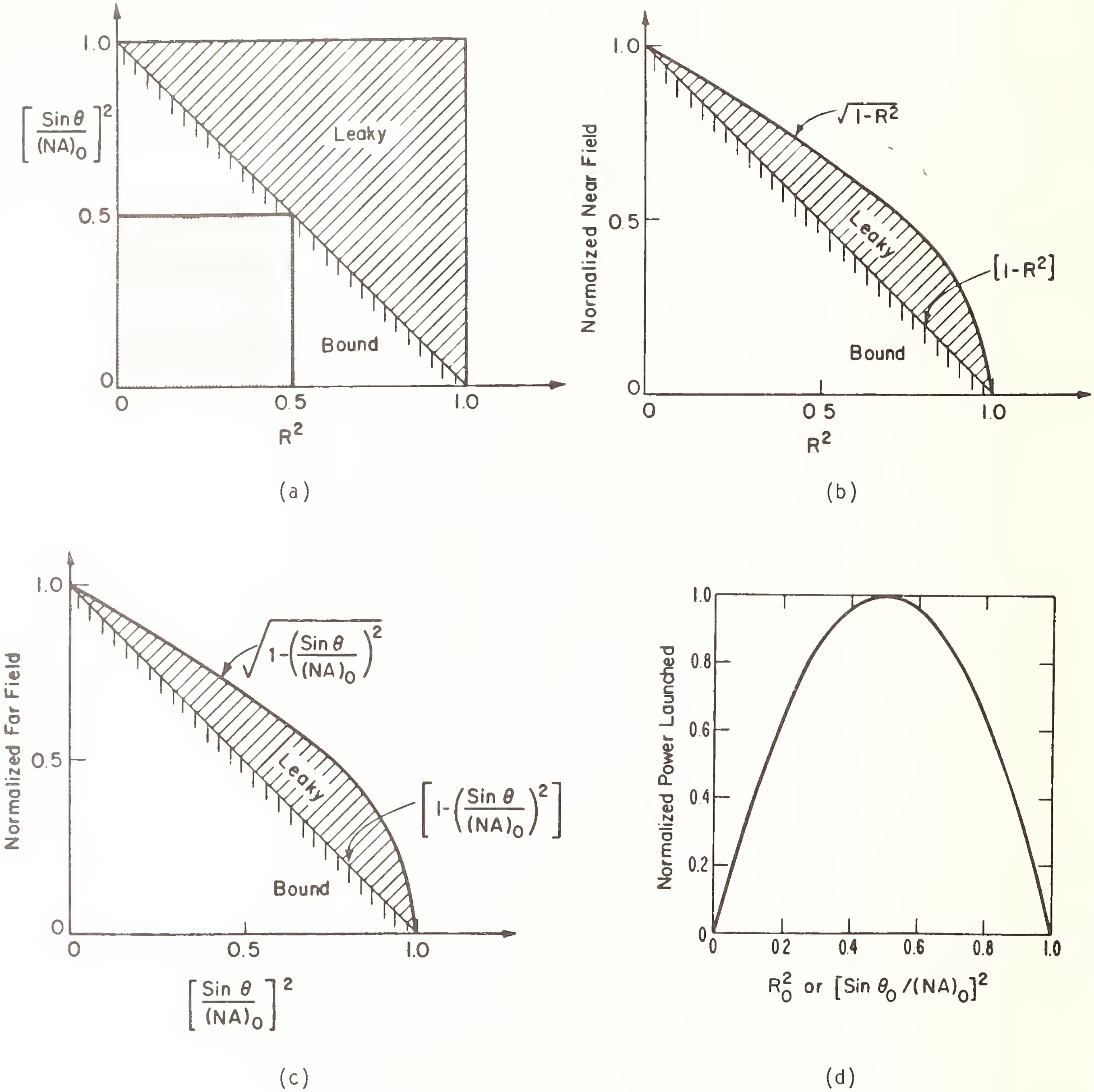

Figure 7. (a) The phase space of a graded-index fiber. Darkened area shows the phase space excited by the LPS launch.
(b) The normalized near field of a parabolic profile fiber (g = 2).
(c) The normalized far field of a parabolic profile fiber (g = 2).
(d) Normalized power launched into a parabolic profile fiber (g = 2) under the condition that R_0 and $\sin\theta_0$ are chosen so no leaky modes are excited but that maximum power is coupled into the fiber. Uniform launch condition.

Holmes [9] has discussed the launch condition described here. He defined the EMV (effective mode volume) of a fiber in terms of the far-field and the near-field intensity distributions of the fiber. EMV is the square of the product of the normalized full width at half maximum (FWHM) of the near-field distribution and the normalized sine of the half width at half maximum (HWHM) of the far-field radiation pattern. Figures 7b and 7c relate this definition of EMV to the LPS launch condition illustrated in figure 7a. If leaky rays are excited, the near field and the far field will reveal this. Defining EMV in terms of the far field and the near field is thus obviously related to the modal power distribution, as seen from the figures.

EMV is a convenient device and has proved to be useful in predicting steady-state conditions of the fiber. Once the modal power distribution of a fiber is in equilibrium, the EMV as measured at the fiber output is independent of fiber length; this is the condition sought when predicting attenuation of concatenated links. The EMV at the input of a fiber depends on launch spot size and launch numerical aperture as shown in the figures.

The concept of EMV is helpful and its use led to a useful launch condition. Recent work demonstrates the complexity of the problem, however, and EMV clearly is not sufficient to circumscribe the variabilities in attenuation measurements. A comparison of several filters and/or mode mixers shows that each has its limitation but fortunately the fiber attenuation is relatively insensitive to the fine details of launched modal power distribution [12,13].

Figure 7d relates the 70-70 launch condition to power launched under the restriction that spot size and launch numerical aperture are chosen so no leaky modes are excited but that power coupled into the fiber is maximum. This maximum power condition is not the primary reason for selecting the 70-70 launch condition. It does represent a happy coincidence, however.

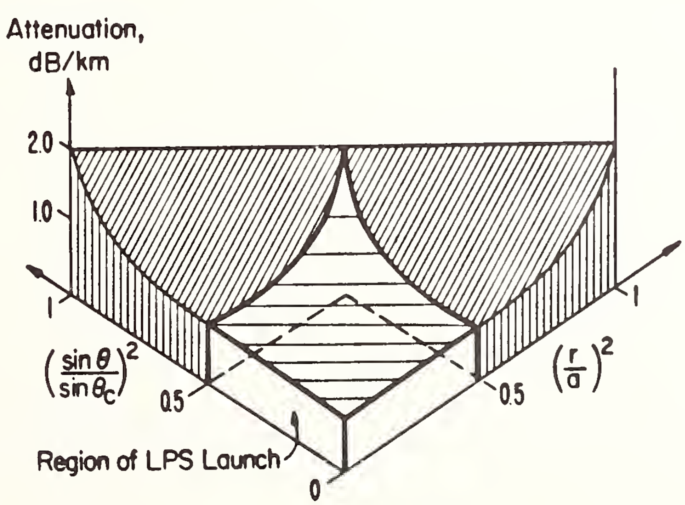

Figure 8. Attenuation as a function of ray parameters (after ref. 14).

Figure 8 [14] further illustrates the reason for the limited launch. The figure gives attenuation along the vertical axis with launch variables in the horizontal plane. The measured attenuation depends on how effectively various modes are excited. If the fiber core and numerical aperture are fully filled at launch, attenuation is skewed by the high-loss modes, giving results that would not be useful in predicting the loss in a system of several kilometers length.

2.1.1 A Summary of Phase Space Concepts

The definitions and connecting relationships given above form the basis of fundamental and important concepts in optical coupling, including the coupling of light energy between a source and a fiber. Phase space is a four-dimensional space that is defined in terms of geometrical optics and light rays. Two of the four dimensions are associated with the momentum of a ray [eq (4)] and the other two are associated with the ray's spatial position. Each point in the four-dimensional space has a one-to-one relationship to the ray's position in space and its direction (or momentum). This is important because a ray enters a fiber at a point in space (on the fiber core) with a momentum determined by its angle with respect to the fiber axis [cf. eq (5)].

The ray is bent as it passes from air into the fiber core according to Snell's law. The bending can be described in terms of phase space by invoking the concept of the density of points in phase space, denoted above by ρ. Neither the density of points nor the volume enclosing a fixed number of points in phase space can change with z, the axial coordinate. Snell's law is a direct result of this conservation principle. The conservation of density (ρ) and of volume (ψ) is a manifestation of Liouville's theorem in statistical mechanics. The conservation of radiance is a consequence of these conservation principles [see eq (15)].

Equation (12) shows that incremental volume in phase space is the product of area, solid angle, and the square of refractive index. [The refractive index is squared because the angle is two dimensional (solid).] It is precisely this product that is controlled in the LPS launch. The product is conserved in going from air to fiber core. The product is also the determinant of power launched into the fiber. That is the thrust of eqs (16) to (29), as illustrated in figures 7a to 7d.

Equation (29a), when used in conjunction with figure 7a, can be used to deduce power coupled into a fiber under several conditions. When a uniform source is assumed, the calculation can be done easily in closed form. The figure helps in defining limits of integration. In particular, if a spatially uniform light spot of radius r_0 is focused onto the end of the fiber, the total power coupled into the fiber (neglecting reflection losses) is

$$P = 2\pi \int_0^{r_0} rdr \int_0^{\theta_0} \int_0^{2\pi} \sin\theta \cos\theta \, d\theta \, d\phi,$$

where θ_0 is the limiting value of θ; several values of θ_0 and r_0 will now be considered.

If the fiber is filled, $r_o = a$, $\theta_o = \theta_c$ as given in eq (25c). The corresponding value of P will be referred to as P_{TOT}. For the LPS launch, $\sin^2\theta_o = (NA)_0^2/2$ and $r_o = a/\sqrt{2}$ (cf. fig. 7a). The corresponding power launched will be referred to as P_{LPS}. The power coupled into guided modes, to the exclusion of leaky modes (referred to below as P_g), is found by taking $\sin^2\theta_o = (NA)_0^2[1 - (r/a)^2]$ and $r_o = a$. To complete the picture, we will refer to $P_g - P_{LPS}$ as $2P_d$. The region outside the shaded square but below the straight diagonal line in figure 7a represents the power $2P_d$. Finally, the amount of power in the leaky modes (P_ℓ) is $P_\ell = P_{TOT} - P_g$. The following relationships are obtained from the integration, assuming a parabolic fiber with uniform mode excitation.

$$P_g/P_\ell = 3, \tag{30a}$$

$$P_g/P_{TOT} = 3/4, \tag{30b}$$

$$P_\ell/P_{TOT} = 1/4, \tag{30c}$$

$$P_{LPS}/P_{TOT} = 3/8, \tag{30d}$$

$$P_d/P_{LPS} = 1/2. \tag{30e}$$

These ratios will be used later.

Equation (29d) gives the power coupled into a parabolic profile fiber as a function of launch spot size and launch angle. It is again the product of area and solid angle that is the determinant of power launched. The equation shows that launching power is a matter of matching the phase space of the source to the phase space of the fiber. Only the phase space of each (aside from a multiplying constant) appears in the equation. The maximum value of the right hand side is K and that obtains when the phase space of the source equals that of the fiber; i.e., the fiber is filled and all bound modes are excited. In that case, $R_0 = 1$ and $\sin\theta_o = (NA)_0$.

The equations reveal an interesting picture of power coupled into the bound modes of a parabolic fiber. If launch angle and launch spot size are independently adjusted so only bound modes are excited, then maximum power is coupled into the fiber when launch spot diameter is 70 percent of core diameter and launch numerical aperture is 70 percent of fiber numerical aperture, provided the launch spot is in focus and exactly centered on the fiber core.

Finally, the connecting relationships and figure 7 lead to what has been called the EVM (effective mode volume) of a fiber [9]. EMV is defined as the square of the product of the full width at half maximum of the near-field pattern and the half width at half maximum of the far-field pattern. That this is so is discussed above. Thus, the 70/70 launch condition is based on both the near field and the far field of the fiber. The mode filter launch, described later, is based only on the far-field pattern of the fiber. The question of equivalence of the methods arises naturally, then. The question cannot be answered definitely but some intuitive arguments in this regard are given later.

2.2 LPS Launch

Figure 9 is a block diagram of the system used to control launch spot size and launch numerical aperture independently, in accordance with the requirements of the LPS technique. The method is sometimes referred to as the beam optics method of launch.

The light source is a tungsten strip lamp powered by a regulated power supply to maintain stability during the measurement. The strip lamp is preferable to coiled filament lamps because it produces a spatially uniform spot. The lens L_1 converts the diverging beam to a beam of parallel rays that pass through the interference filter for wavelength selection. The filters have a 10 nm spectral width. The wheel that houses the several filters allows white light as one option; this option can be used for alignment, as occasionally required. Lens L_2 focuses the beam onto the aperture A_1, called the source aperture, which is imaged onto the specimen. The size of A_1 can be changed to adjust the launch spot size.

The beamsplitter shown in the figure serves a dual purpose. First, the arm marked power monitor goes to a reference detector which monitors the stability of the light source. Correction can be made in the final results if the output light power drifts during measurement. Experience has shown that with a stabilized power source for the lamp, correction is almost never required and measurements are often made without the monitor arm activated. The computer program that controls data acquisition allows the operator to monitor the source or not, as he sees fit. The beamsplitter also allows viewing the fiber end with the vidicon.

Aperture A_2 controls the launch numerical aperture by restricting the beam angle. Thus, A_1 and A_2 must both be adjustable, in accordance with the needs of the LPS launch.

The magnification ($m < 1$) introduced by the optics between A_1 and the fiber end must be known. The spot size on the fiber end is determined from m and the size of A_1. The launch spot size (A_L) is:

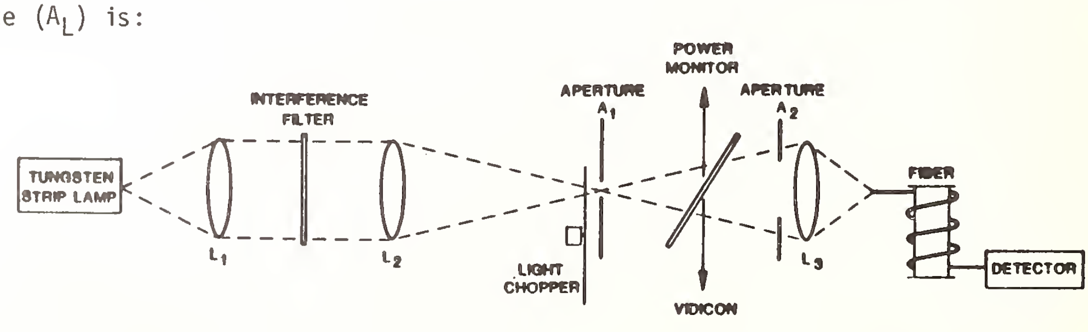

Figure 9. Block diagram of attenuation measurement system. The system allows launch spot size and launch numerical aperture to be controlled independently.

$$A_L = A_1 (\ell_3/\ell) = mA_1 ,$$

where ℓ_3 is the distance from L_3 to the image plane and ℓ is the distance from A_1 to L_3. Dimensions are not accurately known so m is determined by measurement. A pinhole detector (small compared to expected spot size) scans the image plane of L_3 to measure launch spot size for a known size of aperture A_1. Magnification is then calculated. In a similar manner, the launch NA effected by aperture A_2 is determined by measuring the far-field beamwidth as a function of aperture size. A catalog is thus easily established, allowing for selection of A_1 and A_2 to meet the needs of the LPS launch method. Commonly accepted tolerances on A_L and launch NA are as follows:

$$A_L/d = 0.707 \pm 0.05 \tag{31}$$

$$\frac{\text{launch NA}}{\text{fiber NA}} = 0.707 \pm 0.05 \tag{32}$$

where d is nominal fiber core diameter.

The launch NA called for in eq (32) is measured at distances considerably greater than $10\ d^2/\lambda$, which is the usual definition of far field. The launch angle is obtained from geometry, knowing the distance from the focal plane of L_3 to the measurement plane and having obtained the measured beamwidth at that plane. The distance from the focal plane of L_3 to the measurement plane is accurately known because the detector is mounted on a micropositioner stage.

The standard cut-back technique is used to calculate fiber attenuation from the measured values of power; see eq (3). An alternative technique, also based on the cut-back technique, can be used if the fiber ends are prepared with suitable care and input alignment is carefully controlled. In this case, a short piece of the fiber under test is prepared in advance, as is the test fiber. A two-fiber bed on a translation stage allows the input to be focused alternately on the short fiber and the test fiber. The two fibers are likewise coupled to the detector so one can measure the power transmitted through the short piece or the test fiber, alternately and conveniently. The ratio of the two readings gives attenuation, but the technique depends on good agreement in the input coupling for the two fibers. Such agreement is especially important in low-loss fibers, for which a true cut-back technique is preferred. In this one-fiber technique, the input end (which is the more critical end) is unchanged in the course of the measurement. Thus, the modal power distribution established at launch is the same for both measurements. The two-fiber method allows input coupling errors on two counts. First, the preparation of the two fiber ends may differ, even though slightly, allowing for differences in input coupling loss. Second, the alignment may differ, leading to a difference, however slight, of the launched modal power distribution. These two effects may be cumulative, leading to inconsistent power readings and unreliable loss values. With the true cut-back technique, using only a single fiber, the input coupling efficiency and modal power distribution are the same for both test and reference fiber power measurements.

2.3 Mode Filter Launch

The purpose of defining a standard launch condition is to simulate a fiber having an equilibrium modal power distribution. The measured attenuation will then allow prediction of the attenuation expected in field installations, where long fibers are encountered and an accurate prediction of system loss is essential. Linear addition of attenuation is crucial and will be possible only if the measured attenuation for a test fiber is based on steady-state or equilibrium conditions.

Both the LPS launch and the mode filter launch yield results that scale linearly with distance [10]. Both launch conditions were used for attenuation measurements reported in this document.

A mode filter is a device used to select, reject, or attenuate a certain mode or modes [11]. A mode scrambler is a device for inducing mode coupling in an optical fiber [11]. Our purpose is to establish the equilibrium modal power distribution; i.e., the power distribution that prevails at the end of the long test fiber. Whether the modes are filtered or scrambled is thus an academic question. In fact, workers do not agree on just how the equilibrium state is established [2,12,13] or how best to accomplish the desired end. Reference 13 indicates that modal power distribution is affected in different ways by different filters and scramblers on different fibers.

The method of the mode filter launch is based on the assumption that the relative modal power distribution at the end of a long fiber without the mode filter is the same as it is at the end of a short reference fiber with the mode filter in place. Furthermore, the method assumes that the far-field radiation pattern is a suitable indicator of whether or not the modal power distributions are, in fact, the same. If those patterns are the same, or nearly so, the mode filter has served its purpose, having eliminated certain modes and induced an equilibrium modal power distribution which is equivalent to that at the end of a long fiber.

The mode filter probably does more than just eliminate certain high-order modes. It may induce mode coupling as well, to establish a balance between intermodal power transfer and modal attenuation. The primary function of the filter, however, is to eliminate the high-order modes.

The power distribution in the far field of a fiber depends on modal power distribution. If all modes carry the same power, then each incremental area of the core cross section at the fiber end will uniformly illuminate its cone of acceptance. Therefore, all areas on the fiber core that have a local numerical aperture greater than $\sin\theta$ will contribute equally to the far-field power at angle θ, where θ is the angle between the fiber optical axis and the reference point in the far field. The far-field pattern is therefore a function of fiber numerical aperture. In practice, mode coupling and mode-dependent loss lead to unequal power distribution among the modes at the output end of the fiber. In that case, not all modes contribute equally to the power at angle θ. Nevertheless, the far-field pattern width is still a measure of fiber numerical aperture, although the specification of how pattern width is defined now becomes a consideration.

In the mode filter method, the adequacy of the mode filter is based on a comparison of the far-field patterns of two fibers (the test fiber without a filter and the reference fiber with the filter). If the angles agree at the 5 percent intensity points, modal power distribution is assumed to be approximately the same.

The mode filter is qualified as follows. Power is launched into the long test fiber with a spot size greater than the fiber core size and with launch numerical aperture greater than the fiber numerical aperture. This will be refered to as overfilling the fiber. The far-field radiation pattern is then measured, where far field means distances greater than 10 d^2/λ from the fiber end, and where d is fiber core diameter. A short reference fiber is then prepared for the purpose of "qualifying" the mode filter. The reference fiber is overfilled and then subjected to the mode filter. The far-field radiation pattern of this reference fiber is measured and the mode filter is adjusted to produce a far-field pattern which is equivalent (within tolerance) to the pattern of the long fiber without the filter. The filter is deemed acceptable if the pattern widths are the same at the 5 percent intensity points. The tolerance is given below [eq (33)].

The procedure uses the arrangement shown in figure 10 [15]. A filter is normally qualified for only one fiber. Changing the test fiber usually calls for a change (even though slight, in some cases) in the filter. Once the filter has been qualified, attenuation is measured using simple launch optics. The fiber is overfilled and the filter is in place for power measurements on both the long test fiber and the short reference fiber, to insure that the insertion loss of the filter is accounted for.

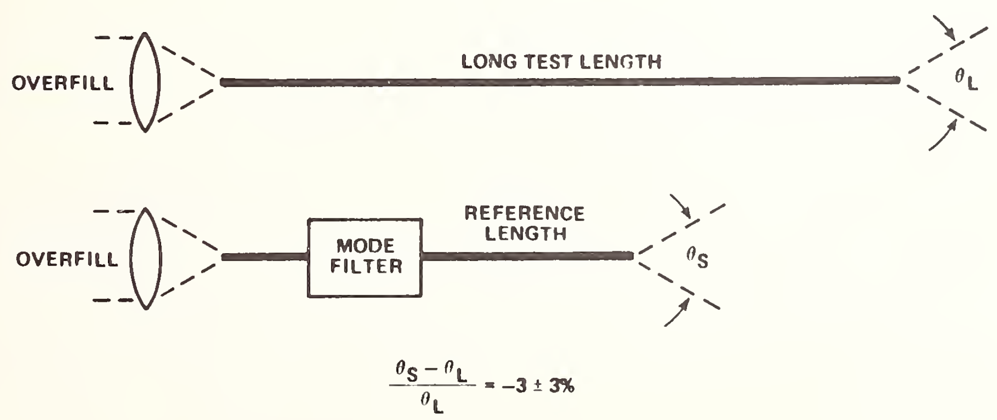

Figure 10. Arrangement for qualifying a mode filter.

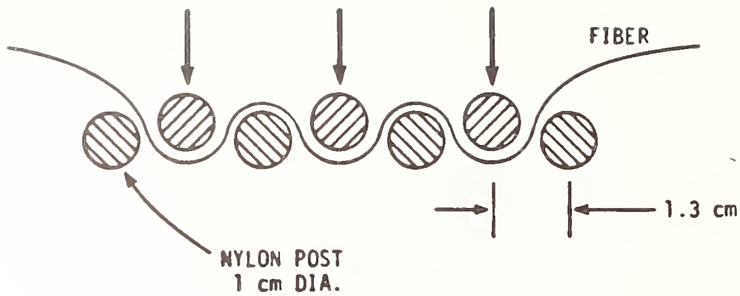

Figure 11. Mode filter used for measurements reported herein.

Workers have used several forms of mode filter, including dummy fibers, macroscopic-bend mandrel wraps and serpentine bends [16]. The measurements reported in this document were taken with a serpentine bend filter, which is shown schematically in figure 11. This design is similar to that used by other workers [17]. The filter consists of seven nylon posts, each of 1 cm diameter. The posts are on 1.3 cm centers. Three of the posts are on a translation stage, allowing for movement of those posts to adjust the strength of the filtering.

The mode filter technique requires knowledge of θ_L (see fig. 10); θ_S is then measured using a short length of reference fiber taken from the spool of test fiber. Moving the posts of the filter (fig. 11) changes the angle θ_S. The requirement is [18]

$$\Delta\theta = \frac{\theta_S - \theta_L}{\theta_L} = -0.03 \pm 0.03. \qquad (33)$$

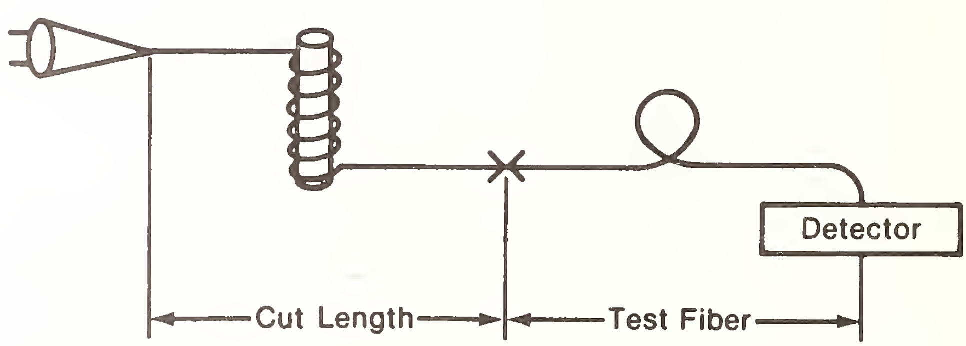

Figure 12. Experiment arrangement for attenuation measurement using a mandrel wrap mode filter [12].

The equation is defined so $\Delta\theta$ is not positive. A negative value for $\Delta\theta$ results from excessive filtering. In that case, the mode filter causes θ_S to be slightly smaller than (or, at most, equal to) θ_L. Equation (33) discourages the acceptance of high-order modes that are known to lead to inaccurate loss measurements. A positive value of $\Delta\theta$ implies inadequate mode filtering.

The experimental arrangement for the mode filter launch is simpler than that for the LPS launch because careful control of the spot size and launch numerical aperture are not required. The fiber must be overfilled and this is easily accomplished without much fuss. A typical experimental arrangement is shown in figure 12, where the mode filter is shown as a mandrel wrap [10]. The attenuation measurement technique is as follows (cf. fig. 12): After the filter is qualified, it is used in the long test fiber and detector power is measured. The fiber is then cut as shown in the figure and power is measured out of the cut length under the same launch conditions. The ratio of the two powers provides the loss using the cut-back formulas.

That the mode filter launch and the LPS launch should yield comparable loss measurements is not obvious. It seems intuitive that different amounts of power are coupled into the test fiber under the two launch conditions. Furthermore, the LPS launch is based on both near field (launch spot size) and far field (launch numerical aperture) information. The mode filter launch is based entirely on the far field. A question naturally arises then as to whether one can expect the two methods to establish equivalent modal power distributions in the fiber. Most important in this regard is the attenuation or elimination of high order and leaky modes. Either method is effective in this regard. Beyond that, however, we are forced to conjecture on the similarities of the two methods. Figure 7a is useful in visualizing concepts. The darkened area is proportional to power launched under the LPS method. That area represents the product of physical area and angle, as already discussed. According to eq (30d), the ratio of power carried by a fully filled fiber (including leaky modes) to that carried by a fiber filled at the 70/70 level (P_{TOT}/P_{LPS}) is 2.67 or 4.26 dB. If a mode filter eliminates the leaky modes from the filled fiber, the ratio reduces to 3 dB $[(P_{LPS} + 2P_d)/P_{LPS}]$. Thus, the ratio of power launched into an overfilled test fiber with a mode filter to that launched using the LPS method is 3 dB or possibly less. If the mode filter introduces additional loss (which is assuredly the case), the figure will be less than 3 dB.

The mode filter almost certainly does more than just eliminate the leaky rays. It probably attenuates the high-order modes and encourages modal power coupling as well. This seems obvious from the fact that the filter must restrict the far-field pattern of the fiber in order to be acceptable. It seems reasonable, then, to suppose that the mode filter eliminates power associated with the following regions of figure 7a:

$$0.5 \leq \left(\frac{\sin\theta}{\sin\theta_c}\right)^2 \leq 1 - (r/a)^2 \qquad (34)$$

and

$$1 - (r/a)^2 \leq \left(\frac{\sin\theta}{\sin\theta_c}\right)^2 \leq 1. \tag{35}$$

If so, the ratio of power launched with a mode filter to that launched using LPS is $(P_{LPS} + P_d)/P_{LPS}$ or 1.76 dB [see eq (30e)]. This assumes that the filter does not attenuate low-angle rays. It further assumes that the rays specified by eqs (34) and (35) are completely eliminated. A laboratory measurement of power launched into a fiber using the mode filter and the LPS launch yielded a ratio of 1.64 dB.

If what we suggest here is true, then the two launch conditions will yield comparable loss measurements even in fibers having differential mode attenuation. If a fiber has very little differential mode attenuation, the two methods will yield comparable results even if what we suggest is not true.

Appendix A relates these concepts to the fiber mode volume. The latter term is a popular one that is easy to understand since it identifies the number of modes that a fiber can support. Appendix A shows that the ratio of the total number of guided modes supported by a parabolic fiber to the number supported between $r = 0$ and $r = a/\sqrt{2}$, is 1.25 dB. Thus, the preceding discussion suggests that the mode filter may eliminate all of the leaky modes but couples some of the energy into low-order guided modes.

3. COMPONENT AND SYSTEM VARIABILITIES

The measurement system shown in figure 9 will yield meaningful results only if the conditions of the restricted launch (either LPS or mode filter) are met. That they are met is confirmed through measurement. The variabilities encountered in measuring the pertinent parameters are discussed in this section. In addition, linearity and noise are discussed for the dynamic range and wavelength range of interest in the current telecommunications-grade fiber market.

The measurement of magnification (denoted m and discussed in the following section) allows a prediction of launch spot size for a known aperture size A_1. The measurement of m and of launch numerical aperture require the measurement of beam widths. Unfortunately, there are fundamental limits to the accuracy with which one can measure those widths. The limits are imposed by virtue of diffraction and the finite size of the detector aperture.

A similar limit is imposed in qualifying the mode filter. The patterns being measured invariably have sloping skirts which make it difficult to clearly define the 5 percent points of the pattern.

This section also addresses the question of component and system linearity and system noise. For fibers of interest today, the required dynamic range is only a few decibels so acceptable linearity is easily attained. System noise is well below the level of tolerance.

3.1 Spot Size and Launch Numerical Aperture

Independent adjustment of launch spot size and launch numerical aperture is accomplished using apertures A_1 and A_2 of figure 9. The diameter of the spot focused onto the end of the fiber is the magnified diameter of A_1, where the magnification m is approximately

$$m = f_3/\ell \tag{36}$$

where ℓ is the distance from A_1 to L_3 and f_3 is the focal length of L_3. Although m is defined here in terms of distances, in practice it is experimentally determined since ℓ is not known accurately. m is found by measuring the launch spot size (mA_1) using a large aperture. The variation of m with wavelength is shown later. The diameter of A_1 is determined by visual examination using a microscope with a two-dimensional vernier stage to identify edge location.

Measurement of m is accomplished by placing a small aperture in front of a detector and in the image plane of L_3. The combination is scanned across a diameter in that plane to determine spot size. Knowing the size of A_1 then allows the calculation of m.

If the focused image of the aperture had spot has perfectly sharp edges, sweeping the detector aperture through that spot could be described by the convolution of two cylinder functions $CYL(r/d_s) * CYL(r/d_a)$, as shown in figure 13, where

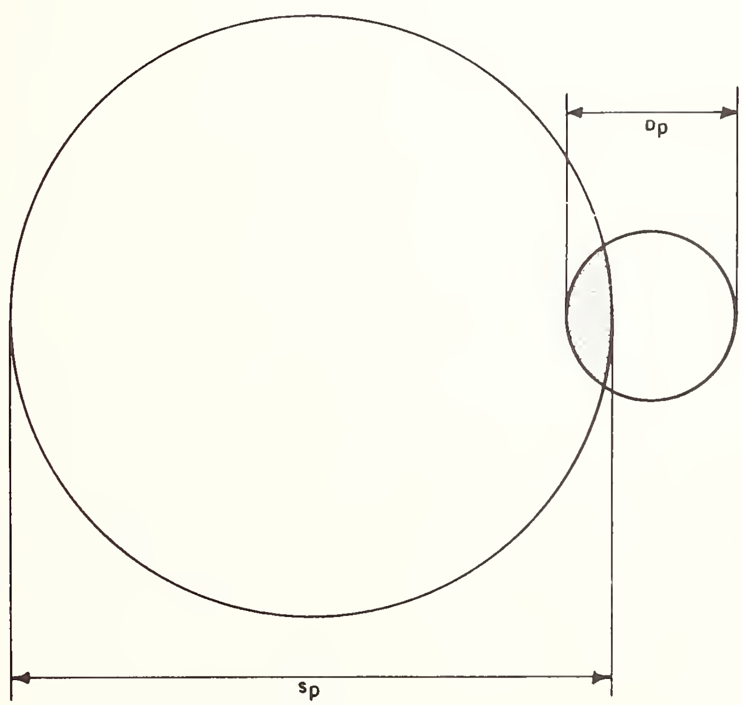

Figure 13. Two cylinder functions, representing an aperture and a spot being measured.

$$\mathrm{CYL}(r/d) = \begin{cases} 1 & , 0 \leqslant r < d/2 \\ 1/2, & r = d/2 \\ 0 & , r > d/2 \end{cases} \quad (37)$$

where d_s and d_a are the diameter of the spot and the aperture and * denotes convolution.

The cylinder function is an accurate description of the transmittance of the circular aperture over the detector but the focused spot invariably has skirts, owing to diffraction. Nevertheless, it is instructive to consider the case of perfectly sharp functions to describe both the spot intensity (in the focal plane of L_3) and the aperture. To estimate potential errors encountered in the system, and to define the "small aperture" alluded to earlier, we consider a one-dimensional problem, the convolution of two rectangular functions, one of width w_s and one of width w_a, where the subscripts refers to spot and aperture; we take $w_s > w_a$. The functions and their convolution are shown in figure 14. This figure shows that the accurate measurement of w_s is difficult. The measured form (fig. 14c) differs from the actual spot (fig. 14a) by an amount that depends on w_a. The FWHM of figure 14c differs from that of figure 14a by w_a.

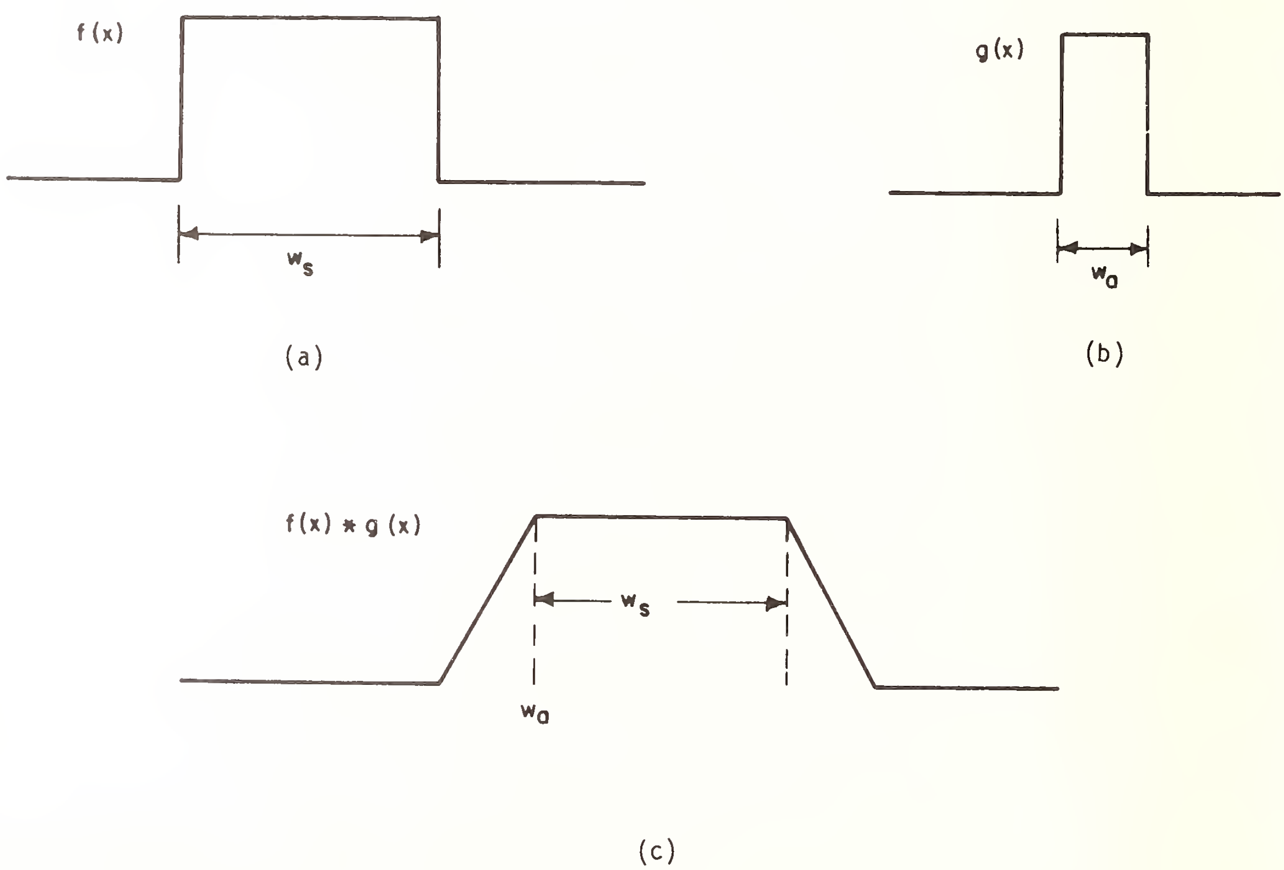

Figure 14. The convolution of two rectangular functions, illustrating the error introduced when measuring f(x) (a) using an aperture g(x) (b) resulting in f(x) * g(x) as shown in (c).

Clearly, we require $w_a << w_s$. If w_a is a delta function, the spot is reproduced exactly in the measurement. However, as w_a is decreased to improve the measurement precision, the signal-to-noise ratio is decreased. Obviously, the measurement of launch spot size calls for a compromise in the name of accuracy. w_a should be as small as possible, commensurate with the need for acceptable signal-to-noise ratio.

Since total measured width is proportional to $w_a + w_s$, the allowed value of w_a is proportional to allowed error on measured w_s. For 1 percent error, w_a must be not more than 1 percent of w_s. If the spot size is defined at the 10 percent intensity points, w_a can be slightly larger: $w_a < 0.0125\ w_s$. The convolution suggested by figure 13 does not differ substantially from that shown in figure 14, if $d_a << d_s$.

This simple approach, based on rectangular functions in one spatial dimension, is useful because it is intuitive. In practice, the measured spot is the convolution of a cylinder function and a two-dimensional function which accounts for diffraction.

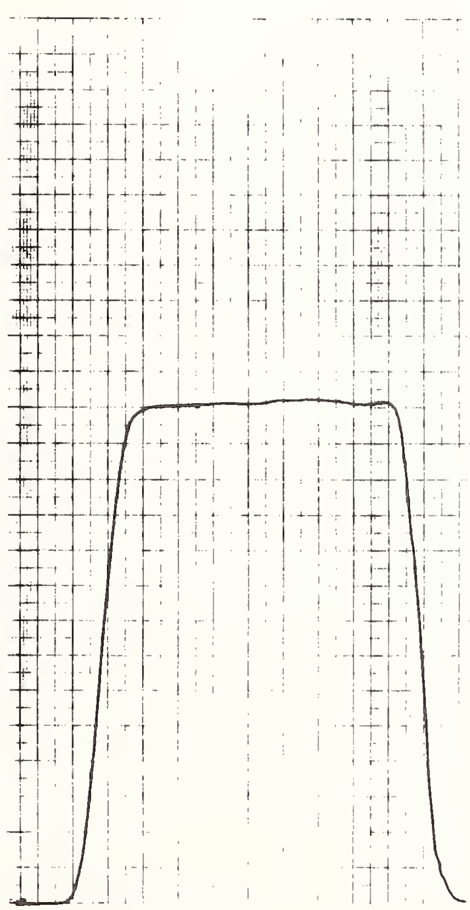

Figure 15. Measured spot in the focal plane of L_3.

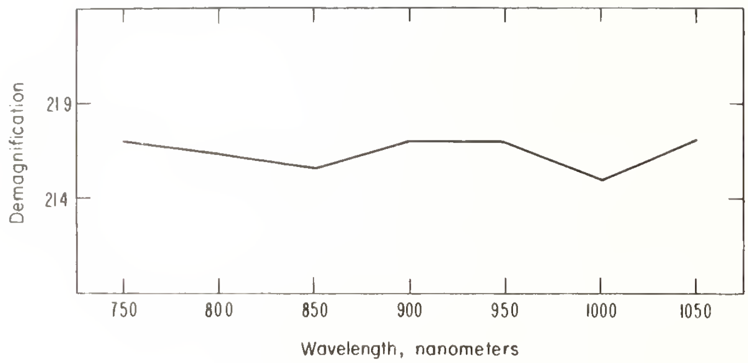

Figure 16. Change of demagnification with wavelength.

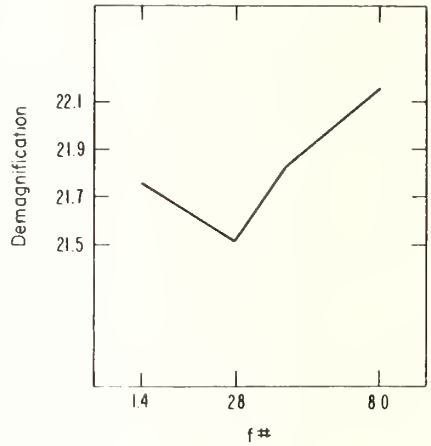

Figure 17. Change of demagnification with f# (aperture size).

Figure 15 shows the measured spot in the focal plane of L_3 with A_1 = 3012 μm at 850 nm, with a 1 μm aperture over the detector. The width at the 10 percent intensity points is 140 μm, indicating that

$$m = 1/21.6. \tag{38}$$

Figure 16 shows how magnification changes with operating wavelength. Obviously, the chromatic aberrations of the intervening lenses and the beamsplitter are not excessive. Variation of m over the range measured is ±0.1 or about 0.5 percent. If the fiber core diameter is 50 μm, the launch spot size should be 35 μm. Invoking the ±5 percent allowance on spot size yields

$$702\ \mu m \leqslant A_1 \leqslant 810\ \mu m. \tag{39}$$

To determine spot size, the vernier of the translation stage that holds the detector is read at the appropriate signal levels.

The magnification is not expected to change with LNA. The accuracy with which one can measure spot size, however, is a function of the size of A_2 (LNA). Figure 17 shows measured values of m as a function of the f-number of the lens L_3. This variation is due primarily to loss of resolution.

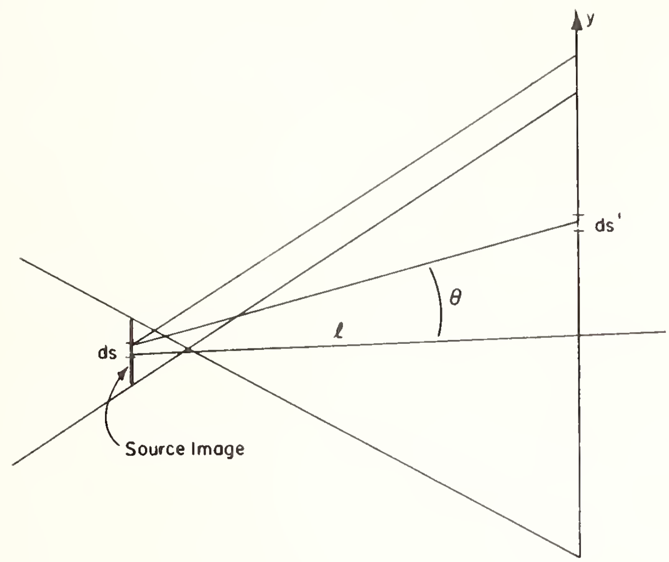

Figure 18. Geometry and angles encountered in measuring LNA.

The method used to determine LNA can be described with the help of figure 18. The source image refered to in the figure is the image of aperture A_1. The source image is in the image plane of L_3. A plane at distance ℓ from the source image is in the far field of that image plane.

Launch numerical aperture is calculated from the pattern width in the far-field plane and the value of ℓ. The pattern width is measured by placing a small aperture in front of a detector and sweeping the combination in the plane at distance ℓ from the source image.

The pattern measurement is difficult because the edges are not sharp and the corners are rounded. One source of distortion of the pattern is a $(\cos\theta)^4$ variation owing to simple geometry, as follows. Assume that the radiance at the source image is N. The incremental power at ds', in the far field, is

$$dP = N\ ds\ \cos\theta\ d\Omega, \tag{40}$$

where

$$d\Omega = \frac{ds'\ \cos\theta}{(\ell/\cos\theta)^2}. \tag{41}$$

Taking

$$N = \begin{cases} N_0 = \text{constant for } \theta \leq \theta_{LNA} \\ 0 \text{ for } \theta > \theta_{LNA} \end{cases}$$

$$dP = \frac{N_0 \, ds \, ds' \, (\cos\theta)^4}{\ell^2}. \qquad (42)$$

For ℓ large with respect to source image, the power pattern seen by a pinhole detector is then

$$P = P_0 (\cos\theta)^4 \qquad (43)$$

where P_0 is the on-axis value, which depends on N_0, ℓ, and source size. The pattern is invariably rounded at the edges, because of this $(\cos\theta)^4$ function [19]. For small values of LNA, a binomial expansion of $(\cos\theta)^4$ yields an expression for P(y)/P(0), where y is the rectangular coordinate perpendicular to the optical axis in the plane of measurement:

$$\frac{P(y)}{P(0)} = \left[\frac{1}{1 + (\frac{y}{\ell})^2}\right]^2. \qquad (44)$$

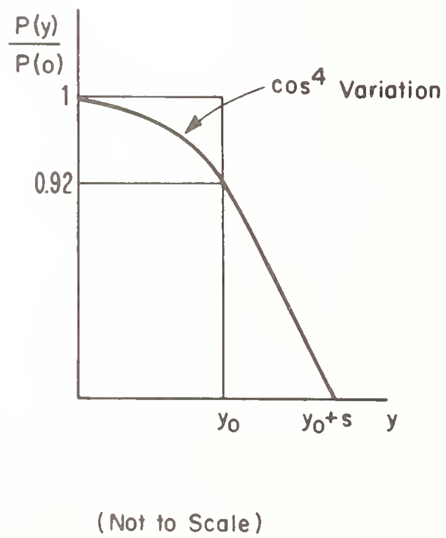

Figure 19. Illustrating the distortion of the pattern edge owing to the $(\cos\theta)^4$ variation.

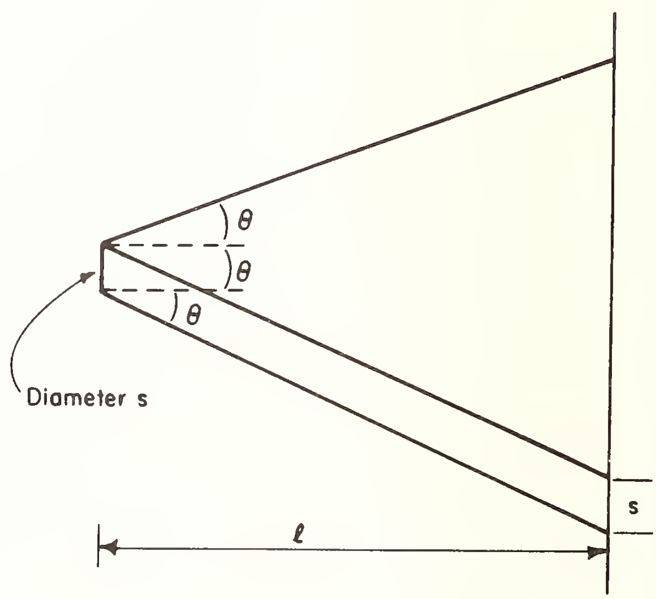

Figure 20. Showing the geometry and angles which cause the skirt shown in figure 19.

Table 1.

f/# or aperture diameter d	Pattern width at 10% points (mm)	LNA
f/# = 1.4	3.72	0.34
f/# = 2.0	2.67	0.25
f/# = 2.8	1.95	0.19
f/# = 4.0	1.41	0.14
d = 3.13 mm	1.42	0.14
d = 6.23 mm	2.89	0.27

The maximum value of y/ℓ of interest is y_0/ℓ

$$\frac{y_0}{\ell} = \tan(\sin^{-1} \text{LNA}). \tag{45}$$

For LNA = 0.2, $P(y_0)/P(0)$ is 0.92 at the edge of the pattern, as shown in figure 19. The pattern measured is further distorted because of the finite size of s (fig. 20), which causes the skirt shown in figure 19. The far-field criterion is therefore

$$\ell \gg \frac{s}{2(\text{LNA})}. \tag{46}$$

For a fiber having a 50 μm core diameter and 0.2 numerical aperture,

$$\ell \gg 125\ \mu\text{m}$$

is required.

Table 1 gives the measured values of LNA taken 5 mm from the focal plane. LNA can be changed by changing either the iris diaphragm of the lens L_3 or by placing an aperture in front of L_3 with its diaphragm open. Both techniques were used. The lens diaphragm consists of leaves which mesh together to only approximate a circular aperture. The aperture placed in front of the lens is circular. However, there was no discernible difference in the far-field patterns of the two openings.

The first column of table 1 gives the f-number setting of the lens when the lens diaphragm was used to restrict LNA. Lens L_3 has a 12.5 mm focal length. When the f-number setting is 4, then, the diaphragm opening is 3.13 mm. The fourth and fifth rows of the table should be the same. The measured values of LNA do agree to within the measurement precision.

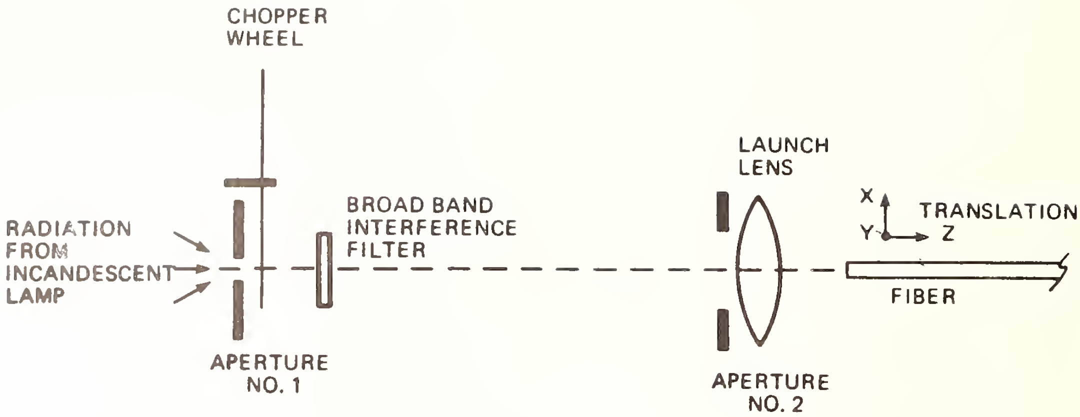

Figure 21. Launch apparatus used to measure near field and far field of fiber.

Arbitrary values of LNA can be obtained by adjusting the iris diaphragm on L_3. This was verified by requiring and obtaining LNA = 0.22. The technique is based on the fact that LNA varies linearly with aperture A_2 if the angles are small. In this case, the widths given in table 1 were used as the starting points. The aperture was adjusted while observing the intensity on a strip chart recorder. Proportional change of pattern width yielded a proportional change of LNA.

Measurements verify that LNA is independent of spot size. There was no discernable difference in measured LNA for a three-fold change of spot size.

3.2 Mode Filter Qualification

Figures 21 and 22 show the launch optics and the measurement apparatus used to qualify the mode filter used in the attenuation measurements [20]. A broadband interference filter is used (fig. 21) to improve signal-to-noise ratio. The 10 nm filters used in the attenuation measurement do not provide adequate signal level for reliable measurements; the filter used here has an approximately 80 nm spectral linewidth. The measurements are relatively insensitive to wavelength, so the increased linewidth does not affect the interpretation of results. More will be said of this later. Aperture 1 determines launch spot size and aperture 2 controls LNA, as before. The fiber is overfilled for these measurements so the launch conditions are not critical. Alignment is straightforward and based on the criterion of maximum signal. The chopper frequency is set at about 45 Hz. The pattern is measured by using a fixed fiber end and a detector that moves along an arc about the center of the fiber end.

The fiber passes through a cladding mode stripper consisting of two 10-cm long felt pads wetted with index-matching fluid. Any buffer coatings are removed from this part of the fiber. Near-field scans have shown that this type of mode stripper effectively removes light from the cladding.

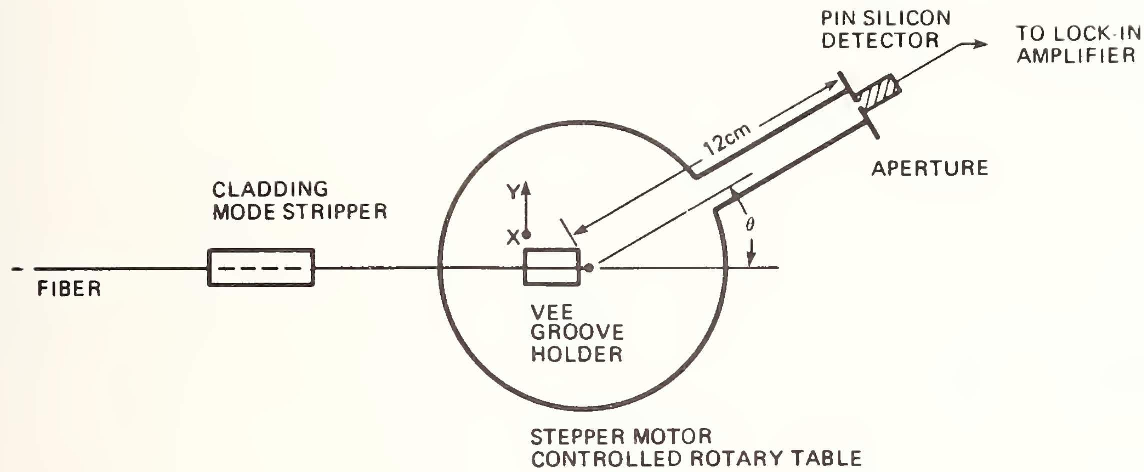

Figure 22. Apparatus used to measure fiber far field. The fiber end is fixed and the detector moves along an arc.

A vee groove positions the fiber to be coincident with the axis of rotation. A small, felt-padded weight holds the fiber in the groove. Before measurement, the fiber end is visually inspected for flatness and perpendicularity. The vee-groove position can be adjusted by a two-dimensional translation stage to assure proper alignment.

Scanning is accomplished with a stepper-motor-controled rotary table, which swings the detector through a 12-cm radius arc. At this distance the far-field criteria is satisfied for core diameters of 100 µm or less. Angular motion (1/2 arc min per step) is fine enough to give smooth far-field curves. Detector aperture size is chosen to give reasonable compromise between resolution and signal-to-noise ratio; the 0.8 mm diameter aperture gives a resolution of 0.38°. A simple one-dimensional model based on a parabolic-shaped far-field pattern with an NA of 0.2 predicts an error of 1.6 percent in radiation angle when the curve is acquired with 0.38° resolution. Measurement precision for determining radiation angle is in the range of 1 to 2 percent when a new output end is prepared and realigned; therefore, a reduction in aperture size would not result in much improvement.

A silicon PIN diode operating in the photovoltaic mode is used as the detector. The detector has an active area of 5.1 mm^2 and a built-in operational amplifier, and is mounted directly behind the aperture. A time constant of 0.4 s is used on the lock-in amplifier. The scanning rate is chosen so one resolution element (0.38°) is scanned in approximately three time constants. At this rate, a far-field pattern is obtained in 3 to 4 min.

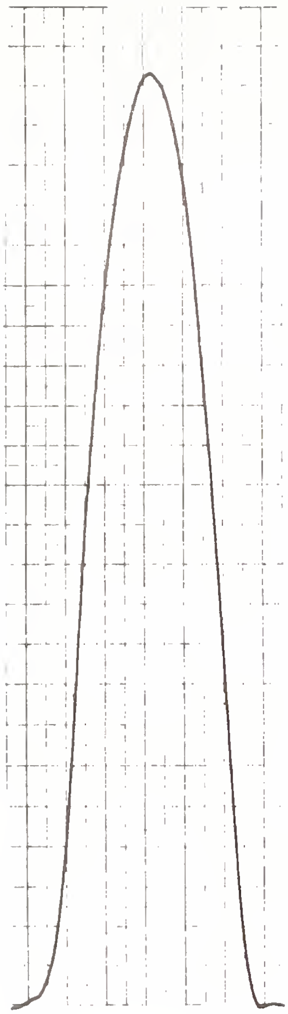

Figure 23. Far-field pattern of test fiber 7502 at 850 nm.

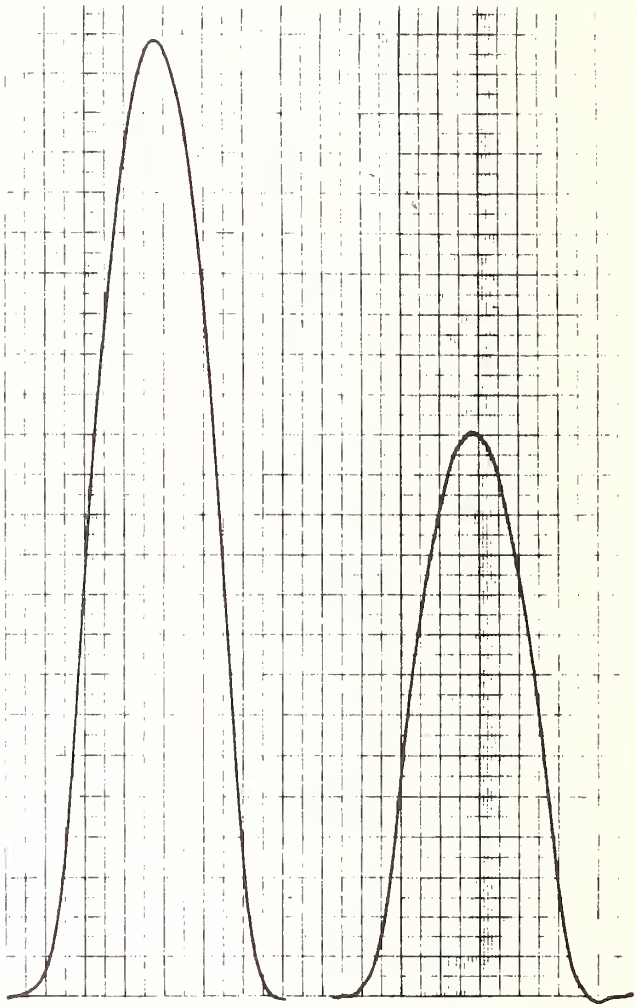

Figure 24. Far-field pattern of reference fiber 7502 with mode filter at 850 nm (left) and 1060 (right).

The output numerical aperture of a fiber is relatively insensitive to wavelength [21] for the range of interest here. Insofar as this is true, the mode filter need not be requalified for a change of wavelength. To verify this important assumption, a mode filter was qualified at 850 nm and then tested at 1060 nm. The resulting far-field patterns are shown in figures 23 and 24. There is virtually no difference in the pattern widths. Unfortunately, the signal-to-noise ratio decreases at 1060 nm, making the graph more difficult to read.

If the differential mode attenuation changes with wavelength, the far-field pattern is a function of wavelength. Indeed, any change in the modal power distribution will produce a change in the far-field pattern. If the differential mode attenuation (DMA) is a function of wavelength, a mode filter that is adequate at 850 nm, may not be so at 1300 nm.

Table 2.

Indicated full-scale voltage	1000	$1000/\sqrt{10}$	100	$100/\sqrt{10}$	10	$10/\sqrt{10}$	1
Measured full-scale voltage (1000 mV range as reference)	1000	317.2	100.3	31.71	10.03	3.165 ±0.01	0.992 ±0.01
Offset (%)		0.3	0.3	0.3	0.3	0.1	0.8

3.3 Component Linearity

Potential nonlinearities exist at the detector and at the lock-in amplifier/digital voltmeter. Because the reference detector and electronics operate at essentially the same signal levels during measurements on the long and short fibers, nonlinearities in those devices are not likely.

Silicon PIN photodiodes are generally found to be linear at power levels of interest ($\leq$ 10 μW total power). The silicon device used here had previously been calibrated against a calorimetric standard at 1 μW and 1 mW with an apparent difference in responsivity of not more than 0.8 percent.

The linearity of the lock-in amplifier/digital voltmeter combination was determined by comparison with a precision inductive voltage divider. The scale factor for individual scales was constant to 0.1 percent (peak to peak) or better from 3 to 100 percent of full scale for each of the scales most often used, increasing to about 0.9 percent (peak to peak) for the most sensitive scale used and to 3 percent for the most sensitive scale on the instrument. Relative offsets between ranges were also measured and are shown in table 2.

This offset error can be avoided by making both measurements on the same scale. A slight adjustment of light power, for example, is often all that is required to insure that a scale change is not required. For our lock-in amplifier, the error encountered in the scale change is about 0.3 percent over most of the range.

3.4 System Linearity

The linearity of the system is most likely to degrade at high intensity points, if at all. System linearity was tested through judicious use of neutral density filters and adjustment of power out of the light source. The test was conducted using narrowband (10 nm) filters to avoid variabilities introduced through the spectrum shift when intensity of the light source was changed. The technique used was as follows: First, a short length of fiber was used to transmit power to the detector. A 2.5 dB filter was then inserted into the launch optics. Attenuation was measured as 2.50 dB. The filter was removed after noting the reading of the DVM (digital voltmeter). The intensity of the light source was then reduced by 2.5 dB so the DVM reading was the same without the filter as it was just before the filter was removed. This represents a new reference reading and the procedure was repeated. The process continues until signal-to-noise ratio is reduced to intolerable limits.

The underlying assumption in this approach is that the attenuation of the filter is independent of power level. Since only relatively low power levels are used, this assumption is reasonable but no attempt was made to verify it. The measurements were made without changing the scale of the lock-in amplifier. At 850 nm and over a dynamic range of 15 dB, the standard deviation of the filter loss was 0.01 dB or 0.4 percent. The results were confirmed at several wavelengths of interest. The system linearity at 1300 nm was tested over only about 7 dB of dynamic range but the results were the same.

3.5 System Noise

System noise contributes to measurement imprecision, but the level of such noise is usually low. Analysis of the expected noise follows [22]. We adopt the following notation:

A	=	measured fiber attenuation, dB
V,M	=	voltage levels at the output of the fiber and the light source monitor, respectively
S(·)	=	standard deviation
subscript s, ℓ	=	short and long fibers, respectively.

In terms of V and M, attenuation is

$$A = 10 \log \left[\frac{V_s/M_s}{V_\ell/M_\ell}\right] \tag{47}$$

and

$$S(A) = 4.34\left[\left(\frac{S(V_s)}{V_s}\right)^2 + \left(\frac{S(M_s)}{M_s}\right)^2 + \left(\frac{S(V_\ell)}{V_\ell}\right)^2 + \left(\frac{S(M_\ell)}{M_\ell}\right)^2\right]^{1/2}. \tag{48}$$

Digitizing noise in the five digit DVM establishes a level of about 10^{-4} for each of the ratios $S(V_s)/V_s$, $S(M_s)/M_s$, $S(V_\ell)/V_\ell$, $S(M_\ell)/M_\ell$. Hence,

$$S(A) \cong 0.001 \text{ dB}. \tag{49}$$

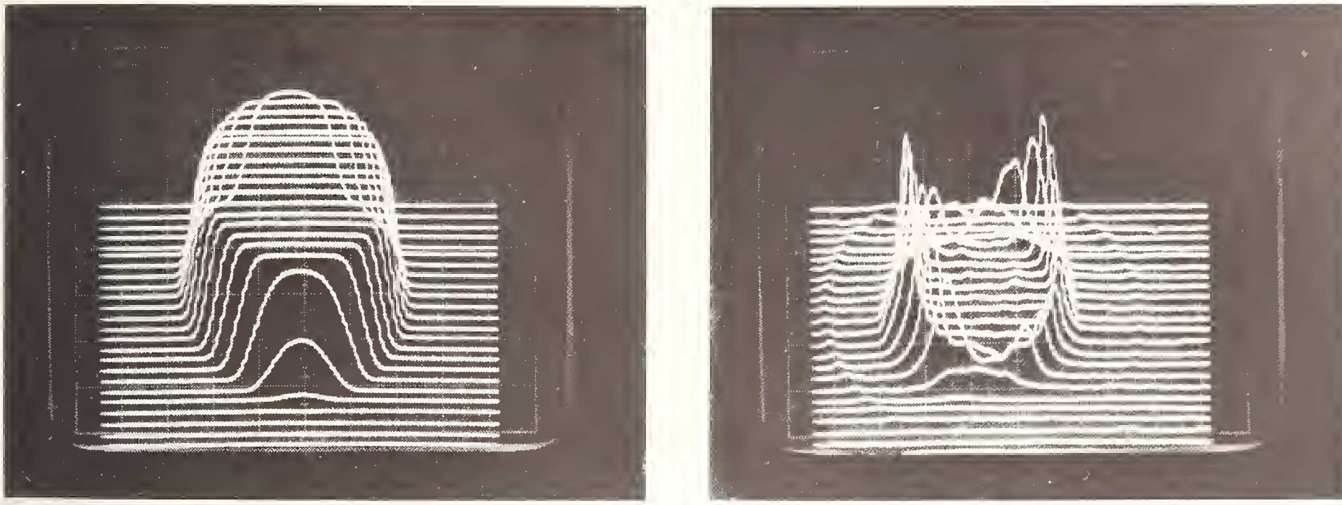

(a) (b)

Figure 25. Response of silicon (a) and germanium (b) detectors.

For high-loss fibers, $S(V_\ell)/V_\ell$ may limit the dynamic range of the system. Experience has shown, however, that such a limit is not a practical problem since telecommunication-grade fibers of interest seldom have attenuation of more than 3 to 5 dB/km.

Measurement of fibers in the laboratory yielded the following values

$$\frac{S(V)}{V}, \frac{S(M)}{M} \lesssim 5 \times 10^{-3} \text{ at } \lambda = 1300 \text{ nm},$$

$$\frac{S(V)}{V}, \frac{S(M)}{M} \lesssim 5 \times 10^{-4} \text{ at } \lambda = 850 \text{ nm}.$$

The system noise contribution to the standard deviation of the attenuation measurement is therefore about 0.001 dB at 850 nm and 0.01 dB at 1300 nm.

3.6 Detector Uniformity

Figures 25a and b show detector response over the surface of the detector. Figure 25a is silicon; figure 25b is germanium. The silicon detector exhibits uniform response, even at its edges. The germanium is uniform over the central region of its surface, but not at the edges. Use of the germanium detector therefore requires more care than does the silicon one. Avoiding the edge is only a minor invonvenience and presents no technical problems. In each case, the detector surface is about 1 cm diameter.

3.7 Measurement Procedure

The cut-back method of measuring attenuation is based on eq (3); it calls for the measurement of relative power transmitted through two lengths of the fiber under test. In the notation of eq (3), we use L_0 to refer to a short length (the reference length) of the fiber under test; L_1 is the full length of test fiber. The measurement can be performed in either of two ways. To distinguish, we will refer to the first as the two-fiber method; it is suitable for measuring attenuations of more than about 4 to 5 dB. In the two-fiber method, length L_0 is obtained, in advance of any measurements, from the test fiber. Both fibers are prepared and the two input ends are placed on a translatable bed, allowing the light source to be coupled alternatively to length L_0 or L_1, as appropriate. Both output ends are likewise coupled to the detector by placing them side by side on a bed that allows equivalent coupling conditions between the fiber and the detector. In this procedure, care must be taken to ensure that the input ends of the fiber are of similar quality. Input coupling loss can vary, leading to unreliable results if such care is not taken.

In the cut-back method, power transmitted through length L_1 is measured. Without disturbing the launch conditions, the fiber is cut at a point about 2 m from the input, thereby obtaining the reference fiber of length L_0. The cut end is prepared and the power transmitted through L_0 is measured. Equation (36) is used in either case to obtain attenuation.

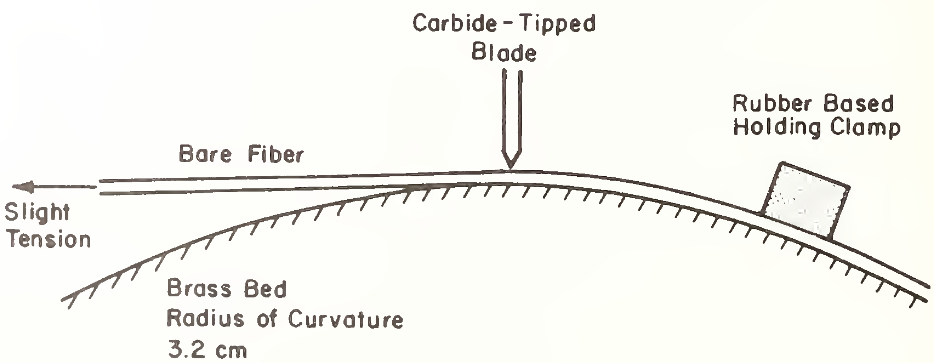

Figure 26. Method of cleaving the fiber.

Each of the methods has advantages and disadvantages. The cut-back procedure insures that the long and short lengths are excited with identical launching conditions and also involves the preparation of three rather than four high-quality end surfaces. It therefore is expected to yield better precision, especially with low-loss fibers. The two-fiber procedure, on the other hand, facilitates repeated measurements.

Systematic tests were conducted to determine the sacrifice in precision suffered in using the two-fiber method. The method may introduce as much as 0.1 dB variation in the measured attenuation unless extreme care is taken in preparing the input ends. Only then will input coupling loss be the same for the two fibers. The cut-back method introduces less than 0.03 dB variation in measured attenuation. The output coupling loss is small and is not sensitive to the quality of the cleave, at least if the cleave is reasonably good.

For either measurement method, about 10 cm of bare fiber is required on both ends to accommodate mode strippers. Fiber ends are prepared by scribing with a hand-held silicon carbide razor blade while the fiber is under tension. The method is shown in figure 26.

Cleaved ends are visually inspected for acceptability with both a 40 power and a 100 power microscope having NA = 0.12 and 0.25. Acceptance is based on a subjective evaluation of smoothness without hackle, lips, breakover or deep notches at the point of scribing, and perpendicularity. Glass chips or foreign material (dirt, jacketing material, etc.) adhering to the end are removed with adhesive tape.

Visual inspection with only one orientation can be deceptive. For this reason, the ends are examined from different angles and under different types of illumination.

The input end is mounted on the x-y-z positioner with the mode stripper in place. The launch spot and the fiber end is viewed for alignment with the vidicon and monitor. The fiber output ends are taped to a flat surface in front of the detector so the axes of the two fibers, if extended, would intersect at the surface of the large area detector. Care is taken to ensure that all the power out of the fiber is collected by the detector.

With the source aperture in place, the appropriate diaphragm set at the launch lens, and the filter wheel set, the positioner is adjusted to place the input face of the fiber at image plane of L_3. Minor axial repositioning to maximize transmitted power is done at each wavelength. When small input spot sizes are used other position criteria may be used. Increasing LNA to improve focusing resolution is sometimes useful.

The lock-in amplifier scale is selected on the basis of expected attenuation and the need to avoid scale change, if possible. The amplifier meter in our case has a decibel scale which can be used to assist in this regard. In so doing, recall that the scale measures electrical power, not volts; thus, 2 dB optical loss will be reflected as 4 dB on the electrical scale.

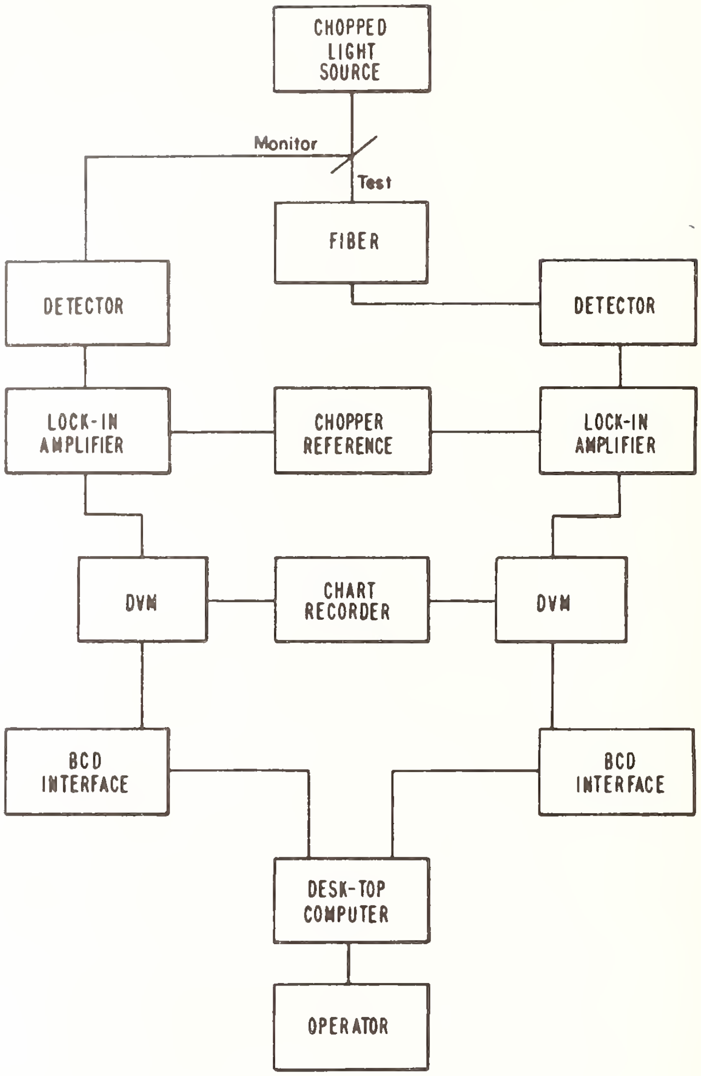

Figure 27. Block diagram of measurement configuration.

Figure 27 is a block diagram of the configuration. The operator is offered three options in the course of taking data. Each option is offered by a screen prompt followed by a computer pause. The operator must respond before the program will proceed. First, the option of monitoring the light source for drift is offered. Experience has shown that a stabilized power supply eliminates drift, so monitoring the source is not often required. If the source is monitored, a correction for drift is imposed in calculating attenuation. The correction is normally small.

Second, the operator is asked to specify the number of data points taken and the time (in milliseconds) between readings. The selected pause between readings is based on the time constant of the lock-in amplifier. The readings must, of course, be independent, which requires that several time constants elapse between readings. It is sometimes true that the signal-to-noise ratio depends on the number of time constants between readings. If so, the

Table 3.

Fiber idenfication	Wavelength (nm)	Method*	Number of measurements	Average attenuation (dB)	Standard deviation (dB)
4103	850	MF	5	2.81	0.05
4103	850	LPS	5	2.75	0.04
4103	1300	MF	3	1.62	0.04
4103	1300	LPS	2	1.65	0.02
5202	850	MF	4	1.98	0.09
5202	850	LPS	3	2.18	0.04
5202	1300	MF	3	1.03	0.01
5202	1300	LPS	3	0.92	0.02
7502	850	MF	5	5.83	0.07
7502	850	LPS	2	5.61	0.01
7502	1300	MF	6	1.85	0.05
7502	1300	LPS	3	1.59	0.01

*MF = mode filter; LPS = limited phase space

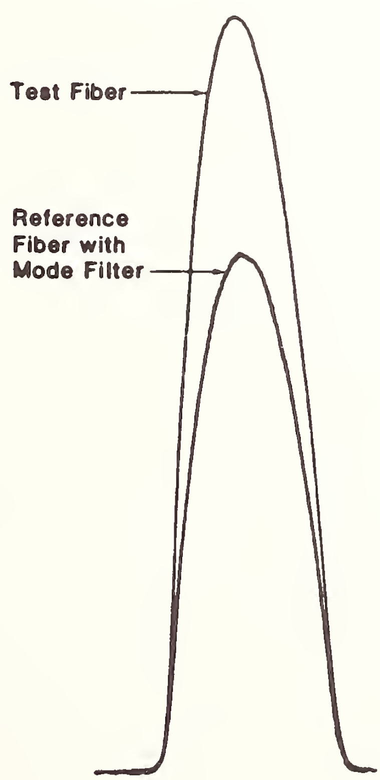

Figure 28. Typical far-field pattern of test fiber and reference fiber with mode filter at 850 nm.

selected pause is adjusted accordingly. The average reading and the standard deviation of the readings reach steady state after about 25 readings. Typically, 30 to 50 readings are taken for each measurement. The additional time consumed by taking 50 data points rather than 30 is small and leads to more confidence in the results.

3.8 Some Results

Measurement results are presented here for three telecommunication-grade fibers. Attenuation was measured at 850 nm and 1300 nm. The mode filter was qualified only at 850 nm for each fiber. Figure 28 shows the far-field patterns taken for one of the fibers. These plots are typical of those seen by the system being used here. Table 3. gives the results of the measurements of the three fibers; the measurement precision is ±0.1 dB.

The data show no clear indication of one launch condition yielding attenuation values consistently lower or higher than the other. The greatest difference encountered is about 0.3 dB on fiber 7502 at 1300 nm. In that case, the mode filter launch yields attenuation that is higher than that found using the LPS launch. Fiber 4103 has nominal length of 0.97 km, fiber 5202 is about 1.1 km long and fiber 7502 is about 2.2 km. The data for fiber 5202 was taken using a mixture of the cut-back and the two-fiber methods. The data show that the standard deviation was not adversely affected in going from one method to the other.

4. MEASUREMENT COMPARISONS AND RESULTS

The procedures discussed in this document have evolved over several years; they are based on the desire to define techniques that lead to usable and realistic predictions of attenuation in long fiber links. The procedures described are approved and sanctioned by the EIA (Electronics Industries Association), who drafted them and guided them through the approval stage.

A comprehensive interlaboratory comparison was conducted during 1980 to establish confidence and provide a definitive evaluation of the EIA procedure [23]. In the following, we discuss that interlaboratory test. The material presented here is exerpted from reference 23.

4.1 Participants and Instructions

The participants in the interlaboratory comparison included NBS and nine vendors who are members of the EIA. These included most US and some Canadian manufacturers of fiber or fiber cable. Participants were given a brief description of the physical characteristics (manufacturer's specifications) of the test fibers and special handling instructions. The following instructions were given.

For mode filter launch:

1. Overfill the test fiber in both spot size and numerical aperture, then measure the long fiber far-field radiation pattern and determine θ_1, the full width at the 5 percent intensity points.
2. Apply a mode filter to the test fiber and adjust until the far-field radiation pattern at the 5 percent intensity points from a 1.8 m length is θ_1 with a tolerance of +0, -7 percent (the current tolerance is -3 ± 3 percent). This procedure qualifies the mode filter for the attenuation measurement.
3. Apply the same mode filter to the test fiber, then measure the attenuation (mode filter is in place and undisturbed for both long and short length measurements) using a reference (cutback) length of 1.8 ± 0.1 m and some type of cladding mode stripper.

For LPS launch:

1. Use beam optics to produce a launch spot with a diameter at the 50 percent intensity points of 70 ± 5 percent of the core diameter.
2. The launch numerical aperture determined at the 5 percent intensity points shall be 70 ± 5 percent of the fiber numerical aperture.
3. Use manufacturer's numbers for core size and NA.
4. The launch spot shall be centered on the fiber core.
5. Attenuation shall be measured using a reference length of 1.8 ± 0.1 m and some type of cladding mode stripper.

In addition to a test of the restricted launch conditions, the interlaboratory tests provided an opportunity to compare the results with those obtained using an overfilled launch condition. This provided additional insight into the effect of the two launch conditions on measured attenuation. The participants were asked to measure attenuation using overfill conditions, according to the following instructions.

Overfilled Launch:

1. Use a launch spot size which overfills the fiber core.
2. Use a launch numerical aperture of 0.24 or the next larger size available to you.
3. In making the measurement, use a reference (cutback) length of 1.8 ± 0.1 m and some type of cladding mode stripper.

The test fiber parameters are given in table 4.

Table 4. Nominal properties of comparison fibers.

Fiber	Cladding O.D., μm	Core dia., μm	Buffer coating thickness, μm	Numerical aperture	Reel dia., cm	Length, km
A	125	60	170	0.24	26	2
B	125	50	70	0.16	32	2
C	125	60	70	0.18	22	2
D	125	60	thin polymer	0.20	30	0.9

4.2 Comparison Results

This interlaboratory comparison yielded data on the stability of fibers that are subjected to repeated handling and shipping. The fibers were returned to NBS and remeasured after each participant's measurement, to identify trends. One of the four fibers (fiber B) tended toward decreasing attenuation so it was retired after five participants. The one standard deviation spread for fibers A, B, C, and D was 0.06, 0.10, 0.08, and 0.10 dB/km; precision of the NBS measurement system was typically 0.1 dB/km at 850 nm, the wavelength of interest in this comparison test.

Each participant was told the fiber length and results were reported in dB/km. Participants typically used 10 m of fiber to complete all measurements and were requested to use no more fiber than needed to make two measurements of each quantity. NBS monitored the fiber length so results could be given in dB/km.

Attenuation results from 10 participants are summarized in figures 29 through 32, table 5, and table 6. A few reported values were clearly outside the dominant distributions. Of 60 reported values, 3 were eliminated as being unrepresentative. Error bars represent participants' estimates of their own system precision, plus or minus one standard deviation, based on their experience with other fibers. Average system precision for the ten participants is 0.15 dB/km. One standard deviation measurement spread is 0.24, 0.11, 0.12, and 0.43 dB/km for fibers A, B, C, and D; the average is 0.23 dB/km. Approximately two-thirds of the participants used the mode filter procedure; the remainder chose the LPS method. Mode filters included mandrel wraps, serpentine bends, and a dummy fiber. The average mode filter value minus the average beam optics value is +0.15, -0.02, -0.07, and +0.30 dB/km for fibers A, B, C, and D. In all cases these offsets are less than one standard deviation of the mode filter values by themselves. Therefore, systematic differences between the two approaches are too small to appear in the comparisons with a significant level of confidence. Greater differences between the two techniques might appear in fibers which have high differential mode attenuation. The next section gives measurement results on two fibers which have high differential mode attenuation. These data, supplied by P. Reitz of the Corning Glass Works, indicates little systematic difference between the two techniques (for these fibers) if the mode filter far-field pattern from the reference length is

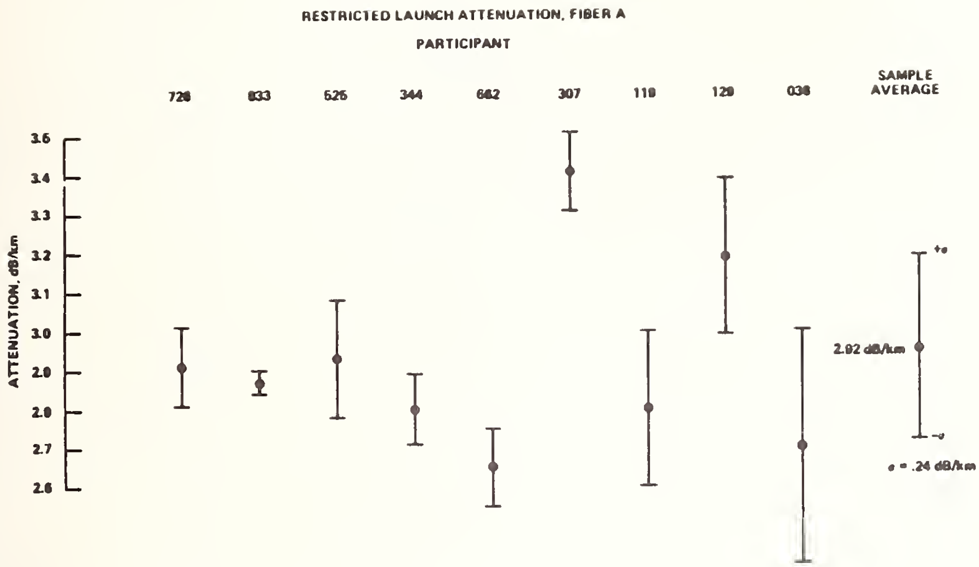

Figure 29. Results of restricted launch attenuation measurements, fiber A.

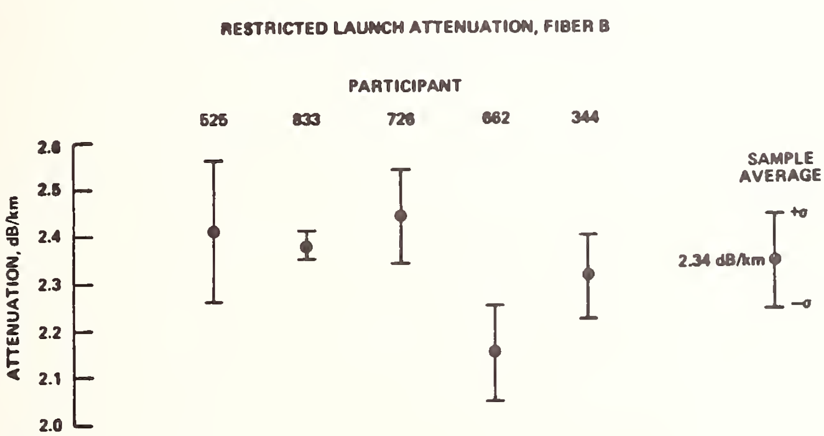

Figure 30. Results of restricted launch attenuation measurements, fiber B.

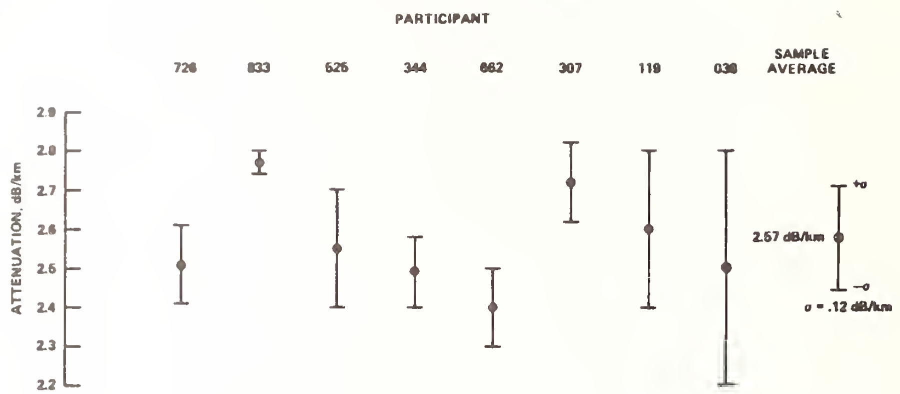

Figure 31. Results of restricted launch attenuation measurements, fiber C.

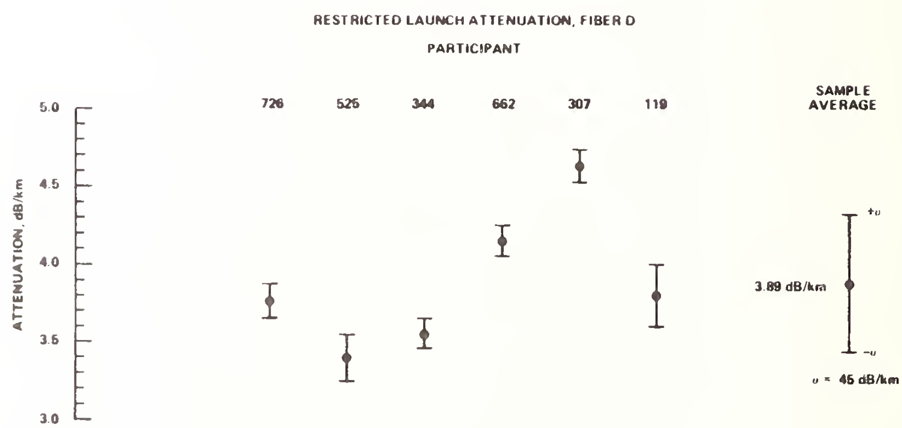

Figure 32. Results of restricted launch attenuation measurements, fiber D.

Table 5. Restricted launch attenuation, 850 nm (dB/km).

Participant	Fiber A	Fiber B	Fiber C	Fiber D
726	2.91	2.44	2.51	3.77
833	2.87	2.38	2.77	-
525	2.93	2.41	2.55	3.40
344	2.80	2.31	2.49	3.56
662	2.65	2.15	2.40	4.15
307	3.41	-	2.72	4.6
119	2.8	-	2.6	3.8
129	3.19	-	-	-
038	2.7	-	2.5	-
902	-	-	-	-
Mean	2.92	2.34	2.57	3.89
Standard deviation	0.24	0.12	0.12	0.43

Table 6. Overfilled launch attenuation, 850 nm (dB/km).

Participant	Fiber A	Fiber B	Fiber C	Fiber D
726	3.26	2.67	2.60	4.95
833	3.08	2.46	2.63	-
525	3.03	2.78	2.55	4.31
344	3.04	2.55	2.54	4.97
662	-	-	-	-
307	3.38	-	2.60	4.77
119	3.2	-	2.6	5.2
129	3.48	-	-	-
038	3.3	-	2.66	-
902	4.29	-	2.58	3.94
Mean	3.34	2.62	2.60	4.69
Standard deviation	0.39	0.14	0.04	0.47

chosen to be in the center of its allowed tolerance. (See additional comments in the following section.)

Overfilled launch results are given in table 6 for the four fibers. One standard deviation is 0.39, 0.14, 0.04, and 0.47 dB/km for fibers A, B, C, and D; the average is 0.26 dB/km. Seven participants reported initially aligning the fiber under test for peak transmitted power while two placed the fiber at the center of the launch spot; there is no significant difference between the two alignment methods for overfilled launch conditions. An earlier comparison had a 0.6 dB/km standard deviation [20]. Also, the average of the standard deviations obtained for overfilled launching conditions, 0.26 dB/km, does not differ much from the 0.23 dB/km resulting from the restricted launch.

Participants did significantly better on some fibers than on others. This may be due to differences in the DMA (differential mode attenuation) for the fibers. The smallest measurement spread is for fiber C, which exhibits almost no differential mode attenuation. The difference between overfilled and restricted launch attenuations is a measure of differential mode attenuation in a fiber; differences for the four fibers in ascending order are 0.03, 0.28, 0.42, and 0.80 dB/km for fibers C, B, A, and D, respectively. This same order occurs when fibers are listed according to increasing measurement spread. The attenuation in high DMA fibers is more sensitive to launching conditions.

Fiber D has a high OH^- concentration. The proximity of the 875 nm OH^- absorption line to the 850 nm measurement wavelength may have affected the results. For example, the slope of the spectral attenuation for fiber D at 860 nm is +0.06 dB/nm, whereas when loss is limited by a Rayleigh scattering as in C, the same slope is -0.01 dB/nm. A small positive offset from the measurement wavelength in addition to a broad source linewidth would result in a higher measured attenuation (fig. 33) (some participants reported using 20 nm source linewidths).

4.3 Attenuation Measurements in High-DMA Fibers

The largest discrepancies between the LPS or beam optics and the mode filter launch conditions occur in fibers having high DMA. This section gives results for two 1-km fibers that have higher DMA than the comparison fibers. For these fibers, attenuation differences between overfilled and restricted launch at 850 nm are 1.74 and 0.72 dB/km. Table 7 shows the difference between the LPS and the mode filter launch implemented at the mid-point and extremes of the specified tolerance on the match of far-field radiation patterns. Mode filters are specified from the far-field radiation angle at the 5 percent intensity points. If θ_L is the radiation angle produced using overfilled launching conditions to the test fiber without a mode filter, and θ_S is the radiation angle from the short (reference) length with the mode filter applied, then $\Delta\theta = (\theta_S - \theta_L)/\theta_L$. For the comparisons, the mode filters had to produce $\Delta\theta$ values between 0 and -7 percent. At both 850 and 1300 nm, the mode filter attenuation values at the tolerance extremes (0 and -7 percent) straddle the LPS values. At

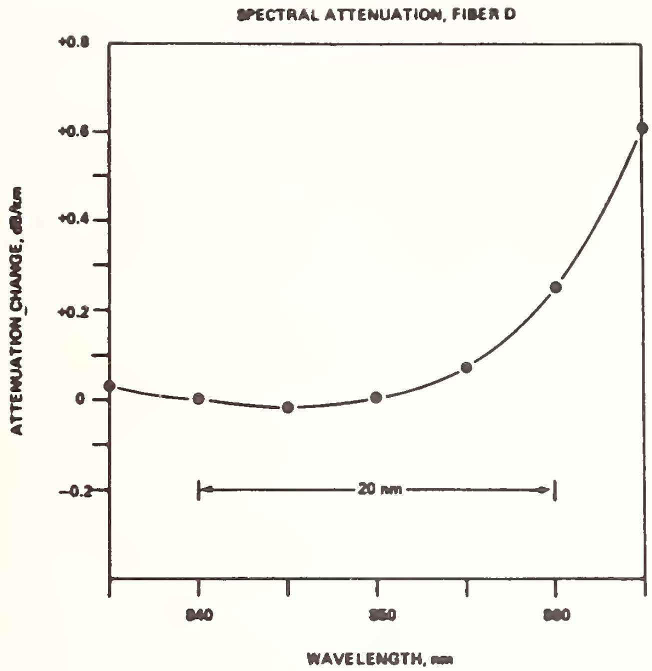

Figure 33. Spectral attenuation change with respect to the comparison wavelength of 850 nm for fiber D. An OH^- absorption line occurs at 875 nm.

Table 7. Attenuation using mode filter and beam optics launches in two high DMA fibers at wavelengths of 850 and 1300 nm (dB/km).

	Fiber #1		Fiber #2	
	850 nm	1300 nm	850 nm	1300 nm
Overfilled launch	4.16	2.97	3.25	1.74
LPS launch; 70% core, 70% NA	2.42	1.11	2.53	0.94
Attenuation difference	1.74	1.86	0.72	0.80
Mode filter attenuation - 70/70 beam optics attenuation for various values of Δ the fractional far-field radiation angle mismatch parameter				
Δ = 0	+0.16	+0.11	+0.20	+0.38
Δ = -3%	-0.05	-0.04	+0.03	+0.12
Δ = -7%	-0.27	-0.29	-0.11	-0.08

-3 percent, near the tolerance mid-point, attenuation values obtained by the two approaches are nearly the same.

The results experienced in these tests may not be typical of the results from other high DMA fibers. This is because the exact nature of DMA may be instrumental to the relationship between the LPS and the mode filter launch. Some fibers may experience high DMA among low order modes but low DMA among high order modes. For other fibers, the converse may be true. For still other fibers, high DMA may prevail only in the mid-range of modes. The results given in table 7 are not typical of the results that would obtain under these diverse conditions.

4.4 Summary of Interlaboratory Comparisons

The results described above suggest the following:

1. Measurement agreement for attenuation has improved since the last NBS-sponsored comparisons [24].
2. Uncabled fibers exhibit good stability as comparison fibers if proper attention is given to buffering and winding configuration.
3. Restricted and overfilled launching conditions for attenuation measurements yield similar standard deviations on some types of graded-index fiber.
4. The LPS and mode filter launch conditions yield nearly the same attenuation on many types of long graded-index fibers.
5. The 0.12 and 0.04 dB/km standard deviations obtained for fiber C indicate systematic differences between participants. These arise from various non-modal effects such as failure to strip cladding light, nonlinear detection, and incorrect wavelength. Systematic differences are near or less than the average claimed system precision of 0.15 dB/km. As DMA decreases in future high-quality fibers, measurement agreement is expected to improve.
6. Standard deviations on some fibers are near typical system precisions. Further improvements will require better system precisions or the use of many measurements and confidence intervals.

The authors are indebted to Dr. M. A. Holzman, Mr. A. G. Hanson, Mr. P. R. Reitz, and Dr. A. H. Cherin for constructive comments. The discussion on phase space, in particular, was revised after lengthy discussions with Mel Holzman. His help is sincerely appreciated. Finally, we acknowledge the gracious and expert editorial assistance of Edie DeWeese.

5. REFERENCES

[1] Olshansky, R.; Blankenship, M. G.; Keck, D. B. Launch-dependent attenuation measurements in graded-index fibers. Second European Conference on Optical Fibre Communication, Paris; 1976.

[2] Vella, P. J.; Abe, K.; Kapron, F. P. Precise measurement of fiber attenuation. Technical Digest, Symposium on Optical Fiber Measurements. Nat. Bur. Stand. (U.S.) Spec. Publ. 641; 1982.

[3] Personick, S. D. Time dispersion in dielectric waveguides. Bell Syst. Tech. J. 50:843; 1971.

[4] Chinnock, E. L.; Cohen, L. G.; Holden, W. S.; Standley, R. D.; Keck, D. B. The length dependence of pulse spreading in the CGW-Bell-10 optical fiber. Proc. IEEE 61:1499; 1973.

[5] Keck, D. B. Spatial and temporal power transfer measurements on a low-loss optical waveguide. Appl. Opt. 15:1882; 1974.

[6] Olshansky, R.; Oaks, S. M. Differential mode attenuation measurements in graded-index fibers. Appl. Opt. 17:1830; 1978.

[7] Olshansky, R.; Oaks, S. M.; Keck, D. B. Measurement of differential mode attenuation in graded-index optical waveguides. Technical Digest, Topical Meeting on Optical Fiber Transmission, Williamsburg; Paper TuE5; 1977.

[8] Arnaud, J. A. Beam and fiber optics (chapt. 4). Academic Press: New York; 1976.

[9] Holmes, G. T. Propagation parameter measurements of optical waveguides. In Fiber Optics for Communications and Control, SPIE Publication 224; 1980.

[10] Gallawa, R. L. On the definition of fiber numerical aperture. Electro-Optical System Design, 46; April 1982.

[11] Hanson, A. G.; Bloom, L. R.; Cherin, A. H.; Day, G. W.; Gallawa, R. L.; Gray, E. M.; Kao, C.; Kapron, F. P.; Kawasaki, B. S.; Reitz, P.; and Young, M. Optical waveguide communications glossary. Nat. Bur. Stand. (U.S.) Handb. 140; 1982.

[12] Cherin, A. H.; Head, E. D.; Lovelace, C. R.; Gardner, W. B. Selection of mandrel wrap mode filters for optical fiber loss measurement. Fiber Integ. Opt. 4:49; 1982.

[13] Agarwal, A. K.; Karstensen, H.; Unrau, U. Modal behavior of various mode mixers and mode filters for optical fiber measurements. Technical Digest, Symposium on Optical Fiber Measurements. Nat. Bur. Stand. (U.S.) Spec. Publ. 641; 1982.

[14] Reitz, P. R. Measuring optical waveguide attenuation: The LPS method. Opt. Spectra, 48; August 1981.

[15] Franzen, D. L.; Day, G. W.; Gallawa, R. L. Standardizing test conditions for characterizing fibers. Laser Focus, 103; August 1981.

[16] Technical Digest, Symposium on Optical Fiber Measurements. Nat. Bur. Stand. (U.S.) Spec. Publ. 597; 1980.

[17] Tokuda, M.; Seikai, S.; Yoshida, K.; Uchida, N. Measurement of baseband frequency response of multimode fibre by using a new type of mode scrambler. Electron. Lett. 13:146; 1977.

[18] Electronics Industries Association. Light launch conditions for long length graded-index optical fiber spectral attenuation measurement. FOTP 50; 1982.

[19] Young, M. Optics and lasers, an engineering physics approach. New York: Springer-Verlag; 1977.

[20] Kim, E. M.; Franzen, D. L. Measurement of far-field and near-field radiation patterns from optical fibers. Nat. Bur. Stand. (U.S.) Tech. Note 1032; 1981.

[21] Sladen, F. M. E.; Payne, D. N.; Adams, M. J. Definitive profile-dispersion data for germanium-doped silica fibres over an extended wavelength range. Electron. Lett. 15:469, 1979.

[22] Mandel, John. The statistical analysis of experimental data. New York: Interscience Publishers; 1964.

[23] Franzen, D. L.; Day, G. W.; Danielson, B. L.; Chamberlain, G. E.; Kim, E. M. Interlaboratory measurement comparison to determine the attenuation and bandwidth of graded-index optical fibers. Appl. Opt. 20:2412; 1981.

[24] Day, G. W.; Chamberlain, G. E. Attenuation measurements of optical fiber waveguides: An interlaboratory comparison among manufacturers. Nat. Bur. Stand. (U.S.) NBSIR 79-1608; 1979.

APPENDIX A. MODE VOLUME AND LIMITED PHASE SPACE

This appendix is addressed to the plausibility of agreement in the measured results when using the LPS and the mode-filter launch conditions. The LPS launch depends only on conditions at the input face of the fiber. The mode-filter launch is based on the far-field pattern of the fiber. Nevertheless, the plausibility of agreement is discussed in section 2.3. The subject is pursued further by examining the number of modes excited by a limited phase space launch.

The number of guided modes (M) in a heavily overmoded fiber having a power-law refractive index profile is found by integrating the normalized wave number over the fiber core and multiplying by 2 to account for the two allowed polarization states:

$$M = \frac{2}{4\pi} \int \int [k^2(x,y) - k_2^2)\, dx\, dy. \qquad \text{(A-1)}$$

Converting to circular cylindrical coordinates and assuming a power-law profile with profile parameter g:

$$k^2 = \left(\frac{2\pi}{\lambda}\right)^2 n_1^2[1 - 2\Delta(r/a)^g], \qquad \text{(A-2)}$$

$$k_2^2 = \left(\frac{2\pi}{\lambda}\right)^2 n_1^2[1 - 2\Delta], \qquad \text{(A-3)}$$

where n_1 is the refractive index at r = 0 and

$$n(r) = n_1[1 - 2\Delta(r/a)^g]^{1/2}. \qquad \text{(A-4)}$$

Consider the mode volume (the number of guided modes) between r = 0 and r = u:

$$M(u) = \left(\frac{2\pi}{\lambda}\right)^2 \frac{2\Delta\, n_1^2}{2\pi} \int_0^{2\pi} \int_0^{u} \left[1 - (r/a)^g\right] r\,d\phi\,dr. \qquad \text{(A-5)}$$

Several special cases are of interest ($V = (2\pi a/\lambda)\sqrt{n_1^2 - n_2^2}$):

Case I: $u = a,\ g = \infty$ (step index fiber) (A-6)
$M = V^2/2$

Case II: $u = a,\ g = 2$ (parabolic profile) (A-7)
$M = V^2/4$

Case III: $u = a/\sqrt{2},\ g = 2$ (A-8)
$M = (V^2/4) \cdot 3/4$

Cases I and II are well known; they imply a 3 dB loss when coupling from a step-index fiber to a parabolic profile fiber. Cases II and III are of interest to this discussion. They imply a loss of 1.25 dB in coupling a filled parabolic fiber (filled in both core size and numerical aperture) to an identical fiber through an aperture of radius $a/\sqrt{2}$, using a perfect butt joint.

This 1.25 dB loss is consistent with the concepts of LPS. To see this, note first that leaky modes should be ignored since thev were not included in the foregoing. Consider, then, eqs (2-27):

$$\frac{P_{LPS} + P_d}{P_{LPS} + 2P_d} = 3/4 \text{ (1.25 dB)}, \qquad \text{(A-9)}$$

Which agrees with eqs (A-8) and (A-7).

Chapter 2

Measurement of Optical Fiber Bandwidth in the Frequency Domain

G. W. Day

The design, evaluation, and performance of a system for determining the magnitude of the transfer function (hence, the bandwidth) of a multimode optical fiber are presented. The system operates to about 1450 MHz using a tracking generator/spectrum analyzer combination for narrowband detection. It is constructed, almost entirely, from commercially available components. The system is less complex and easier to use than an equivalent time domain system and the measurement precision is comparable. Background information on time and frequency domain specifications, fiber bandwidth limitations, and alternate frequency domain techniques is also presented.

CONTENTS

		Page
1.	INTRODUCTION	59
2.	TIME DOMAIN AND FREQUENCY DOMAIN SPECIFICATIONS: CONCEPTS AND TERMINOLOGY	59
	2.1 Time Domain Concepts	60
	2.2 Frequency Domain Concepts	63
	2.3 Correspondence Relations	66
	2.4 Specification Choices	68
3.	BANDWIDTH LIMITATIONS IN MULTIMODE FIBERS	68
	3.1 Distortion Mechanisms	68
	3.1.1 Intermodal Distortion	68
	3.1.2 Intramodal Dispersion	70
	3.2 Separation of Chromatic and Monochromatic Distortion	71
	3.3 Length Dependent Effects and Launching Conditions	73
4.	FREQUENCY DOMAIN TECHNIQUES AND SYSTEMS	74
	4.1 Systems	74
	4.1.1 Systems Using Wideband Detection	75
	4.1.2 Systems Using Narrowband Detection	75
	4.1.3 Network Analyzers	78
	4.2 Choosing a System and the Matter of Phase	78
5.	DESCRIPTION OF MEASUREMENT SYSTEM	79
	5.1 Source	79
	5.2 Mode Scrambler	82
	5.3 Launching Optics	84
	5.4 Specimens	87
	5.5 Detection	89
	5.6 Electronics	92
	5.7 Computation	92
6.	SYSTEM PERFORMANCE	94
	6.1 Measurement Procedure	94
	6.2 Precision and Accuracy	95
	6.3 Limitations	95
7.	SUMMARY	96
8.	REFERENCES	98

1. INTRODUCTION

In determining the parameters of optical fibers, measurement practice is evolving rapidly as the accumulated experience of manufacturers and users and the work of standards groups leads toward uniformly accepted techniques. This chapter is intended to describe the present design and capability of fiber measurement systems now in use at the National Bureau of Standards. These systems are perhaps representative of current practice in the industry. Many of the techniques described will also be relevant to future systems. The topic of this particular document is the measurement of fiber bandwidth as a means of specifying the maximum rate at which information may be transmitted through the fiber. In particular, it describes a frequency domain measurement system generally used to characterize graded index fibers in the 820 nm spectral region. Much of the discussion is general and can be applied to other bandwidth measurement systems.

Sections 2 and 3 are tutorial and are designed to facilitate an understanding of the later sections. Section 2 is a compilation of the concepts and terms used in the specification of the bandwidth of any transmission medium. Both time domain and frequency domain concepts and correspondence relations are included to accommodate those who may have a preference for one or the other approach. Section 3 is a review of those characteristics of fibers that determine bandwidth limitations. It is, by necessity, only a brief overview though the indicated references should be sufficient to guide the reader to more complete treatments.

Various frequency domain methods have been used for fiber characterization. Section 4 summarizes these methods and discusses some of the relative merits of each.

Section 5 describes the design of the system now in use at NBS in some detail. Section 6 describes the measurement procedure used and the quality of measurements obtained.

2. TIME DOMAIN AND FREQUENCY DOMAIN SPECIFICATIONS: CONCEPTS AND TERMINOLOGY

Most frequently, information is transmitted through an optical fiber by intensity modulating an optical carrier. The modulation may be digital, that is, in the form of discrete states, or it may be analog. In either case, the maximum rate at which information may be transmitted is determined by the way that the fiber, through various mechanisms, acts to modify or distort the modulation. In this section we discuss the different ways that these limitations may be specified, before examining the specific limiting mechanisms in section 3.

In all cases we assume that the fiber will behave linearly with respect to the <u>intensity</u> rather than the <u>amplitude</u> of the optical field. We know that this will be true for a

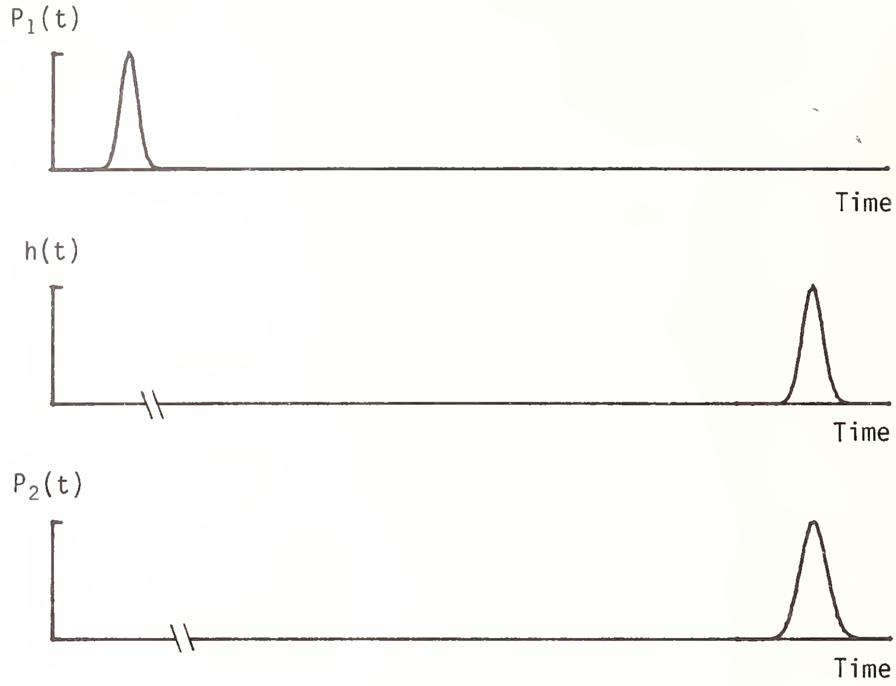

Figure 1. The output waveform of a linear system, $p_2(t)$, can be described as the convolution of the input waveform, $P_1(t)$ and the impulse response, h(t), of the system. In a transmission medium the impulse response, that is the response to an impulse at t=0, is characterized by a delay corresponding to the propagation time and distortion.

sufficiently incoherent source, that is, a source having a sufficiently broad spectral width. It will not be true for a coherent or monochromatic source. Generally the assumption of linearity in intensity is believed to be adequate when the spectral width of the source is large compared to the highest frequency components of the modulating signal [1]. As a point of reference, a 1 nm spectral width at 850 nm corresponds to a frequency range of 415 GHz.

2.1 Time Domain Concepts

With the assumption of linearity and time invariance we can relate the time dependence of the modulating signal at the output to that at the input through the convolution integral. We write

$$p_2(t) = \int_{-\infty}^{\infty} p_1(t)\ h(u-t)\ du \equiv p_1(t) * h(t), \qquad (1)$$

where $p_1(t)$ is the modulating signal applied at the input, $p_2(t)$ is the modulation observed at the output, and h(t) is the modulation waveform that would appear at the output when a modulation waveform that was sufficiently brief that it could be considered to be a true impulse was applied at the input (fig. 1). The effect of propagation through the fiber is thus completely specified through a knowledge of h(t), which is known as the impulse response of the fiber. If h(t) could be reliably determined it would therefore be a particularly well suited parameter for measurement.

As a practical matter, it is often not feasible to provide an input waveform that is of sufficiently brief duration to be considered an impulse, nor may it be possible to solve eq (1) accurately for h(t) given $p_1(t)$ and $p_2(t)$. Therefore one commonly resorts to approximate methods of describing h(t).

One common but in general highly approximate method is to use the concept of FDHM (full-duration-half-maximum) pulse-broadening. If the measured input waveform is a pulse with a FDHM of D_1, and the measured FDHM of the output waveform is D_2, then the FDHM of h(t), D_h, may be estimated by

$$D_h \sim \left(D_2^2 - D_1^2\right)^{1/2}. \tag{2}$$

The attractiveness of this approximation results from the ease with which it may be applied. Its usefulness depends on the shape of $p_1(t)$ and h(t), (and therefore on $p_2(t)$) and on their relative durations.

The approximation in eq (2) becomes an equality when $p_1(t)$ and h(t) have Gaussian time dependences. For high quality graded index fibers, h(t) frequently resembles a Gaussian shape. Therefore, if $p_1(t)$ also resembles a Gaussian, as it does in many cases of interest, the approximation may be useful, improving, of course, as D_1 is made smaller. When h(t) assumes other shapes, as for example in a step index fiber, the approximation becomes rather poor.

A better approximate method of characterizing h(t) is through an examination of its moments. The moments of a time varying function f(t) are defined as [2]

$$M_n = \int_{-\infty}^{\infty} t^n f(t)\, dt, \tag{3}$$

where n is an integer. The zeroth moment, M_0, is a simply the area under f(t). The first moment, when normalized to M_0, is known as the central time,

$$T = M_1/M_0. \tag{4}$$

The variance, which is related to the first three moments, turns out to be a particularly useful analytic tool in characterizing the impulse response approximately with a single number. It is given by

$$\sigma^2 = \frac{1}{M_0} \int_{-\infty}^{\infty} (t-T)^2 f(t)dt \tag{5}$$

$$= \frac{M_2}{M_0} - T^2. \tag{6}$$

The square root of the variance of h(t), σ_h, is known as the rms pulse broadening.

The variance possesses a very useful attribute related to the operation of convolution. It is that the variance of f(t) convolved with g(t) is exactly equal to the sum of the variances of f(t) and g(t) [2]. That is, since [eq (1)]

$$p_2(t) = p_1(t) * h(t)$$

then

$$\sigma_{p_2}^2 = \sigma_{p_1}^2 + \sigma_h^2. \tag{7}$$

Thus, if we could accurately measure σ_{p_1} and σ_{p_2} we could obtain σ_h. The usefulness of σ_h in system design has been discussed by Personick [3].

Unfortunately, for technical reasons, it is difficult to measure directly σ_{p_1} and σ_{p_2}. The variance of the impulse response and the rms pulse broadening are thus less useful means of experimentally characterizing a fiber than one might like or suppose.

Another measure of the duration of the impulse response that may be useful is its equivalent duration defined as

$$D_{eq} = \frac{\int_{-\infty}^{\infty} h(t)\, dt}{h(T)}. \tag{8}$$

D_{eq} is thus the duration of a rectangular waveform that has the same "height" as h(t) and encompasses the same area as h(t). The usefulness of D_{eq} arises primarily from a correspondence relation described in section 2.3 below; it is most useful when h(t) is even, that is symmetric, about its central time.

The relationship among σ_h, D_h, and D_{eq} for a Gaussian impulse response is shown in figure 2.

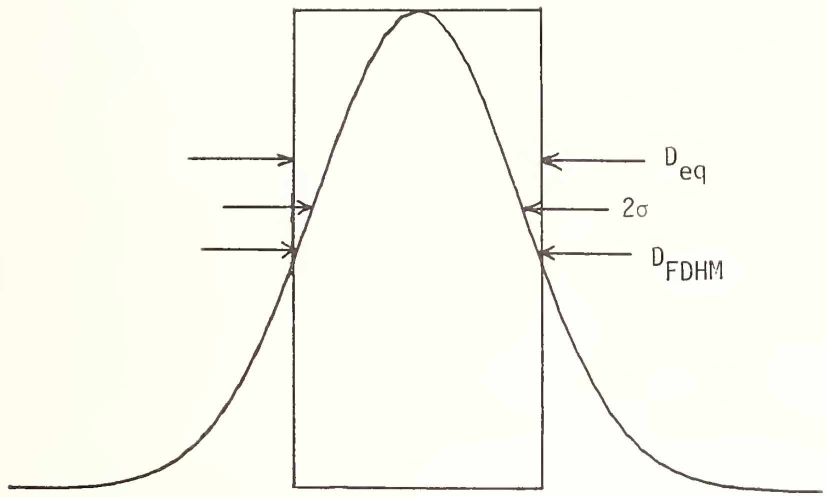

Figure 2. The relationship among three methods of characterizing a Gaussian impulse response. $D_{FDHM} = 2.33\ \sigma$; $D_{eq} = 2.48\ \sigma$.

2.2 Frequency Domain Concepts

The same conditions that allow the use of the convolution integral [eq (1)] to relate input and output waveforms allow us to develop equivalent relations in the frequency domain through the use of the Fourier transformation, or if the integrals of the waveforms are unbounded, through the Laplace transform. For this work we choose the symmetrical form of the Fourier transform pair:

$$F(f) = \int_{-\infty}^{\infty} f(t)\, e^{i2\pi ft} dt$$

$$f(t) = \int_{-\infty}^{\infty} F(f)\, e^{-i2\pi ft} df. \tag{9}$$

We use the convention that frequency domain functions are identified by upper case symbols with the corresponding lower case symbols for the corresponding time domain function.

F(f) is, in general, a complex function,

$$F(f) = \mathrm{Re}\,[F(f)] + i\,\mathrm{Im}\,[F(f)]. \tag{10}$$

Since f(t) is a real function, certain things can be said about the real and imaginary parts of F(f). In particular, F(f) is Hermitian; that is the real part is even with respect to f = 0 and the imaginary part is odd with respect to f = 0. Furthermore, if f(t) is even about t = 0, $\mathrm{Im}[F(f)] \equiv 0$.

It is frequently convenient to write F(f) in polar form,

$$F(f) = |F(f)|\; e^{i\phi_F(f)} \tag{11}$$

which is related to the rectangular form through

$$|F(f)|^2 = (\mathrm{Re}[F(f)])^2 + (\mathrm{Im}[F(f)])^2 \tag{12}$$

and

$$\phi_F(f) = \tan^{-1}\,(\mathrm{Im}[F(f)]/\mathrm{Re}[F(f)]). \tag{13}$$

The usefulness of these representations comes largely from the frequency domain analog of convolution. Specifically if eq (1) holds, then it is easy to show that

$$P_2(f) = P_1(f)\; H(f). \tag{14}$$

H(f), the Fourier transform of h(t), is generally known as the transfer function of the fiber. It is sometimes also called the frequency response, or to emphasize that $p_1(t)$ and $p_2(t)$ are modulation functions it may be called the modulation transfer function. $|H(f)|$ is known as the magnitude of the transfer function and represents the diminution that each spectral component of the input waveform suffers during propagation. $\phi_H(f)$ is known as the phase of the transfer function and represents the shift in phase angle that each spectral component incurs. With respect to $\phi_H(f)$ it is useful to define the group (or envelope) delay as

$$\tau_g(f) = -\frac{1}{2\pi}\,\frac{d\phi_H(f)}{df} \tag{15}$$

which represents the delay that the spectral components at frequency f of the envelope of p_1 incur (fig. 3). This is distinguished from the delay that individual components suffer which is known as the phase delay given by

$$\tau_p(f) = -\frac{1}{2\pi}\,\frac{\phi_H(f)}{f}. \tag{16}$$

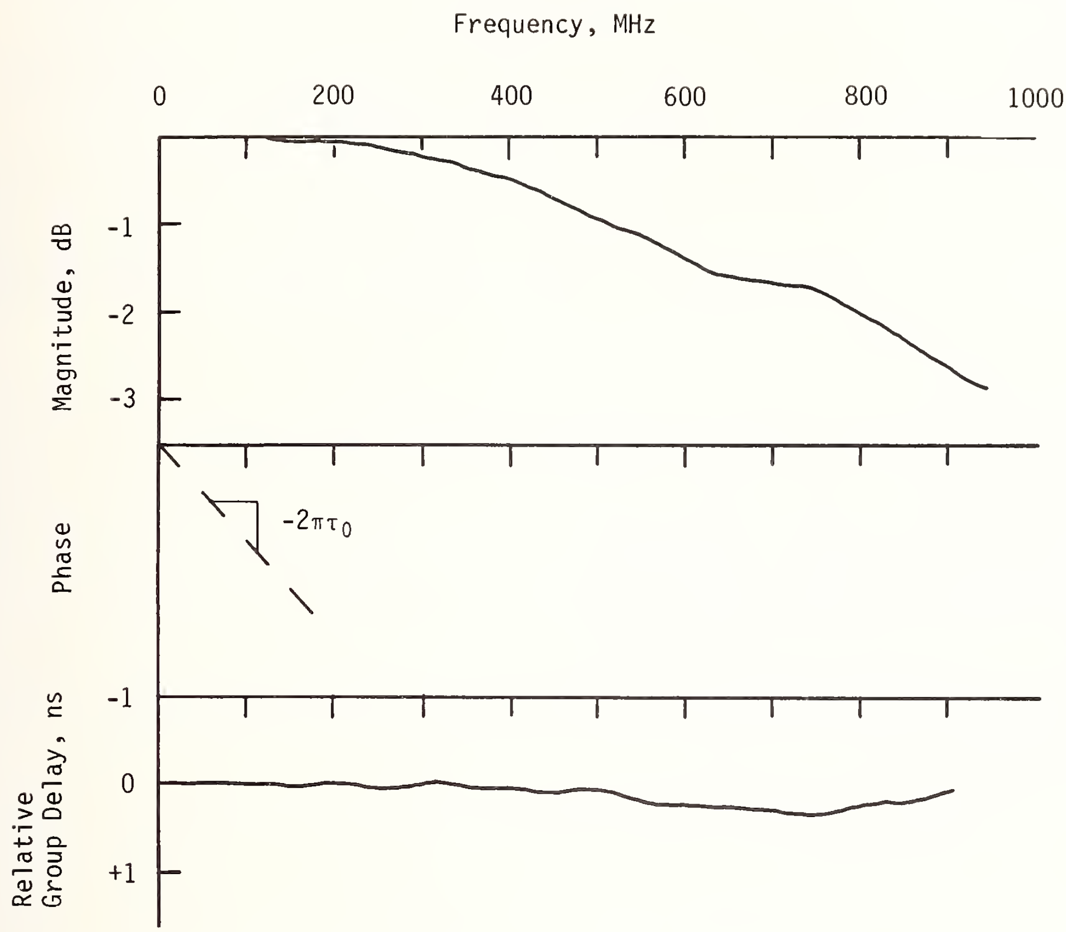

Figure 3. Characteristics of a high bandwidth fiber having an approximately Gaussian impulse response. The magnitude, if plotted linearly, would be approximately Gaussian, as well. The phase, if measured, would be nearly linear with a slope of $-2\pi\tau_0$ rad/Hz, where τ_0 is the propagation time. The group delay is nearly independent of frequency. (These measurements were taken with a developmental system similar to that shown in figure 5.)

The shift theorem states that if F(f) is the transform of f(t) then $F(f)e^{-2\pi ifT}$ is the transform of f(t-T). Therefore, when the impulse response is characterized in part by a time delay, as in the case of a fiber or other transmission medium, the phase of the transfer function contains a term linear in frequency which accounts for the distortion-free delay plus a term that represents phase distortion,

$$\Phi_H(f) = -(2\pi\ \tau_0 f + 2\pi\ \gamma(f)). \quad (17)$$

Thus the group delay in this case consists of a constant, τ_0, plus a frequency dependent term, $d\gamma(f)/df$. It is this latter term, together with $|H(f)|$, which represents the total distortion and which therefore determines the highest rates at which information can be transmitted. It may be useful to think of $|H(f)|$ as contributing a symmetric distortion and $\gamma(f)$ as contributing an antisymmetrical distortion [4].

In the time domain representation, it was noted that h(t) was a complete representation of the system. In the frequency domain it can be shown that since the system is causal (output does not begin before input) that either Re[H(f)] or Im[H(f)] is a complete representation and in fact one can be computed from the other through the Hilbert transform [2]. However, neither $|H(f)|$ nor $\gamma(f)$ is a complete representation of a system, except for those systems known as minimum phase systems. Fibers are not, in general, minimum phase systems [5].

In spite of its incompleteness, $|H(f)|$, typically normalized to its value at f = 0, is often used as the principal means of specifying a fiber. To futher reduce the characterization to a single number rather than a function it is common to indicate the -3 dB bandwidth, that is the lowest frequency at which $|H(f)| = 0.5$ or $|H(f)|_{db} = -3$ dB. Alternatively, one might choose a specification of bandwidth at another level, say -6 dB, or -1.5 dB. The latter value may be attractive since in a detector or source an electrical quantity, current or voltage, is proportional to optical power. Electrical power is thus proportional to optical power squared and $|H(f)|_{db} = -1.5$ dB corresponds to a -3 dB specification in terms of electrical power.

2.3 Correspondence Relations

In addition to the correspondence between convolution in the time domain and multiplication in the frequency domain, many other relations between time and frequency domain quantities can be derived. Some are useful for component characterization; others are not.

The similarity theorem [2] states that if f(t) has the Fourier transform F(f) then f(at) has the transform $|1/a|\ F(f/a)$. Thus, when comparing two impulse responses of identical shape, the ratio of durations at any arbitrarily defined points, say the 50 percent points, is inversely proportional to the ratio of bandwidths at an independently chosen level, say -6 dB.

The moments of h(t) can be expressed in terms of frequency domain quantities through [2]

$$M_n = \int_{-\infty}^{\infty} t^n h(t)dt = \frac{H^n(o)}{(-2\pi i)^n}, \qquad (18)$$

where $H^n(0)$ is the value of the nth derivitive of H(f) evaluated f = 0. These relations are probably not directly useful in metrology because of the difficulty in reliably evaluating $H^n(0)$. However, they do lead to what may be useful approximations.

From eq (18) and the reciprocal nature of the transform we can relate the equivalent width of the impulse response to the equivalent width of the transfer function, as follows:

$$\frac{\int_{-\infty}^{\infty} h(t)dt}{h(0)} = \frac{H(0)}{\int_{-\infty}^{\infty} H(f)\, df}, \qquad (19)$$

or somewhat more generally using the shift theorem

$$\frac{\int_{-\infty}^{\infty} h(t)dt}{h(T)} = \frac{H(0)}{\int_{-\infty}^{\infty} H(f)e^{ia\pi fT} df}. \qquad (20)$$

This expression is probably most useful where f(t) is symmetrical about T, for then the argument of the integral on the right side of eq (20) is real and equal to the transform of h(t-T).

Because of the additive property of the variance in convolution it would be desirable to usefully relate the variance to frequency domain quantities. The relation that arises from eq (18) is probably not useful for the reasons noted before. An alternate approach might be to express the transform in terms of the moments of h(t) by writing $e^{i2\pi ft}$ as a power series

$$H(f) = \int h(t) \left(1 + \frac{i2\pi ft}{1!} + \frac{(i2\pi ft)^2}{2!} + \ldots\right)dt.$$

Then

$$H(f) = M_0 + i2\pi M_1 f - \frac{(2\pi)^2}{2} M_2 f^2 + \ldots$$

and

$$|H(f)|^2 = H(f)\, H^*(f)$$

$$= M_0{}^2(1-(2\pi)^2\sigma_h{}^2 f^2 + \ldots). \qquad (21)$$

Thus one may, at least in principal, obtain σ_h by fitting $|H(f)|^2$ to a power series in f and isolating the coefficient of f^2. The practical usefulness of this approach has not as yet been explored.

2.4 Specification Choices

Given the array of parameters outlined in the above sections, it is often not clear how best to specify the information carrying capacity of a fiber. The choice undoubtedly depends on the type of fiber, the characteristics of the system in which it will be used, measurement considerations, and the experience and preference of the designer.

It is sometimes suggested that time domain specifications should be used for digital systems and frequency domain specifications for analog systems. Since the larger fraction of fiber systems will be digital, one might expect time domain specifications to dominate. Such has not been the case in industry.

In the U.S., the majority of manufacturers use time domain measurement methods but specify their product by the -3 dB bandwidth. The reasons are several. Early in the development of fiber systems it was easier to obtain suitable sources for pulsed measurements than for cw measurements. However, it is difficult, for technical reasons, to obtain an accurate impulse response or an accurate value for rms pulse broadening; hence frequency domain computations. And, perhaps more importantly, it seems to be the preference of most designers to use bandwidth specifications. In Japan, a different situation has evolved in that many manufacturers use both frequency domain specifications and frequency domain measurement techniques.

If frequency domain specifications continue to dominate, it seems likely that frequency domain measurements will grow in popularity. With presently available components, frequency domain systems are easier to construct, simpler to operate, and more direct in computation. Their precision is comparable to time domain systems on short fibers; for long fibers they offer easier signal averaging.

3. BANDWIDTH LIMITATIONS IN MULTIMODE FIBERS

3.1 Distortion Mechanisms

Regardless of general preferences for time domain or frequency domain representations, it turns out to be more convenient to consider the limiting mechanisms in the time domain, specifically as sources of variation in propagation time. These variations, which lead to waveform distortion, arise in two separable categories. One comes from differences in propagation constants between individual modes or mode groups, and is called <u>intermodal distortion</u>. The other comes from the variation in the propagation constant of individual modes with wavelength, called <u>intramodal dispersion</u>. For a non-zero source spectral width, intramodal dispersion results in additional waveform distortion.

3.1.1 Intermodal Distortion

In a step index fiber, if one assumes that the angle that a light ray makes with the axis corresponds to a particular mode designation it is intuitive that high order modes (high angle rays) will propagate more slowly than low order modes. Thus a propagating pulse will be broadened. It has long been known that by properly tailoring the refractive index distribution these intermodal differences can be minimized.

For a optical waveguide in which the maximum difference in refractive index between the core and cladding is about a percent, Gloge and Marcatilli [6] have shown how the refractive index profile may be optimized. They considered a class of profiles given by

$$n\,(r) \equiv \begin{cases} n_1\,[\,1-2\Delta(r/a)^g]^{1/2} & \text{for } r<a \\ n_1[1-2\Delta]^{1/2} \equiv n_2 & \text{for } r>a \end{cases}, \qquad (22)$$

where $n(r)$ represents the refractive index as a function of radius, n_1 is the refractive index on axis, a is the core radius, n_2 is the refractive index in the cladding and Δ is a parameter related to the difference between n_1 and n_2 given by

$$\Delta \equiv \frac{n_1^2 \;-\; n_1^2}{2\;n_1^2} \approx (n_1 \;-\; n_2)/n_1. \qquad (23)$$

The parameter g, known as the profile parameter, takes on values between 1 and ∞. As it does so one may consider a broad range of profiles from triangular (g = 1) to parabolic (g = 2) to step (g = ∞).

Analysis of these profiles shows that the duration of the impulse response is a function of g and Δ. In particular, under the assumption that $n(r)$ is independent of wavelength, it was shown [6] that for a particular value of g given by

$$g_{opt} = 2 - 2\Delta \qquad (24)$$

the duration of the impulse response goes to zero.

Olshansky and Keck [7] have extended the work of [6] to include the variation in refractive index with wavelength. They give an approximate expression for the rms duration of the impulse response due to intermodal effects as follows:

$$\sigma_{INTER} \approx \frac{LN_1\Delta}{2C}\;\frac{g}{g\,+\,1}\;\frac{g\,+\,2}{3g\,+\,2}\;\left|\;\frac{g\,-\,2\,-\,P}{g\,+\,2}\;\right|, \qquad (25)$$

where

$$N_1 \equiv n_1 \,-\, \lambda\,\frac{dn_1}{d\lambda} \qquad (26)$$

is known as the material group index and P, sometimes known as the profile dispersion parameter, is given by

$$P = -2 \frac{n_1}{N_1} \frac{\lambda}{\Delta} \frac{d\Delta}{d\lambda}. \qquad (27)$$

From eq (25), g_{opt} is seen to be

$$g_{opt} = 2 + P \qquad (28)$$

or, from a more exact version of eq (25) [7],

$$g_{opt} = 2 + P - \Delta \frac{(4+P)(3+P)}{(5+2P)}. \qquad (29)$$

For P = 0, eq (29 is approximately equal to eq (24).

In any case, it is apparent from eq (25) and (29) that even though P is small, its effect can be to make σ_{INTER} and hence the fiber bandwidth a strong function of wavelength, particularly when the fabrication of the fiber is such that $g \approx g_{opt}$. Several authors [8] have studied the variation in the intermodal distortion with wavelength experimentally and have observed large variations.

3.1.2 Intramodal Dispersion

To understand the broadening that occurs within a single mode it is necessary to identify those parameters that determine the velocity of propagation of a mode. Consider the effective phase index of a mode, $n_{\mu\nu}$, which is the ratio of the speed of light in vacuum to the phase velocity of the mode. For each mode $n_{\mu\nu}$ varies between n_1 at short wavelengths (far above cutoff) where the power is confined near the axis to n_2 at cut-off where the power propagates through the cladding. For a specific mode, $n_{\mu\nu}$ depends on the core radius, the wavelength explicitly, and on $n_1(\lambda)$, $\Delta(\lambda)$, and $g(\lambda)$. That is,

$$n_{\mu\nu} = f(a, \lambda, n_1, \Delta, g). \qquad (30)$$

It should not be inferred from this relation that the dependence of $n_{\mu\nu}$ on these parameters is separable. However, it is usual to identify the dependence on a/λ, which would be present even if the waveguide were composed of dispersion-free glass, as waveguide dispersion. Then $n_1(\lambda)$ is said to give rise to material dispersion, $\Delta(\lambda)$ to profile dispersion, and $g(\lambda)$ to what might be called profile parameter dispersion.

For those modes farthest from cut-off

$$n_{\mu\nu} \rightarrow n_1(\lambda). \qquad (31)$$

We therefore expect that material dispersion will be the dominant contributor to intramodal dispersion except perhaps near where $dn_1/d\lambda = 0$.

In the limit of expression (31) the velocity of propagation (both phase and group) approaches that of a plane wave in a medium of refractive index $n_1(\lambda)$. The propagation constant in that case is $\beta = 2\pi n_1(\lambda)/\lambda$. The time for a pulse to propagate a distance L is

$$\tau_{\mu\nu} = \frac{L}{v_g} = L\frac{d\beta}{d\omega} = \frac{L}{c}\left(n_1 - \lambda\frac{dn_1}{d\lambda}\right) \equiv \frac{L}{c}N_1, \tag{32}$$

where v_g is the group velocity and N_1 is the material group index as stated earlier.

The intramodal pulse broadening then becomes

$$\sigma_{INTRA} \approx \sigma_{Material} = \sigma_s\frac{d\tau_{\mu\nu}}{d\lambda} = \sigma_s\frac{L}{c}\frac{dN_1}{d\lambda}$$

$$= -\sigma_s\frac{L}{c}\frac{d^2n_1}{d\lambda^2} \equiv -\sigma_s LM, \tag{33}$$

where $\sigma_{material}$ is the rms pulse broadening due to material dispersion, σ_s is the rms spectral width of the source, and M is known as the material dispersion parameter.

For most glasses M is zero at a wavelength near 1.3 μm. At shorter wavelengths it is positive and at longer wavelengths negative. M is not a strong function of glass composition. At 800 nm its value for most glasses falls in the range of 120-150 ps/nm•km and at 900 nm, 70-90 ps/nm•km.

3.2 Separation of Chromatic and Monochromatic Distortion

With regard to measurements, the most important aspect of the above discussion is the extent to which the total distortion or bandwidth depends on the spectral characteristics of the source. Because the material of which the fiber is composed is dispersive, both σ_{INTRA} and σ_{INTER} depend on wavelength. Further, σ_{INTRA} is proportional to the spectral width of the source (σ_s). Within the limits of the analysis σ_{INTER} is independent of σ_s. The problem, then, is in interpreting measurement results.

The variation of intermodal pulse broadening with wavelength is not readily predictable. It is thus difficult to use measurements at one wavelength to design a system that will operate at another wavelength. Appropriate sources are available over most of the range at which systems are likely to operate but economic considerations generally preclude routine spectral bandwidth measurements.

The dependence of bandwidth on source spectral width generally causes greater difficulty in measurements. It is usually not possible to choose a source for measurement that will have the same spectral line shape as will be found in the system in which the fiber will ultimately be used. It is also difficult to accurately separate chromatic and monochromatic effects in a measurement result that depends significantly on both.

Usual practice therefore is to set limits on the spectral width of the source used for measurements so that one or the other effect dominates. The focus is usually on intermodal effects since they vary much more between fibers and since in most systems they represent the limitation.

If the total distortion can be written as the convolution of the "intermodal impulse response" with the "intramodal impulse response" we can write

$$\sigma_h^{\,2} = \sigma^2_{INTER} + \sigma^2_{INTRA}. \qquad (34)$$

We may decide arbitrarily that intermodal effects dominate whenever

$$\sigma^2_{INTRA} \equiv \sigma_s^{\,2}\, M^2\, L^2 \leqslant 0.21\, \sigma_h^{\,2}, \qquad (35)$$

that is, whenever intramodal effects account for no more than ten percent of a measured σ_h. This leads to

$$\sigma_s^{\,2} \leqslant \frac{0.21\, \sigma_h^{\,2}}{M^2\, L^2}\,. \qquad (36)$$

If the source line shape and the impulse response are both reasonably modelled as Gaussians, eq (36) may be rewritten as

$$\Delta\lambda < \frac{0.2}{|M|\, L\, f_{-3dB}}\,, \qquad (37)$$

where $\Delta\lambda$ is the FWHM (full-width-half-maximum) of the source spectrum and f_{-3dB} is the frequency at which the measured transfer function equals -3 dB.

Table 1. Values of the parameter $0.2/|M|$ for a germanium-phosphorus-doped silica fiber [10]. Gaussian impulse response shapes and Gaussian pulse shapes were assumed to generate these data.

λ(nm)	0.2/|M| (GHz km nm)	λ(nm)	0.2/|M| (GHz km nm)
800	1.6	1200	18.
820	1.7	1250	42.
840	1.9	1300	220.
860	2.1	1340	40.
880	2.3	1510	11.
900	2.5		

Equation (37) has been used by standards committees [9] as a necessary condition for a valid measurement of "intermodal bandwidth". As indicated in section 3.1.2, M is a fairly weak function of glass composition but a strong function of wavelength. Table 1 gives the quantity $0.2/|M|$ for a germanium-phosphorus-doped silica fiber [10]. From this data one concludes, for example, that to measure a 1 km-long fiber having a 1 GHz bandwidth at 850 nm a source spectral width of less than 2 nm is required. In the longer wavelength region a much greater source spectral width could be used.

3.3 Length Dependent Effects and Launching Conditions

In multimode fibers several mechanisms act to render the fiber bandwidth a nonlinear function of length. These effects can make the interpretation of data very difficult.

Certain non-ideal characteristics of a fiber result in power being coupled between modes, an effect known as mode coupling or mode mixing. The transfer of power from modes with low group velocities to those with high group velocities and vice versa means that fiber bandwidth will decrease more slowly with length than would otherwise be the case. The actual functional dependence frequently falls in the range of $L^{-1/2}$ to L^{-1}, depending on the degree of mode coupling present [11].

Mode coupling may arise from defects introduced during manufacturing; for example, variations in diameter or index profile with length. Mode mixing also arises from bending of the fiber, particularly from bends that have spatial periods of the order of a millimeter. This means that the manner in which a fiber is cabled or handled can have a major effect on a bandwidth measurement. Particular care is required in the measurement of unbuffered fiber wound tightly on a spool.

Differential modal attenuation can also cause fiber bandwidth to be a nonlinear function of length. If high order modes of the fiber are excited and if, as is frequently the case, these modes suffer from higher attenuation than low order modes, then the rate at which bandwidth decreases with length is likely to be greatest near the input, where the complete range of mode groups is encountered.

The combined effects of mode coupling and differential modal attenuation may result in a complex functional dependence of bandwidth on length. For example, when both effects are important the bandwidth has been observed to decrease as L^{-1} near the input, progressing gradually to perhaps $L^{-1/2}$ after a substantial distance [12], and stabilizing at that value. Such a condition, where the functional dependence of bandwidth on length is stable, is sometimes known as modal equilibrium because it occurs when the distribution of power among the modes changes no further with length. The attenuation coefficient presumably becomes independent of length in this case, as well.

Another factor that effects the dependence of bandwidth on length is variations in index profile. If, in attempting to produce a fiber in which the group velocities of all modes are equal, some parts of the fiber are overcompensated* and other parts are undercompensated, equilization occurs.

This leads to a higher bandwidth than would otherwise be expected and to a very complex variation of bandwidth with length. Such variations in the degree of compensation frequently appear between fibers joined together in a link, and make the prediction of system performance difficult.

All of the problems described above make the choice of launching conditions for bandwidth measurements very difficult. Until such time as better methods of describing the variation of bandwidth with length are found it is probably wisest to simply choose measurement (launching) conditions that are well defined and easy to verify and which therefore may be expected to yield reproducible results. Certain standards groups [9] have therefore suggested that bandwidth measurements be made in such a way that all the modes of the fiber are excited. This means that light should be coupled into the fiber over the full area of the core and over a range of angles as large as the acceptance angle of the fiber. These are the criteria generally adopted in this chapter.

4. FREQUENCY DOMAIN TECHNIQUES AND SYSTEMS

Many techniques have been developed for the characterization of rf components in the frequency domain and instruments and devices for use in these measurement systems are widely available. With care, much of this same technology can be applied to the characterization of optical fibers. This section provides a survey of several potentially appropriate measurement methods, one of which has been extensively evaluated and is described in detail in subsequent sections.

4.1 Systems

It may be useful to separate frequency domain techniques into two groups: those that use wideband rf detection and those that use narrowband rf detection. Wideband detection generally leads to a simpler and less expensive measurement system but suffers from a lack of harmonic rejection and may give inferior noise performance. Narrowband detection is more complex but provides freedom from distortion, an important consideration when the system includes lasers or LEDs.

*A properly compensated fiber is one in which the group velocities of all modes are the same. Overcompensation is the case where low order modes propagate more slowly than higher order modes (in the power law representation, $g<g_{opt}$). Undercompensation is the opposite case.

4.1.1 Systems Using Wideband Detection

One of the simplest systems that might be used is shown in the block diagram of figure 4. An rf sweep generator provides a controlled input signal, the frequency of which can be varied or swept over the range of interest. This signal is applied to the system under test, which in the case of a fiber would include the optical source and detector. The output rf signal is detected by a wideband, linear (in power) rf detector. If the signal-to-noise ratio is not an important consideration this arrangement may be sufficient to determine the magnitude of the transfer function by comparing the ratio of output-to-input signal level as a function of frequency with the test system in place to the same ratio with it removed. If the losses in the test system are large, the signal-to-noise ratio can be improved by amplitude modulating the input at a low frequency and using a lock-in amplifier as shown.

Probably the greatest difficulty in using this system for fiber measurements is that most suitable optical sources introduce harmonic distortion to the signal. With typical sources this problem may be sufficient to result in a several percent error in the transfer function (see section 5.1).

A variation of the system shown in figure 4 that allows the determination of group delay as well as transfer function magnitude [13] is shown in figure 5. In this case, the input is amplitude modulated at a relatively high frequency--perhaps 10 MHz for a sweep range from 30 MHz to 1.5 GHz. The output of the rf detector then goes into a vector voltmeter which gives the ratio of the output (envelope) magnitude to input magnitude and the phase shift in the envelope. The group delay (section 2.2) is related to this phase shift by the relation [13]

$$\tau_g = \frac{\phi_e}{360\ f_m},$$

where ϕ_e is the phase shift in the envelope, in degrees, and f_m is the modulation frequency.

This is probably the simplest method of obtaining phase data on a fiber. It has been used by the author to evaluate several fibers and except for the problem of harmonic distortion works quite well.

4.1.2 Systems Using Narrowband Detection

The wide choice of detection bandwidth, gain, sweep rate, averaging, etc. generally available in commercial rf spectrum analyzers make that instrument a good choice for the detector in systems using narrowband detection (fig. 6). To fully exploit its capability, however, it must be used with a signal source that is frequency locked to the local oscillator of the spectrum analyzer. Thus, the source output frequency will vary coincidentally with the sweep of the spectrum analyzer. Such sources, known as tracking generators, and designed for use with specific spectrum analyzers are available from several manufacturers.

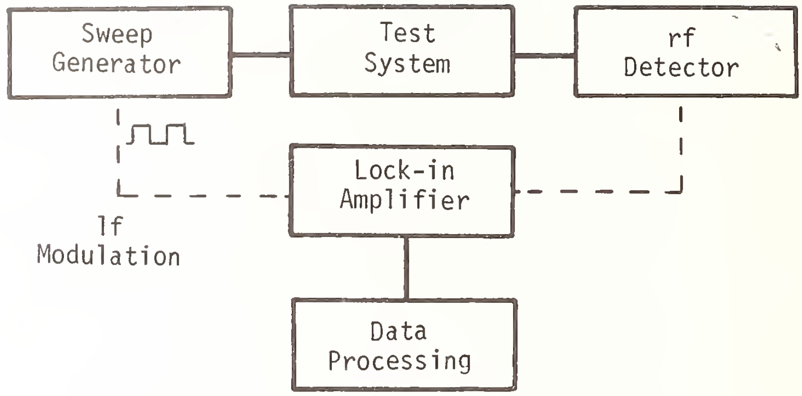

Figure 4. Block diagram of a simplified frequency domain measurement system. When the signal-to-noise ratio is high, the lock-in amplifier may not be necessary.

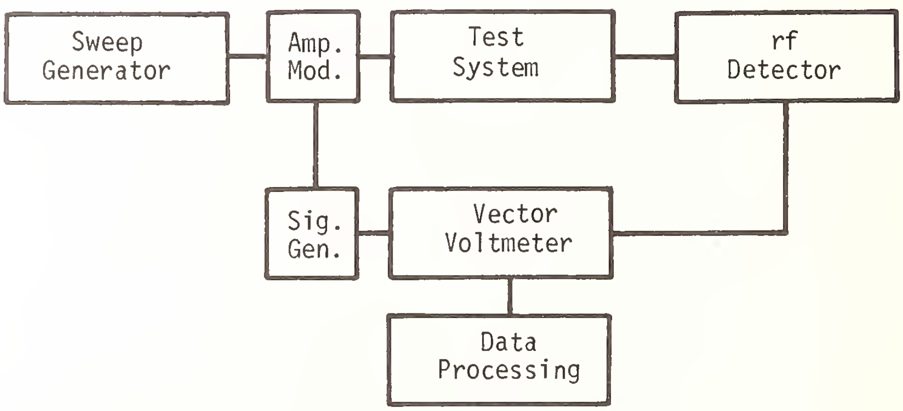

Figure 5. A modification of the system of figure 4 which allows both magnitude and group delay measurements. The signal generator operates at a relatively high frequency and the vector voltmeter determines both the magnitude and phase of the input and output modulation envelopes.

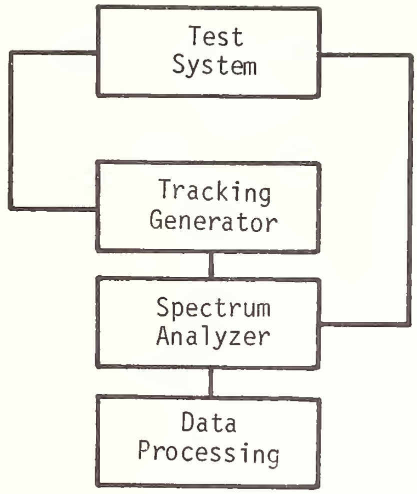

Figure 6. A simplified frequency domain system using narrowband detection. This arrangement forms the basis of the system described in detail in section 5.

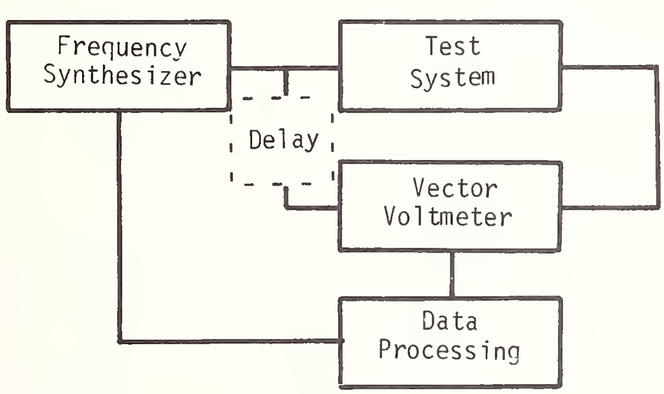

Figure 7. A narrowband system that can provide phase information. The system works best if a compensating delay is inserted in the reference channel of the vector voltmeter.

The system bandwidth is generally limited by the degree to which the lock between the tracking generator and spectrum analyzer can be maintained. The simplicity of construction and operation of this system probably make it the best choice for fiber measurements whenever magnitude information is sufficient.

In the testing of discrete rf components, a vector voltmeter is frequently used to obtain both magnitude and phase information. It is not generally used in the testing of systems characterized by long propagation delays because of the difficulty in separating the phase distortion information from the large linear phase shift associated with the delay. Two techniques shown in figure 7 allow one to avoid these difficulties to a degree. One approach is to use a frequency synthesizer instead of a conventional sweep generator [14]. The synthesizer provides a discretely variable source frequency that can be varied arbitrarily slowly over the range of interest allowing more accurate phase measurements to be made. The other approach is to insert a system characterized by a similar delay but much smaller distortion in the reference line [15]. The phase distortion is then a much larger portion of the total phase shift. A single mode fiber would be a suitable choice for a system designed to characterize multimode fibers.

4.1.3 Network Analyzers

The four measurement systems described above are fundamentally similar in function and form to more elaborate rf measurement systems known as network analyzers which measure the S-parameters of microwave devices and circuits. Commercially available network analyzers can also be grouped into wide and narrowband detection types. They will measure the magnitude of the transfer function (i.e., S_{12}, S_{21}) and, depending on type, will provide some form of phase characterization. Generally, they are also designed to measure other parameters important in rf circuit design (e.g., impedance, S_{11}, S_{22}). Thus, a network analyzer suitable for carrying out fiber transfer function measurements is generally an expensive alternative to the limited purpose systems described.

4.2 Choosing a System and the Matter of Phase

Performance, convenience, and cost together determine the choice of measurement system. Several of the methods described in section 4.1 have been used at NBS and of them, provided that only magnitude information is needed, the system shown in figure 6 seems to be the most appropriate choice. This brings us again to the question of whether the incomplete characterization of the information carrying capacity by $|H(f)|$ is sufficient.

Most high quality graded-index fibers designed for telecommunications applications have an impulse response that is nearly symmetrical about its central time and therefore show very little variation of group delay with frequency. The phase distortion that is present is therefore probably of little consequence as long as the problems noted in section 3.3 continue to complicate the interpretation of bandwidth measurements.

Step-index and other non-optimum profiles generally do not have symmetric impulse responses. It is conceivable that in certain systems using such fibers or in other special purpose systems phase distortion may be important. However, it appears that at this time these cases arise infrequently and most of the needs of the industry can be met with magnitude data alone.

The system of figure 6 was therefore chosen for further evaluation and use. The design and performance details of the version now in use at NBS are given in the following sections.

5. DESCRIPTION OF THE MEASUREMENT SYSTEM

Figure 8 shows a block diagram of the system. The optical design is similar to that of a time domain system described elsewhere [16], though certain refinements have been incorporated. Almost all of the components are commercially available; their important characteristics are described below along with the basic system design.

5.1 Source

The source normally used in this system is a commercially available "laser transmitter". It consists of a single-transverse, multi-longitudinal mode GaAlAs laser diode coupled directly to a 2 m length of 50/125 μm core/cladding diameter, graded-index fiber. The laser is mounted on a temperature controlled substrate. Output from the laser is further stabilized by using the detected light from the back face of the laser to control the bias current. Radio frequency signals may be superimposed upon the bias current using a single R-C network, thus providing wide-bandwidth amplitude modulation. The entire unit, excluding power supply, measures about 3.5 by 7 by 4 cm (fig. 9).

The specified output power at the laser is 2.5 mW with an amplitude stability of 0.1 percent. Measured power at the fiber output is about 1.25 mW, where a long term drift of 1 to 2 percent is noted. This drift probably results from changes in optical feedback (reflections from the fiber ends) with temperature.

Figure 10 shows the spectrum of the source as measured with a 0.5 m Ebert-type spectrometer, with a resolution indicated by the width of individual longitudinal modes. The relative power of the modes varies somewhat with time with the result that a specificiation of spectral linewidth based on the FWHM of the envelope becomes uncertain. However, for purposes of estimating the frequency at which chromatic effects begin to effect a bandwidth measurement (section 3.2) we choose $\Delta\lambda = 0.9 \pm 0.15$ nm. This suggests that for a typical germanium-phosphorus doped silica fiber material dispersion does not become a contributor to the measurement below 1.9 GHz which is outside of the operating range of the system.

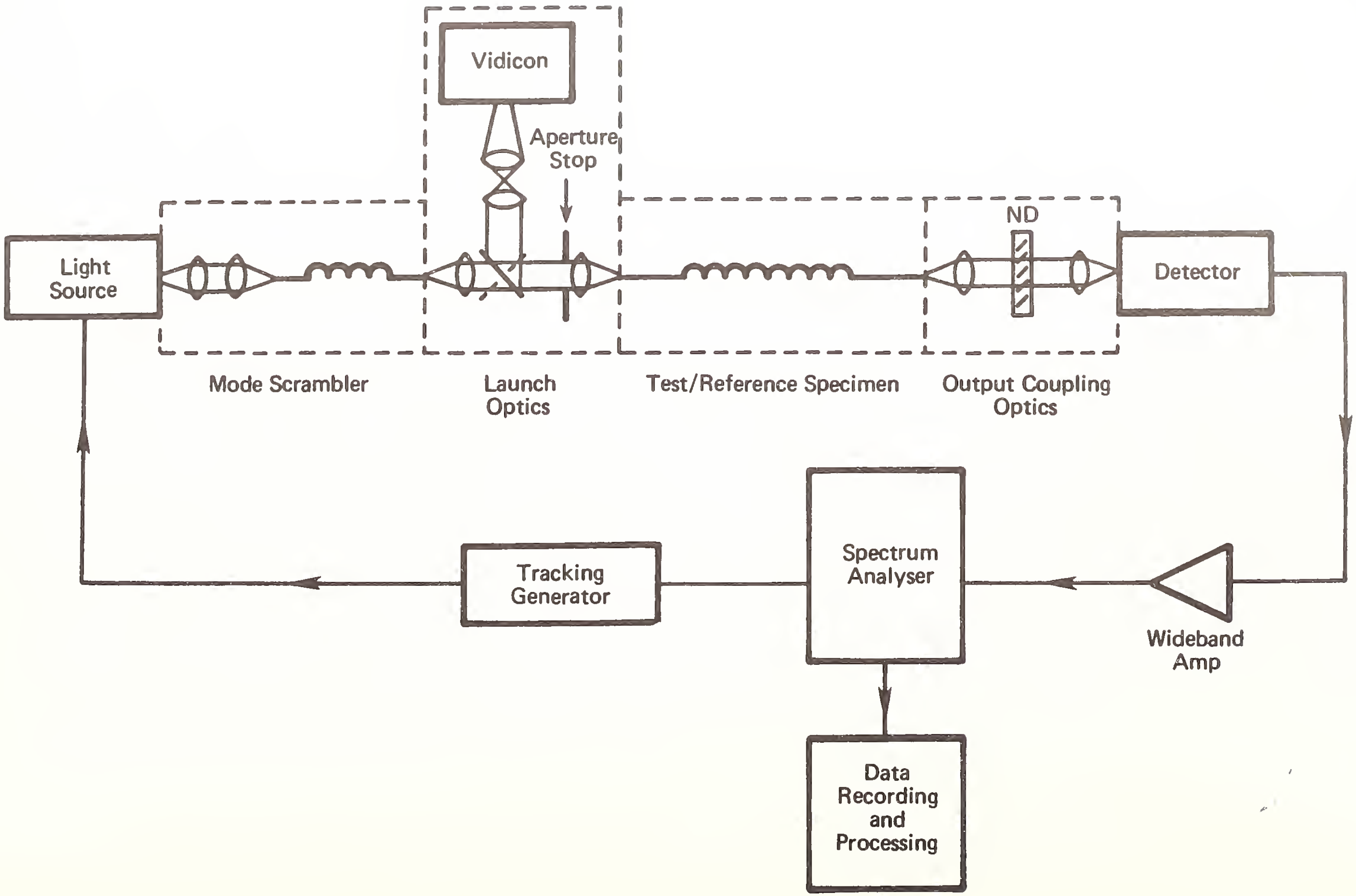

Figure 8. Block diagram of frequency domain fiber bandwidth measurement system.

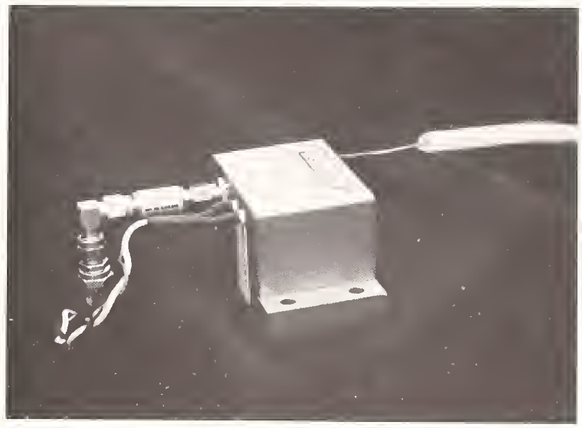

Figure 9. Photograph of "laser transmitter" used as the source.

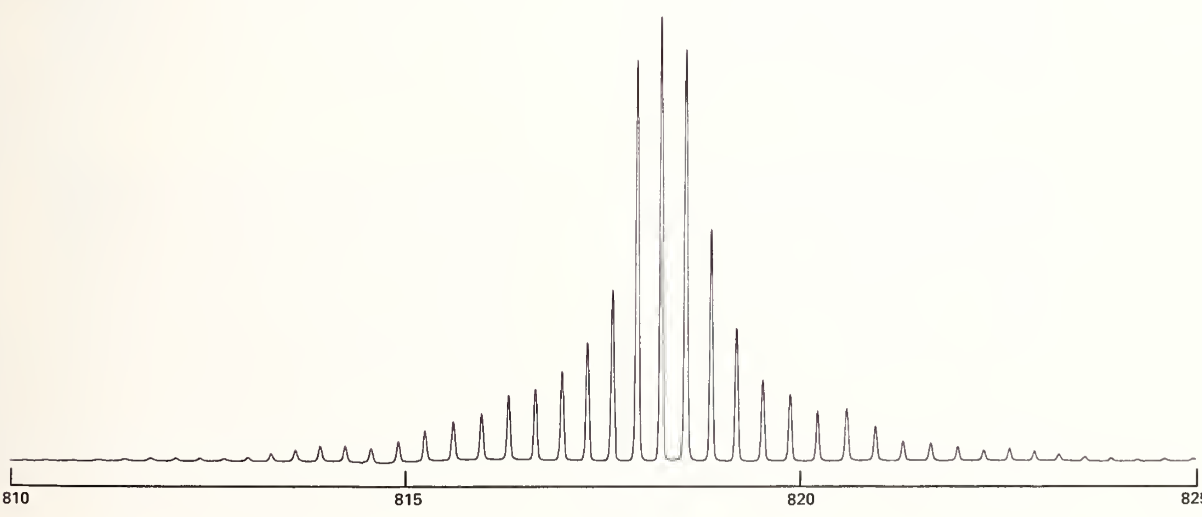

Figure 10. Output spectrum of source obtained with a 0.5 m Ebert-type spectrometer.

Figure 11 shows the variation in modulation index (optical power modulation/rf drive) versus frequency. The modulation index is essentially independent of frequency from a few tens of hertz to 600 MHz (specified bandwidth is 500 MHz). The index decreases by about 2.5 dB (optical) between 600 and 680 MHz and then increases gradually to a value about 4 dB (optical) above its low frequency value at 1430 MHz near the limit of the system. Independent tests on the detector used in this measurement indicate that the variations in modulation index are not measurably affected by the detector. The increase at the highest frequencies may be related to self pulsing in the laser because the noise spectrum of the laser output shows a similar increase. The dip at 680 MHz is of unknown origin.

Harmonic distortion in the source output can, as noted in section 4, cause difficulties when broadband detection is used. Figure 12 shows the distortion produced by this source. At a drive frequency of 100 MHz and an rf signal level of 0 dBm, the second harmonic is about 38 dB below the fundamental (manufacturer's specification: 40 dB). However, as the drive frequency is increased the harmonic distortion increases until at a fundamental frequency of 500 MHz both the second and third harmonics are only about 20 dB down. This would be unacceptable for broadband detection.

5.2 Mode Scrambler

Since the results of a fiber bandwidth measurement depend rather strongly on the spatial and angular characteristics of the input light, that is to say the input mode volume, it becomes necessary to minimize the effects of such changes in the source. This problem is somewhat less severe in the frequency domain system than in the time domain system [16] since the cw laser diodes are inherently more stable spatially than those used in time domain systems.

The usual way of maintaining launch stability is to couple the output of the source through a specially designed spatial filter. The spatial filter has the properties that the spatial and angular characteristics of its output are independent of those of the input. In practice, the spatial filter usually consists of a piece or pieces of suitably chosen fiber [16,17]. For this reason it has come to be known as a mode scrambler.

The mode scrambler used in this system consists of two pieces of fiber. The first is the 2 m section of 50/125 μm core/cladding diameter, graded-index fiber directly coupled to the laser by the manufacturer. The second is a similar length of 80/125 μm core/cladding diameter, step-index fiber spliced onto the first fiber in a loose tube. The radiation angle of each fiber is nominally 0.2 rad.

Figure 13 shows the characteristics of the device. The near-field profiles are obtained by imaging the output face of the fiber onto a silicon target vidicon. The video signal is processed with commercial equipment in such a way that the intensity of the image along a line normal to the raster is determined and plotted on the monitor screen.

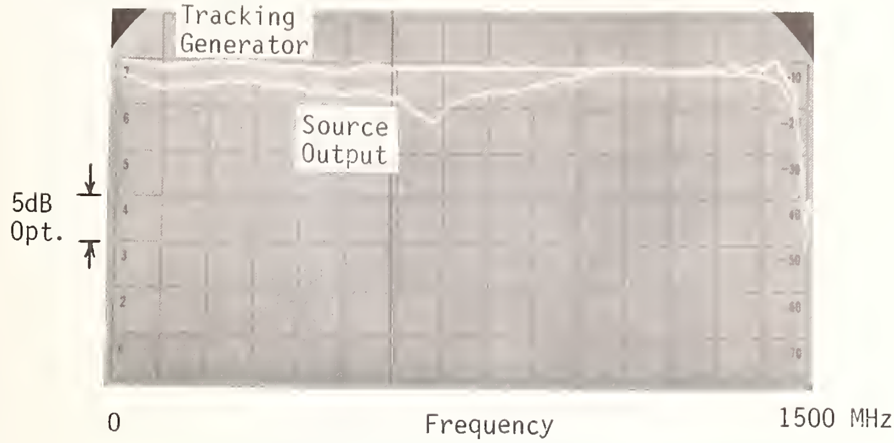

Figure 11. Modulation index of source as a function of frequency. The output of the tracking generator was applied to the source and the output of the graded-index pigtail from the source focused onto the detector.

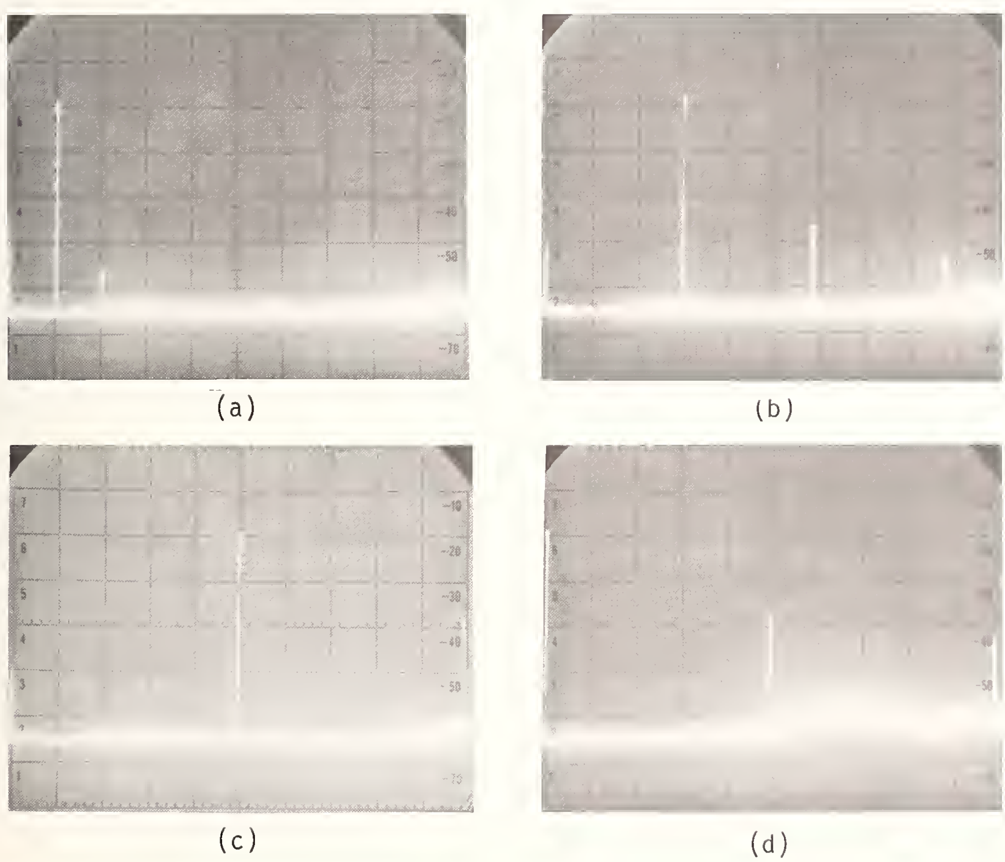

Figure 12. Distortion in source output. Drive level was approximately 0 dBm and the vertical scale 10 dB (electrical)/div in each case. (a) Drive: 100 MHz, Scale: 0-1000 MHz; (b) Drive: 300 MHz, Scale: 0-1000 MHz; (c) Drive: 500 MHz, Scale: 0-1000 MHz; (d) Drive: 500 MHz, Scale: 500-1000 MHz.

The near field of the output from the graded-index fiber shows a rounded profile as expected, with a great deal of variation due to speckle. At the output of the step fiber the core is completely filled and the variations due to speckle appear somewhat reduced.

The far-field pattern from the step fiber was obtained by scanning a detector along a circular arc about 10 cm from the fiber end [18]. The far-field radiation angle is about 0.19 at the 90 percent irradiance points.

The speckle evident in all the data of figure 13 represents a fundamental difficulty in controlling the launching conditions for bandwidth measurements. It results from constructive and destructive interference in the superposition of fields from the modes of the fiber and appears whenever the coherence time of the source is long compared to the differences in group delay among the modes. The details of the speckle pattern vary with the relative phase of the modes. Very slight movement or distortion of the fiber will produce such phase shifts as will a change in temperature. These effects make it difficult to precisely define launching conditions. Further, when the speckle pattern shifts with time in a system where mode sensitive devices, such as couplers, are present or where there is significant differential mode attenuation, noise, generally known as modal noise results [19].

One solution to the problem of speckle is to use a less coherent (broader spectral linewidth) source. However, as noted earlier (section 3.2) that can result in additional limitations to the bandwidth from the material dispersion. As a practical compromise, source spectral widths of about 1 nm are reasonable.

Another possible solution for measurement systems might be to deliberately introduce periodic phase shifts through, for example, mechanical distortion by a piezoelectric transducer. This should have the effect of smearing the speckle pattern. This approach has not been seriously pursued, as yet.

5.3 Launching Optics

The section of figure 8 labeled launching optics is designed to image the output of the mode scrambler onto a fiber specimen in a well defined and reproducible fashion. The launching parameters of interest are the size of the image (the "spot size") on the input end of the fiber specimen and the angular extent of the bundle of rays that converge to form the image (the "LNA", launch numerical aperture). With this system (fig. 14) it is possible to control these parameters independently, though rather less conveniently than is necessary in an attenuation measurement system [20]. However, as noted in section 3.3, the greatest interest at present is in measurements made with full excitation of the fiber.

Two microscope objectives form the image. The first, usually a 10X, 0.25 NA lens, collimates the output of the mode scrambler. The second, in most cases identical to the first, focuses the collimated beam onto the specimen. The ratio of the spot size on the end of the test specimen to the spot size at the output of the mode scrambler is equal to the ratio of

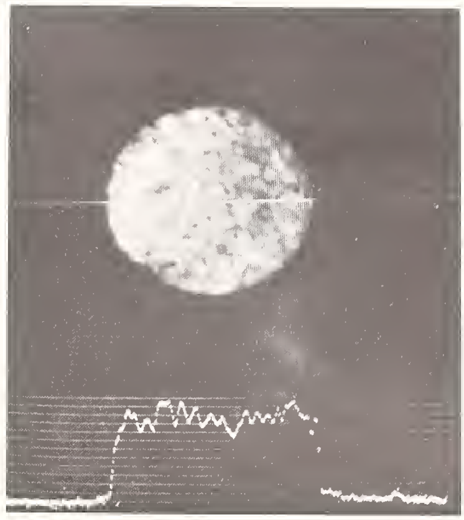

(a)

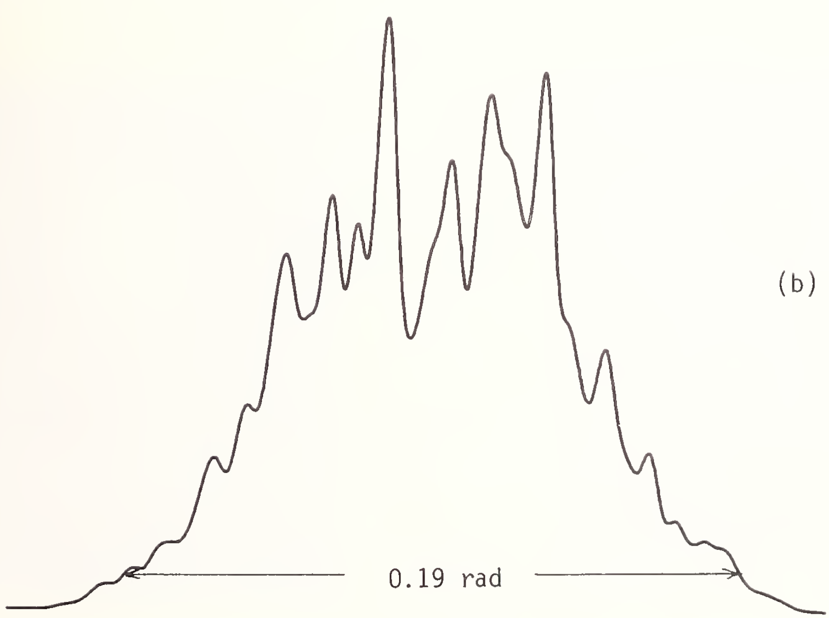

(b)

Figure 13. Characteristics of mode scrambler. (a) Near-field pattern, nominal diameter, 83 μm. Plot at bottom is of intensity along line through image. (b) Scan of far field of mode scrambler.

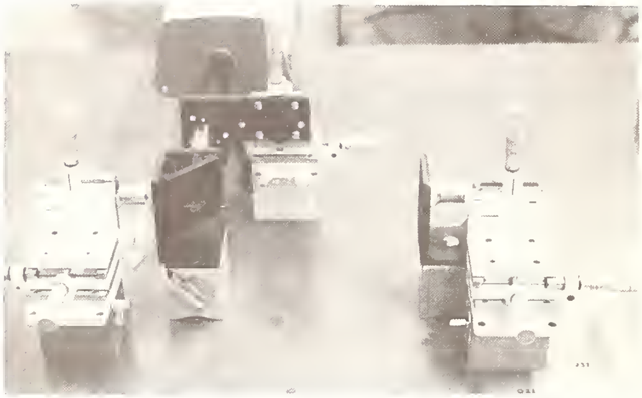

Figure 14. Photograph of launching optics. Output of mode scrambler is on manipulator at right, specimen input on manipulator at left. Pellicle at left of center can be rotated 90° to direct the image of either the mode scrambler output or the specimen input onto vidicon at top of photo (see fig. 8).

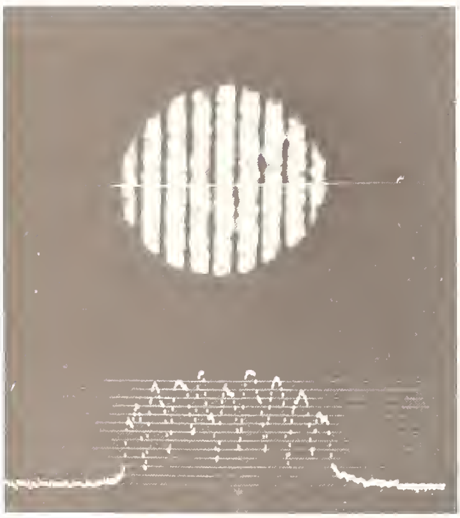

(a)

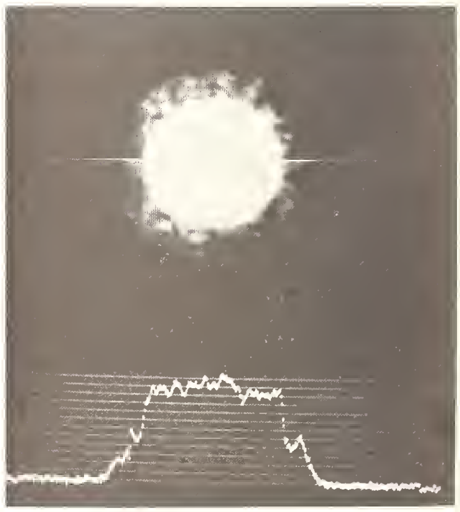

(b)

Figure 15. (a) Image of stage micrometer placed where specimen input would normally be placed, to verify size of launch spot. Line spacing is 10 μm. (b) Image of short step-index specimen. The core appears brighter because of reflected light from output end of fiber.

the focal length of the second objective to that of the first. This is perhaps the easiest way to control the spot size. The launch numerical aperture is somewhat more complicated to predict. If the objectives are identical, the LNA should be the lesser of the sine of the radiation angle of the mode scrambler or the effective NA of the objective. If the objectives are different, a more specific analysis is necessary to predict the LNA. The LNA may be limited beyond that determined by the mode scrambler or lenses by placing an aperture in the collimated portion of the beam.

For purposes of system alignment and evaluation it is convenient to place a pellicle beam splitter in the collimated beam and to thereby image, with some additional magnification, the input end of the fiber specimen as illuminated by the source. Figure 15a shows the image produced on a stage micrometer placed at the image point; verification of the launched spot size is thus obtained from the 10 μm line spacing on the micrometer. Figure 15b shows the image of a short (~ 2m) fiber specimen similarly obtained. The core appears brighter than the cladding due to light reflected back from the output end of the fiber. With a long fiber or with the output end index matched, there is little difference in appearance between the core and cladding.

The launch numerical aperture could be verified by scanning a small detector through the diverging beam beyond the image point. An alternate method is to determine the far-field radiation angle from a short piece of fiber (fig. 16).

5.4 Specimens

In most cases, the test specimen is a known length (typically 1 km) of multimode graded-index fiber. A separate reference specimen representative of the test specimen, generally a piece cut from one end of the test specimen, is chosen. The length of the reference specimen must be such that the magnitude of its transfer function is essentially unity over the frequency range of interest. As a practical matter, it is usually sufficient to limit the length of the reference specimen to 1 percent of the length of the test specimen.

Both ends of each specimen are prepared by cleaving and are inspected with a 400 power microscope for flatness and perpendicularity. Illumination is either collinear with the microscope axis or from the far end of the fiber. Ends with perceptable hackle or breakout within the core region are rejected as are ends on which the entire outer surface of the cladding can not be brought into sharp focus at the same time. The theoretical depth of focus of the microscope is about 3 μm which means that for a 125 μm fiber diameter angles smaller than 1 to 1.5 degree are accepted.

Cladding mode strippers are not used in this system. Unlike the case with attenuation measurements, light that remains trapped within the cladding for the full length of the reference fiber should not affect the measurement.

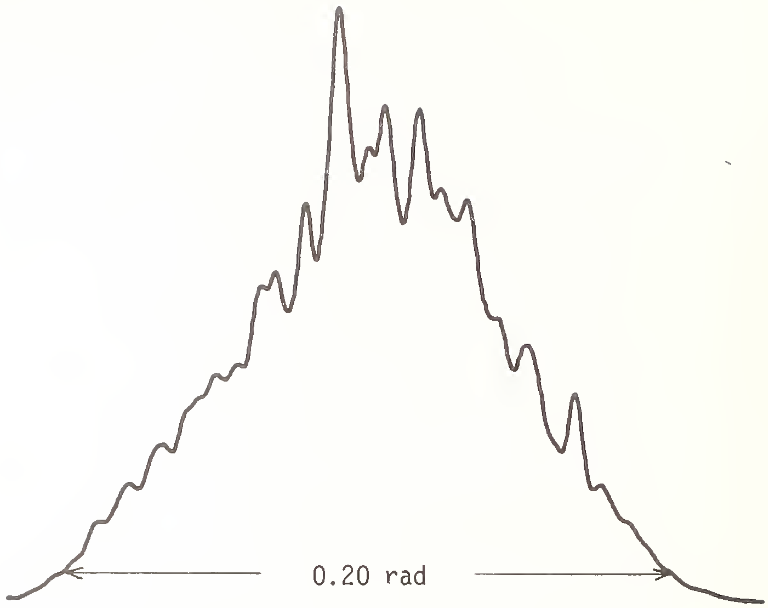

Figure 16. Far-field radiation pattern from a short piece of large acceptance angle fiber placed in test system to verify launch numerical aperture. Fiber specifications: 100 μm core diameter, quasi-step index profile, 0.3 NA.

(a)

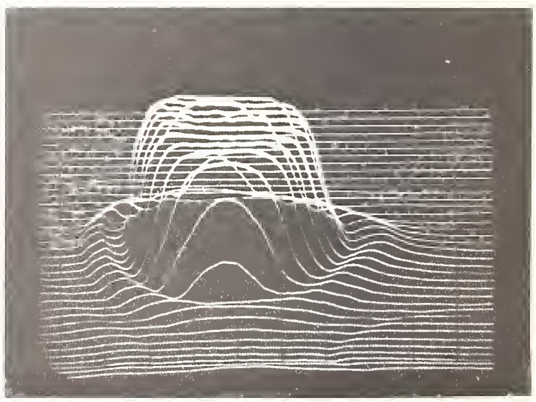

(b)

Figure 17. (a) Photograph of Si APD detector used. Active area is 200 μm diameter. (b) Plot of spatial response uniformity. Detector is uniform to about 5 percent peak to peak.

It is important that the test specimen be handled in such a way that no excess microbending is applied to the fiber. This consideration can be very important when testing uncabled fiber that has a very thin buffer.

5.5 Detection

A suitable detector must have a sufficient frequency response, linearity of response over the range of operating levels, and a uniformity of response over the active area. The detector chosen for this system is a 200 μm diameter Si APD. The characteristics of this detector were described previously [16] and are briefly summarized here. The impulse response duration is about 200 ps which gives a more than adequate frequency response for this system (see also fig. 10). The uniformity of response (fig. 17) is about 5 percent peak to peak.

The pulse linearity is good [16]. At the higher average currents (50-100 μA) used in this system perceptable heating occurs. This is sufficient to cause a few percent change in detector gain but allowing the detector to stabilize before measurements eliminates most of the difficulty. Further compensation for temperature changes by the method described below fully eliminates the problem.

The detector is mounted in a coaxial mount similar to one described by Green [21] (fig. 18) and biased with the circuit of figure 19, which differs somewhat from the bias circuit used with the time domain system [16].

The detector is normally biased at a point (typically 140 V) where the gain is between 5 and 10. To compensate for any temperature induced change in gain or change in laser output the dc current is monitored with a 10 Ω sensing resistor. The slopes of the dc and rf load lines being nearly equal (1/60 versus 1/50 Ω^{-1} when the ammeter is shorted) a change in this reference voltage is proportional to any laser output or detector gain induced changes in detected rf level.

It is necessary that the outputs of the test and reference fibers are completely coupled to the uniform detector to insure that all mode groups are equally detected. This is done with two microscope objectives, as shown in figures 8 and 20. Usually the objective nearest the fiber output is a 10 X, 0.25 NA while the second is a 5 X, 0.1 NA to provide a larger spot on the detector and thus average over spatial nonuniformities.

Neutral density filters (fixed and circularly variable) are placed in the collimated region to set the signal levels for test and reference specimens equal, minimizing the effect of detection nonlinearities.

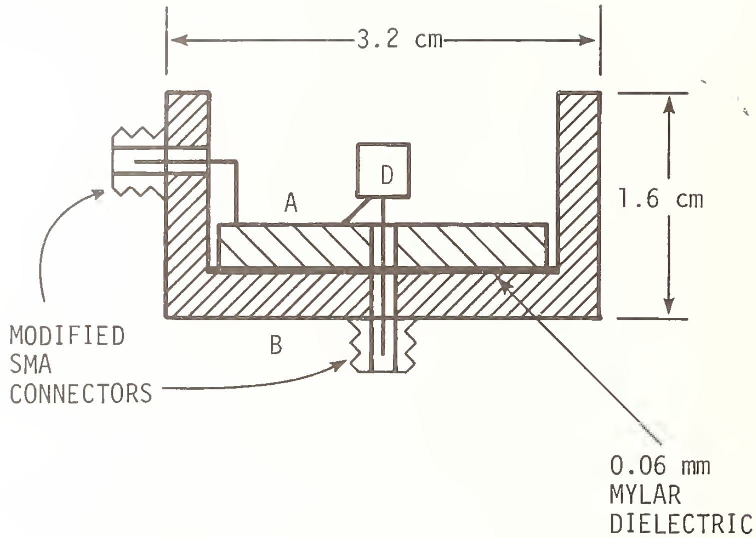

Figure 18. Diagram of detector mount.

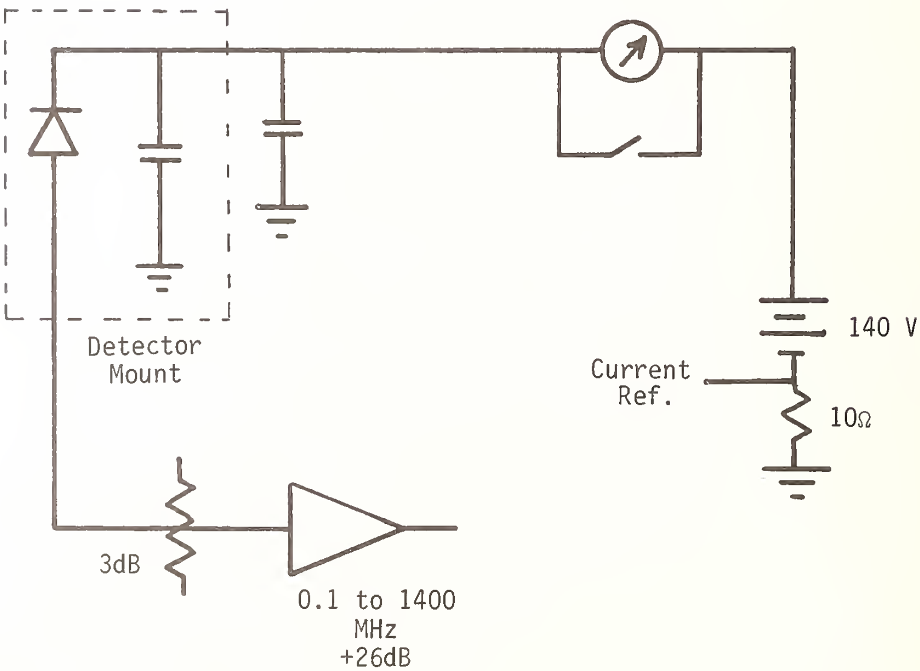

Figure 19. Detector bias circuitry.

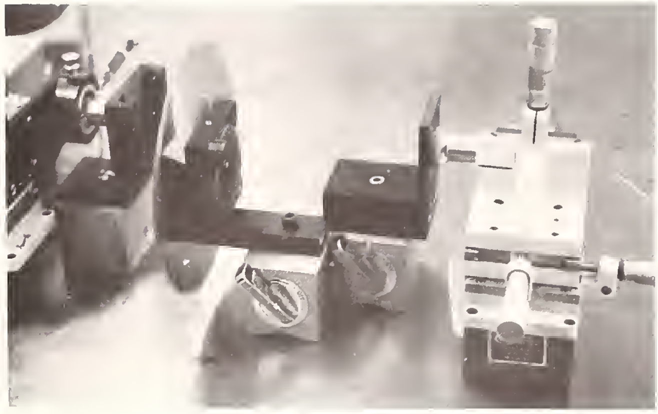

Figure 20. Photograph of output coupling optics. Specimen output is on manipulator at right. Fixed and circular-variable neutral density filters are placed between microscope objectives. Detector is in cylindrical mount at left (see fig. 8).

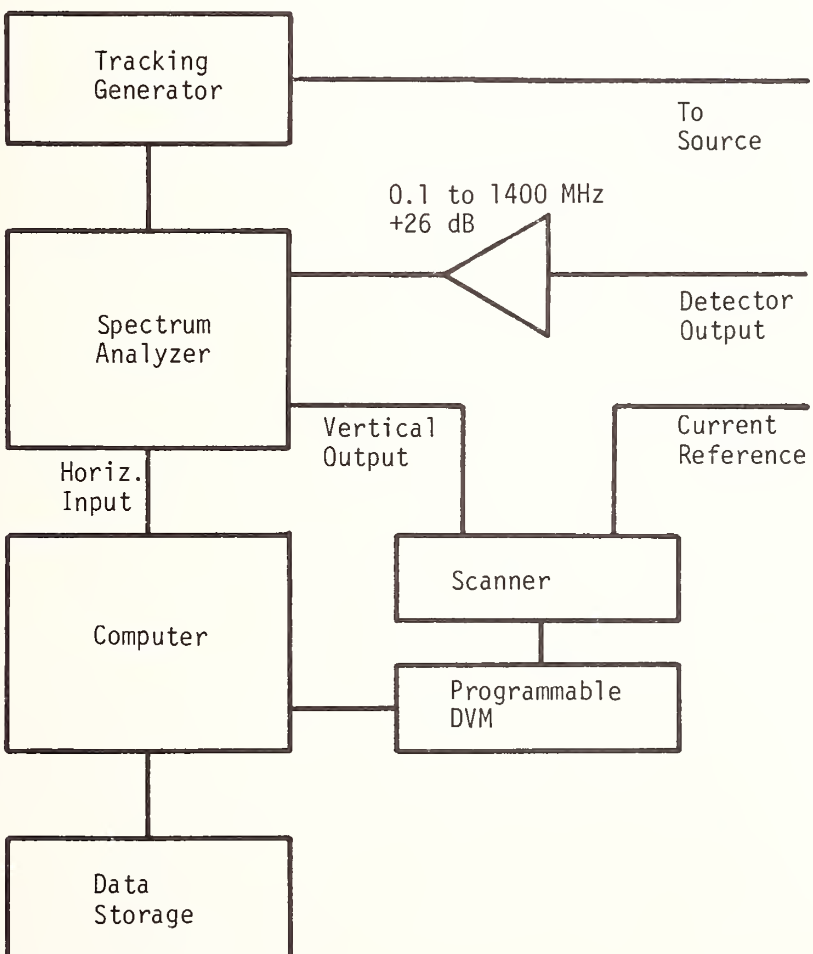

Figure 21. Block diagram of electronics.

5.6 Electronics

A more detailed block diagram of the electronic portion of the measurement system is shown in figure 21. The heart of the system is the spectrum analyzer/tracking generator combination. These two instruments function together in such a way that the output frequency of the tracking generator always coincides with the detection frequency of the spectrum analyzer. The modulation frequency applied to the laser transmitter is thus swept over the range of interest by controlling the sweep (horizontal) input to the spectrum analyzer.

The system operates under computer control, the operator choosing the range of frequencies over which measurements are to be made and the nominal resolution. Using a fitted linear calibration function relating sweep input voltage to tracking generator output frequency (fig. 22) the computer provides to the spectrum analyzer a sequence of voltages corresponding to the measurement frequencies. After an appropriate settling time at each point the computer records the vertical output voltage of the spectrum analyzer and the dc detector current using the programmable DVM (digital voltmeter)/scanner combination.

The vertical output of the spectrum analyzer is calibrated using a signal gnerator and a set of precision attenuators. Calibration points are taken at 1 dB electrical (0.5 dB optical) intervals. The attenuators were chosen for their reproducibility and frequency independence. The specified values were verified or adjusted using a bolometer-type rf-microwave power meter accurate to 1 percent. This power meter thus becomes the magnitude reference standard for the system. Calibration at several frequencies indicates that single frequency calibration is sufficient. Vertical calibration data relative to a suitably chosen reference level are shown in figure 23, along with a linear least-squares fit.

5.7 Computation

For both the test and reference specimens the vertical output is converted to decibels, corrected for any changes in detector gain (normally negligible) using the dc detector current as a reference, and plotted as the data are acquired. Since the test and reference spectra are obtained using the same set of frequencies the two arrays may be subtracted directly to yield the magnitude of the transfer function.

Verification of the computations was obtained by inserting the precision attenuator set between the tracking generator and spectrum analyzer in place of the usual test apparatus. The attenuators were switched at intervals as the usual sweep range was covered (fig. 24). Deviations from calibrated values (averaging over several stnading wave periods where necessary) are all less than 0.03 dB.

From the magnitude of the transfer function, the bandwidth is computed as the lowest frequency at which the magnitude drops 3 dB below its value at the lowest frequency of measurement.

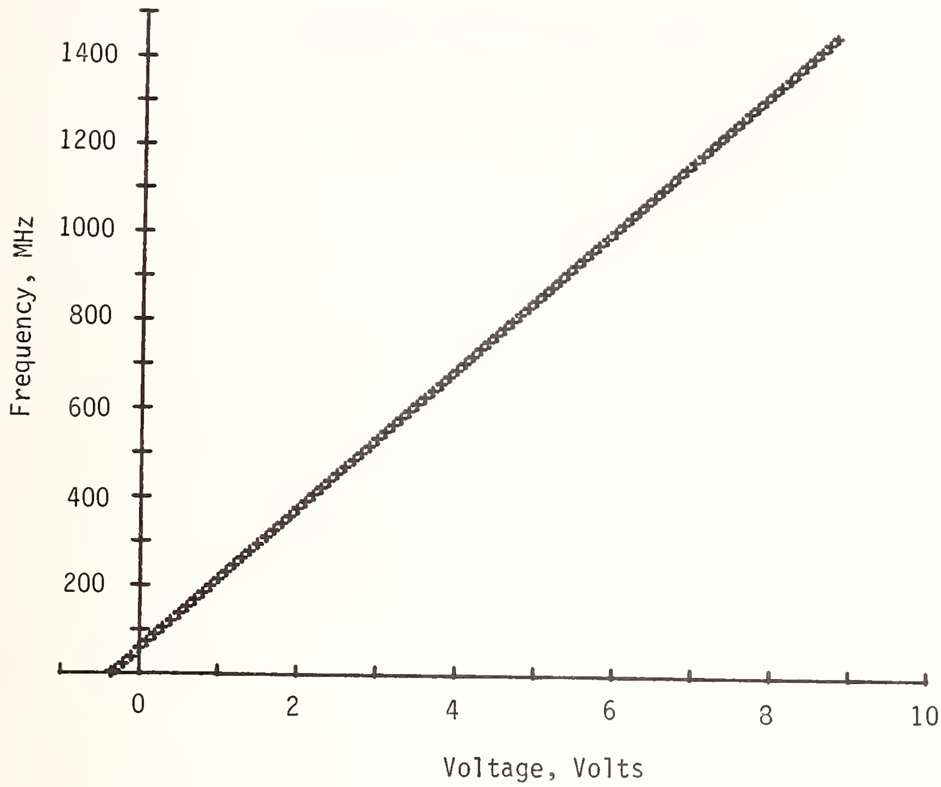

Figure 22. Frequency calibration data.

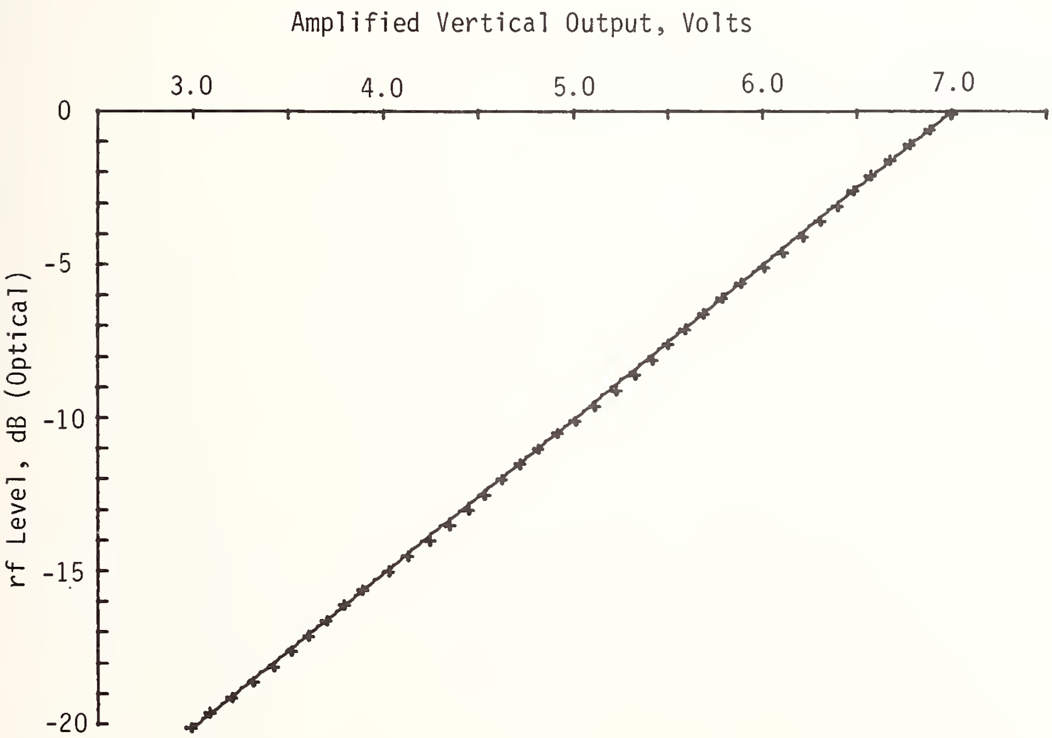

Figure 23. Vertical calibration data.

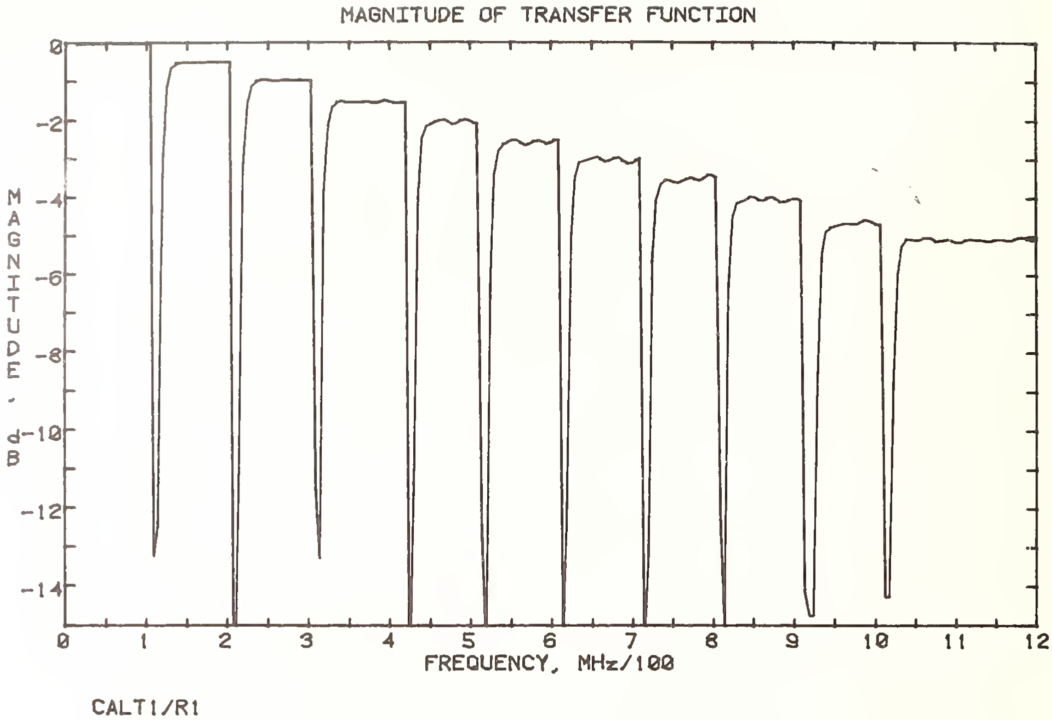

Figure 24. Result of replacing test system with a set of precision, step-variable attenuators and switching at intervals during scan.

6. SYSTEM PERFORMANCE

6.1 Measurement Procedure

Following preparation of the test and reference specimens as indicated in section 5.4, the two fibers are placed into the system. Generally, the test specimen is evaluated first. The alignment procedure consists of observing the fiber end on the monitor and adjusting the end position so that both the end and the spot striking it are in focus and the spot is visually centered within the core circumference. At the fiber output the image of the output end is located on the detector by adjusting the focus for maximum signal and adjusting the transverse position to center the spot on the detector.

The signal level is adjusted with discrete and variable neutral density filters to a satisfactory value not exceeding the limits of the detector. (If a high-loss fiber is measured no ND is used with the test specimen.) The tracking generator is adjusted for proper tracking, the spectrum analyzer is set to scales and conditions on which calibration data is available, the sweep is begun, and data are recorded.

The procedure is repeated for the reference specimen. In this case, the average current level at the detection is set equal to that with the test specimen and care is taken to ensure that the same spectrum analyzer parameters are chosen.

6.2 Precision and Accuracy

Given the difficulty of interpreting bandwidth measurements, the most important aspect of bandwidth measurement quality at the present time is the precision, or reproducibility. To test the precision of this system repeated measurements were made on each of two selected fibers, using the procedure of section 6.1. The two fibers were chosen because in each case a substantial history of both bandwidth and attenuation measurements was available [16,22] indicating stability of characteristics. The nominal characteristics of the fibers are summarized in table 2. Each measurement consisted of separate test and reference data with a completely new alignment and resetting of levels for each specimen. The results are shown in figures 25 and 26.

It is useful to specify precision in two ways. One is reproducibility in determining the frequency at which the magnitude reaches a specified level, say -3 dB, -6 dB, -9 dB, etc. The other is the reproducibility in magnitude at a specified frequency. In figures 25 and 26 a one standard deviation precision at several levels and frequencies is indicated. Note that the precision on fiber I308 is significantly better than for fiber I223. This difference appears to be related to the fiber characteristics--presumably differences in mode coupling and differential attenuation--and was noted in previous work. (I308 was identified as fiber A and I223 as fiber B in [16].) In fact, the precision obtained in that previous work is very similar in both cases to the precision obtained here (table 3). This is not at all surprising since the optical part of the system in all probability determines the system precision and the optics in the two systems are very similar.

6.3 Limitations

The frequency range over which this system is operated, 10 to ~ 1200 MHz is sufficient to test most commercial fibers--the highest commercial specification at this time appears to be 1000 MHz•km. However, experimental fibers with a bandwidth of 2 to 3 GHz•km and higher have been reported, and it would be desirable to extend the range of the system.

Table 2. Characteristics of fiber used in precision determinations.

Fiber	I308	I223
Length	1.3 km	1.1 km
Size	50/125 μm	50/125 μm
NA	0.25	0.25
Attenuation	6.0 dB/km @ 850	6.0 dB/km @ 850

Table 3. Comparison in precision between a time domain system [16] and the frequency domain system described here. The variation in FD precision on I308 at the -3, -6, and -9 dB levels probably results from the different slopes of the transfer at these points.

Fiber	Level (dB)	TD-Precision (%)	FD-Precision (%)
I308	-3	0.6	1.7
I308	-6	1.	0.06
I308	-9	1.	0.06
I223	-3	4.	3.4
I223	-6	3.	3.3

Several factors limit the upper frequency of the system as it now exists. The presently used wideband amplifier and the tracking generator/spectrum analyzer all have limitations in the 1400 MHz region. Each could be upgraded somewhat, though material dispersion due to source linewidth becomes a significant factor somewhat near 2 GHz. Using a more coherent source will decrease material dispersion contributions but will increase problems in specifying launching conditions due to speckle. Unless the speckle problem can be eliminated by other means, 2 GHz is probably the maximum useful frequency for a system of this sort at this wavelength.

It is becoming increasingly important to be able to measure long systems with substantial loss. The dynamic range of this system has not been carefully studied, but is clearly limited, at present, to roughly 20 dB loss as a result of direct electrical coupling from input to output. Signal-to-noise measurements indicate that when this problem is eliminated fibers with a loss of at least 30 to 40 dB could be measured.

7. SUMMARY

Based on data and experience obtained to date and reported in previous sections, the frequency domain system described in this chapter seems well suited for the routine measurement of fiber bandwidth. It is relatively simple to construct using components that are almost all commercially available. It is easy to use and requires fewer and less complex computations than time domain systems. The precision obtained is comparable to that obtained in the time domain and well within the uncertainties observed between laboratories [23]. Certain improvements in the system and an extension to the 1.3 or 1.55 μm region would allow it to perform most of the multimode fiber bandwidth measurements required in the foreseeable future.

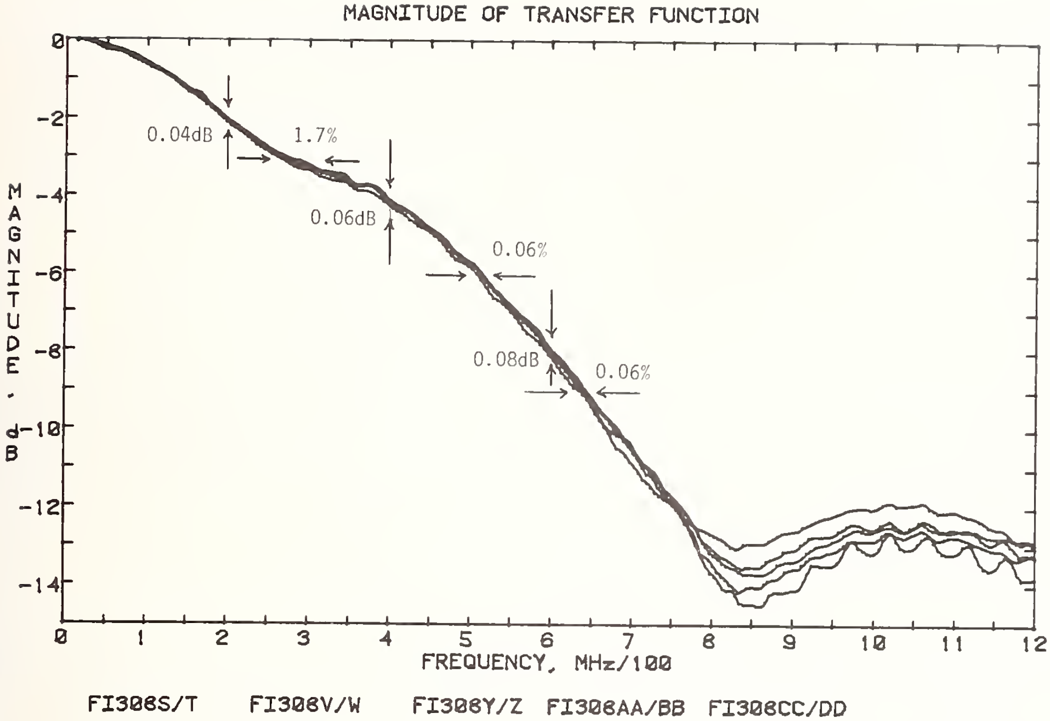

Figure 25. Superposition of the results of five independent measurements on fiber I308. Arrows indicate the one standard deviation imprecision at the -3, -6, and -9 dB levels in percent and at frequencies of 200, 400, and 600 MHz in dB.

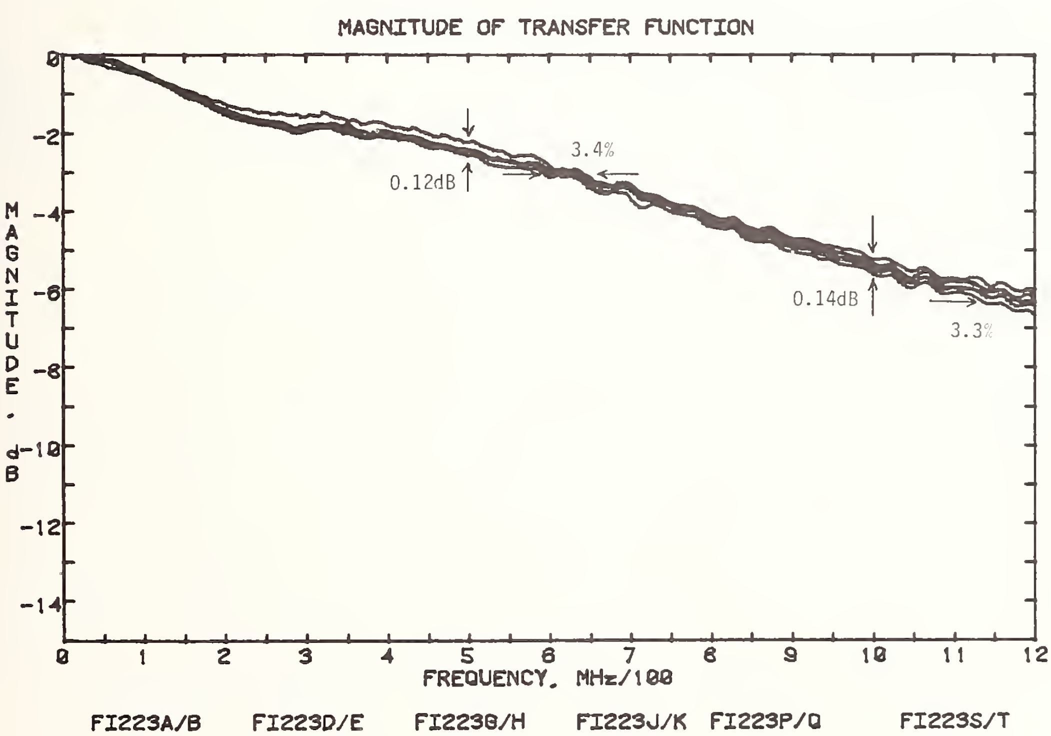

Figure 26. Superposition of the results of five independent measurements on fiber I223. Arrows indicate the one standard deviation imprecision at the -3, and -6 dB levels in percent and at the frequencies of 500, and 1000 MHz in dB.

While this and other work suggest that the measurement of bandwidth on a specific length of fiber is well in hand, a great deal of work needs to be done on the length dependence of fiber bandwidth. Until new approaches to this problem are developed it is likely that the most appropriate measurement conditions for bandwidth measurements will continue to be a full excitation of the fiber modes.

The author is indebted to D. L. Franzen, R. L. Gallawa, and P. A. Hudson for helpful consultations and to J. Skudler and R. Hunter for technical assistance. The Department of Defense, Calibration Coordination Group and the U.S. Army Electronic Proving Ground, Ft. Huachuca, Arizona, provided partial funding for this work.

8. REFERENCES

[1] (a) Persionick, S. D., Hubbard, W. M., and Holden, W. S. Measurement of the baseband frequency response of a 1 Km fiber. Appl. Opt. 13:266-268; 1974.
(b) Personick, S. D. Baseband linearity and equilization in fiber optic digital communications systems. Bell Sys. Tech. J. 52:1175-1195; 1973.
(c) Vassallo, Charles. Linear power responses of an optical fiber. IEEE Trans. Microwave Theory Tech. MTT-25:572-576; 1977.

[2] Bracewell, Ron. The Fourier transform and its applications. McGraw-Hill; 1965.

[3] Personick, S. D. Design of repeaters for fiber systems, in Fundamentals of optical fiber communications. Barnoski, Michael K., ed. Academic Press; 1976.

[4] Goldman, Stanford. Frequency analysis, modulation, and noise. McGraw-Hill; 1948.

[5] (a) Sandberg, I. W.; Kaminow, I. P.; Cohen, L. G.; and Mammel, W. L. . On the phase of the modulation transfer function of a multimode optical-fiber guide. Bell Sys. Tech. J. 57:99-109; 1978.
(b) Sandberg, I. W. A note concerning optical-waveguide modulation transfer functions. Bell Sys. Tech. J. 57:3047-3057; 1978.

[6] Gloge, D. and Marcatili, E. A. J. Multimode theory of graded-core fibers. Bell Syst. Tech. J. 52:1563-1578; 1973.

[7] Olshansky, Robert and Keck, Donald B. Pulse broadening in graded-index optical fibers. Appl. Opt. 15:483-492; 1976.

[8] (a) Cohen, Leonard G.; Kaminow, Ivan P.; Astle, Harry W.; and Stulz, Lawrence W. Profile dispersion effects on transmission bandwidths in graded index optical fibers. IEEE J. Quantum Electron. QE-14:47-41; 1978.
(b) Horiguchi, M.; Ohmori, Y.; and Takata, H. Profile dispersion characteristics in high bandwidth graded-index optical fibers. Appl. Opt. 19:3159-3167; 1980.

[9] Procedures now under consideration by EIA Committee P6.6--Working Group on Fibers and Materials (Electronic Industries Association, 2001 Eye St., Washington, DC 20006).

[10] Data supplied by P. Reitz, Corning Glass Works, Corning, NY.

[11] (a) Suzuki, S.; Kawahara, T.; Tanaka, G; Yoshida, M.; Kyoto, M.; Nakahara, T.; Kumamaru, H.; Takada, H.; Inagaki, N.; and Kitayama, K. Characteristics of graded-index fiber by VAD method. Proc. Optical Comm. Conf., Amsterdam, 12.6-1--12.6-4; 1979.

(b) Kapron, F. P.; Sladen, F. M. E.; Garel-Jones, P. M.; and Kneller, D. G. Attenuation and pulse broadening along concatenated fiber links. Tech. Digest, Symp. Opt. Fiber Meas.-1980, Boulder, 63-66; 1980. U.S. Govt. Printing Office, Washington, DC 20402.

[12] Cohen, L. G. Shuttle pulse measurements of pulse spreading in an optical fiber. Appl. Opt. 14:1351-1360; 1975.

[13] Swept-frequency group delay measurements. Applications Note 77-4, Hewlett-Packard, Palo Alto, CA 94304.

[14] Kobayashi, Ikutaro. Bandwidth measurement in multimode optical fibers. Tech. Digest, Symp. Opt. Fiber Meas.-1980, Boulder, 49-54; 1980. U.S. Govt. Printing Office, Washington, DC 20402.

[15] Okoshi, T.; Chang, J. C.; and Saito, S. Measuring the complex frequency response of multimode optical fibers. Appl. Opt. 20:1414-1417; 1981.

[16] Franzen, Douglas L. and Day, G. W. Measurement of optical fiber bandwidth in the time domain. Nat. Bur. Stand. (U.S.) Tech. Note 1019; 1980.

[17] Love, W. F. Novel mode scrambler for use in optical-fiber bandwidth measurements. Tech. Digest, Opt. Fiber Commun., Washington, 118-120; 1979. Optical Society of America.

[18] Kim, Ernest M. and Franzen, Douglas L. Measurement of far-field and near-field radiation patterns from optical fibers. Nat. Bur. Stand. (U.S.) Tech. Note 1032; 1978.

[19] Epworth, R. E. The phenomenon of modal noise in analog and digital systems. Digest, Fourth Eur. Conf. Opt. Comm., Genova, 492-501; 1978.

[20] Chamberlain, G. E.; Day, G. W.; Franzen, D. L.; Gallawa, R. L.; and Young, M. Attenuation measurements on multimode optical fibers. Nat. Bur. Stand. (U.S.) Tech. Note (in preparation).

[21] Green, S. I. 50 picosecond detector pulse monitor. Rev. Sci. Instrum. 47:1083-1085; 1976.

[22] Day, G. W. and Chamberlain, G. E. Attenuation measurements on optical fiber waveguides: an interlaboratory comparison among manufacturers. Nat. Bur. Stand. (U.S.) NBSIR 79-1608; 1979.

[23] Franzen, Douglas L.; Day, G. W., Danielson, Bruce L.; Chamberlain, George E.; and Kim, Ernest M. Interlaboratory measurement comparison to determine the attenuation and bandwidth of graded-index optical fibers. Appl. Opt. 15:2412-2419; 1981.

Chapter 3

Measurement of Near-Field Radiation Patterns from Optical Fibers

E. M. Kim

D. L. Franzen

A microcomputer-controlled system is described for measuring TNF (transmitted near-field) radiation patterns from optical fibers. Theoretical considerations, experimental technique, performance, and system calibration are presented. The dependence of TNF profiles on source wavelength, linewidth, fiber sample length, and launch position is given. A comparison of TNF profiles to actual index profiles shows that TNF measurements on graded-index fibers do not benefit from leaky-mode correction. Other profile investigations include curve fitting and iso-intensity contour mapping. Contours were made using the two-dimensional capability of the system along with digital image processing algorithms. Analysis of contours reveals the amounts of core non-circularity. Also investigated was the ability to measure single-mode fiber spot size and cutoff wavelength.

CONTENTS

		Page
1.	INTRODUCTION	103
2.	MULTIMODE FIBER MEASUREMENTS UTILIZING NEAR-FIELD PATTERNS	105
	2.1 Index Profile	105
	2.2 Core Diameter	108
	2.3 Mode Volume Transfer Function	109
3.	SINGLE MODE FIBER MEASUREMENTS UTILIZING NEAR-FIELD PATTERNS	110
	3.1 Fundamental Mode Spot Size	110
	3.2 Second-Order Mode Cutoff	110
4.	DESCRIPTION OF ONE-DIMENSIONAL NEAR-FIELD SYSTEM	111
	4.1 Optics	111
	4.2 Electronics	117
	4.3 Calibration	117
	4.4 Experimental Technique and Performance	120
5.	DESCRIPTION OF TWO-DIMENSIONAL CONTOURING TECHNIQUE	122
6.	EXPERIMENTAL RESULTS FROM NEAR-FIELD MEASUREMENTS ON MULTIMODE FIBERS	126
	6.1 Length Dependence	126
	6.2 Wavelength and Linewidth Dependence	132
	6.3 Launch Position Dependence	137
	6.4 Profile Pathologies	137
	6.5 Comparison of Near-Field Profiles to Actual Index Profiles	149
	6.6 Curve Fitting	149
	6.7 Modified Near-Field	154
	6.8 Two-Dimensional Contouring	154
7.	EXPERIMENTAL RESULTS FROM NEAR-FIELD MEASUREMENTS ON SINGLE-MODE FIBERS	168
	7.1 Spot Size	168
	7.2 Cutoff Wavelength via Spot Size	168
	7.3 Cutoff Wavelength via Near-Field Dip	172
	7.4 Estimating Index Profiles of 1.3 μm Single Mode Fibers by Blue Near-Field Measurements	172
8.	REFERENCES	184

1. INTRODUCTION

The radiation propagating in a multimode optical fiber can take on various spatial and angular distributions depending upon the relative excitation of fiber modes. Useful information about the fiber can be obtained by analyzing the radiation exiting an end. This analysis can take place in either the far- or near-field region. A far-field measurement determines the angular dependence of intensity (irradiance) sufficiently far from the end of the fiber (fig. 1); whereas, a near-field measurement determines the spatial intensity distribution in the plane of the end face.

In the far field, the normalized, angular intensity distribution no longer depends on distance from the fiber. While the intensity at any given angular coordinate decreases as the square of the distance from the fiber end, the normalized pattern remains constant. If the far-field pattern is circularly symmetric about the fiber axis, then a single angular coordinate is sufficient to describe the pattern.

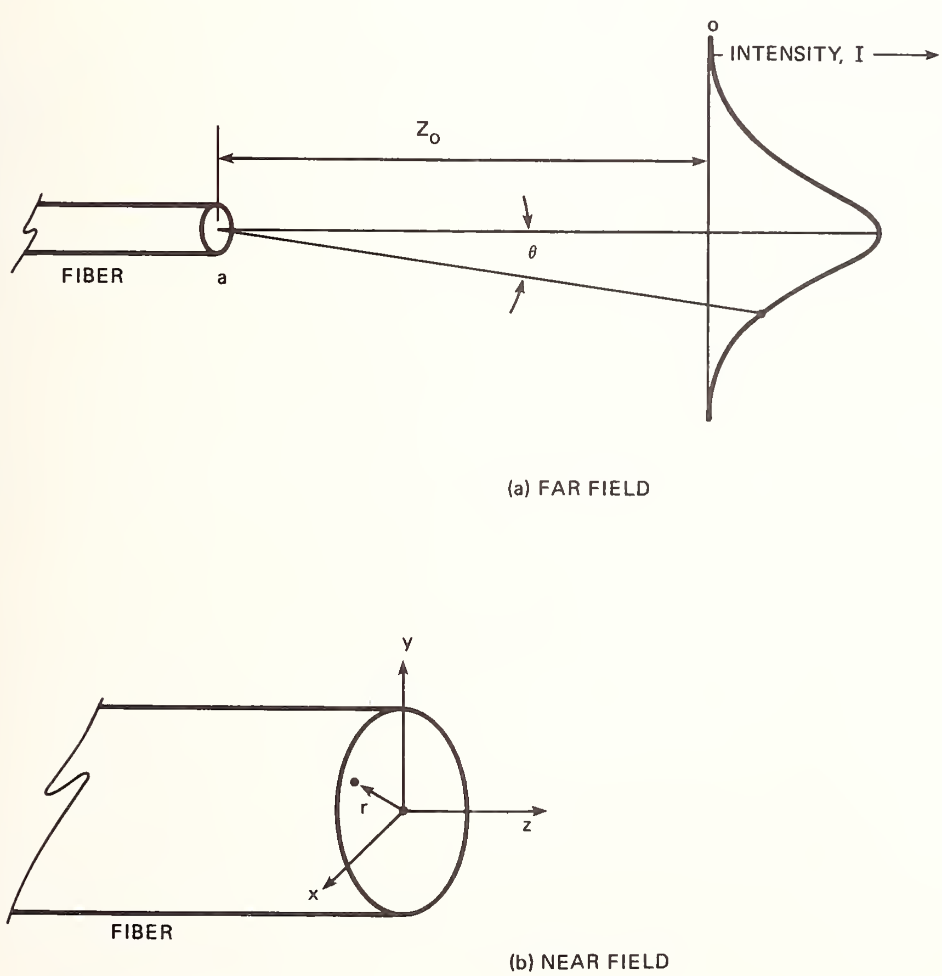

Figure 1. Radiation pattern measurements from optical fibers, (a) far-field intensity is given by $I(\theta)$ at $z >> z_0$, (b) near-field intensity is given by $I(r)$ in xy plane.

The far field, which is synonymous with the Fraunhofer diffraction region, is usually said to start at a distance

$$z_0 = \frac{(2a)^2}{\lambda} \quad (1)$$

from the fiber end, where λ is the wavelength of light and a the core radius [1]. When $z >> z_0$, the amplitude (electric field) distribution in the far-field is closely related to the spatial Fourier transform of the amplitude distribution existing at $z = 0$, [1]. In practice, far-field measurements are made at distances greater than 10 z_0 from the fiber end. For the standard graded-index core diameter of 50 μm and a wavelength of 1 μm, 10 z_0 is 2.5 cm. For the standard step-index core diameter of 100 μm, the distance becomes 10 cm. Both of these lengths represent convenient laboratory working distances.

Radiation patterns are measured on either short or long lengths of fiber, depending upon the application. Frequently, the short length is a 2 m cutback length left over from an attenuation or bandwidth measurement. In this chapter, a long length refers to the entire length of fiber under test and, for telecommunications fibers, generally exceeds 1 km.

Radiation patterns from multimode fibers depend upon launching conditions and contain contributions from both guided and tunneling leaky modes of the fiber [2,3]. In short lengths, patterns result mainly from guided modes with a significant contribution from leaky modes. The relative importance of the leaky mode contribution depends upon the index profile and launching conditions. In long lengths, leaky modes have generally decayed and the patterns result from guided modes modified by differential mode attenuation and mode coupling. Far- and near-field patterns resulting from overfilled launching conditions on graded-index fibers generally become restricted with further propagation along the fiber. This occurs because differential mode attenuation is generally higher for higher order modes. Eventually an equilibrium is reached between mode coupling and differential mode attenuation to yield a steady state pattern. However, steady state is seldom observed in practice since mode coupling lengths in good fibers are several kilometers [4] if not tens of kilometers [5].

Radiation patterns from single-mode fibers indicate the intensity distributions of the fundamental waveguide mode associated with the index profile. The near-field pattern of the fundamental or first order mode is generally Gaussian shaped and independent of structural details in the index profile. Since the Fourier transform of a Gaussian is another Gaussian, the far-field pattern from a single-mode fiber is also approximately Gaussian. In fact, the radial dimensions of the near-field pattern (spot size) can be determined using either a near-field or far-field measurement [6]. Tables 1 and 2 give various measurement applications of radiation patterns from multimode and single-mode fibers, respectively.

Table 1. Measurement applications of radiation patterns from multimode fibers.

Application	Fiber length employed: short (2 m)	Fiber length employed: long	Radiation pattern: far field	Radiation pattern: near field	Launching condition	General comments
1 Radiation angle	X		X		Overfilled	Meridionally defined NA approximated for near parabolic graded-index fibers. Special considerations necessary for step index.
2 Attenuation using restricted launch via a mode filter	X	X	X		Overfilled	Used to qualify mode filters; applies to graded-index fibers over 1 km in length.
3 Index profile	X			X	Overfilled	Little or no leaky mode correction required for near parabolic graded-index fibers; large correction for step index. Limited resolution information on guiding regions of fiber only.
4 Core diameter	X			X	Overfilled	Possible uncertainty due to low index "barrier" layer, poor resolution near core-cladding boundary, is easy to implement.
5 Mode volume transfer function	X	X	X	X	Restricted	Applies to graded-index fibers; measurement system must have ability to control launch mode volume and therefore beam optics systems capable of independently variable launch spot and NA are usually required.

2. MULTIMODE FIBER MEASUREMENTS UTILIZING NEAR-FIELD PATTERNS

2.1 Index Profile

When a multimode optical fiber having a large number of modes is uniformly illuminated to equally excite all bound modes, the near-field pattern approximates the refractive index profile of the core [7]. A simple relationship between the refractive index profile and the intensity distribution across the exit face of the fiber can be found. In this case, an assumption will be made that there are only bound modes present.

For the simple model of a fiber, only the radiation which is contained in a cone of θ_c can propagate in the fiber. This angle, called the acceptance angle, is used to calculate a numerical aperture. Often, numerical aperture is defined as the largest cone of meridional rays (rays that pass through the center axis) that can enter or leave an optical element. For our purposes, NA (numerical aperture) is the sine of the acceptance angle of the fiber

Table 2.
Measurement applications of radiation patterns from single-mode fibers.

Application	Radiation pattern far field	Radiation pattern near field	General comments
1 Spot size		X	Direct measure of spot size from fundamental mode shape.
2 Spot size	X		Spot size obtained by transform to near field. Gaussian assumption usually made. Hankel transform more rigorous.
3 Cutoff wavelength		X	Cutoff wavelength occurs when near-field pattern exhibits on-axis dip due to presence of second- order mode.
4 Cutoff wavelength	X	or X	Cutoff wavelength occurs approximately when spot size as a function of wave-length is a minimum.

[8]. The mathematical equation for NA as a function of radial position (local numerical aperture) is

$$NA(r) = \sqrt{n(r)^2 - n_2^2} \quad (2)$$

$$= \sin \theta_c . \quad (3)$$

Uniform illumination of the fiber requires a diffuse Lambertian source. The angular dependence of such a source acts as a cosine function. The brightness of the Lambertian source is therefore given by

$$B(\theta) = B\cos\theta. \quad (4)$$

Then the intensity accepted into the cone defined by the NA is

$$I(r) = \int_0^{2\pi} d\phi \int_0^{\theta_c(r)} B(\theta)\sin\theta d\theta. \quad (5)$$

Substituting in the expression for $B(\theta)$, the intensity accepted as a function of radius becomes

$$I(r) = \pi\sin^2\theta_c(r). \quad (6)$$

Normalizing this equation to the maximum intensity which occurs at r = 0 for a graded-index fiber, eq (6) yields,

$$\frac{I(r)}{I(o)} = \frac{\sin^2\theta_c(r)}{\sin^2\theta_c(o)}. \tag{7}$$

This can be expressed in terms of index as

$$\frac{I(r)}{I(o)} = \frac{n^2(r) - n_2^2}{n^2(o) - n_2^2}. \tag{8}$$

Assuming all modes are equally attenuated, the output near-field replicates the input acceptance. By assuming that the mathematical model for the fiber index profile given by Gloge and Marcatili [9], eq (8) becomes

$$\frac{n^2(r) - n_2^2}{n^2(o) - n_2^2} = 1 - (\frac{r}{a})^g \tag{9}$$

where a is the core radius and g is a constant. Therefore the near-field radiation pattern will also appear as a power law profile

$$\frac{I(r)}{I(o)} = 1 - (\frac{r}{a})^g. \tag{10}$$

This indicates that in the ideal case, the near-field intensity distribution does correspond to the refractive index profile.

This is, however, a simplistic relationship between the index profile and the near-field radiation pattern. To fully understand the actual intensity distribution at the exit end of the fiber, rigorous modal or optical ray analysis must be performed. Since the near-field radiation pattern depends on the modal power distribution of the fiber, modal analysis may be more appropriate.

In short lengths where differential mode attenuation and mode coupling are negligible, the deviation of the near-field pattern from the actual index profile is due mainly to the presence of tunneling leaky modes. Sladen, et al. have derived a leaky mode correction factor allowing one to obtain the index profile from transmitted near-field data [2]. The radial index profile difference, $n(r) - n_2$, is given by

$$n(r) - n_2 \approx \frac{n(o) - n_2}{C(r,z)} \frac{I(r)}{I(o)} \tag{11}$$

where $n(r)$ is the index in the core, n_2 the cladding index, $I(r)$ the near-field intensity as a function of radius, and $C(r,z)$ the correction factor. $C(r,z)$ is zero at the core center and gradually rises to a maximum near 0.9 a, where a is the core radius. As an example [7], for a 1 m length of fiber having a near-parabolic index profile, a core diameter of 80 μm, an NA of 0.18, and at a wavelength of 0.9 μm, the correction factor is 8 percent at 0.6 a, rising to 20 percent at 0.85 a.

Whether a leaky-mode correction should be made for near-parabolic profile, graded-index fibers is still open to debate. Calculations by Petermann [9] indicate a slight core ellipticity can cause leaky modes to attenuate more rapidly than indicated in references 2 and 7 and corrections would not be necessary for practical near-parabolic fibers. Leaky-mode correction factors have been derived for elliptical-core fibers [10].

Regardless of the appropriateness of a correction, the near field is a close approximation to the index profile for near-parabolic fibers. Also, corrections mainly affect the 0.5 a to 0.9 a region and the apparent width of the pattern near the baseline is not affected. This is of importance in determining core diameter from near-field measurements.

For step-index fibers, leaky modes are definitely significant and for short lengths the near-field profile differs substantially from the index profile.

The near-field intensity distribution gives information on the spatial location of power in the fiber. Thus, one is measuring only the guiding regions of the fiber. What happens at the core cladding interface or in the cladding is not indicated.

It should be pointed out that the above comments apply only to multimode fibers with large numbers of modes. In fibers with single or few propagating modes, the near-field intensity distribution is given by the mode patterns themselves which can differ substantially from the index profile shape.

2.2 Core Diameter

Core diameter is usually defined from the fiber refractive index profile. In one recommended definition, the core diameter is that diameter on the index profile where the refractive index of the core exceeds that of the cladding by k times the difference between the maximum refractive index in the core and the minimum index in the cladding, where k is a specified constant ($0 < k < 0.05$) [11] (fig. 2). Near-field measurements can be used to determine core diameter in some circumstances because of the close relationship between near-field and refractive index profile. Leaky-mode corrections, if they are even necessary for near parabolic index fibers, do not affect the measured width of the near-field pattern near the baseline. A core diameter measurement based on the full width at the 2 to 5 percent intensity points is appropriate [12]. A more serious uncertianty in determining core diameter results from the use of low index "barrier" layers between the core and cladding. How the near field is affected by such fluctuations near the cladding has not been completely established. Also, in graded-index fibers, there is a loss of resolution near the core-cladding boundary due to the decrease in local numerical aperture [13]. Some of these problems may be alleviated in a recently described "modified near-field" technique [14]. Despite some limitations, near-field measurements do indicate where power is spatially located in the fiber and, in some practical situations, this may be more important than the core diameter determined from the index profile.

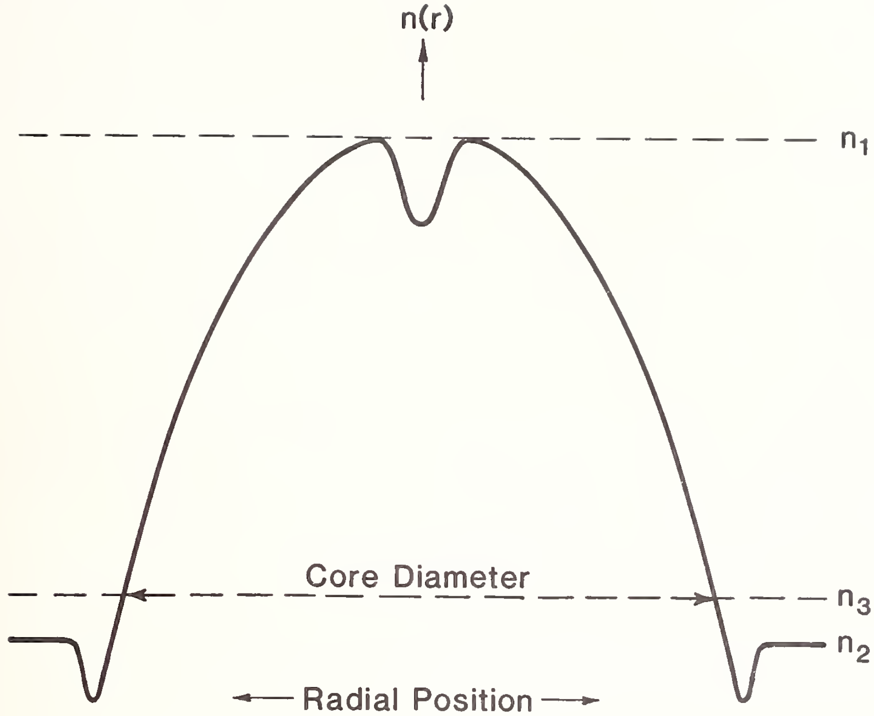

Figure 2. Points on a typical graded-index profile used for determining core diameter. Absolute index values do not have to be known.

2.3 Mode Volume Transfer Function

Holmes, et al., have introduced a concept describing the effect of propagation on spatial and angular intensity distributions in graded-index fibers [15]. They define an "EMV" (effective mode volume) based on far- and near-field intensity distributions. Specifically, the EMV at a given point along the fiber is the square of the product of the FWHM (full width at half maximum) of the near-field and the sine of the HWHM (half width at half maximum) of the far-field.

EMV is related to the number of modes excited in the fiber. This can be intuitively seen when applied to the expression for the total number of guided modes, N, in a fully excited graded-index fiber having a power law profile, g [16].

$$N = \frac{g\Delta}{2 + g} \left(\frac{2\pi n_1 a}{\lambda}\right)^2 \qquad (12)$$

where a is the core radius, λ the wavelength, and other terms have been previously defined. After arranging terms,

$$N = \frac{g}{2 + g} \left(\frac{2\pi^2}{\lambda^2}\right) [(NA) \cdot a]^2 \qquad (13)$$

$$\approx \frac{g}{2 + g} \left(\frac{2\pi^2}{\lambda^2}\right) \cdot \text{EMV}. \qquad (14)$$

Of interest is the EMV transfer characteristic for a fiber. This describes how various EMVs propagate in the fiber and is a plot of output EMV versus input EMV. By controlling launch spot and NA, various input EMVs can be generated. Input EMVs are determined from radiation patterns exiting a 2 m length at the input. The corresponding output EMVs are obtained from radiation patterns exiting the long length.

The EMV transfer characteristic gives information on mode coupling, differential mode attenuation, and quasi-steady-state EMV. A fiber without mode coupling or differential mode attenuation appears as a 45° line on the transfer characteristic plot; i.e., the output EMV is equal to the input EMV.

A principle use of the EMV concept is in the prediction of concatenation. EMV transfer characteristics and attenuation versus EMV for all the fibers in the link allows one to predict accurately the concatenated attenuation for any input EMV [15].

3. SINGLE MODE FIBER MEASUREMENTS UTILIZING NEAR-FIELD PATTERNS

3.1 Fundamental Mode Spot Size

The size of the fundamental mode is an important parameter for single-mode fibers. For most index profiles, the mode profile shape is close to Gaussian. A Gaussian curve can be described by a number of constants including FWHM, 1/e diameter, and $1/e^2$ diameter. Definitions have not been standardized at the present.

Spot size is important in determining splice loss when two fibers are joined. With the low losses available in single-mode fibers (0.16 dB/km), a mismatch in spot size can cause attenuation equivalent to several kilometers of fiber.

The near-field method of determining spot size is perhaps the most fundamental of all the techniques available because it gives directly, by definition, the radial intensity variation of the fundamental mode. Other methods for determining spot size include transforming far-field patterns, measuring power loss from lateral splice offset, and analyzing light from the fiber with various gratings and rulings [17,18].

3.2 Second Order Mode Cutoff

Another important parameter for single-mode fibers is the wavelength where the second-order mode first appears. At wavelengths longer than the cutoff wavelength, the fiber supports only a single waveguide mode. The presence of a second mode is undesirable because at those wavelengths where only a few modes propagate, the differential group velocities are rather large (several nanoseconds) and give rise to widely separated multiple pulses.

Cutoff wavelength can be determined by measuring the spot size as a function of wavelength [19]. Near cutoff, the spot size is close to a minimum. At wavelengths longer than cutoff, more power propagates in the cladding and spot size increases. At wavelengths shorter than cutoff, the second-order mode adds to the first-order mode to give a larger spot size. These measurements require a fair amount of calculation because data must be acquired and fit to give spot size for each wavelength.

Another near-field method for determining cutoff utilizes the pattern shape. The second-order mode has an on-axis minimum while the fundamental mode is Gaussian shaped with an on-axis maximum. Cutoff is defined as that wavelength where the central portion of the near-field pattern flattens out and just begins to exhibit a dip due to the presence of a small amount of second-order mode power [20].

It should be pointed out that both of the above methods for determining cutoff depend on the length of fiber sample. All methods based on transmission suffer from this problem [21]. At cutoff the loss of the second-order mode is exceptionally high, approaching 1000 dB/km. Thus, the ratio of second-order mode power to first-order mode power is a function of fiber length and true cutoff would require a very short sample--perhaps less than 1 mm. With this in mind, the cutoff wavelength determined by the above methods on a few meters of fiber might well be referred to as an "effective cutoff." While it is not the actual cutoff, it is sufficient for system design.

4. DESCRIPTION OF ONE-DIMENSIONAL NEAR-FIELD SYSTEM

In a near-field system, light is launched into the fiber sample at one end and the intensity distribution across the exit end face is measured. This pattern is acquired by translating an apertured detector across a magnified image. Reference 7 gives a brief description of one of the first near-field systems. Arnaud and Derosier demonstrate a variation of the standard near-field technique by measuring the transmitted power as a small area of illumination is translated across the input end face [22]. This type of apparatus is not commonly used today. A recently proposed method called the modified near-field technique is an interesting variation of the standard method. An absolute measure of the index difference is possible with this method. A more detailed description will be given later in this section.

This section describes the optics, electronics hardware, and calibration of the NBS system. Experimental technique and system performance are also discussed.

4.1 Optics

The system optics are divided into two parts--the launch optics and the exit optics. Both parts must be designed properly for optimum system performance.

The launch optics are shown in figure 3. The radiation source is a tungsten-halogen projection lamp. Since there is a coil structure to the filament, the bulb is frosted using

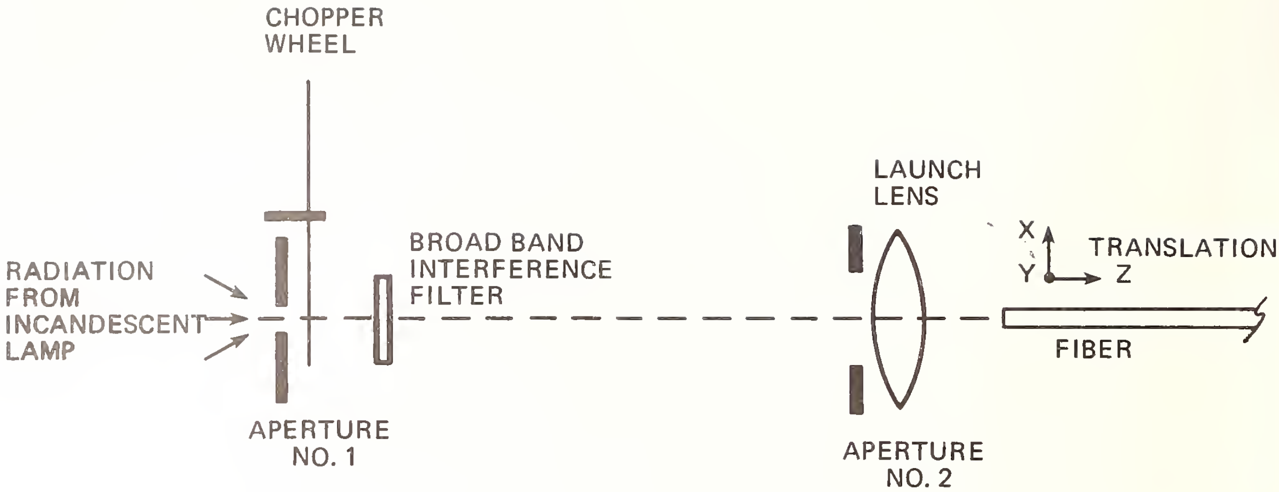

Figure 3. Launch optics used with near-field systems.

a "grit" blast to provide a diffuse source. This eliminates spatial variations in the radiation and approximates a Lambertian source. An aperture (aperture #1) is placed near the bulb. The spot size on the launch end of the fiber is controled by the size of aperture #1. For overfilled launch conditions, where the spot size is larger than the core diameter, aperture #1 is typically 2000 μm in diameter; this gives a 100 μm diameter spot on the fiber.

A chopper wheel is placed immediately after aperture #1. The chopper wheel acts as an "on-off" switch to convert the dc white light source into a train (in the time domain) of square pulses. The chopper enables the use of phase-sensitive detection and substantially increases the S/N (signal-to-noise) ratio.

After the chopper wheel, the radiation passes through a broadband interference filter. Wavelength selection is accomplished with this filter. A wide linewidth bandpass is used to reduce modal ripple caused by the summation of a finite number of modes [23]. The filters used in the system are centered at 850 and 600 nm and have full half intensity widths of approximately 80 nm. An 850 nm filter is often used since this is a wavelength common to fiber telecommunications links.

After the interference filter, the light is focused onto the fiber by a lens assembly. The camera lens assembly can be modeled as an aperture (aperture #2) and a simple lens. The DMAG (demagnification) ratio is given approximately as

$$DMAG \approx L/F, \tag{15}$$

where F is the focal length of the lens and L is the distance from aperture #1 to the lens. The spot size on the fiber is equal to the size of aperture #1 divided by DMAG. The usual

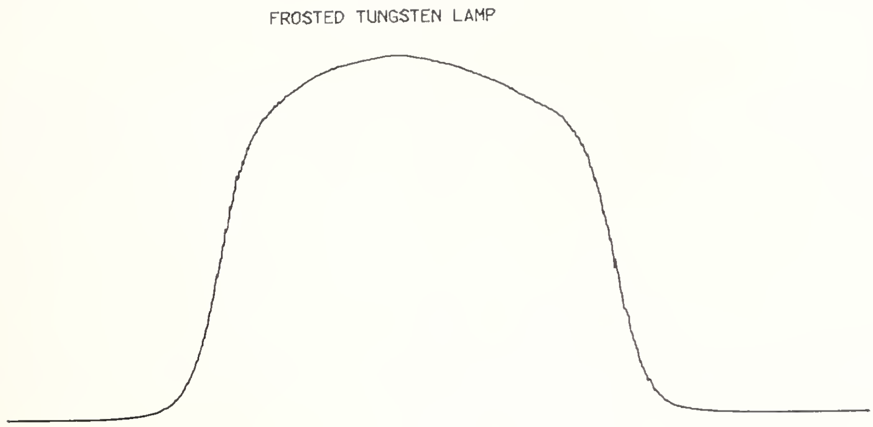

Figure 4. The radiation pattern of the "grit-blasted" envelope tungsten-halogen lamp image at the fiber entrance face.

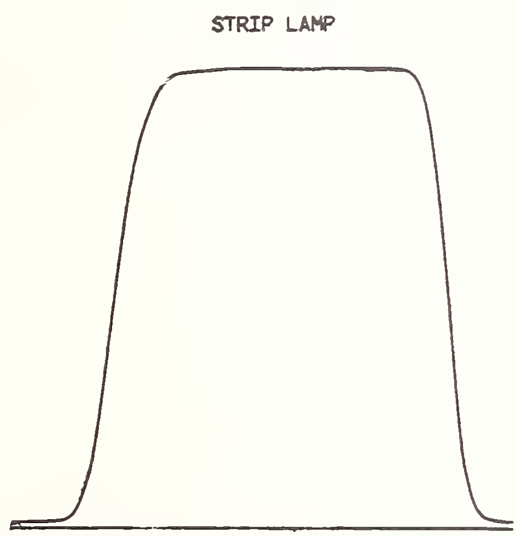

Figure 5. The radiation pattern of the flat tungsten strip lamp image at the fiber entrance face. Note that a more uniform pattern is launched.

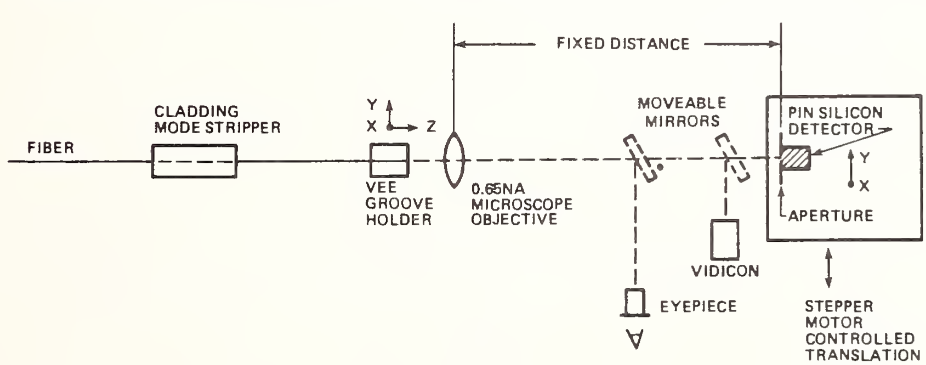

Figure 6. Exit optics for the system. The fiber enters from the left and is magnified by the microscope objective onto the apertured PIN detector. Alternatively, the eyepiece or vidicon may be used to inspect the fiber exit face.

100 μm diameter spot spatially overfills 50 μm diameter core fibers. Figure 4 gives the radiation pattern of the source at the fiber entrance face. If a flat tungsten strip lamp is used, a much more uniform pattern results (fig. 5).

The numerical aperture of the launch is totally dependent on the f number controlled by aperture #2. The conversion from the f number to NA is made with the help of the following equation

$$NA = \sin[\tan^{-1}(\frac{1}{2f\ \text{number}})]. \tag{16}$$

For an f number of 1.3, the launch NA is 0.36. Since the fiber NA rarely exceeds 0.2, an angular overfill condition is met for an f number of 1.3.

Light is launched from the camera lens into the bare fiber which rests on a vee-groove holder. The fiber is held in the vee-groove by a piece of adhesive tape and a small padded weight. The vee-groove is fastened to an xyz translation stage for ease of focusing and positioning. The bare fiber is placed in a cladding mode stripper which removes light from the cladding. The stripper is made of black felt soaked in index-matching oil. The bare fiber is laid on the felt and sandwiched by a second oil-soaked strip of black felt; the cladding mode stripper is 10 cm long.

For many reasons it is important that the fiber be angularly and spatially overfilled. This condition assures that all modes are excited. If the fiber is underfilled, a restricted mode distribution exists at the exit end of the fiber and would yield an incorrect result in the case of core diameter measurement.

Exit optics for the system are shown in figure 6. The coating is again removed and the fiber placed through a cladding mode stripper. Here the mode stripper is much shorter than at the launch end and is attached to the vee-groove which holds the fiber. Any residual cladding light is stripped out at this point. The vee-groove/mode stripper assembly is mounted on an xyz translation stage for positioning and focusing. The exit end face of the fiber is magnified by a 0.65 NA, 40X metallurgical objective designed for a tube length of 210 mm. The image plane scanned by the detector is 240 mm from the objective. Operating at or near the recommended tube length of the objective reduces spherical aberrations. A metallurgical objective is used because it does not require a cover slip for proper correction.

A detector is placed 240 mm from the objective and scans the intensity distribution of the magnified image. The magnification at the detector is approximated by the simple ratio

$$\frac{240\ \text{mm}}{210\ \text{mm}} = \frac{M}{40}, \tag{17}$$

where M is the magnification. This equation yields an approximate magnification of 45. A more accurate measurement of the magnification is made when calibrating the system. A 35 μm diameter aperture is placed in front of the detector to increase the resolution. The detector-aperture therefore could at best resolve 35 μm/45 or 0.75 μm as referenced to the fiber end.

The resolution of the near-field system is not determined by the apertured detector but by the fiber or magnifying optics. Since the objective collects all the light emitted from the fiber, the resolution is determined by the fiber NA. Adams, et al. [23] showed that the resolution is related to the number of propagating modes by analysis not unlike that used for the spatial resolution of a lens. Using a WKB argument, they showed that the half period of ripples in a near-field pattern yields the spatial resolution of the method. The limit of resolution, R_1, for a parabolic fiber is

$$R_1 = \frac{\lambda}{\pi(NA)}, \tag{18}$$

where NA ≈ 0.2 for typical fibers. For λ = 850 nm, this expression yields a resolution of 1.3 μm. In classical optics, the resolution limit of a lens is related to the Fraunhaufer diffraction pattern of a circular aperture illuminated by a uniform source, i.e., the spatial distance from the center maximum to the first dark ring of the Airy disk. If D is the diameter of the lens, F is the focal length, and r the radial distance from the maximum to the first dark ring of the Airy disk, then the resolution R_2

$$R_2 = \frac{1.22\ \lambda F}{D}. \tag{19}$$

Using the approximation,

$$NA = 0.5/f \text{ number}, \tag{20}$$

eq (19) can be expressed as a function of NA,

$$R_2 \approx 0.61 \frac{\lambda}{NA} \tag{21}$$

where f number = F/D. This is the common expression for the limit of resolution of a microscope objective [24]. This gives the minimum spatial separation of two points whose Airy disks might be distinguished in the image plane. That is, if the distance is 0.61 λ/NA, then the maximum of one disk corresponds to the first zero of the other; this is the so called Rayleigh criterion.

Using this criterion, the resolution is approximately 2.6 μm which is twice the figure given by eq (18). By coincidence, the resolution limit of eq (18) is equal to the 1/e width of the minimum spot size of a Gaussian beam in the focus of a lens.

Table 3. Different resolution limit definitions.

Type	Resolution	How derived	Normalized to Airy disk definition
Rayleigh criterion	$0.61\lambda/NA$	Distance from maximum to first dark ring of Airy disk pattern. From diffraction theory.	1
Gaussian	$\lambda/\pi(NA)$	Distance from max to $1/e^2$ of max of a Gaussian. From diffraction theory.	0.52
Adams, et al. (step)	$\lambda/4(NA)$	Half period of near-field pattern ripples. From mode theory.	0.41
Adams, et al. (parabolic)	$\lambda/\pi(NA)$	Half period of near-field pattern ripples. From mode theory.	0.52

Table 3 summarizes the different definitions of resolution limit. Normalized to the Rayleigh criterion, the remaining definitions show better resolution limits for the same parameters. Experimental data for the near field system discussed here indicates a resolution limit of 1.3 μm to 1.7 μm. These numbers were arrived at by measuring the half period of the ripples in the near-field pattern at a wavelength of 850 nm. At any rate, table 3 shows that there is a factor of two difference in the resolution depending on the analysis and definitions.

Alignment and focusing are accomplished by the use of movable mirrors, eyepiece, and vidicon as shown in figure 6. First, a fiber is imaged onto the detector at the measurement wavelength (typically 850 nm) and is focused using the on-axis index dip common to most fibers. Then, using a 600 nm filter, the first movable mirror is positioned to illuminate the eyepiece. The eyepiece is adjusted until the image appears in sharp focus. Now, when a fiber end is in focus at the eyepiece, it will be in focus at the detector when the mirror is moved out of position. The position of the vidicon is also determined as with the eyepiece, only with 850 nm light. In addition, the correct spatial position of the image is marked by cross-hairs on the video monitor. This guarantees that the fiber lies in the optic axis of the objective, and is in the optimum position for imaging. When the image of the fiber end on the video monitor is in focus and bisected by the cross-hairs, it will be in focus at the detector when the mirror is moved out of position.

4.2 Electronics

The detector is a silicon PIN diode in the photovoltaic mode [25]. This detector has a 5.1 mm^2 active area and a built-in operational amplifier. The output signal from the detector goes to the input of a lock-in amplifier. The reference signal for the lock-in originates from the chopper. The chopping frequency is approximately 400 Hz and the time constant of the lock-in amplifier is typically 40 ms. The dc output voltage from the lock-in is read by a DVM (digital voltmeter) and interfaced to computer memory.

The detector is mounted on two orthogonal stepper motors giving two degrees of freedom in the plane perpendicular to the optical axis of the objective. The motors are identical and have movements of 0.4 µm/step. Each motor has its own controller which contains the electronics required for stepping the motor. Controllers have TTL compatible interfaces for computer control of the electronics. A Z8 microcomputer is used to translate and take voltage readings from the detector. The microcomputer accomplishes the translation and voltage readings via its input/output ports.

4.3 Calibration

The accuracy of core diameter measurements would be suspect without a dimensional calibration. A calibration device has been developed for near-field systems [26]. It consists of a reticle illuminated by a large core/NA fiber and is intended to fit into a system in place of the fiber under test. The image in the detector plane is that of the reticle rather than a fiber endface. Photolithographic techniques common to integrated circuit fabrication are used to make the reticles. The substrate is glass 1.6 mm thick covered with 100 nm thick chromium film. Fine transparent lines appear in the opaque chromium film (fig. 7). Three 1.2 µm wide vertical lines are separated by 50 µm. A pair of horizontal lines 5 µm wide are located 100 µm on either side of the vertical lines. These lines aid in making scans perpendicular to the vertical lines. When a scan intersects both horizontal lines, the tilt of the vertical lines is less than 1° and the central regions are measured. The tilt error in measuring a 100 µm distance is less than 0.5 percent. The reticle is placed in a fixture and illuminated through a diffuser by a 2 m long, large core (300 µm), large NA (0.4) plastic fiber. Therefore, light fills up the NA of the objective. From eq (21) the resolution is approximately 0.9 µm for λ = 850 nm.

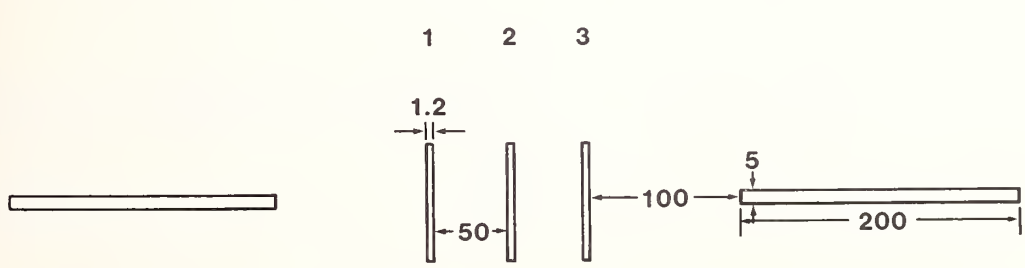

Figure 7. Calibration pattern on test reticle, all distances in micrometers. The calibration bars are in transmission.

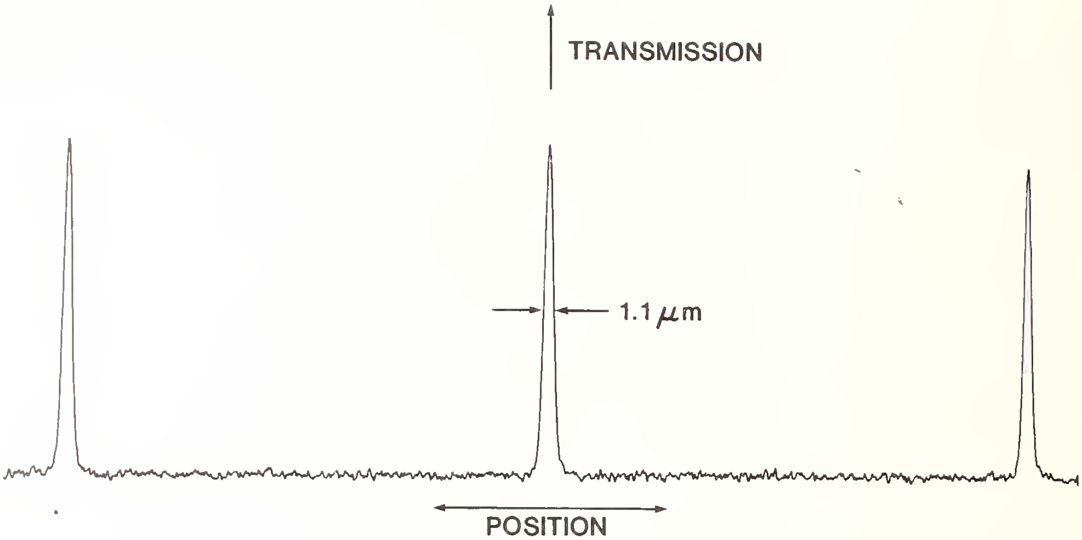

Figure 8. Analog results of a calibration scan using the NBS TNF system. Full-width-half-maximum of the calibration bars is 1.1 μm, consistent with expectations.

An analog result of a calibration scan is given in figure 8. A FWHM (full width half maximum) linewidth of 1.1 μm was measured in general agreement with expectations. The measurement of the width of the line is not the most important factor. The distance between the peaks is the critical parameter. The nominal distance between lines 1 and 3 is 100 μm. Fourteen repeated measurements of the 1 to 3 distance on the reticle were made, with it being refocused each time. These measurements showed that at λ = 850 nm the magnification of the near-field system is 45.5. Referenced to the fiber end face, the system acquires a data point every 0.22 μm. The standard deviation of 14 calibration measurements is less than 0.22 μm. The resolution limit of the objective does not limit the precision of the calibration since the resolution defines the ability to distinguish two lines close together whereas these measurements determine distances between centers of lines that are far apart. The measurement is limited by the motor movement which is 0.22 μm.

The linearity of the system can be determined by measuring the difference between lines 1 and 2 and lines 2 and 3. The 1 to 2 minus 2 to 3 distance was 0.3 μm. This is approximately the distance between data points (0.22 μm) indicating good linearity.

The stability of the apparatus was also tested using the calibration reticle. The detector was positioned at the peak of the center vertical calibration line. The drift of the system was determined by checking for decreases in intensity which are related to displacement from the peak of the calibration line, viz. figure 8. Rather surprisingly, the system exhibited a drift of less than 0.2 μm over a period of 30 min.

Calibration was also performed at λ = 600 nm. The magnification for this wavelength is 0.4 percent greater than that for λ = 850 nm. The difference is not significant enough to warrant correction to the data taken with the red filter. This also indicates the objective is well corrected for chromatic aberration.

Absolute calibration of the reticle is accomplished by comparing the distance between vertical lines to the wavelength of the 632.8 nm transition of the HeNe laser. Using a piezoelectrically driven stage, the reticle is smoothly translated across a focused (1 μm spot) HeNe laser beam. A large area detector is placed behind the reticle so that it is illuminated by the focused beam as the transparent calibration lines move across the HeNe spot. A Fabry-Perot interferometer is used with a second HeNe laser to measure the displacement by fringe counting as the reticle is translated. Since a short Fabry-Perot cannot resolve the individual modes of a HeNe laser, the transmission fringes occur every half wavelength or 316.4 nm. The tranmission fringes from the interferometer are recorded by another large area detector. The experimental apparatus is shown in figure 9; reticle transmission and the corresponding Fabry-Perot fringes are also shown. The distance between lines 1 and 3 is measured to be 100.1 μm. The precision of the data was determined to be 0.1 μm (one standard deviation) for six measurements. The difference between lines 1 and 2 and lines 2 and 3 is 0.0 ± 0.1 μm.

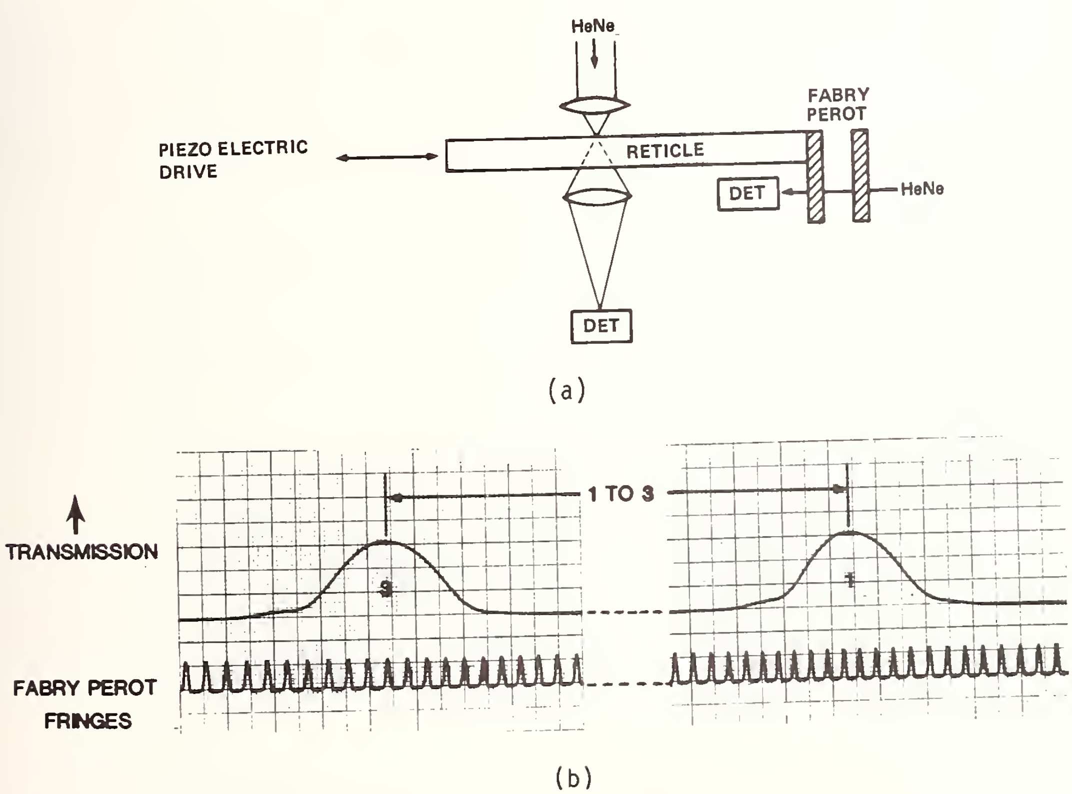

Figure 9. (a) Method used for placing absolute calibration on reticle. (b) Line spacing referenced to Fabry-Perot fringes, in this example the 1 to 3 distance is 316.5 fringes.

4.4 Experimental Technique and Performance

The system acquires the near-field intensity distribution by magnifying the fiber end face and scanning a detector across the diameter of the image. In figure 6, the apertured detector is at a fixed distance from the objective which insures that the magnification ratio (and therefore the calibration) remains constant and independent of system adjustments.

Care must be taken in preparing good ends on the fiber sample especially for core diameter measurements. First the buffer coating is stripped back about 15 cm before the ends are cleaved. End faces should be inspected with a microscope to insure cracks or foreign matter do not exist in the core region. They should also be inspected for flatness and perpendicularity to the axis. This can be accomplished by shining a HeNe laser on the end face parallel to the axes. Four percent of the light is reflected off the end. If the surface is not perpendicular light will reflect off at some angle. Any nonuniformity of the end surface will cause a deformation in the intensity distribution of the reflected light. The use of a concentric ring pattern at the laser gives a quantitative measure of the nonperpendicularity of the cleave. End faces that are nonperpendicular by more than 1.5° are rejected. Gross deformations of the reflected spot on the target are also grounds for rejection.

At the launch end, the fiber is placed in the vee-groove. The cladding mode stripper is used on the bare part of the fiber to eliminate unwanted cladding light. The other end of the fiber is placed in the vee-groove/cladding mode stripper assembly at the imaging optics. Using the 600 nm (red) filter, the image of the fiber end is brought into the field of view of the eyepiece via the movable mirror and focused. The red filter is then replaced by the 850 nm filter, the eyepiece mirror is translated from the optical axis of the objective, and the image is detected by the vidicon via its turning mirror. The image is centered (usually at the trough of the index dip) on the electrically generated cross-hairs of the video monitor. The image is then projected on the detector plane by removing the mirror from the light path. Fine spatial adjustments to find the trough of the index dip are performed at the detector by manually moving the motor.

The signal from the detector is acquired by the lock-in amplifier. To optimize the voltage reading, the phase adjustment is tuned to yield the maximum. The launch optics are then adjusted to maximize the signal. The system is now ready to take data in either the vertical or horizontal axis. Usually 320 data points are taken for multimode fibers, corresponding to approximately 35 μm on each side of the starting point. A 320 point scan usually takes about 6 min.

Performance of the system can be determined by its accuracy, stability, precision, and dynamic range. Precision is a statement of measurement repeatability. It is not to be confused with "systematic" error which is the offset of the average of a large number of measurements from the true value. Best precision is obtained when a measurement is repeated without disturbing any parameters. For a typical 50 μm diameter multimode graded-index fiber, measurement of the core diameter at 5 percent points is repeatable with a one standard deviation of ±0.2 μm (±0.4 percent). Here, the near-field measurement was made six times without disturbing any parameters. It was accomplished with an overfilled launch condition at a wavelength of 850 nm. This indicates that the system does not have appreciable drift, thus confirming the stability data.

For practical purposes however, near-field measurements are made with new fiber ends and system alignment. To determine precision under these conditions, six successive lengths of fiber were cut and measurements were performed on each length. Six different fibers from four different manufacturers were tested in this way. All of these fibers exhibited smooth backscatter signatures indicating very little diameter variation with length. The average precision (one standard deviation) for core diameter on these 50 μm graded-index fibers was ±0.4 μm (±0.8 percent).

Typical signal-to-noise ratios of the system are about 40 dB for an unattenuated source at a wavelength of 850 nm. The minimum tolerable S/N is about 17 dB. Therefore, the dynamic range of the system is 23 dB. Figure 10 is an analog near-field profile with the source attenuated by 22 dB. When the voltage is digitized, typical maximum to minimum digitized outputs are between 400:1 and 1000:1 depending on the scale of the lock-in amplifier.

Improvements in the dynamic range may be made by increasing the source linewidth or the lock-in time constant. However, if the lock-in time constant is increased, the time required to gather the data will also increase. This may not be an acceptable trade-off. A summary of the system specifications is given in table 4 for typical 50 μm diameter fibers.

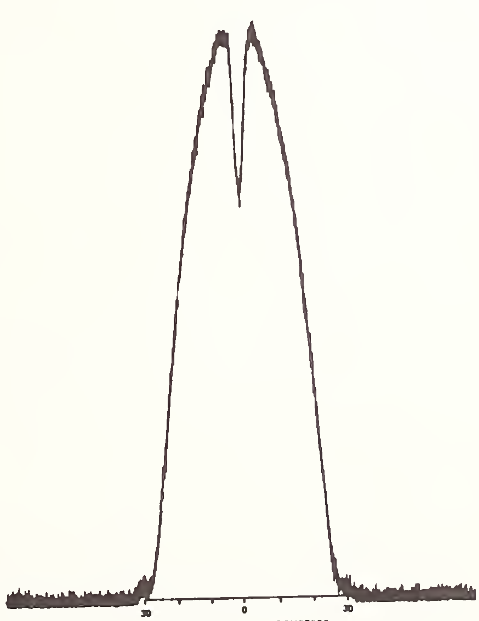

Figure 10. Analog near-field plot from a 2 m length of graded-index fiber with source attenuated by 22 dB. Signal-to-noise ratio in this figure is 17 dB.

Table 4. Near-field specifications for multimode fibers.

Characteristic	Performance
Magnification	45.5 at 850 nm 45.8 at 600 nm
Resolution	1.3 to 1.7 μm
Accuracy	0.5 μm
Stability	<0.2 μm over 30 minutes
Precision	±0.5 μm or ±0.8% (one standard deviation)
Dynamic range	23 dB at 850 nm

5. DESCRIPTION OF TWO-DIMENSIONAL CONTOURING TECHNIQUE

Determination of core noncircularity is of interest to standards groups. Knowledge of this parameter allows the user to properly select connectors and evaluate splice loss. In addition, for graded-index fibers the circularity of the core theoretically affects the leaky mode attenuation coefficient. The more elliptical a core, the more rapidly the leaky modes attenuate.

Standards organizations have yet to specify the amount of core noncircularity allowed. A noncircularity (maximum minus minimum diameter) of 6 percent has been recommended by the CCITT and 8 percent by the IEC [27]. Corresponding to tolerance fields of ±3 μm and ±4 μm for 50 μm core fibers. Both organizations are studying a four circle tolerance method. In this method four concentric circles are used such that the cladding/air boundary is contained within the ring defined by the outer two circles and the core/cladding interface is contained within the ring defined by the two inner circles (fig. 11). The width of these rings is called the tolerance field. For simplicity, the tolerance field in this chapter refers to the core/cladding interface only. Generally, the field is constructed by determining the smallest circle that circumscribes the interface and defining it to be the outer circle. The inner circle is that circle which has a radius equal to the distance between the center of the circumscribing circle and the closest core/cladding point. A microscope method is commonly used in which the template of four concentric circles is superimposed on the image of the fiber cross section to determine if the boundaries lie within the rings. This is strictly a "go-no go" test to see if the fiber geometry lies within the tolerances. Inspection is often performed by an operator.

Due to the properties of the human eye, this method of inspection is not reliable. Not only does the eye respond as a logarithmic function of incident light intensity, it suffers a response "over shoot" around the boundary of regions of different intensity. This phenomenon, called the Mach-band effect [28], is an important physical limitation of th

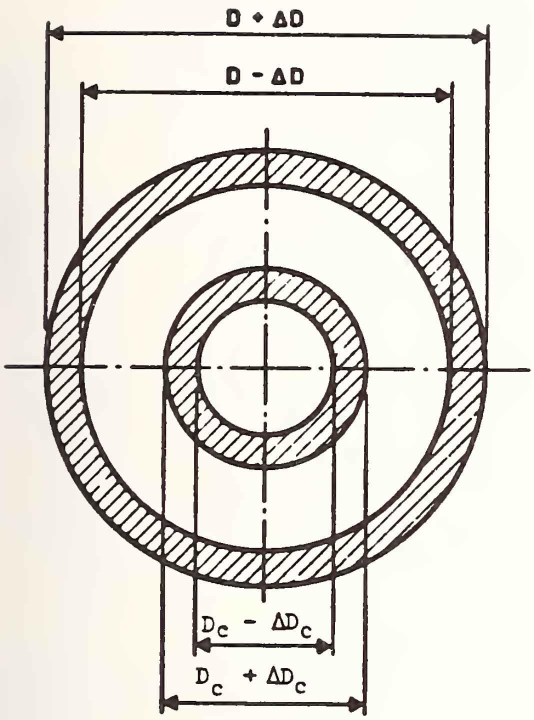

Figure 11. The four circle tolerance field for determining core and cladding noncircularity.

microscope method where inspection is performed by a human operator. Therefore, the Mach-band effect coupled with subjective human judgement make the use of an operator inspected microscope method for determining core diameter undesirable.

Alternate methods for determining ellipticity have been proposed in lieu of a tolerance template. The focusing [29], scattering [30], and Fourier transform methods [31] have been suggested. These techniques, however, take much processing time for simply contouring a boundary. A more promising method for making geometric measurements was proposed by Marcuse and Presby [32] in which a vidicon with a video digitizer scans a near-field image to find the core/cladding and the outside diameter. The image is usually digitized to 8 bits or an intensity resolution of 255:1. Although attractive, the vidicon target may be spatially nonuniform and require a point-by-point calibration [33]. In addition, many cameras have an intensity dependent gain which can cause nonlinear processing if care is not taken.

A method is described in which the near-field system is used to map an isointensity contour of the core. Use of the orthogonal stepper motors enables the detector to be positioned at any location on the fiber image. The cursor-like property of the detector can be used to locate and circumscribe the core boundary. Algorithms commonly used in digital image processing are used to perform the contouring. The LML rule (T Algorithm) [34] with a simplification of Freeman's chain code [35] programmed into the computer controlling the motors is used for locating the spatial coordinates of the core/cladding boundary. The data is then analyzed by another program to find the tolerance field. The experimental apparatus, procedure, and electronic hardware are the same as that for the conventional near-field system.

Again, the Z8 microcomputer is used for acquiring the data. In this case however, both motors are translated for a single map of the core. Also, the data recorded in memory is not the voltage of the DVM but the spatial (x,y) coordinates of the isointensity points. Analysis is performed by a graphics computer to yield the tolerance ring and the isointensity contour map.

In order to minimize data acquisition time, a finite number of data points (locations) are recorded. Too few data points result in large errors in the contour, whereas too many take time. This problem can be modeled by assuming the fiber core boundary can be described by an ellipse. Essentially, this equation has four parameters: (1) the x-position; (2) the y-position; (3) the major axis; and (4) the minor axis. Using the spatial analog to the Nyquist frequency criteria, the minimum number of samples required to describe an ellipse without major errors (aliasing) is 4 x 2 = 8. Better approximations may be made with 16 isointensity locations. Sixteen data points appeared to provide sufficient information to construct a good contour map and were therefore chosen as the number of points gathered.

The use of the LML rule proved to be adequate for contouring a constant intensity level. The chain coding scheme adapted well to the T algorithm. The LML rule is used to decide the direction of travel of the cursor (detector) out of each point relative to the direction of entry into that point. The cursor is always looking toward its left to see if the intensity is the same as the reference intensity.

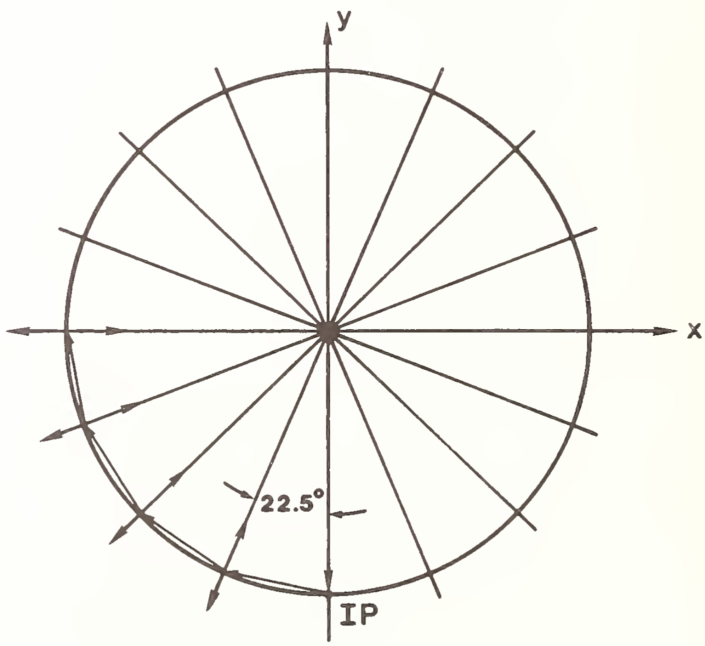

Figure 12. A diagramatic representation of the algorithm used to acquire the iso-intensity points for a contour map of the core.

In the contouring algorithm used, the LML restricts the cursor to the inside of a hypothetically circular isointensity boundary. Also, only 16 isointensity locations are sought. These 16 points are of equal angular spacing. Figure 12 is useful for explaining the contour algorithm. Before any mapping is performed, the fiber end is focused onto the detector. The detector is moved to the central extremum location of the fiber image. The extremum, taken as the origin (0,0), is usually the trough of an index depression in the profile and is at or near the geometric center of the image. The contouring program is activated and records the 16 equi-angular points as follows:

1. The operator is prompted to give the initial point (IP) in micrometers. This is usually the 5 percent core diameter which has been determined previously.
2. The computer moves the detector in the -y direction to the specified location and records the number of motor steps in cartesian coordinates. It also stores the intensity at the IP. This intensity is used as the reference for the isointensity contour.
3. The computer calculates the number of x- and y-axis motor steps required for 22.5° translations of the detector in a single quadrant at the same radius as the IP. This information is used for all four quadrants of a circle. It is expected that the cursor will move clockwise from the IP and stay inside of the imaginary perfect circle calculated by the computer.
4. The computer moves the detector clockwise 22.5° on the calculated perfect circle and takes the intensity reading of the fiber image at that location.
5. The computer makes a decision--is the intensity greater, equal, or less than the reference? If greater, the detector is moved radially out of the circle and the intensity is read every 0.1 μm relative to the image. When encountering an intensity less than or equal to the reference intensity, that location is recorded in memory as (x,y), where x and y are the x-axis and y-axis motor steps taken. If the intensity reading is less than the reference upon completion of the 22.5° rotation, a radial search is performed toward the center of the image at 0.1 μm intervals. Upon encountering a measured intensity greater than or equal to the reference, that location is recorded. If the intensity of the point on the calculated circle is equal to the reference, that location is recorded. This routine is repeated until the detector wraps around to the IP. The 16 points are typically gathered in 6 to 7 min.

The data is processed to yield a tolerance field containing all of the 16 isointensity locations. Determining the noncircularity is not as simple as just finding the maximum and minimum radii from the origin (central extremum). It is more accurate to find the smallest circle that circumscribes the data points. The origin of such a circle will most likely be offset from the central extremum location. The inner circle of the tolerance field is formed by finding one of the 16 data points whose distance is closest to the center of the circumscribing circle.

An iterative approach was used to perform the task of finding the circumscribing circle. The method calls for the computer to construct an 11 x 11 grid overlayed on the 16 data points with the grid origin on top of the origin of the cartesian coordinates defining the data locations. The size of the grid is 88 μm x 88 μm. From each grid point, the distances to each of the 16 data points are calculated. The largest of the distances is then compared and the smallest of these distances is selected. The grid point corresponding to this distance is then the new origin and an 11 x 11 grid of 8.8 μm x 8.8 μm is built around it. This process is repeated twice more until an 11 x 11 grid of 0.088 μm x 0.088 μm is formed. Again, the smallest of the largest distances is found. The grid point corresponding to that distance is the center of the smallest circumscribing circle around the 16 data locations. Using that center, the shortest distance between it and the 16 data points is found. This is the inner circle that defines the tolerance field. The radius of the outer circle minus the radius of the inner circle yields the tolerance field (usually given as ±(outer radius-inner radius)). The noncircularity is defined by the difference in the diameters of the inner and outer circle. The circles are plotted along with the relative positions of the data points.

6. EXPERIMENTAL RESULTS FROM NEAR-FIELD MEASUREMENTS ON MULTIMODE FIBERS

6.1 Length Dependence

In multimode fibers, the higher order bound modes generally attenuate more rapidly than the lower order modes. If leaky modes are also excited, the situation becomes more complex. Since the relative amount of power left in each mode is a function of fiber length, near-field core diameter may depend on test sample length. Therefore, a study was conducted in which the core diameter was measured for 1, 2, and 7 m sample lengths. Also, the effects of large bends (loops) in the fiber sample for 1 and 2 m lengths were investigated.

Table 5 gives the core diameter differences between 2 m and 7 m fiber samples. The average difference is 0.4 μm. All the results are positive, indicating a gradual contraction of the radiation pattern owing to increased attenuation for higher order modes (differential mode attenuation). The amount of spatial contraction differs among fibers, but the magnitude of the differences are always small for the lengths studied.

A comparison of core diameters was made between 2 m lengths having one 30 cm diameter loop and straight 1 m samples (see table 6). The average core diameter difference is +0.5 μm. One large loop was used in the 2 m sample to simulate gradual bends that may exist in the fiber when measurements are being made on a typical test bench. Again, the contraction in the pattern was small and the differences positive. Comparisons of the 1 m and 2 m radiation patterns are shown in figures 13 to 18. The average difference in core diameters between samples having two 15 cm loops and straight, 1 m samples (1 m minus 2 m) was +0.9 μm. Results indicate that radial bends less than 30 cm in diameter are not recommended since such bends act as a mode filter and cause increased attenuation for higher order modes which results in smaller measured core diameter.

Table 5. Length dependence of 5 percent core diameter (2 m versus 7 m).

Fiber #		Diameter from 2 m length minus diameter from 7 m, μm
1		+0.2
2		+0.3
3		+0.7
4		+0.1
5		+0.7
6		+0.1
	Average	+0.4

A comparison was made between 2 m and 1 km lengths of graded-index fiber. Figure 19a shows the near-field patterns from 2 m and 1 km lengths of the same graded-index fiber. The 1 km pattern is noticeably contracted. The 5 percent diameter for the 2 m length is 4.2 μm greater than that for the 1 km length. The far-field pattern was also measured under the same conditions (fig. 19b) and it also shows a contraction. For the 1 km length, a contraction of 0.9° or 8 percent is observed. A length comparison of near-field patterns was also made on a multimode step fiber. The 2 m sample shows the distinctive "leaky mode ears" (fig. 20). At 1 km the leaky mode power is not evident.

Table 6. Length dependence of 5 percent core diameter (1 m versus 2 m).

Fiber #		Diameter from 1 m length minus diameter from 2 m, μm
1		+0.7
2		+0.5
3		+0.4
4		+0.5
5		+0.4
6		+0.3
	Average	+0.5

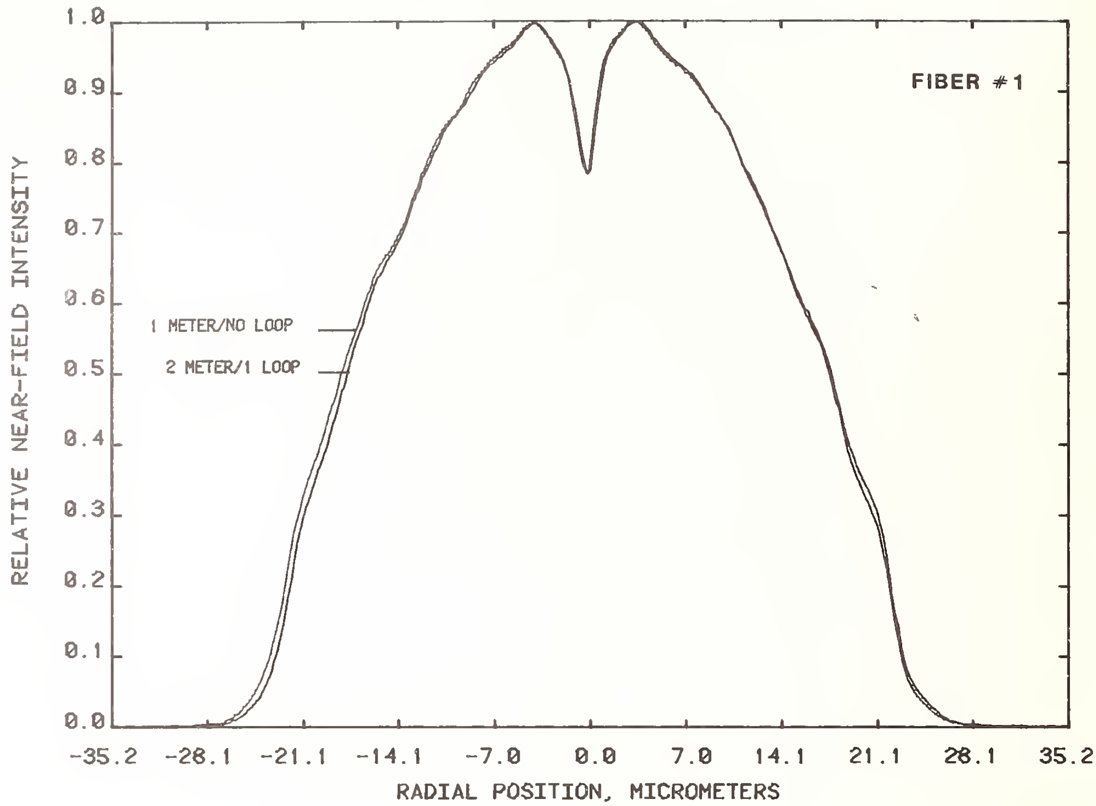

Figure 13. TNF comparisons for 1 and 2 m specimen lengths, 850 nm, fiber #1.

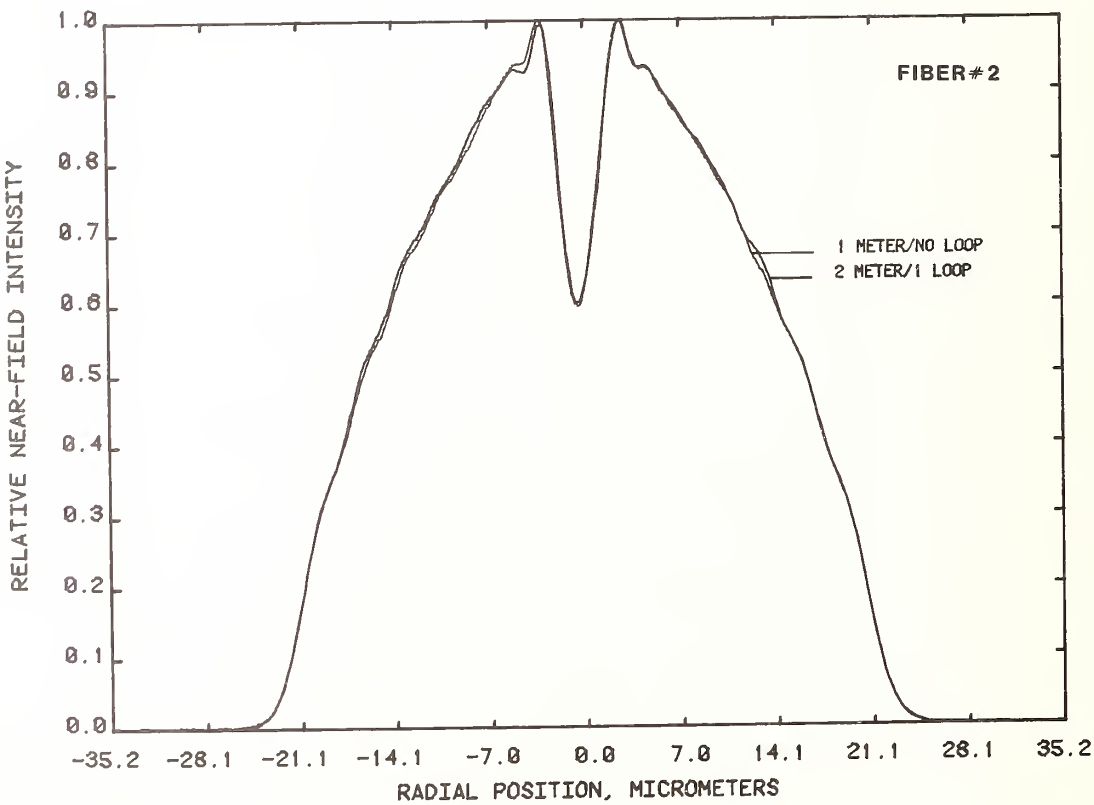

Figure 14. TNF comparisons for 1 and 2 m specimen lengths, 850 nm, fiber #2.

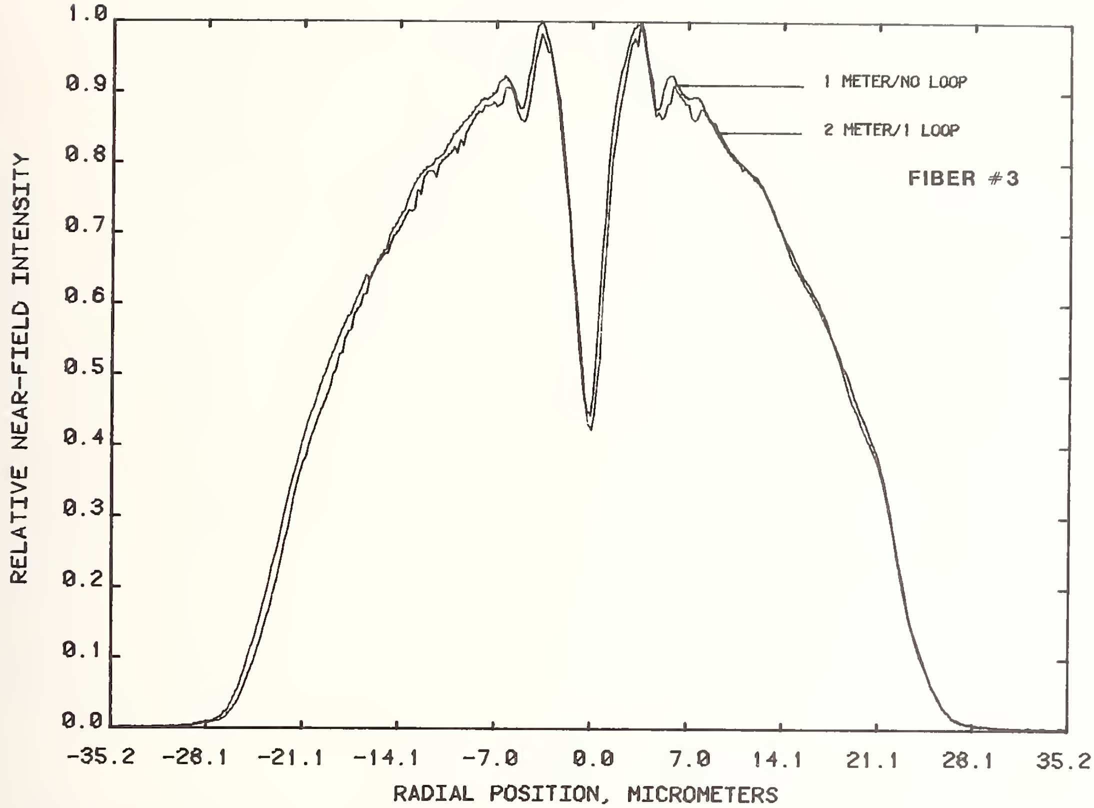

Figure 15. TNF comparisons for 1 and 2 m specimen lengths, 850 nm, fiber #3.

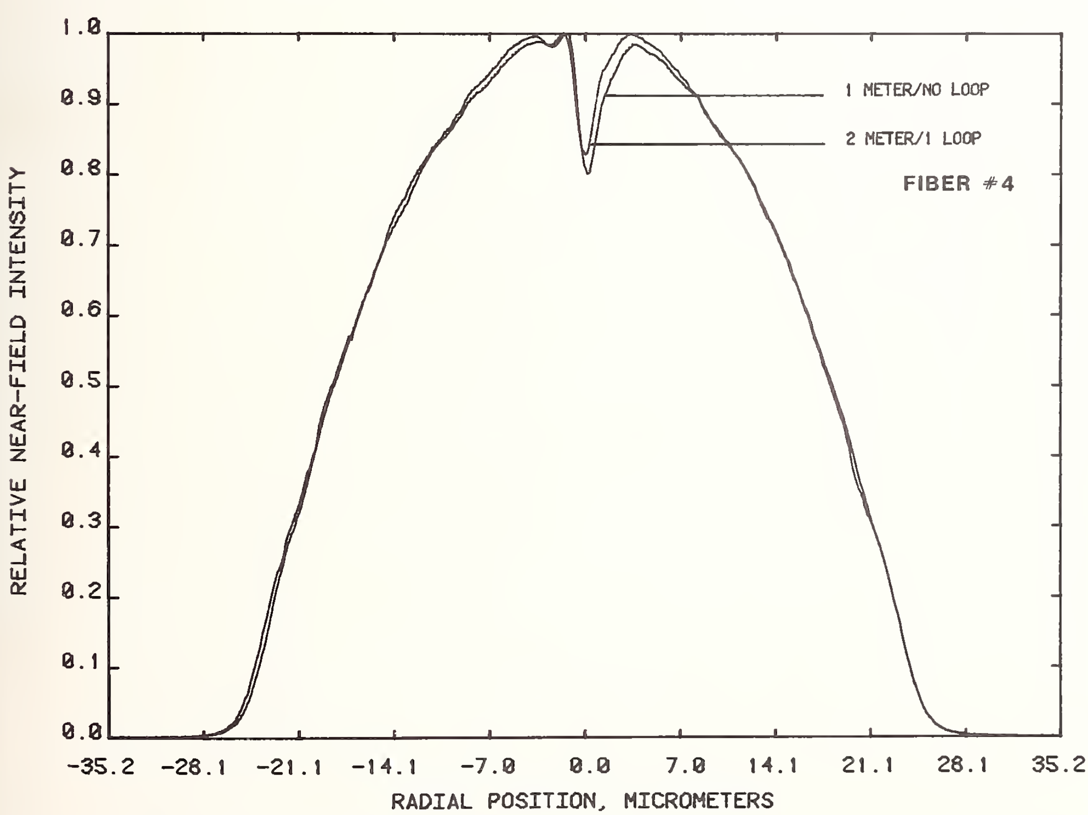

Figure 16. TNF comparisons for 1 and 2 m specimen lengths, 850 nm, fiber #4.

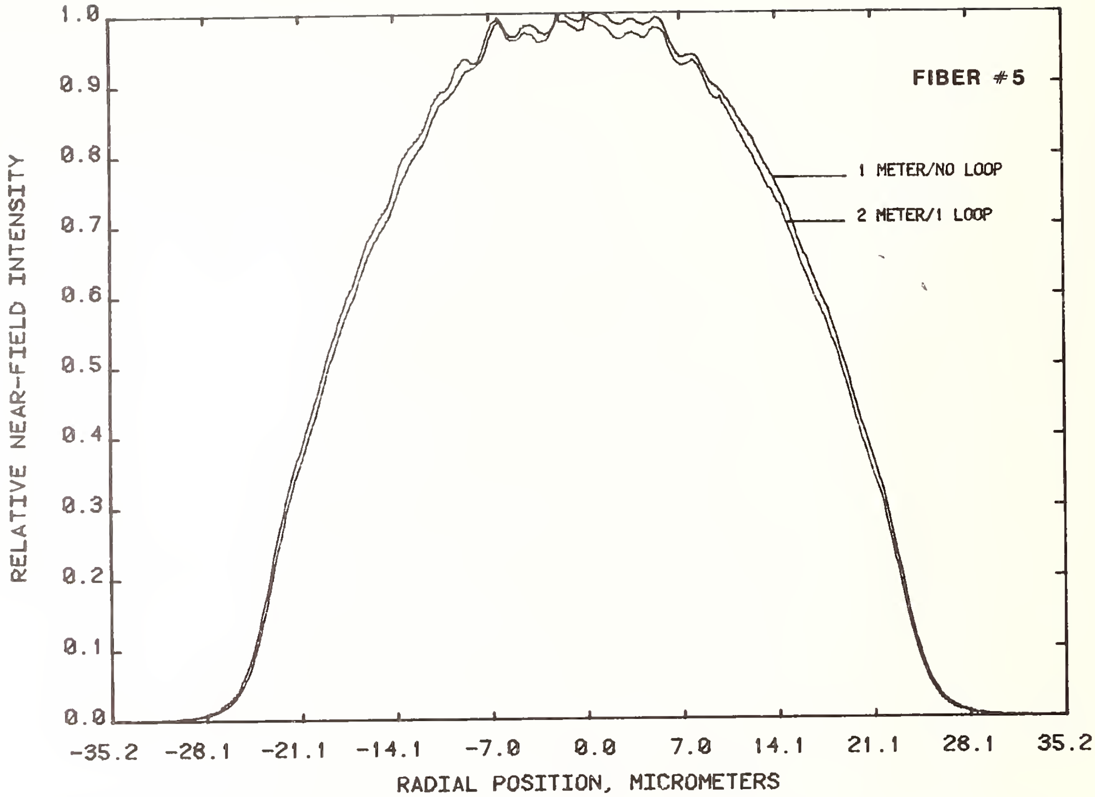

Figure 17. TNF comparisons for 1 and 2 m specimen lengths, 850 nm, fiber #5.

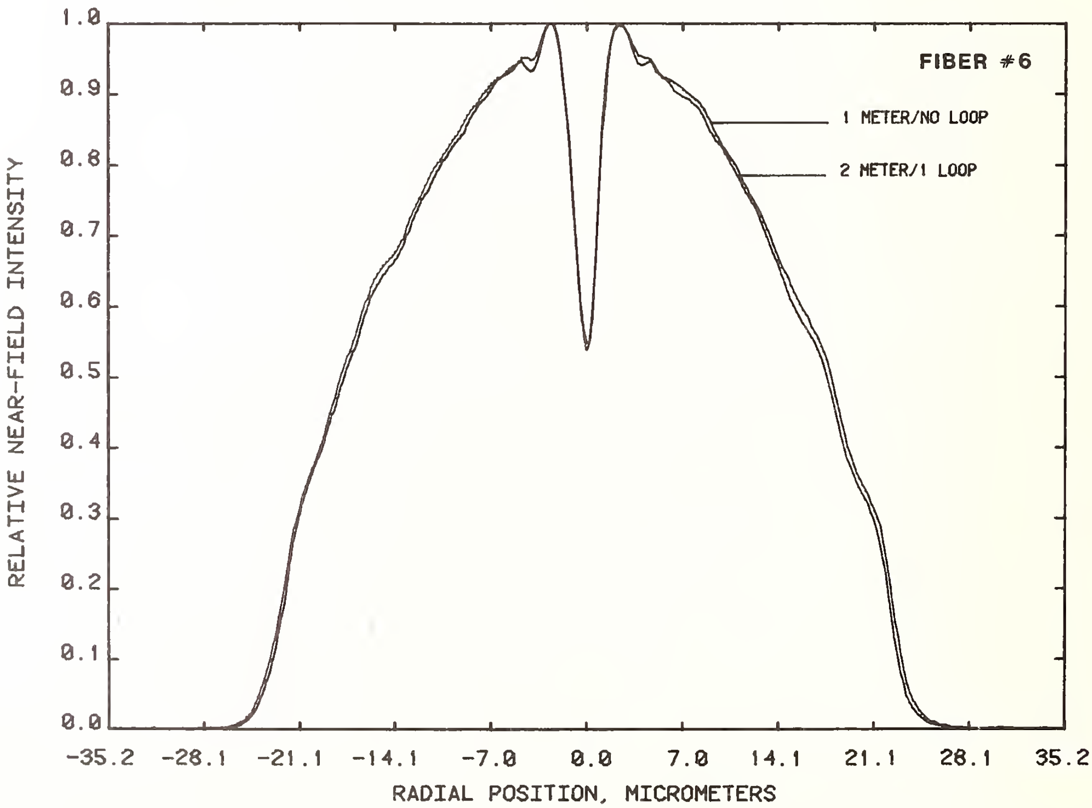

Figure 18. TNF comparisons for 1 and 2 m specimen lengths, 850 nm, fiber #6.

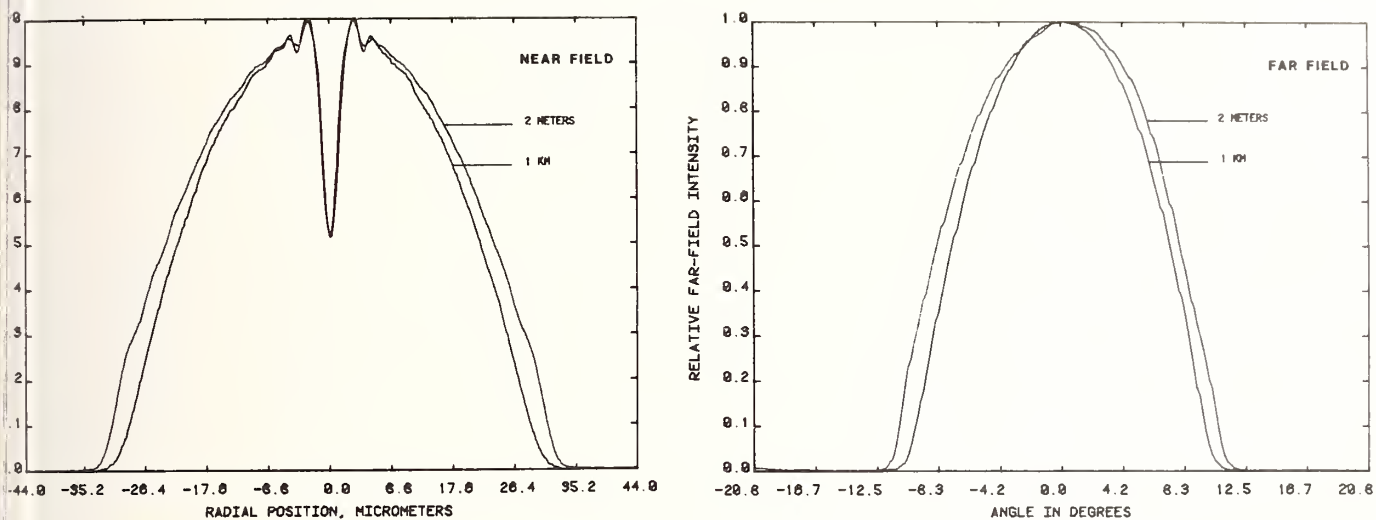

Figure 19. (a) Normalized near-field radiation patterns at 2 m and 1 km from an initially overfilled graded-index fiber. (b) Normalized far-field radiation patterns at 2 m and 1 km for the same fiber and launch conditions. The restriction indicates the loss of power in higher-order modes.

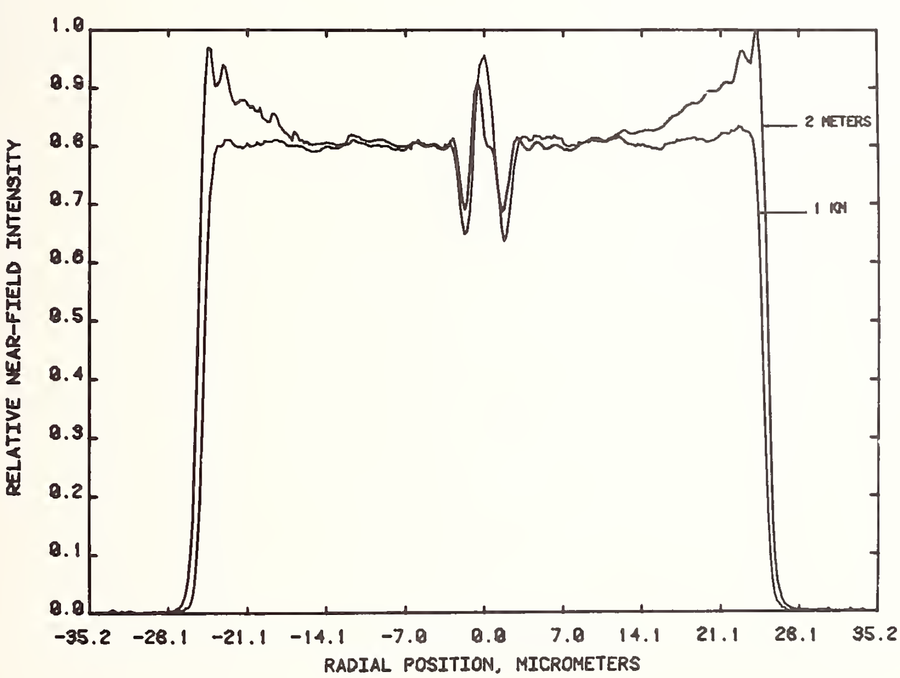

Figure 20. Normalized near-field radiation patterns at 2 m and 1 km from an initially overfilled multimode step-index fiber. The short sample exhibits the distinctive "leaky mode ears."

6.2 Wavelength and Linewidth Dependence

The near-field system was calibrated at wavelengths of 850 nm and 600 nm using the calibration reticle. Although the correction is very small between 850 nm and 600 nm (0.44 percent), it is required to fully interpret core diameter data obtained at the two wavelengths. In order to investigate wavelength dependence in core diameter, the near-field patterns of six fibers were obtained at 850 nm and 600 nm (figs. 21 to 26). Each plot is normalized to its maximum intensity. Note that at the shorter wavelength the resolution is increased showing in more detail the deposition layer structure. This enhancement is very apparent for the fiber in figure 23.

From these patterns, the 5 percent core diameters at 850 nm and 600 nm were determined. Tabulated in table 5 are the diameters taking into account the 0.44 percent chromatic correction factor. The difference between the corrected diameters is less than the distance between data points. Therefore, near-field core diameter is invariant to a change in the wavelength from 850 nm to 600 nm; the inclination therefore is to use shorter wavelengths for better resolution.

The source filter width was changed from 88 nm to 8 nm (centered at 850 nm) to study the effects of various spectral linewidths on near-field patterns. Comparisons of near-field profiles for the two linewidths for two fibers are shown in figures 27 and 28, respectively. Normally, the detected signal is processed using a 40 ms time constant on the lock-in amplifier. However, since the signal-to-noise ratio was low when using the 8 nm linewidth filter, the time constant was increased to 125 ms. This is sufficient time to process each piece of data since data is taken at approximately 1 s intervals. The near-field patterns for the two different filters are essentially the same. It is therefore recommended that a wide linewidth source be used for the sake of increasing the signal. A wide linewidth would also tend to reduce modal ripple should it become a problem [23].

Table 7. Wavelength dependence of 5 percent TNF core diameter.

Fiber #	a. 850 nm μm	b. 600 nm μm	c. 600 nm corrected μm	d. (c - a μm
1	47.2	47.4	47.2	0.0
2	44.5	44.8	44.6	+0.1
3	50.5	50.8	50.6	+0.1
4	49.9	50.2	50.0	+0.1
5	50.4	50.4	50.2	-0.2
6	48.3	48.6	48.4	+0.1

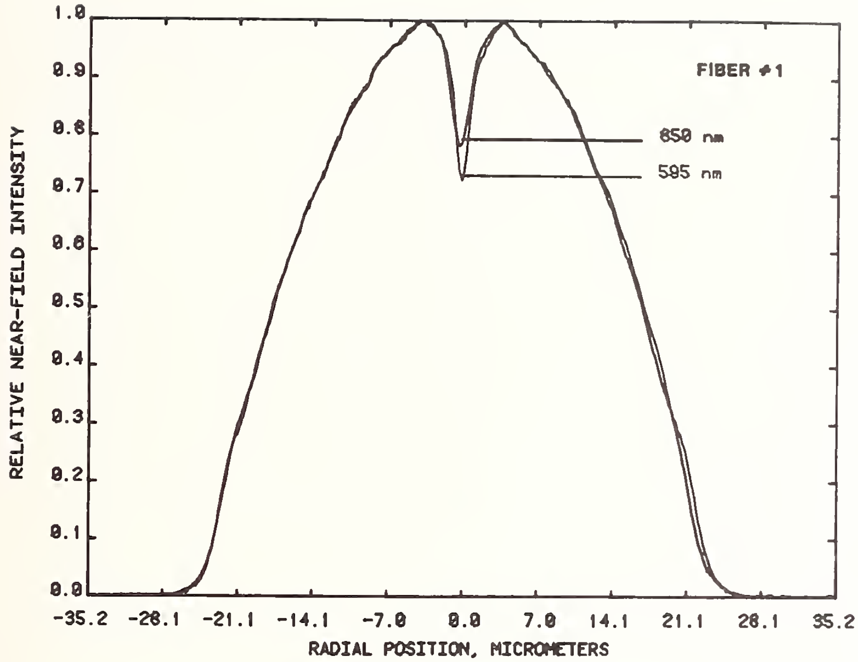

Figure 21. TNF profiles for fiber #1 at 600 and 850 nm.

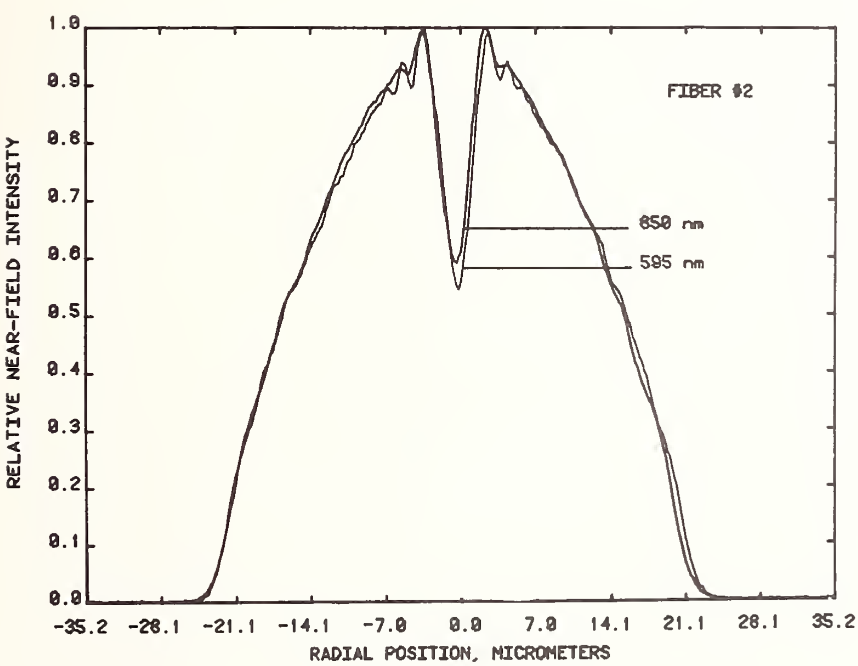

Figure 22. TNF profiles for fiber #2 at 600 and 850 nm.

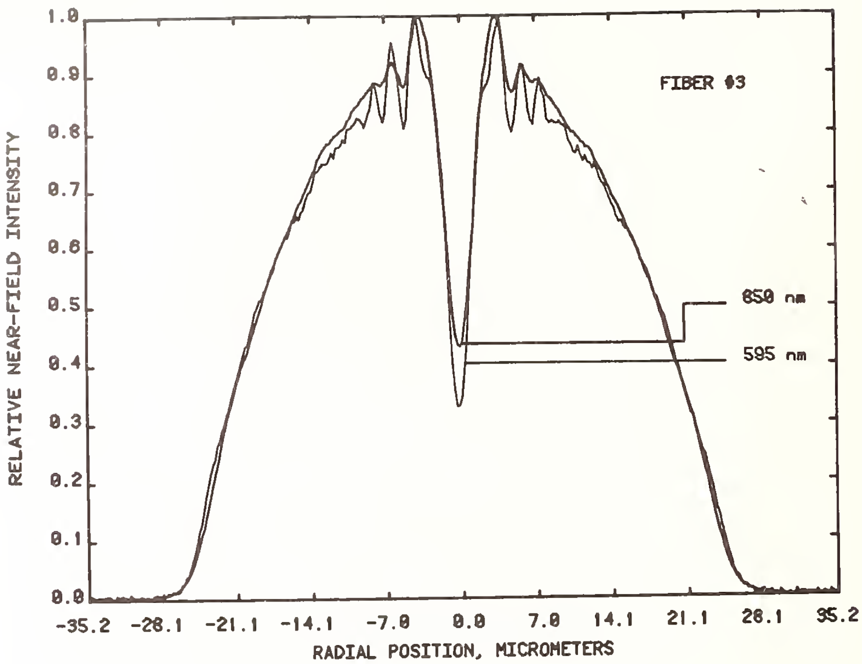

Figure 23. TNF profiles for fiber #3 at 600 and 850 nm.

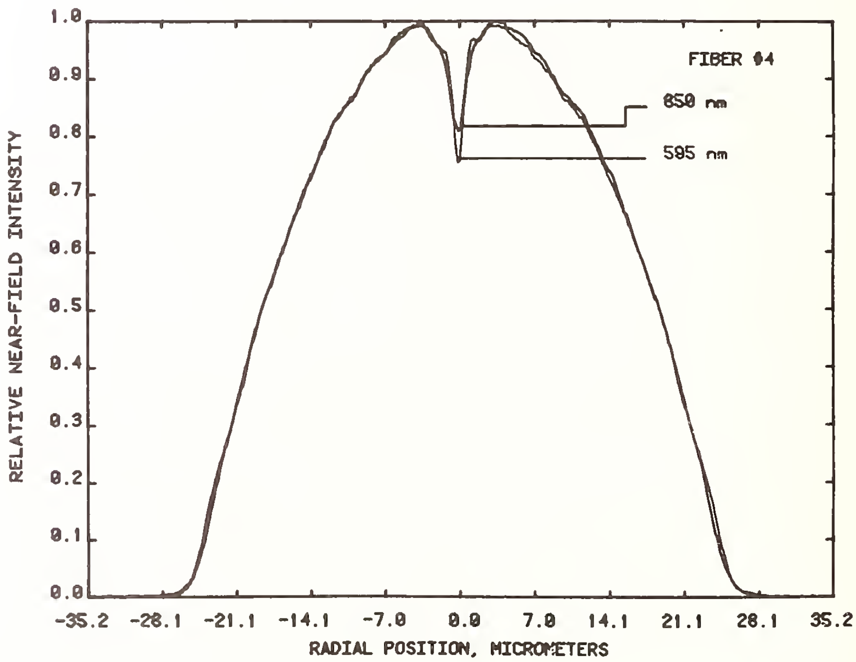

Figure 24. TNF profiles for fiber #4 at 600 and 850 nm.

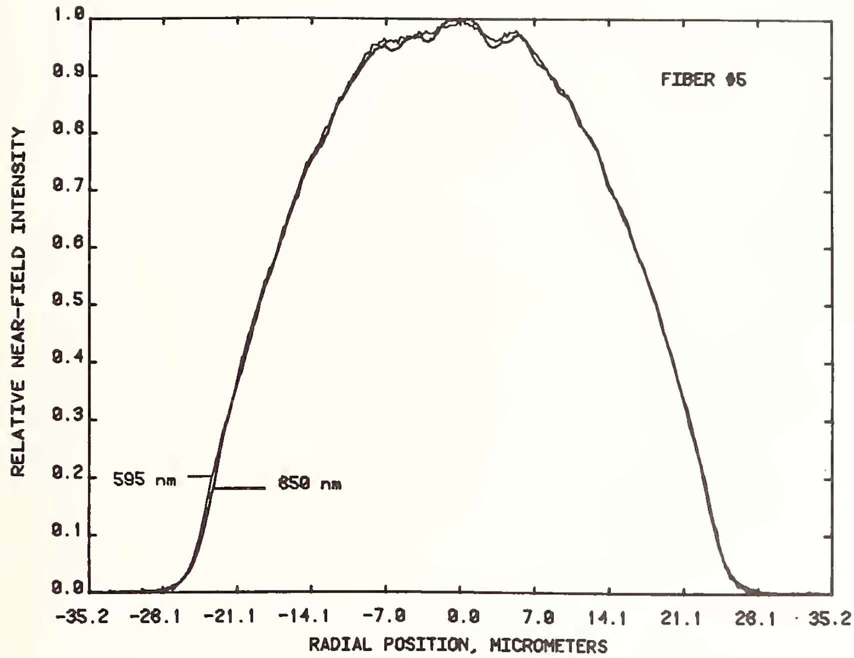

Figure 25. TNF profiles for fiber #5 at 600 and 850 nm.

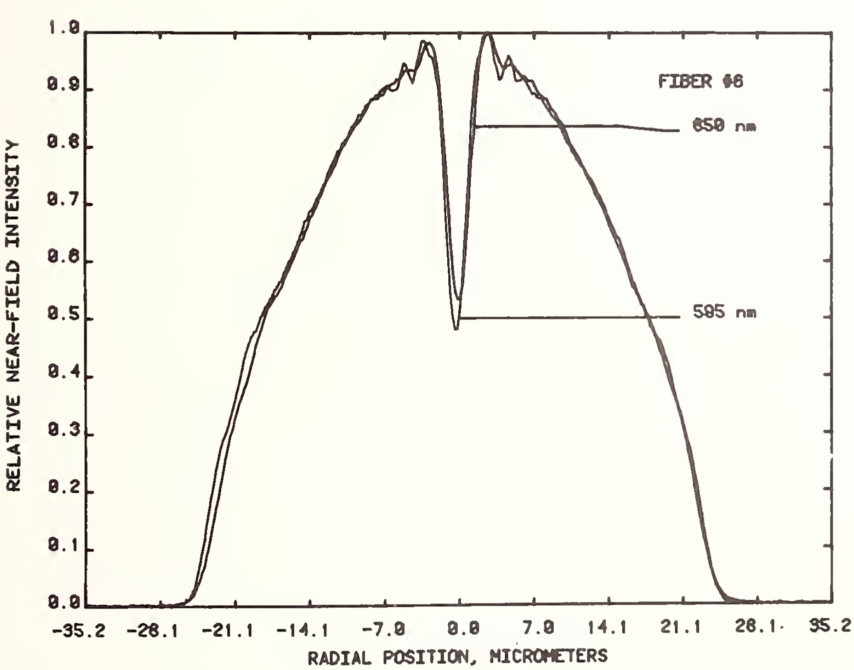

Figure 26. TNF profiles for fiber #6 at 600 and 850 nm.

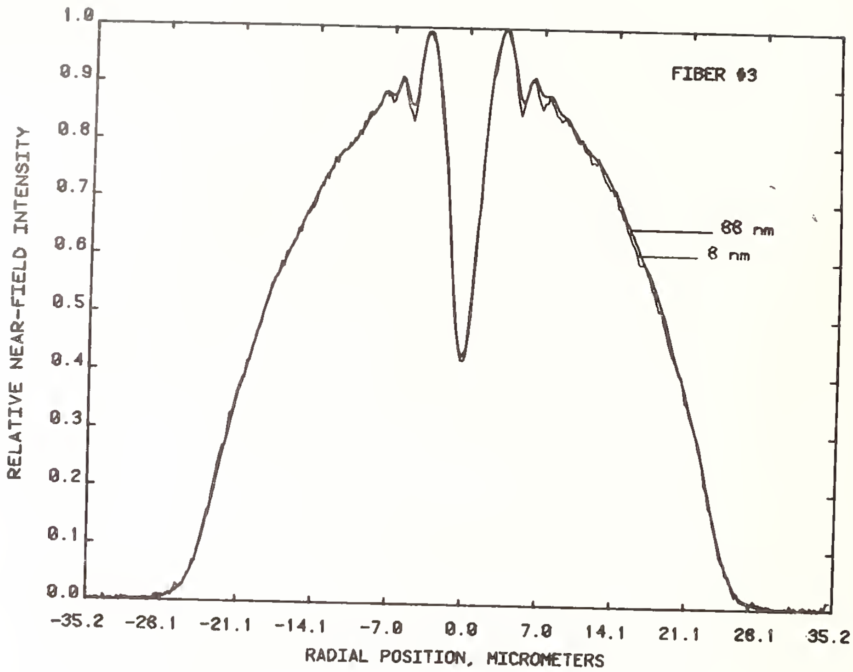

Figure 27. TNF profiles for source linewidths of 8 and 8 nm centered at 850 nm, fiber #3.

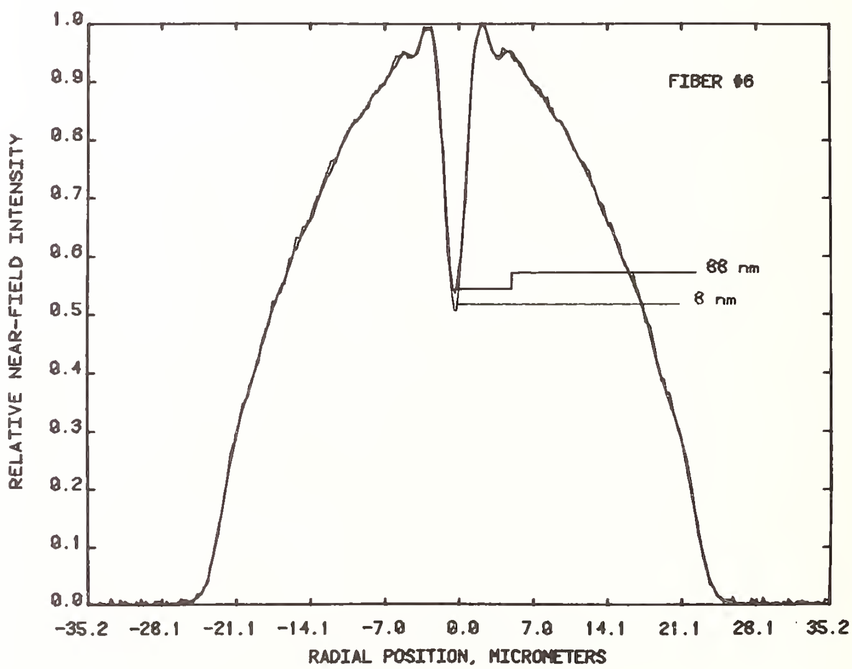

Figure 28. TNF profiles for source linewidths of 8 and 8 nm centered at 850 nm, fiber #6.

6.3 Launch Position Dependence

Launch parameters were varied to determine the sensitivity of near-field measurements to launching conditions. It was presumed that even small deviations from the optimum launch condition would affect core diameter measurements.

For the present apparatus, the optimum launch position is that which maximizes light intensity at the image. Using a large spot launch, launch parameters may be additionally changed by varying the launch NA, axially translating the fiber away from the optimum, and transversely moving the fiber from the optimum.

For launch NA dependence, NA was reduced from 0.36 to 0.24. The effect of changing launch NA for a step-index and a graded-index fiber are given in figures 29 and 30, respectively. In the step fiber case, lowering the NA has the effect of eliminating the leaky mode ears. Measurement of the far-field radiation pattern on this step fiber indicated a fiber NA of about 0.25. Thus, by restricting the launch angle to that which is close to the fiber NA, leaky modes are eliminated and a better approximation to the step-index profile is achieved. There was no appreciable change in the near-field shape of the graded-index fiber when the launch NA was decreased from 0.36 to 0.24. The graded fiber had an NA of 0.18. Since most multimode graded-index fibers have NAs of 0.2, a launch NA of 0.24 still provides an overfilled launch condition. However, in practice, the launch NA should be greater than 0.3 if an overfilled launch is desired. If the launch NA is reduced below that of the graded-index fiber, the near-field pattern will become restricted.

The effects of transverse and axial translation of the fiber are shown in figures 31 and 32 and figures 33 and 34, respectively. Translations of 25 μm perpendicular to the optical axis and 100 μm in the axial direction do not change the shape of the profile, although a decrease in intensity at the output is noticed. There was also little change in the 5 percent core diameters. For the 25 μm transverse offset, fiber 1 showed a change of 0.0 μm, fiber 2 a change of 0.1 μm, and fiber 6 a change of 0.2 μm. For the ±100 μm axial translation, there were no changes in the core diameter. A summary of these results is given in table 8.

6.4 Profile Pathologies

Because optical fibers are fabricated from deposited layers, a wide variety of index profile shapes is possible. The purpose of this section is to point out some of the diverse near-field patterns observed in our laboratory.

Fibers fabricated from the inside MCVD (modified chemical vapor deposition) method frequently have on-axis dips in the index profile. This is caused by the evaporation of germanium during the collapse of the preform. Dopants evaporate from the last layer as the burner temperature is increased. Figure 35 shows one of the deepest dips in the near-field profile observed in our laboratory for a graded-index fiber. Also, there is deposition layer structure apparent adjacent to the dip. The presence of a dip in the index profile

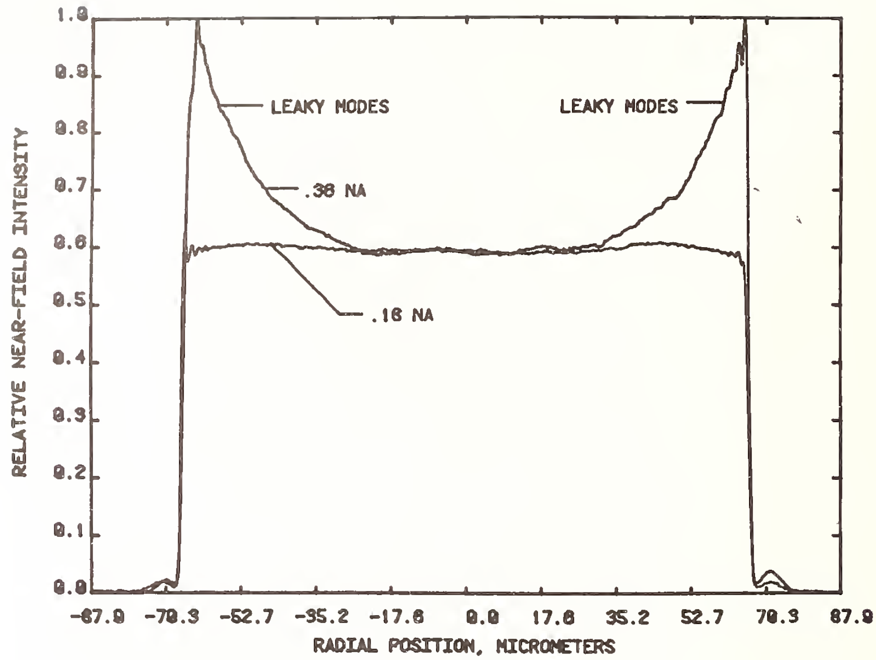

Figure 29. TNF profiles for a large core step-index fiber for 0.18 and 0.36 launch numerical aperture (NA). Note the "leaky-mode ears" for the overfilled launch NA condition.

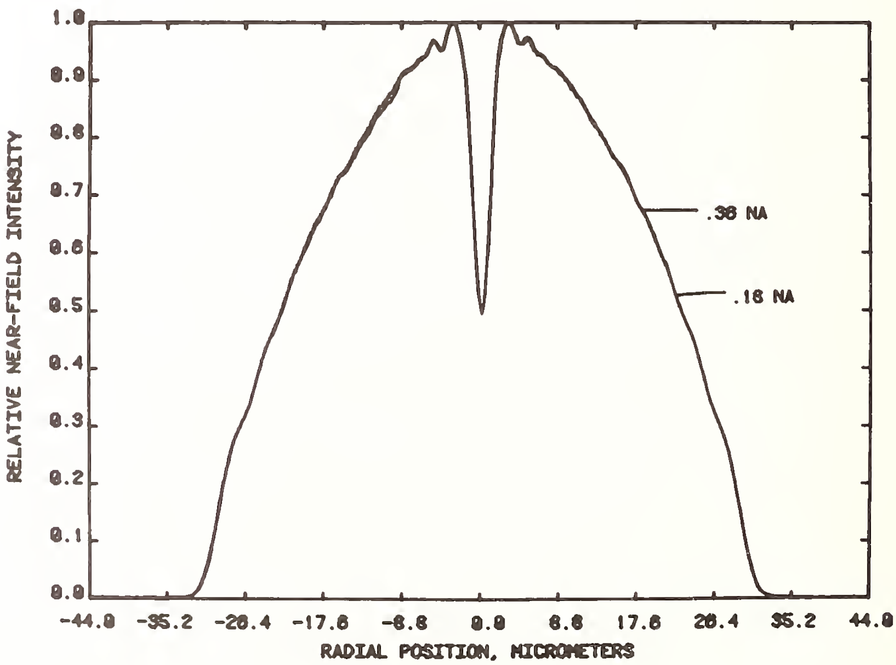

Figure 30. TNF profiles for a graded-index fiber for 0.18 and 0.36 launch numerica[l] aperture (NA). There is little difference in the patterns.

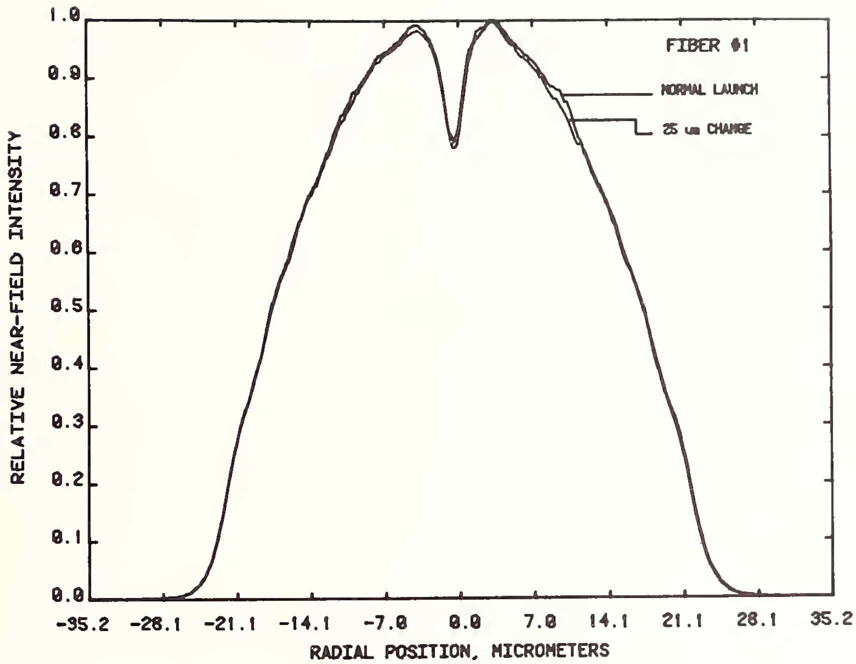

Figure 31. Normalized TNF profiles for an optimum launch and a 25 μm transversely offset launch, fiber #1.

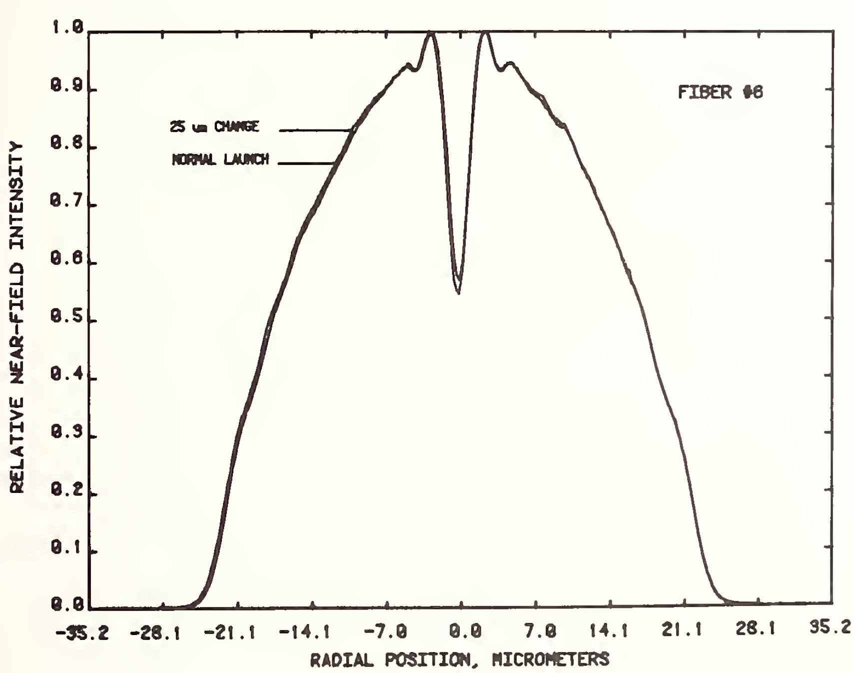

Figure 32. Normalized TNF profiles for an optimum launch and a 25 μm transversely offset launch, fiber #6.

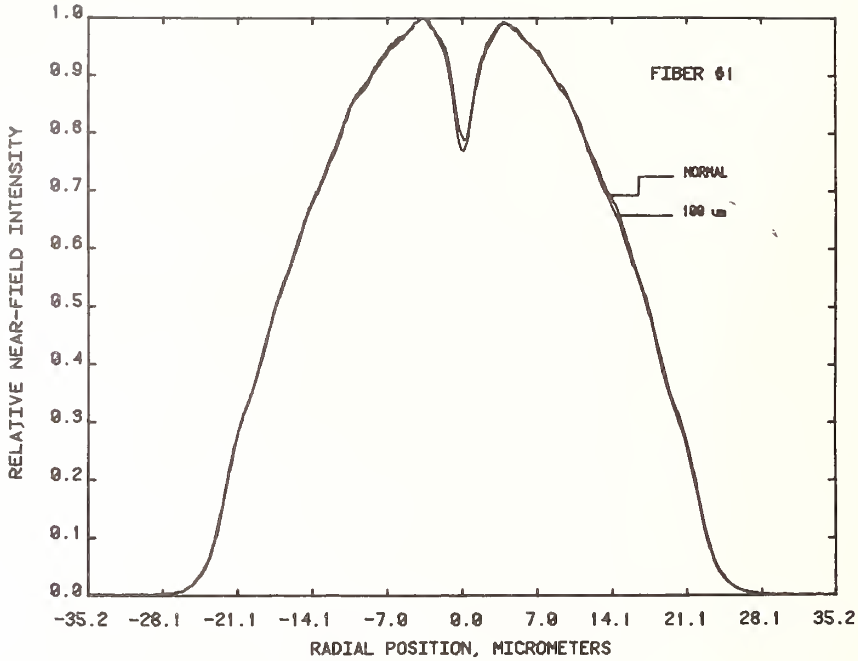

Figure 33. Normalized TNF profiles for an optimum launch and a +100 μm axially offset launch, fiber #1.

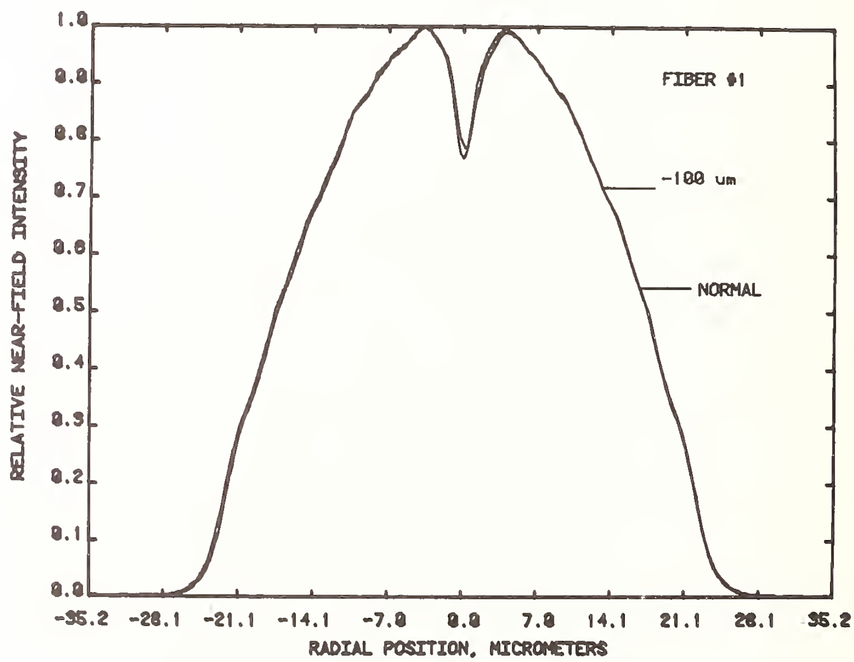

Figure 34. Normalized TNF profiles for an optimum launch and a -100 μm axially offset launch, fiber #1.

Table 8. Core diameter due to changes in launch position (translated minus optimum launch).

Translation	Fiber #	5% core diameter difference (translated minus optimum) μm
25 μm transverse	1	0.0
25 μm transverse	2	+0.1
25 μm transverse	6	+0.2
+100 μm axial	1	0.0
-100 μm axial	1	0.0

does not greatly disturb the attenuation properties of the fiber. Figure 36 gives the spectral attenuation for this fiber plotted as a function of $1/\lambda^4$. The loss out to 1.1 μm is Rayleigh scattering limited and the vertical axis intercept is only 0.2 dB. The index dip does however affect the bandwidth. If one assumes good group delay compensation over the whole profile, one effect of the index depression would be to increase the group velocity for modes near the axis; the result would be a pre-pulse. Figure 37 is the impulse response for this fiber and indeed a low-level pre-pulse is present. Fibers fabricated from the outside CVD process generally have smaller dips than the inside process. Figures 38 and 39 are examples of fibers made by an outside process and exhibit the smallest dips we have observed for graded-index fibers.

Step-index fibers fabricated from MCVD also exhibit on-axis index depressions. Figure 40 is an example of a large-core "fat" fiber having a deep depression in the near-field profile. Here several deposition layers are also evident. The launch NA for this fiber was restricted to eliminate leaky mode "ears". Figure 41 is also a step-index fiber at two different launch NAs showing the presence of leaky modes at launch NAs higher than the fiber NA. This fiber also has a "peak" within the index dip.

Another class of fibers encountered is "quasi-step" fibers. Index profiles for these fibers are not pure step but partially graded to enhance the bandwidth (fig. 42). Bandwidths of quasi-step fibers are intermediate to pure step and parabolic profile fibers.

Occasionally near-field profiles reveal features not desirable for good fiber design. This includes asymmetries in shape, localized peaks in the profile, excessive core ovality, and undesirable profile shape. Figures 43 through 48 give various examples of these kinds of fibers. Fiber 4 has an asymmetric, high-intensity region near the center of the core. Figures 43 and 44 are two orthogonal scans for this fiber. The high intensity region exists over only a small part of the core and is not circular symmetric. Figures 45 and 46 are examples of fibers having excessive core ovality. Orthogonal scans are superimposed to reveal the degree of ovality. Figure 47 is an example of an undesirable profile. This fiber has large ripples superimposed on a near-power law profile. Figure 48 is perhaps the

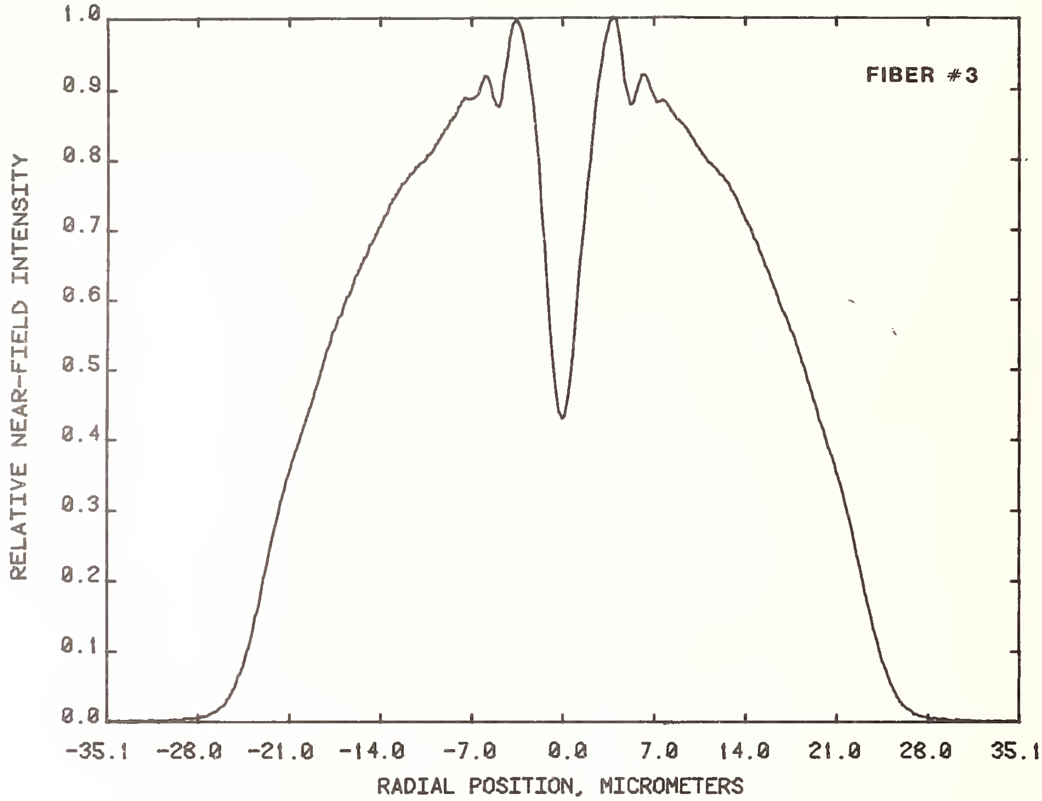

Figure 35. One of the deepest index depressions for a graded-index fiber in a near-field profile was fiber #3.

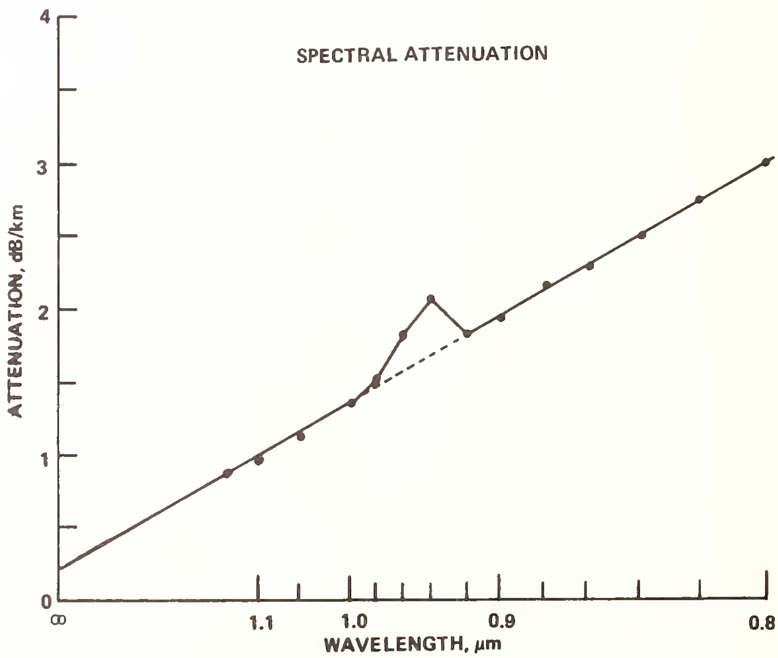

Figure 36. The spectral attenuation as a function of $1/\lambda^4$ for fiber #3.

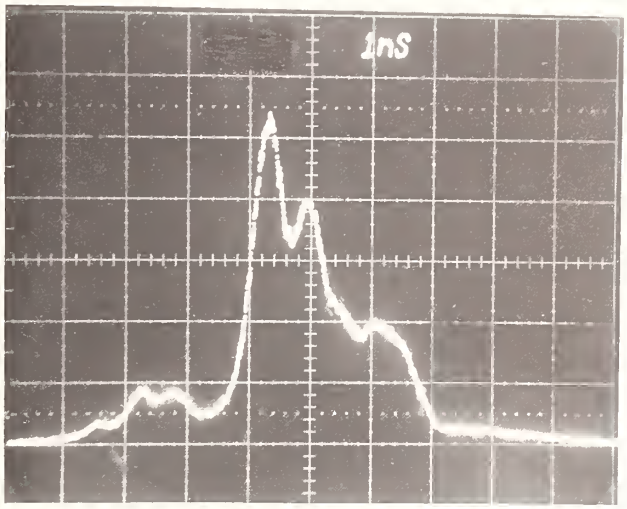

Figure 37. The impulse response of fiber #3 shows a low-level pre-pulse presumably due to the deep index depression.

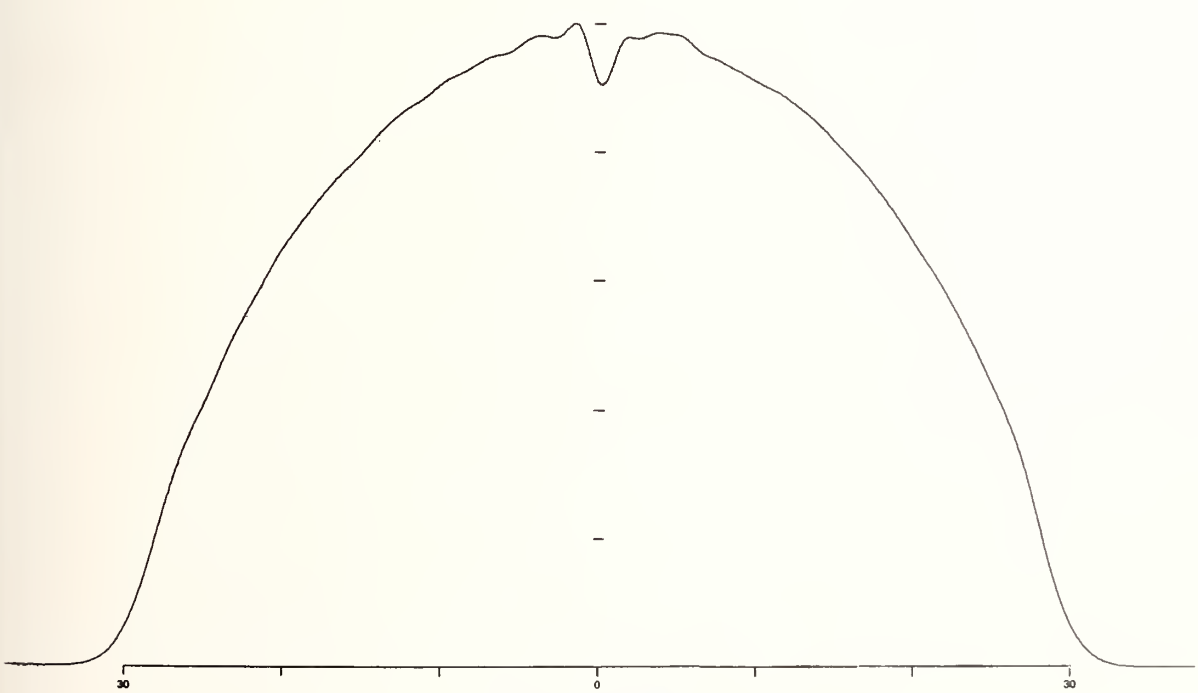

Figure 38. Analog TNF profile of a fiber made by the outside chemical vapor deposition process.

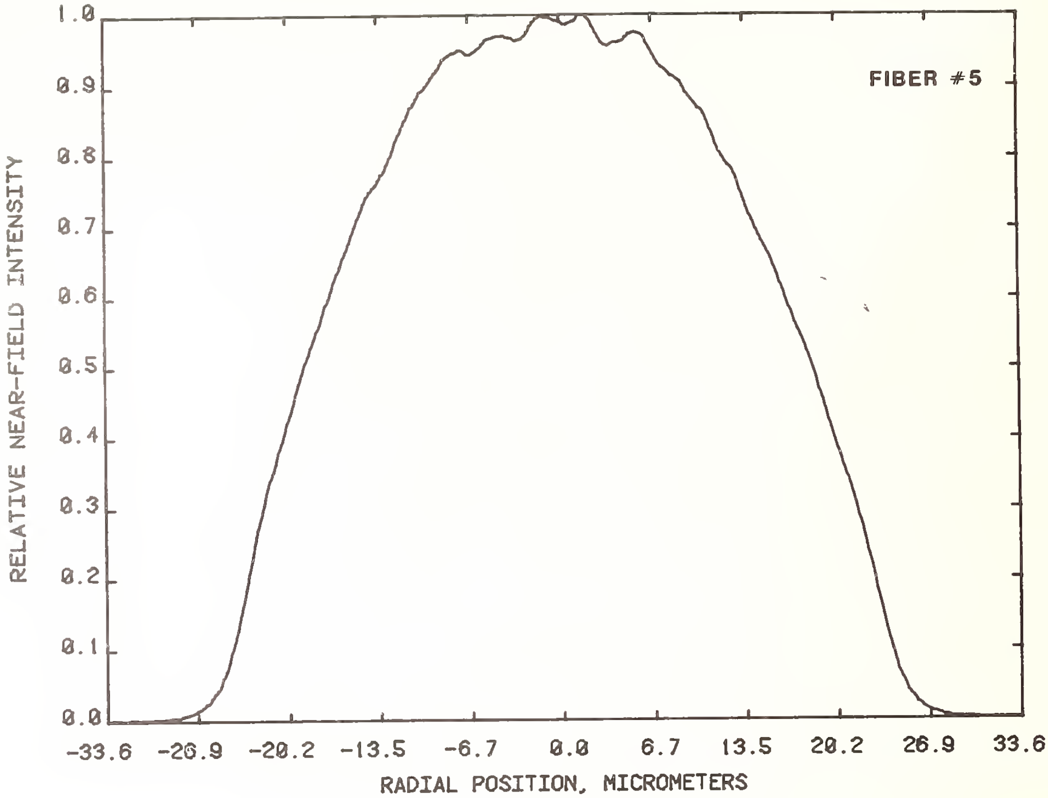

Figure 39. TNF profile of fiber #5 which was made by the outside chemical vapor deposition process.

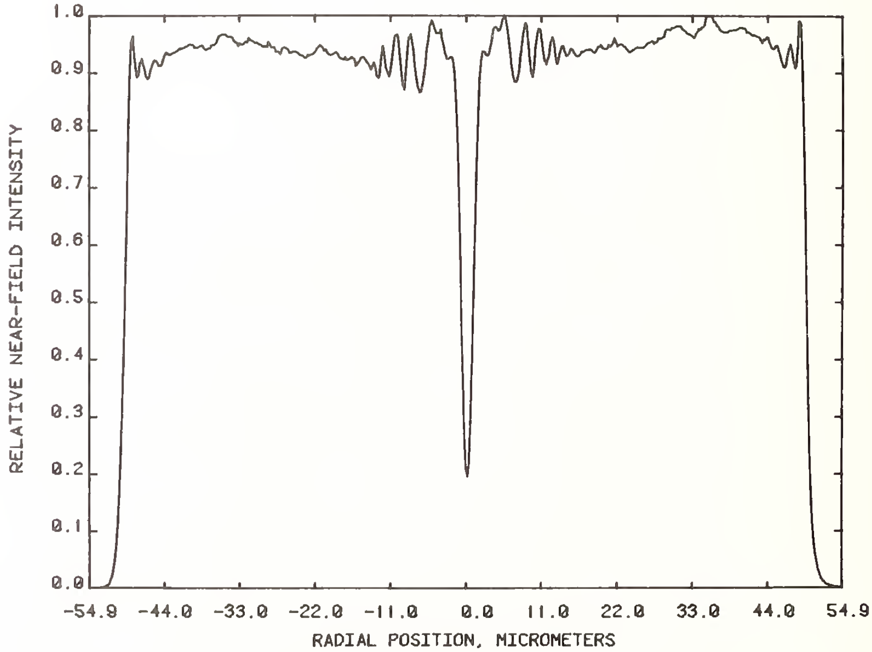

Figure 40. TNF profile of a large core fiber with a deep index depression and pronounce deposition layer structure.

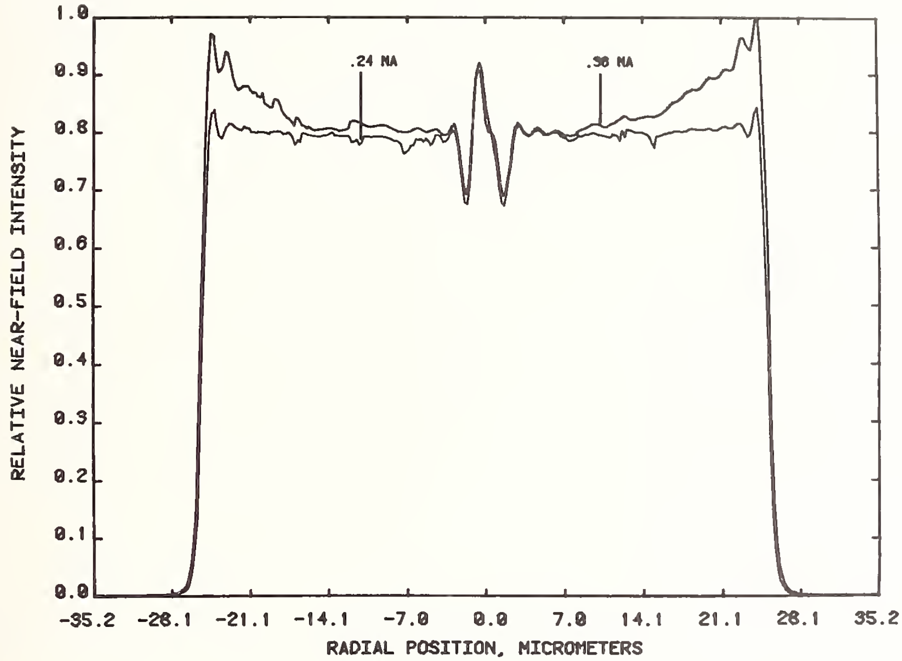

Figure 41. TNF profiles of a multimode step-index fiber for 0.18 and 0.36 launch numerical aperture (NA).

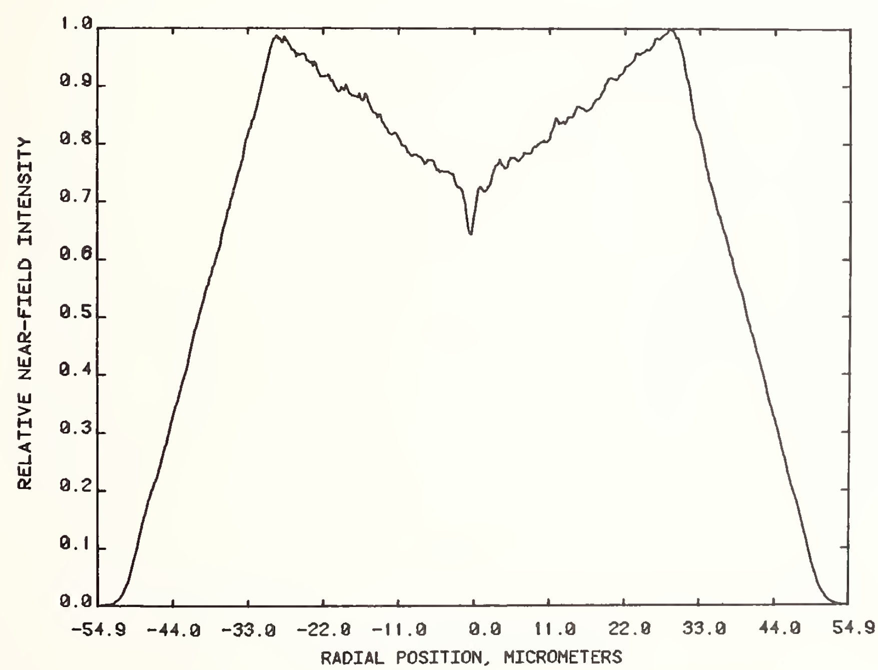

Figure 42. TNF profile of a "quasi-step"-index fiber.

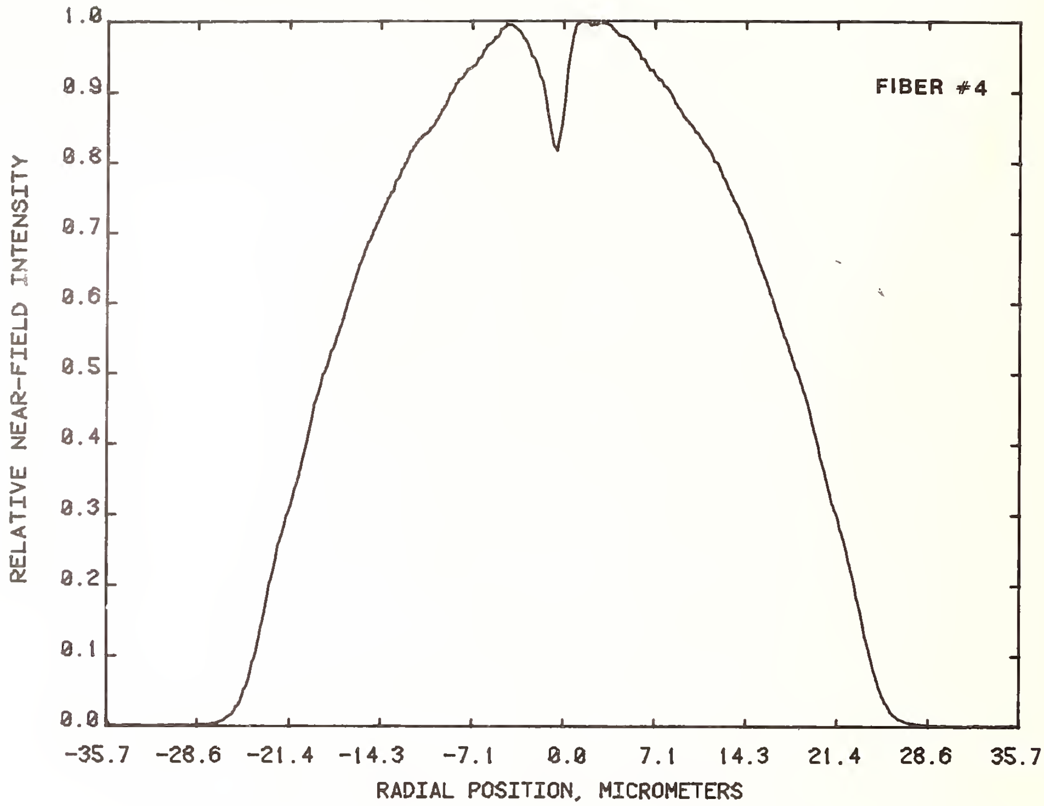

Figure 43. TNF profile of fiber #4, 850 nm.

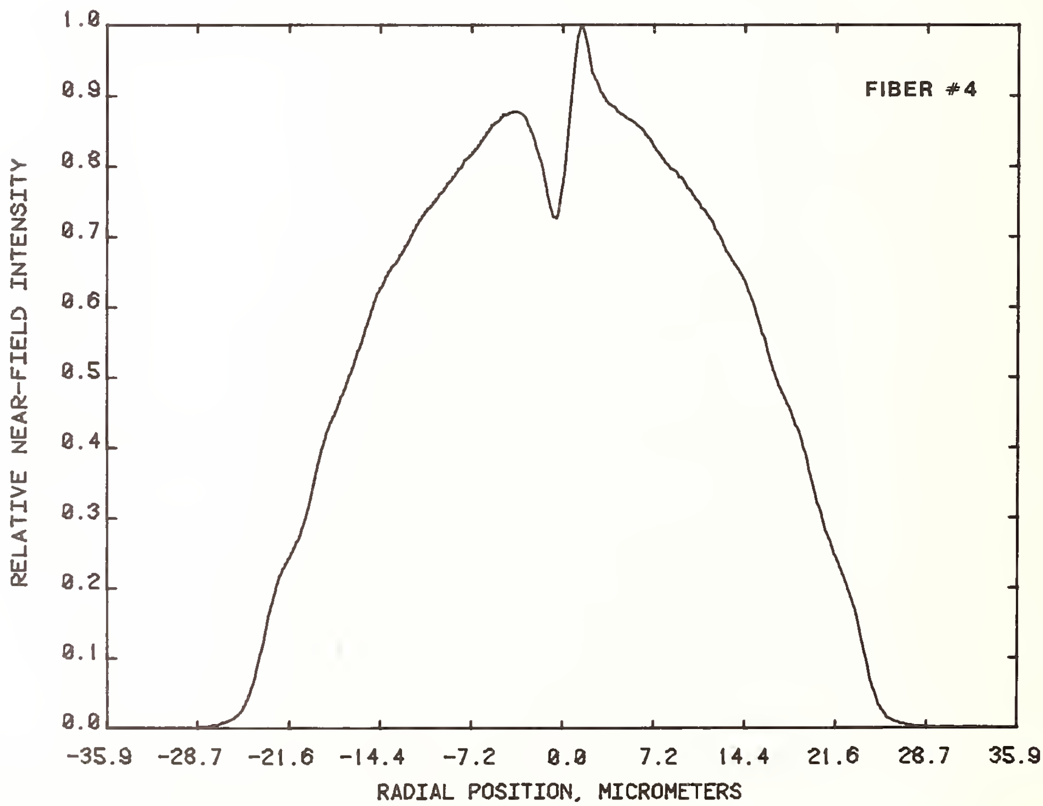

Figure 44. TNF profile of fiber #4, 850 nm. Fiber rotated 90° from figure 26; note lack of circular symmetry at the core center.

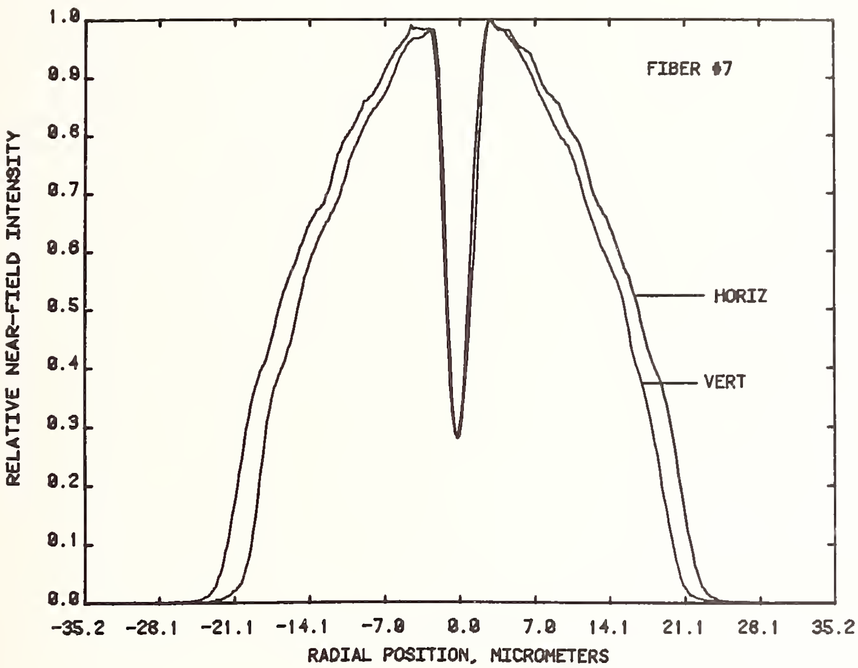

Figure 45. Orthogonal TNF scans of a fiber with excessive core ovality, fiber #7.

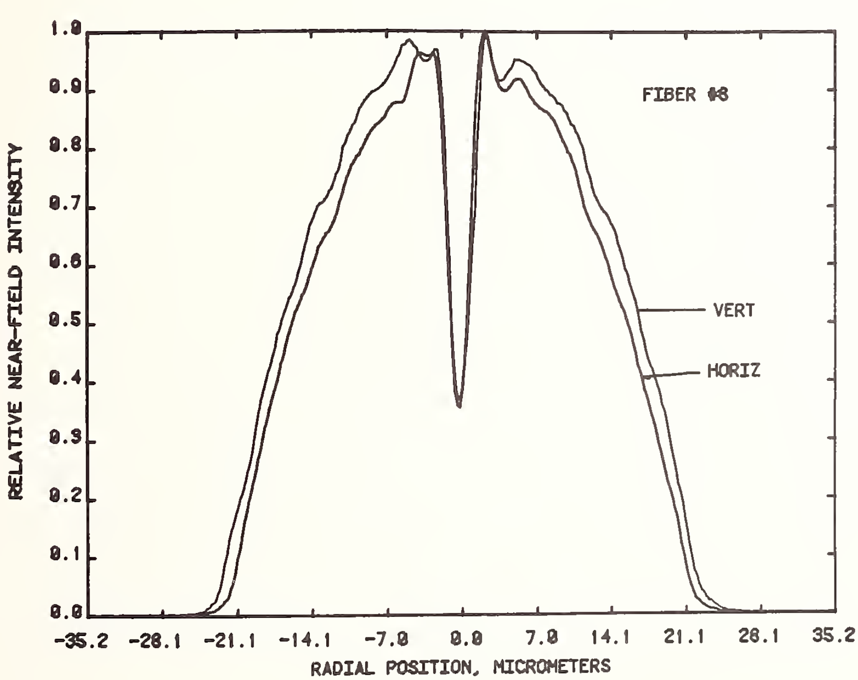

Figure 46. Orthogonal TNF scans of a fiber with excessive core ovality, fiber #8.

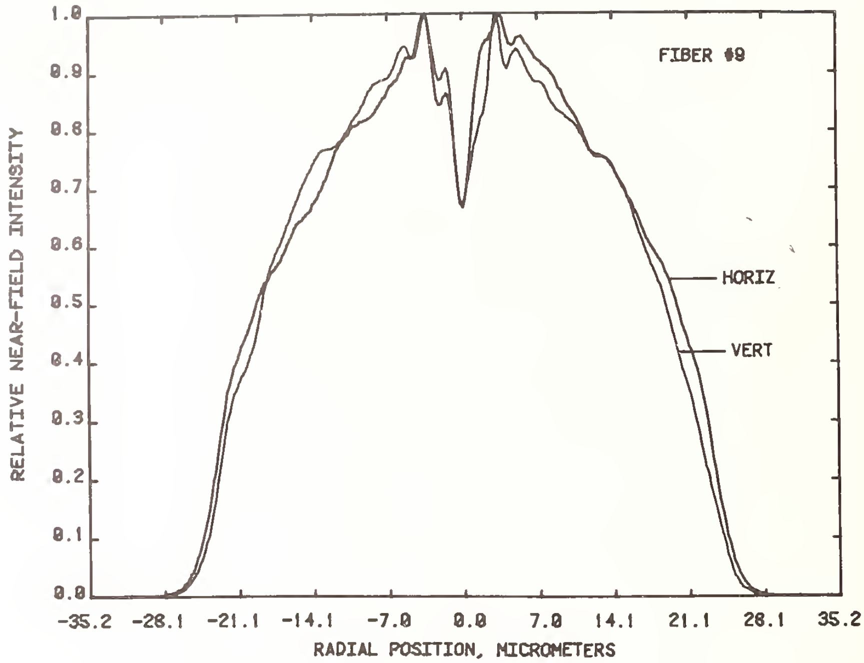

Figure 47. Fiber #9 has excessive ripple superimposed on a nominally parabolic shape.

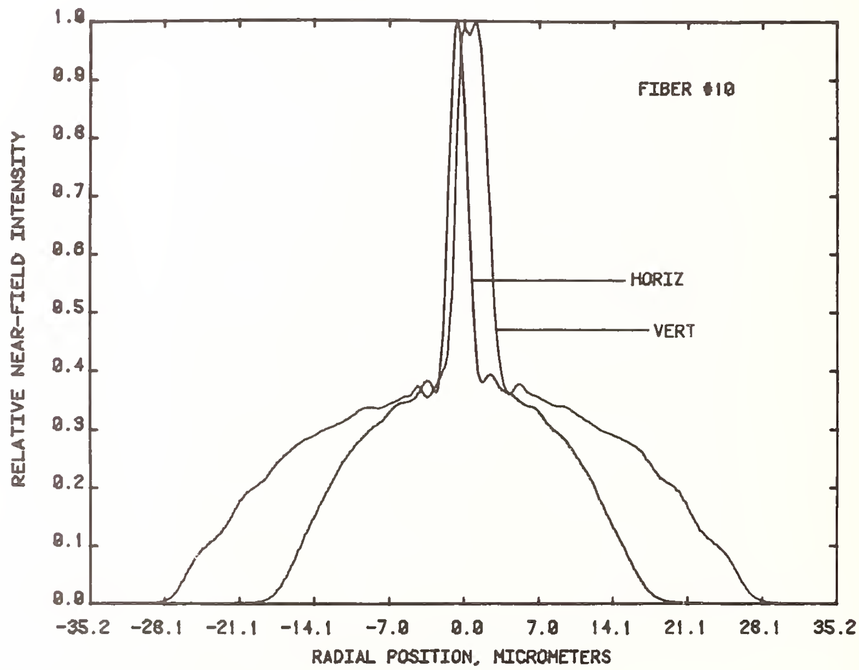

Figure 48. Fiber #10 has an extremely elliptical core coupled with a large on-axis pea
which is also elliptical.

strangest profile observed. Here the core is extremely elliptical and a very large peak occurs on-axis. Large on-axis peaks in the index profile generally lead to trailing pulses caused by low on-axis group velocity [36].

6.5 Comparison of Near-Field Profiles to Actual Index Profiles

Since core diameter is defined from the refractive index profile, it is important to know how well the near-field profile (overfilled launch) matches the index profile. The major source of disagreement is thought to be contributions from leaky modes. Power in these modes would cause the near-field profile to "bulge out" from the actual index profile at medium to high radial values. Whether a leaky mode correction should be made is subject to debate [9]. In this section near-field profiles from six graded-index fibers are compared to actual index profiles.

Refractive index profiles for the six fibers were determined by the refracted ray scanning method (sometimes referred to as RNF, refracted near-field) [37]. RNF gives an accurate measure of the index profile with resolution generally better than 1 μm. RNF profiles were obtained at a wavelength of 632.8 nm using a HeNe laser.

Comparisons are given in figures 49 through 54. Note that in all cases the near-field profiles are to the inside or touching the RNF profiles. Leaky mode corrections would result in a constriction of the profiles and further increase the disagreement. It appears that near-field profiles from graded-index fiber do not benefit from leaky mode corrections.

Other interesting points are brought out in these comparisons. Fiber 1 has an abrupt step in the index profile near the core-cladding boundary. Near-field power does not fill this region of the fiber to indicate the presence of the step. This is of interest for core diameter measurements where behavior near the baseline is of special interest. Fiber 6 has a low index barrier layer between the core and cladding. Note that the near-field profile includes only the region of the core where light is guided, consequently the low index barrier layer does not appear. This is of little consequence for core diameter measurements since index values below the cladding are not considered in the definition.

Near-field profiles reverse curvature near the core-cladding boundary due to a loss of resolution and leakage of light from the core into the cladding. In all cases, the near-field profiles cross the index profile near the core-cladding boundary. This behavior has been taken advantage of by standards groups in setting definitions for core diameter when different measurement methods are allowed. The curves cross over at about the 2.5 to 3.0 percent intensity levels [38].

6.6 Curve Fitting

A serious limitation of the near-field method is the loss of resolution near the core-cladding boundary due to the decrease in local fiber numerical aperture. By curve fitting the profile, this effect can be compensated for. The purpose of fitting the profile is not

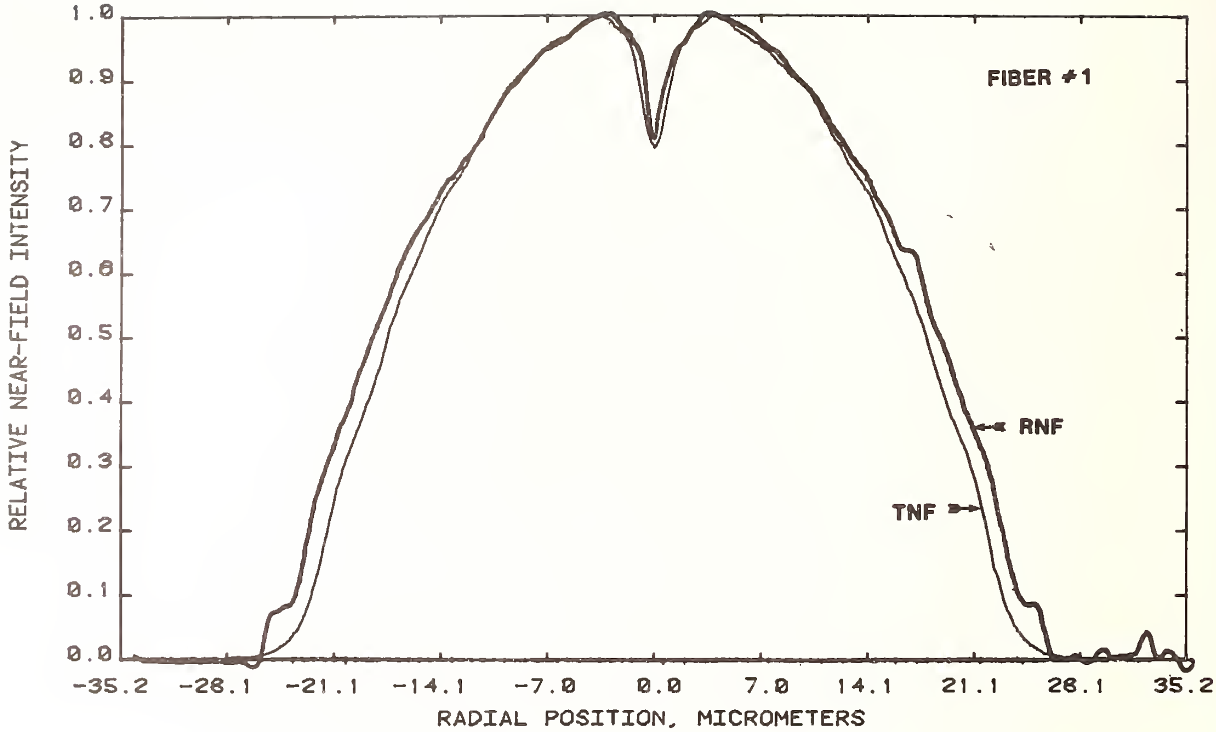

Figure 49. Comparison of RNF (M. J. Saunders) and TNF profiles for fiber #1 which had the largest disagreement in 5 percent core diameter.

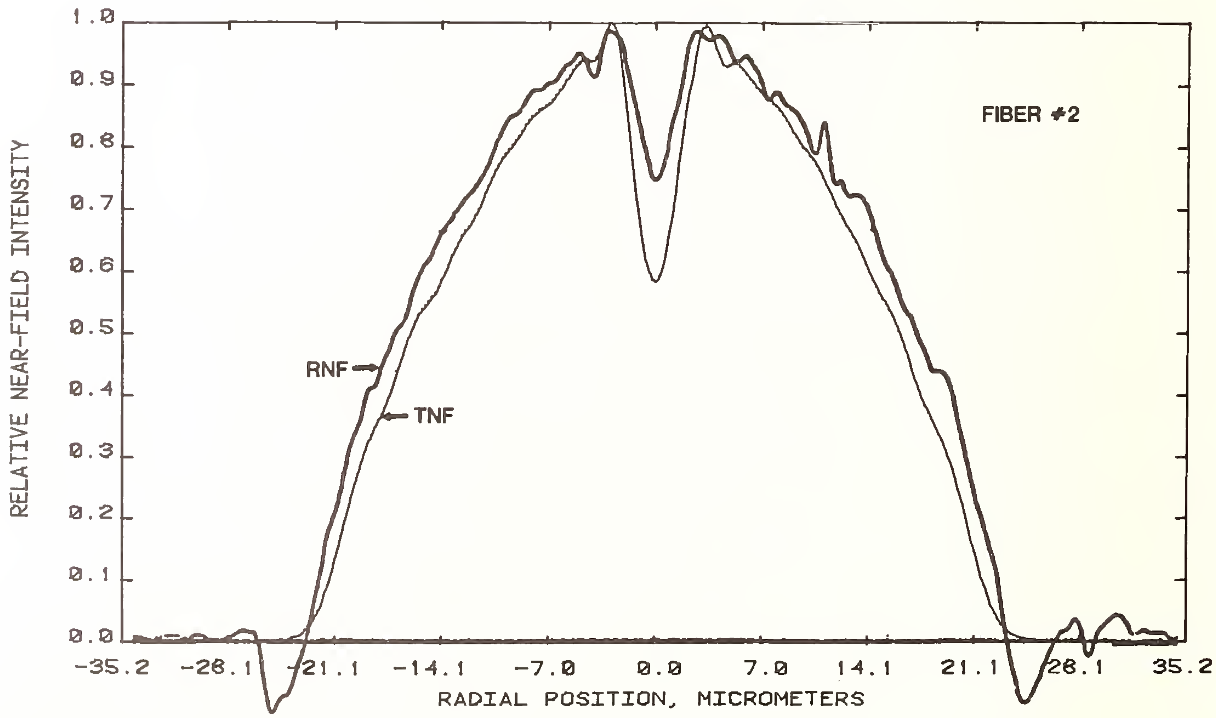

Figure 50. Comparison of RNF (M. J. Saunders) and TNF profiles for fiber #2.

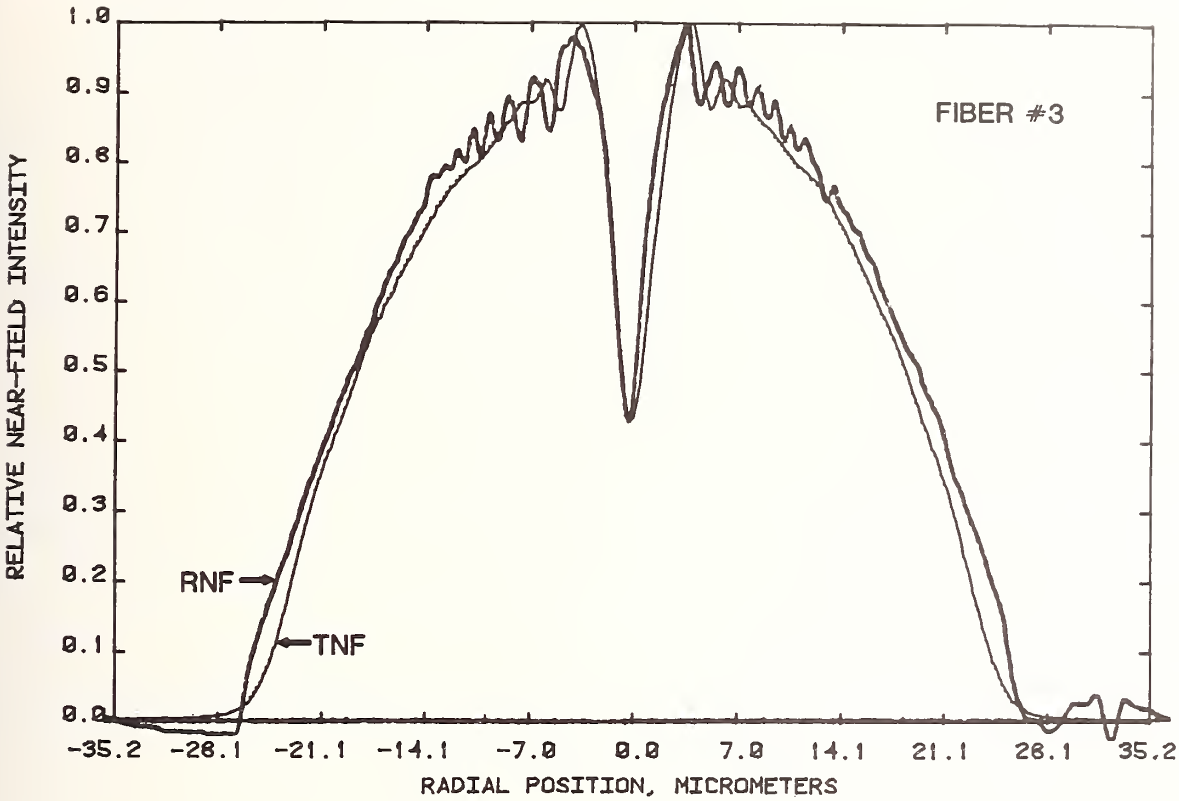

Figure 51. Comparison of RNF (M. J. Saunders) and TNF profiles for fiber #3.

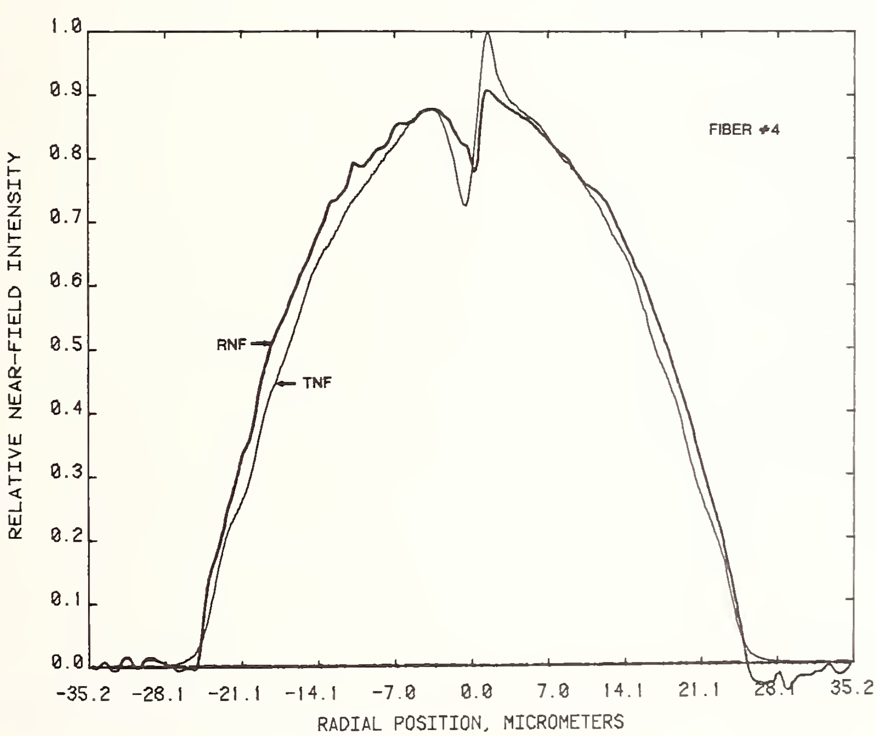

Figure 52. Comparison of RNF (M. J. Saunders) and TNF profiles for fiber #4. Note curves are normalized to left peak. The asymmetric high-intensity peak in the TNF occurs over only a small portion of the core.

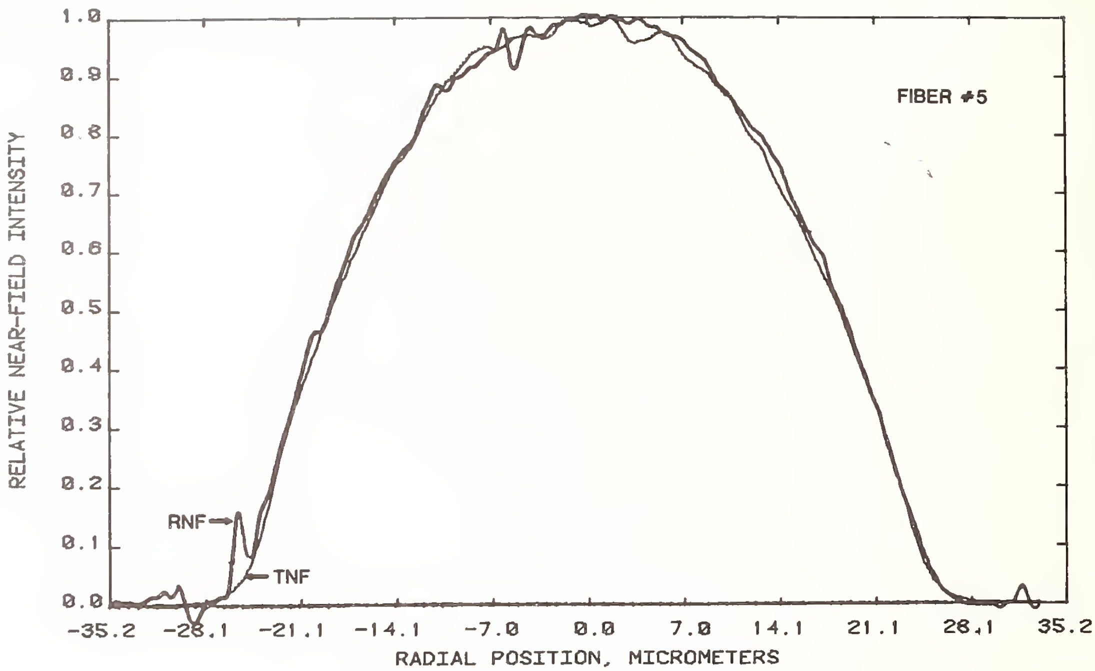

Figure 53. Comparison of RNF (M. J. Saunders) and TNF profiles for fiber #5. A speck of foreign material near the cladding (lower left side of RNF profile) results in an abnormally large value for 5 percent RNF core diameter.

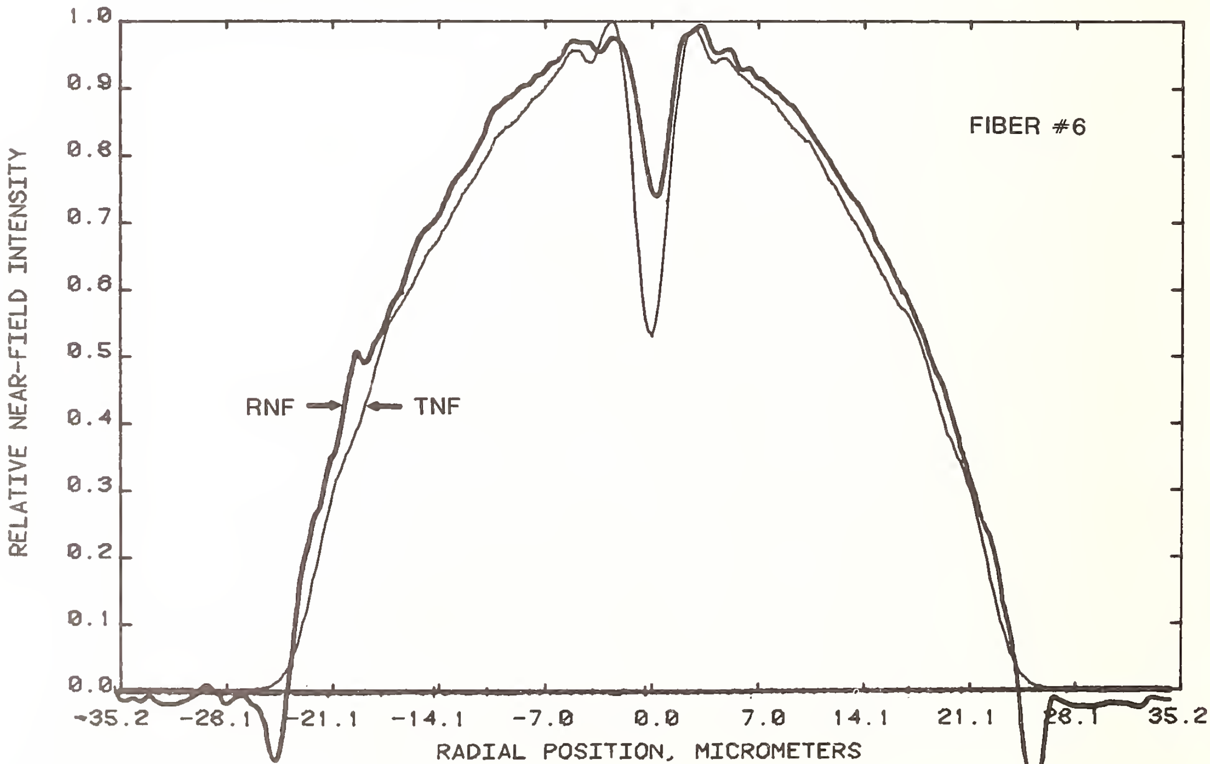

Figure 54. Comparison of RNF (M. J. Saunders) and TNF profiles for fiber #6 which has a lo index barrier layer. Good agreement occurs at the 5 percent diameter.

to find a mathematical formula for approximating a set of data values as is sometimes done, but to "smooth" and average the profile to eliminate bumps or anomalies that may affect the measurement of core diameter. In the near-field method, the diameter of the profile below the 5 percent intensity level is not an accurate measure of the index profile due to the curvature reversal. Usually the actual profile shape is estimated by a fitted curve in this region.

The least squares algorithm was used to fit profiles. The criterion for the best fit is that the sum of the squares of the errors be a minimum [39],

$$\sum e_i^2 = \text{minimum}. \tag{34}$$

The error is the difference between the observed and computed values. The primary advantage of the method of least squares is that methods of calculus can be employed to find the minimum sum of squares of errors.

Two equations were evaluated for their ability to approximate profiles. They were the power law and third order polynomial. The power law equation refers to the ideal near-field intensity distribution exiting a fiber for a Gloge-Marcatili index profile.

$$\frac{I(r)}{I(o)} = 1 - (r/a)^g \tag{35}$$

where r is the radial position, I(r) is the intensity at r, a is the core radius and g is the index profile parameter. In order to use the least squares algorithm, the equation was linearized to yield

$$u = \log\left(1 - \frac{I(r)}{I(o)}\right) = + g\log r - g\log a \tag{36}$$

where the adjustable constants are g and a. The absolute tolerance for displacements is 10^{-3} and the initial values of g and a are 2 and 25 μm, respectively. The third order equation is

$$u = \frac{I(r)}{I(o)} = 1 + a_1 r + a_2 r^2 + a_3 r^3. \tag{37}$$

The maximum number of iterations (adjustments to the constants) for both cases is 700, after which the computer terminates the program.

Because of the reversal of curvature near the core-cladding boundary, deposition layers, and index depressions near the core center, a fit cannot be made to the whole profile. By fitting between the 10 percent to 80 percent intensity points on the profile these anomalies, that are not contributors to the general ideal shape of the profile, can be eliminated. Also, every other data point between 10 percent to 80 percent was used since empirically there was no difference in the final fitted curve. Use of every other data point also decreases processing time. The shape of the fitted curve does however, change appreciably when using every third data point. Residues were also calculated for the fitted curves. The residues are the errors between the actual values and the fitted values.

Results of the power law fit to fibers 1, 2, 4, 5, and 6 are shown in figures 55 to 60. Due to a nonsymmetrical "hotspot" on the profile, two scans of fiber 4 are shown in figures 57 and 58, where the scans are perpendicular to each other. The residues associated with each fit are also shown. Convergence occurred typically after 50 iterations and frequently after 100.

6.7 Modified Near-Field

The MNF method first proposed by Sabine, Donaghy, and Irving [14], is essentially the conventional near-field experiment with different sample preparation. Because of this, drastic differences in interpretation occur. In essence, the MNF method considers a short piece of fiber where both core and cladding are overfilled by the launch. Core and cladding are then treated as the core of one large equivalent step fiber with a central perturbation (the multimode core) and the surrounding lower index material around the fiber as the cladding. The original experiments used the silicone buffer coating as the outer cladding. By treating the whole fiber as a step fiber with a central perturbation, the resolution at the core/cladding interface is improved. Absolute indices can also be assigned to the profile. Theoretical analysis shows the leaky mode corrections all but disappear and that the corrections to the absolute indices are less than 5×10^{-4} in the core region [40].

An attempt was made to implement MNF by modifying the conventional system. The aperture immediately after the source was removed and replaced with opal glass to obtain a diffuse large NA launch. A straight, 15 cm length of bare fiber was butted against the glass. Care was taken not to have index-matching oil touch the fiber. Measurements were then taken as usual.

Results of a MNF scan are shown in figure 61. The light in the cladding could not b increased to the relative amount indicated in previous work [14,41]. Figure 61 does sho however, the barrier layer at the core-cladding boundary otherwise undetectable with th standard near-field method. Since the imaging objective had an NA of 0.65, all the ligh out of the fiber (which is ~1.0 NA) could not be captured.

6.8 Two-Dimensional Contouring

Isointensity contour maps were made for seven 50 μm core graded-index fibers and fi large-core short-haul fibers. Of the seven graded fibers, fiber 6 was extraordinarily rour while fiber 10 was extremely elliptical. The algorithm and system performed well unde these two diverse situations. In addition, the algorithm/system's ability to contour shor haul fibers is shown.

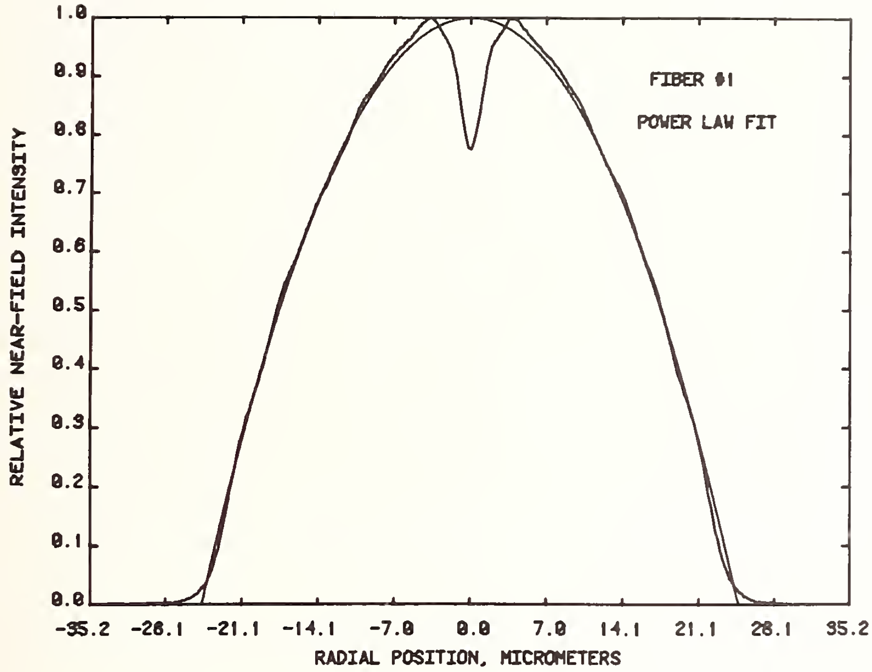

(a)

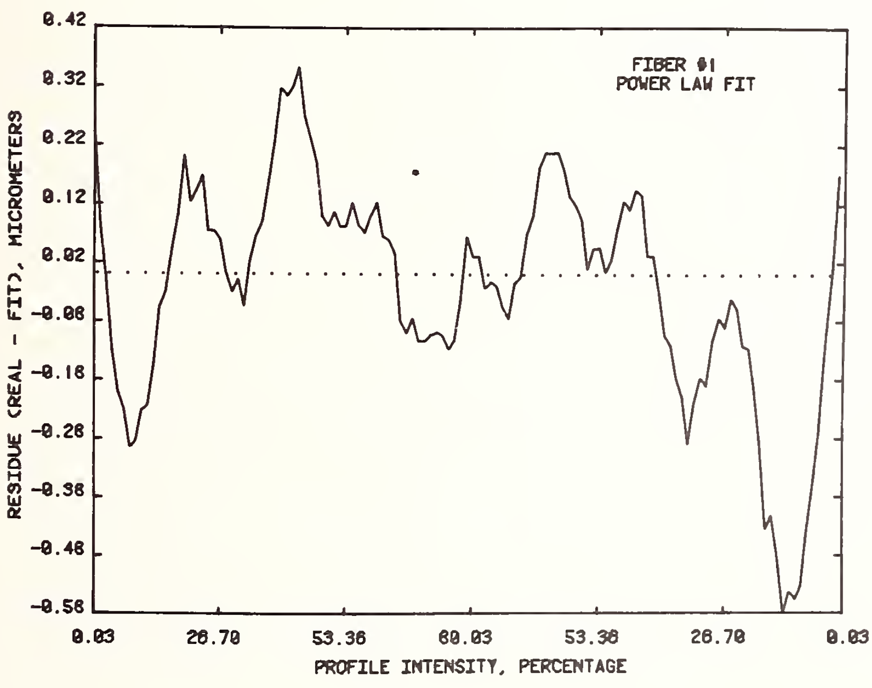

(b)

Figure 55. TNF profile for fiber #1 with superimposed least squares fit to a power law profile; a plot of the residues is also shown.

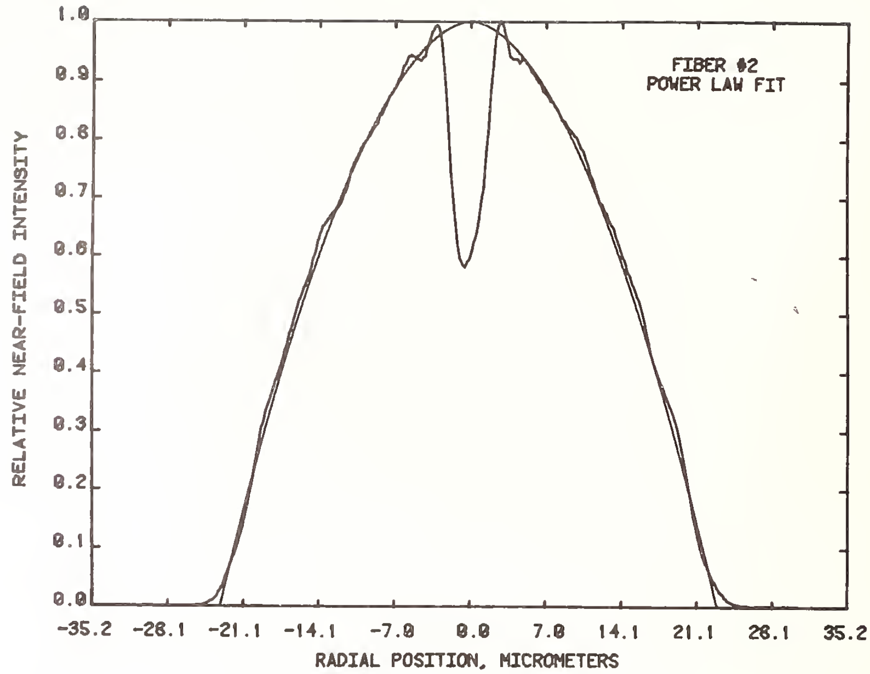

(a)

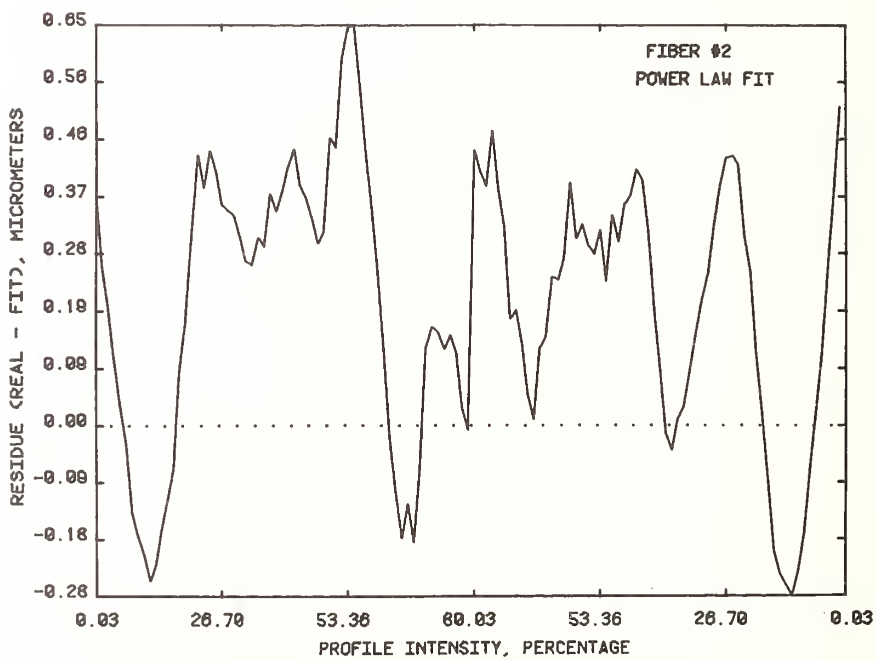

(b)

Figure 56. TNF profile for fiber #2 with superimposed least squares fit to a power law profile; a plot of the residues is also shown.

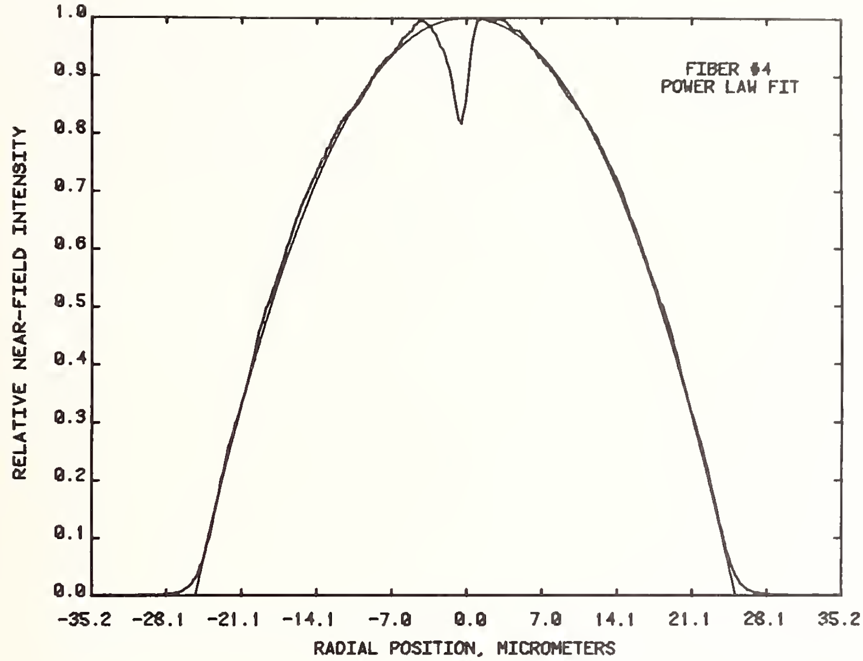

(a)

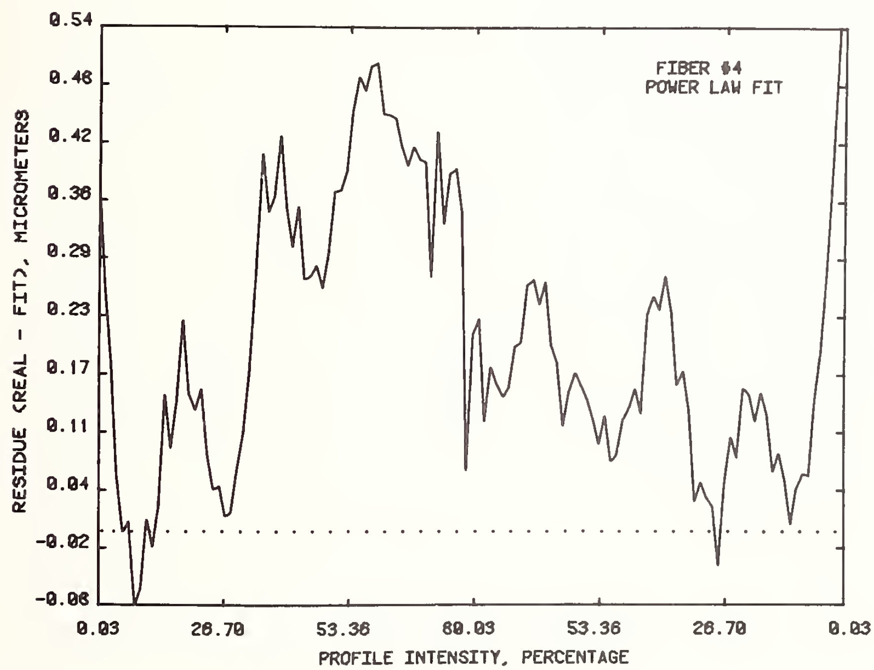

(b)

Figure 57. TNF profile for fiber #4 with superimposed least squares fit to a power law profile; a plot of the residues is also shown.

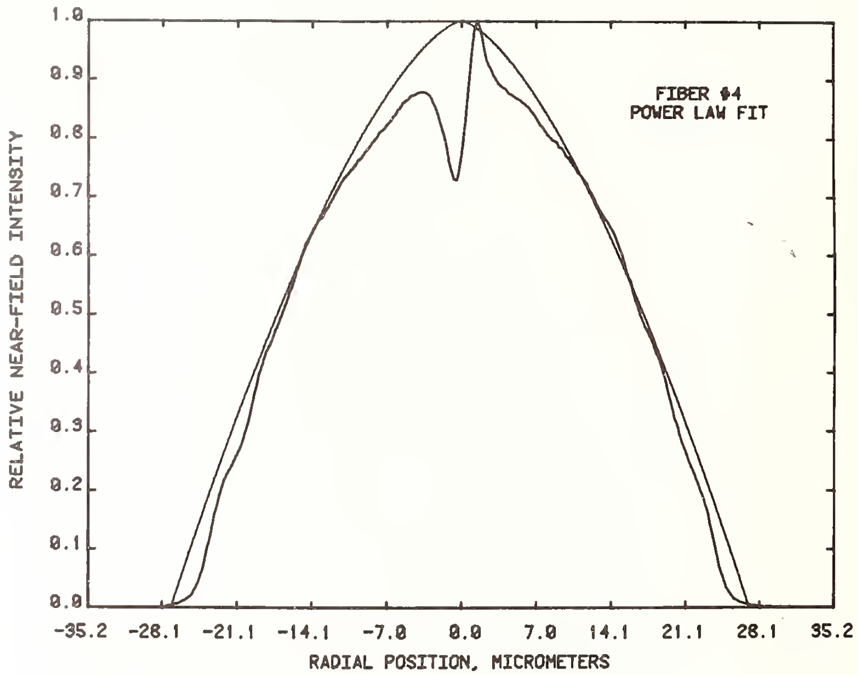

(a)

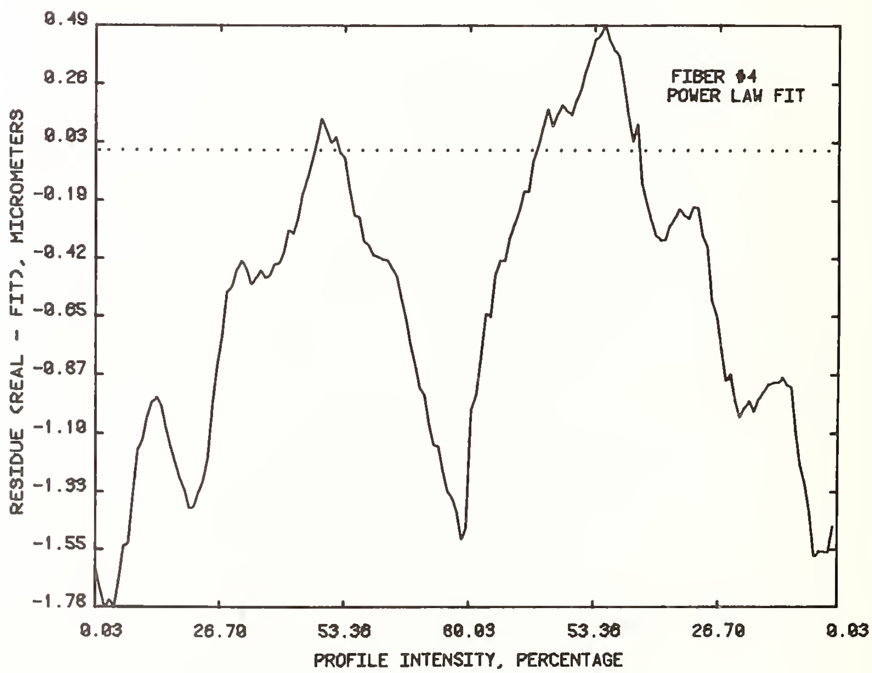

(b)

Figure 58. TNF profile for fiber #4 rotated 90° from figure 57 with superimposed leas squares fit to a power law profile; a plot of the residues is also shown.

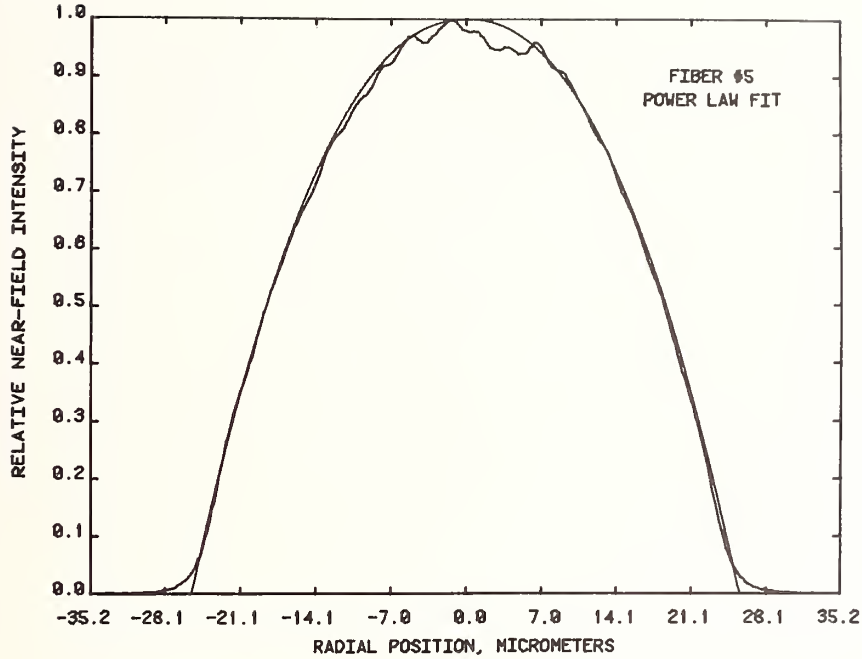

(a)

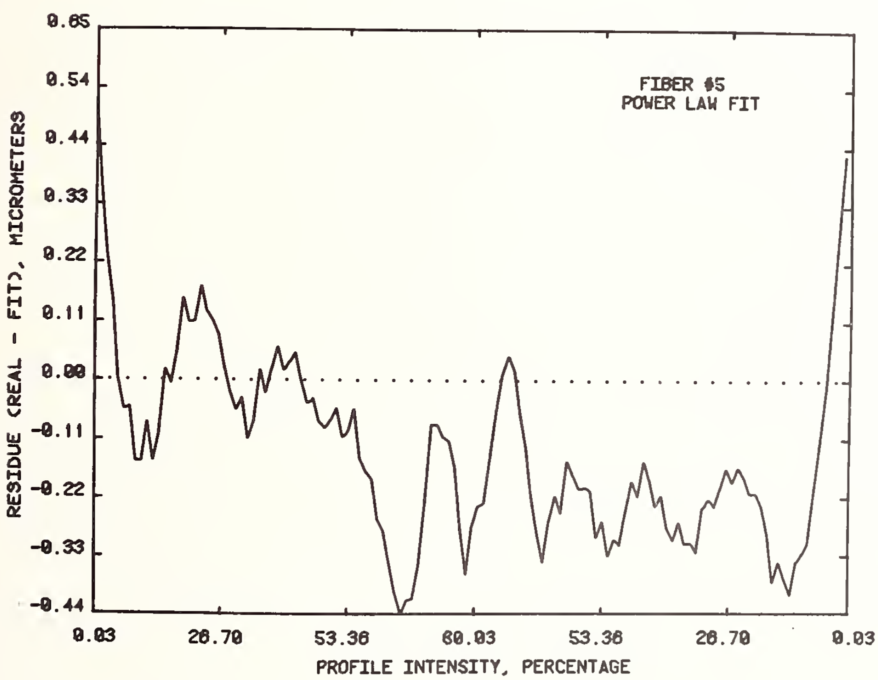

(b)

Figure 59. TNF profile for fiber #5 with superimposed least squares fit to a power law profile; a plot of the residues is also shown.

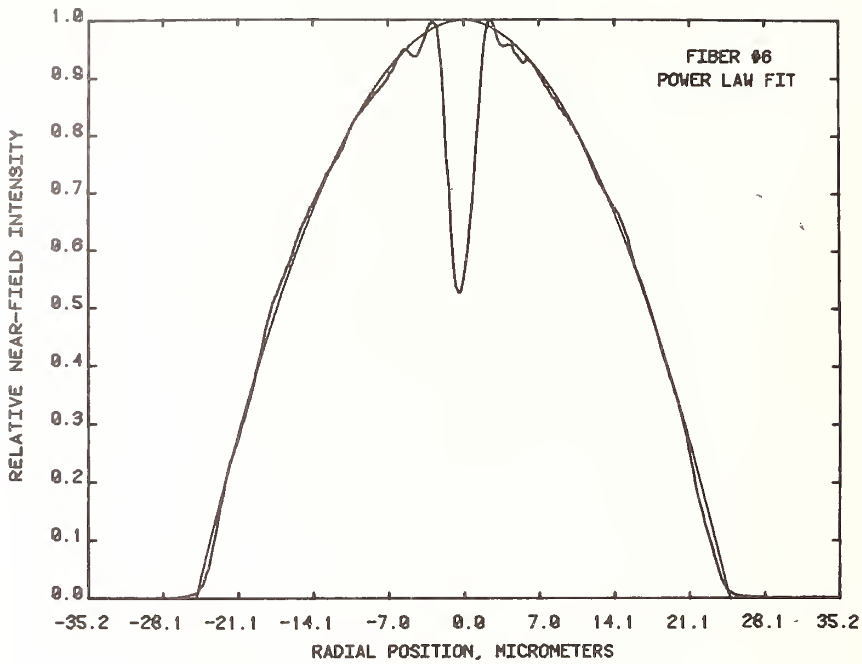

(a)

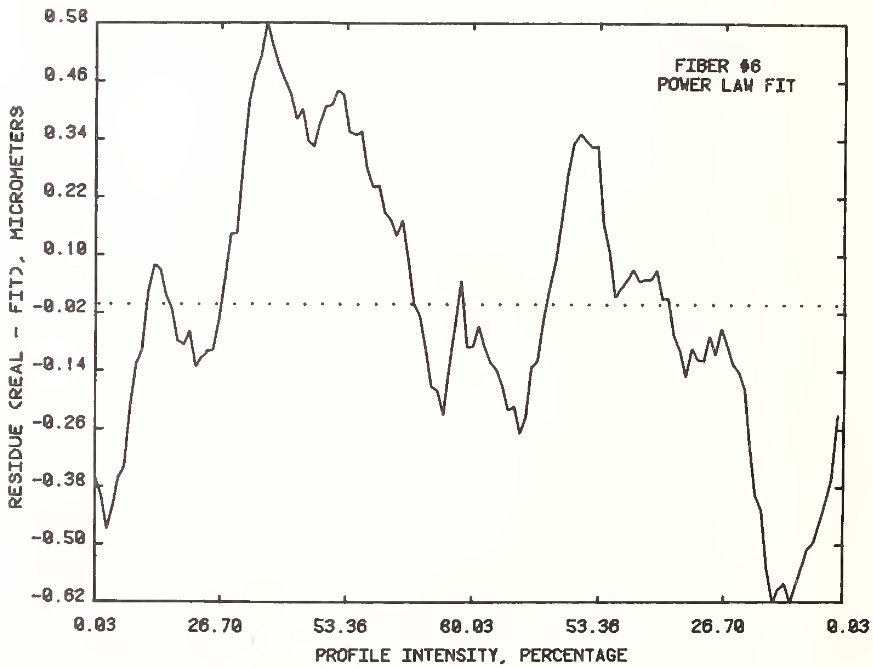

(b)

Figure 60. TNF profile for fiber #6 with superimposed least squares fit to a power la profile; a plot of the residues is also shown.

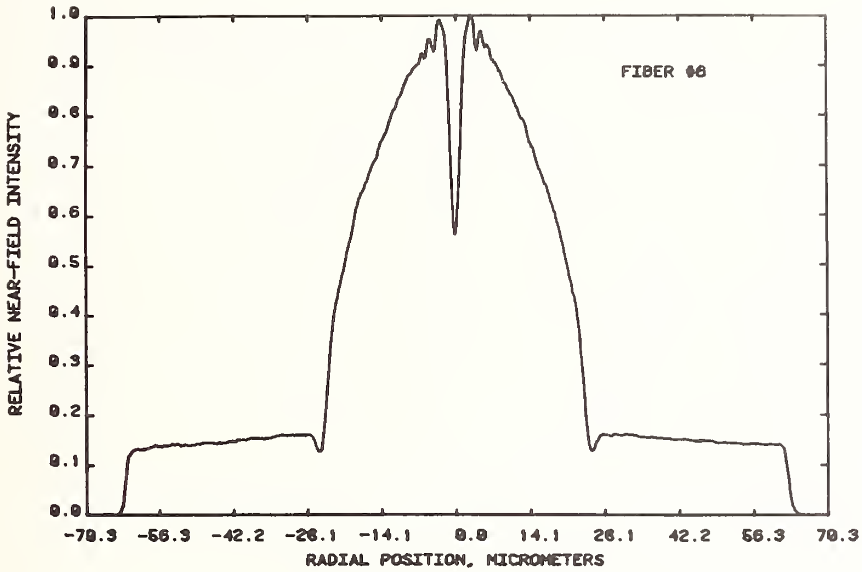

Figure 61. Results of an attempt to implement the MNF method. Although there wasn't as much cladding light as expected, the scan clearly shows the low index barrier layer at the core-cladding interface.

The iso-intensity maps for the graded-index fibers are shown in figures 62 through 68. The tolerance fields are 1.7 μm, 2.8 μm, 1.4 μm, 2.0 μm, 1.6 μm, and 0.9 μm for figures 62 through 67, respectively, and 9.5 μm for figure 68. The ellipticity ε is defined as

$$\varepsilon = \sqrt{1 - b^2/a^2}, \tag{38}$$

where a is the radius of the major axis and b is the radius of the minor axis. The ellipticities of these fibers are 0.36, 0.47, 0.32, 0.38, 0.33, 0.26, and 0.77, respectively. Note that the most circular fiber is given in figure 67 while the most elliptical is figure 68. The central extremum locations in cartesian coordinates whose origin is the center of the concentric circles (cross-hair) are (0.04 μm, 0.13 μm), (-0.40 μm, 0.31 μm), (0.00 μm, 0.22 μm), (0.40 μm, -0.48 μm), (0.40 μm, -1.36 μm), (0.04 μm, -0.40 μm), and (0.48 μm, 0.04 μm), respectively.

The short-haul fibers' contours are shown in figures 69 through 73. Unlike the overfilled launch used in measuring the core diameter of graded-index fibers, the measurements were made with a restricted launch condition. Since the short-haul fiber cores have step or quasi-step index distributions, leaky mode "ears" appear when the input is illuminated by a large NA source. Therefore, the launch NA was reduced to 0.24 to produce patterns without

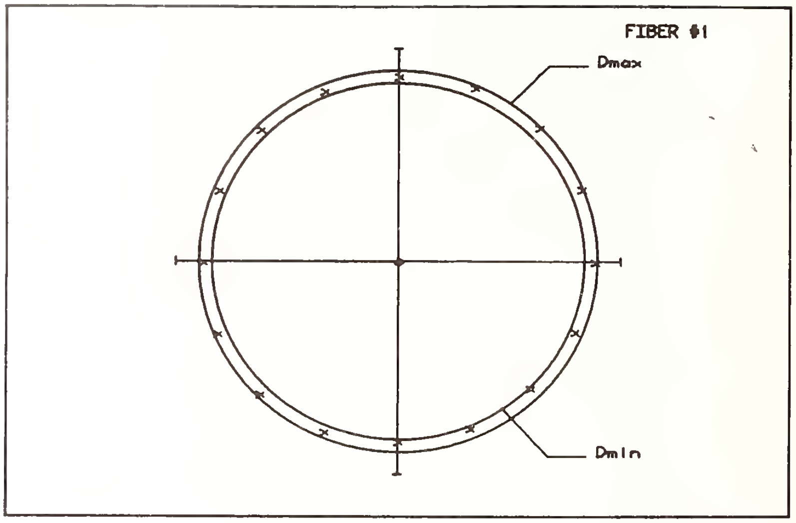

Figure 62. Iso-intensity map of fiber #1. Its tolerance field, $(D_{max} - D_{min})/2 = 1.7$ μm and ellipticity $\varepsilon = 0.36$.

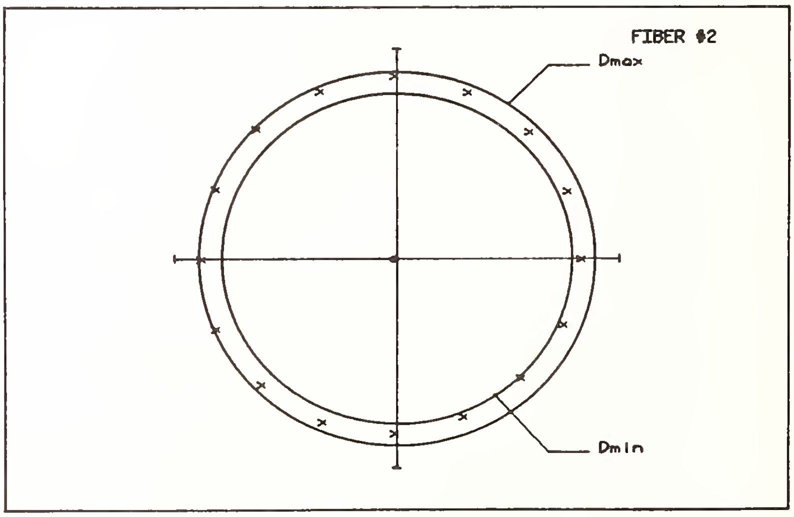

Figure 63. Iso-intensity map of fiber #2. Its tolerance field, $(D_{max} - D_{min})/2 = 2.8$ μm and ellipticity $\varepsilon = 0.47$.

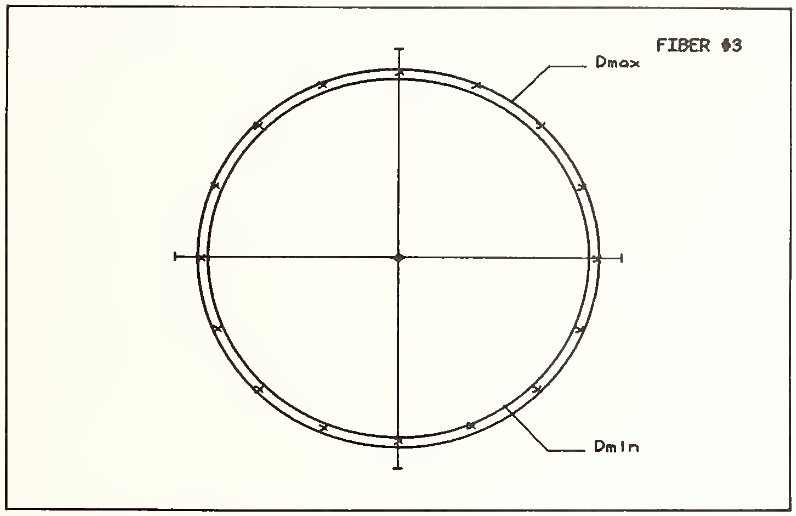

Figure 64. Iso-intensity map of fiber #3. Its tolerance field, $(D_{max} - D_{min})/2 = 1.4$ μm and ellipticity $\varepsilon = 0.32$.

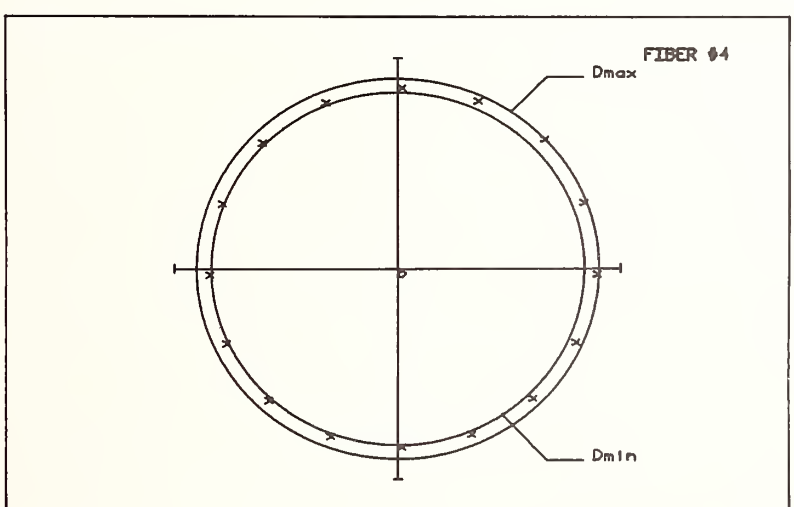

Figure 65. Iso-intensity map of fiber #4. Its tolerance field, $(D_{max} - D_{min})/2 = 2.0$ μm and ellipticity $\varepsilon = 0.38$.

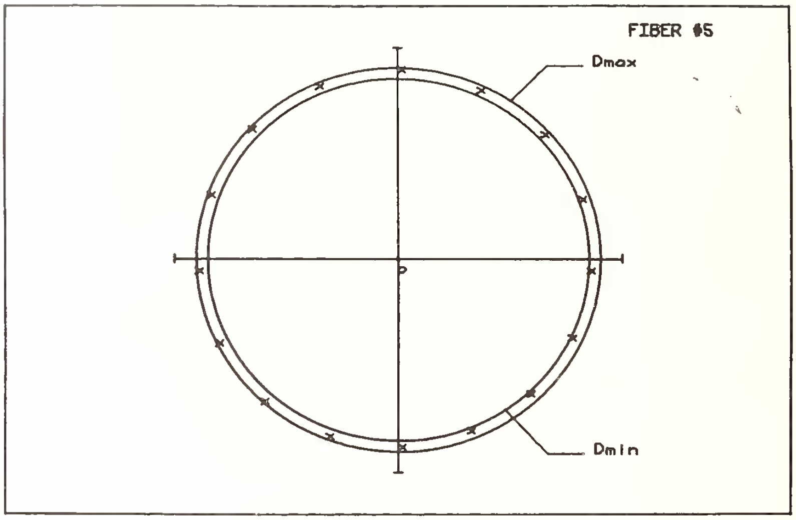

Figure 66. Iso-intensity map of fiber #5. Its tolerance field, $(D_{max} - D_{min})/2 = 1.6$ µm and ellipticity $\varepsilon = 0.33$.

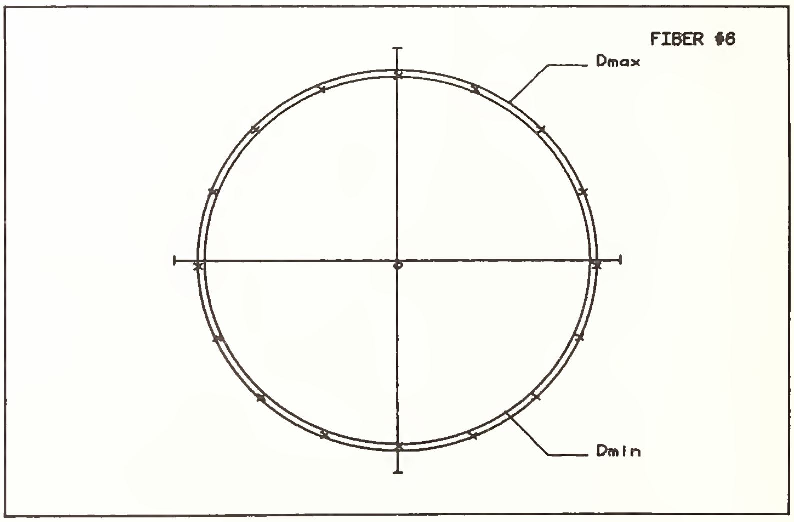

Figure 67. Iso-intensity map of fiber #6. Its tolerance field, $(D_{max} - D_{min})/2 = 0.9$ µm and ellipticity $\varepsilon = 0.26$.

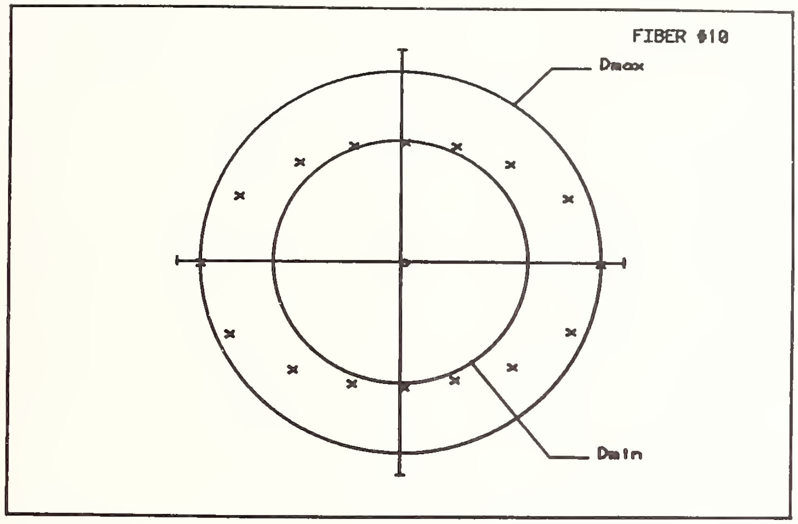

Figure 68. Iso-intensity map of fiber #10. Its tolerance field, $(D_{max} - D_{min})/2 = 9.5\ \mu m$ and ellipticity $\varepsilon = 0.77$.

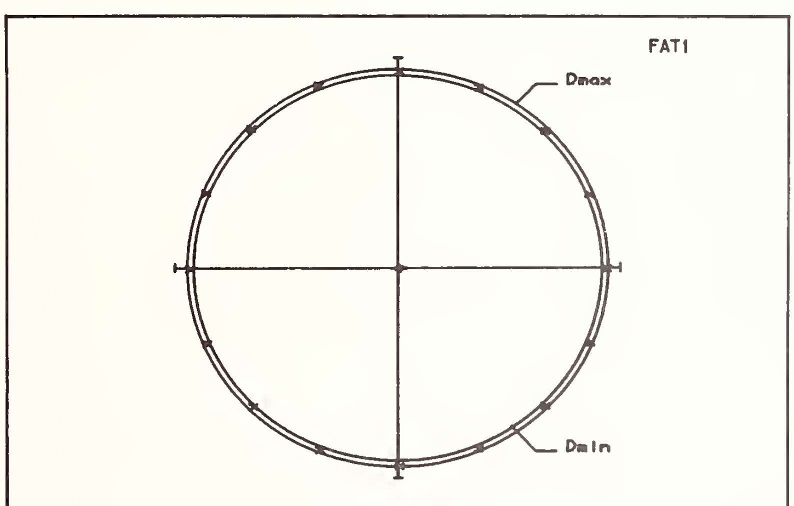

Figure 69. Iso-intensity map of fiber FAT1. Its tolerance field, $(D_{max} - D_{min})/2 = 1.5\ \mu m$ and ellipticity $\varepsilon = 0.24$.

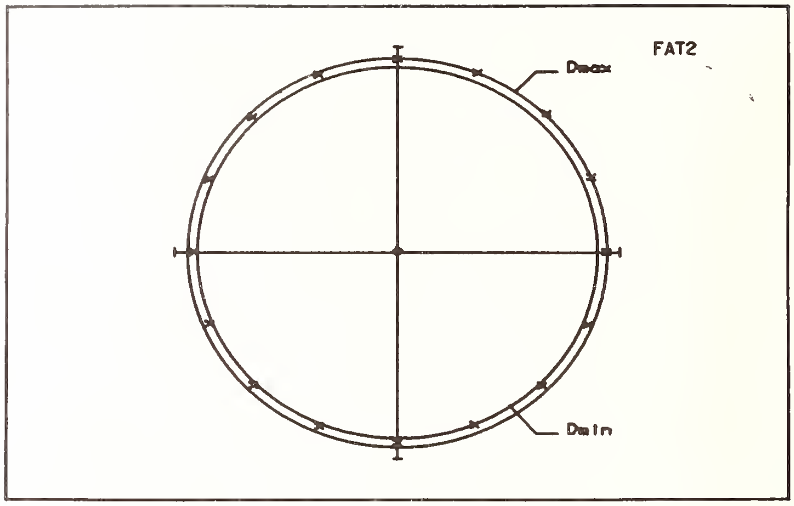

Figure 70. Iso-intensity map of fiber FAT2. Its tolerance field, $(D_{max} - D_{min})/2 = 2.3$ μm and ellipticity ε = 0.30.

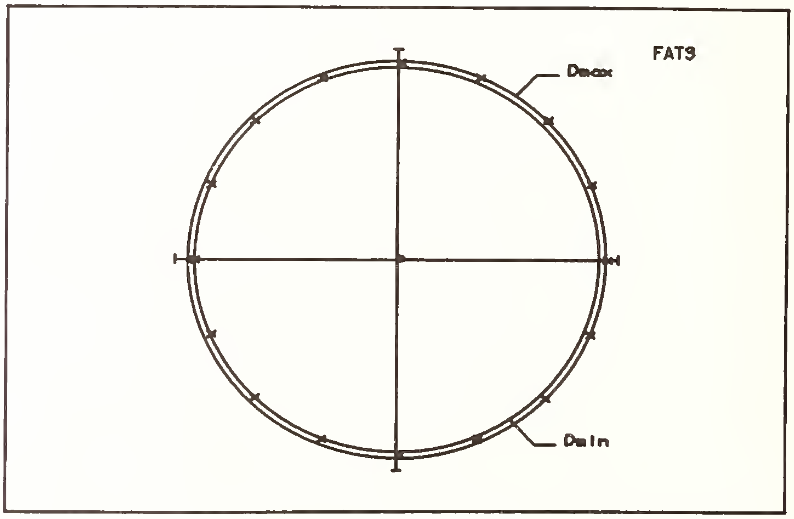

Figure 71. Iso-intensity map of fiber FAT3. Its tolerance field, $(D_{max} - D_{min})/2 = 1.6$ μm and ellipticity ε = 0.24.

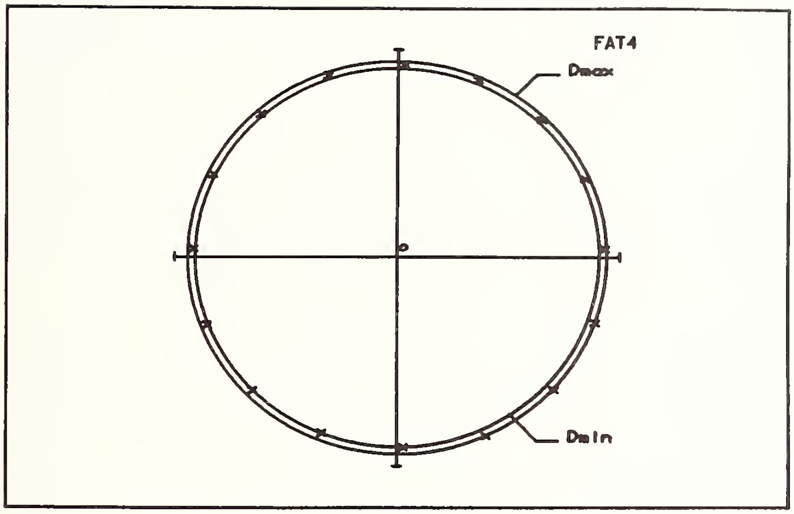

Figure 72. Iso-intensity map of fiber FAT4. Its tolerance field, $(D_{max} - D_{min})/2 = 1.7$ μm and ellipticity $\varepsilon = 0.26$.

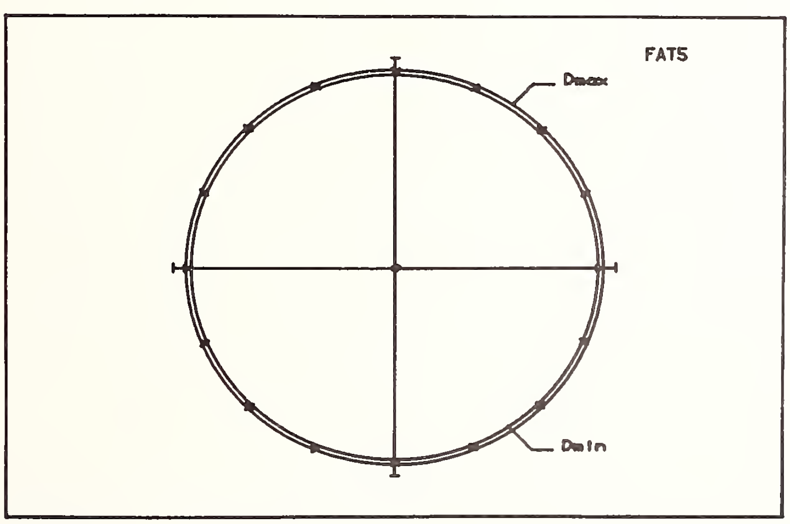

Figure 73. Iso-intensity map of fiber FAT5. Its tolerance field, $(D_{max} - D_{min})/2 = 1.2$ μm and ellipticity $\varepsilon = 0.22$.

the leaky mode "ears." The patterns are then representative of the actual index distribution. The ellipticities of fibers FAT1 through FAT5 are 0.24, 0.30, 0.24, 0.26, and 0.22, respectively. The tolerance fields for FAT1 through FAT5 are 1.5 μm, 2.3 μm, 1.6 μm, 1.7 μm, and 1.2 μm. The central extremum locations relative to the crosshairs are (-0.13 μm, -0.13 μm), (-0.48 μm, 0.31 μm), -0.31 μm, 0.11 μm), (1.01 μm, 2.24 μm), and (-0.31 μm, 0.03 μm).

The data indicate that the tolerance field of large core fibers is approximately the same as that of the 50 μm graded-index fibers. However, the large-core fibers have smaller ellipticities because the tolerance fields are a smaller percentage of the total core diameter.

The use of this type of contouring system could prove useful not only in the quality assurance environment but in the design or use of connectors and terminals. It is also an aid in the study of the effects of geometric perturbations in the transmission properties of fibers. Of particular interest is the effect of core noncircularity on leaky modes for fibers with near-parabolic profiles.

It can be shown theoretically that leaky modes attenuate much more rapidly if the core is noncircular. For near-parabolic telecommunciatons fibers, the smallest ellipticity observed was 0.26. According to theory, the leaky modes attenuate very rapidly for this large an ellipticity. Therefore, for a 2 m length, leaky mode correction factors should not be necessary.

7. EXPERIMENTAL RESULTS FROM NEAR-FIELD MEASUREMENTS ON SINGLE-MODE FIBERS

7.1 Spot Size

The near-field system as previously described can also be used to measure single-mode fibers. This however requires some sacrifice in signal-to-noise ratio. Figures 74, 75, and 76 show single-mode fiber near-field radiation patterns. Fundamental mode shapes are nearly Gaussian and show little resemblance to the index profile. Spot size is usually defined from some point on the curve. Standards groups have yet to decide on a spot size definition. The definition may well involve points on a "best" fit Gaussian curve.

7.2 Cutoff Wavelength via Spot Size

Cutoff wavelength may be determined by measuring spot size as a function of wavelength [42]. Near the cutoff wavelength the spot size is a minimum. Figure 77 shows single mode fiber spot size (i.e., diameter) as a function of wavelength. Different wavelengths were obtained by changing the interference filter. For these measurements the filter transmission widths were approximately 80 nm. In practice, however, narrower linewidths would be used to achieve better resolution. The minimum is readily apparent and figure 77 represents in principle the technique.

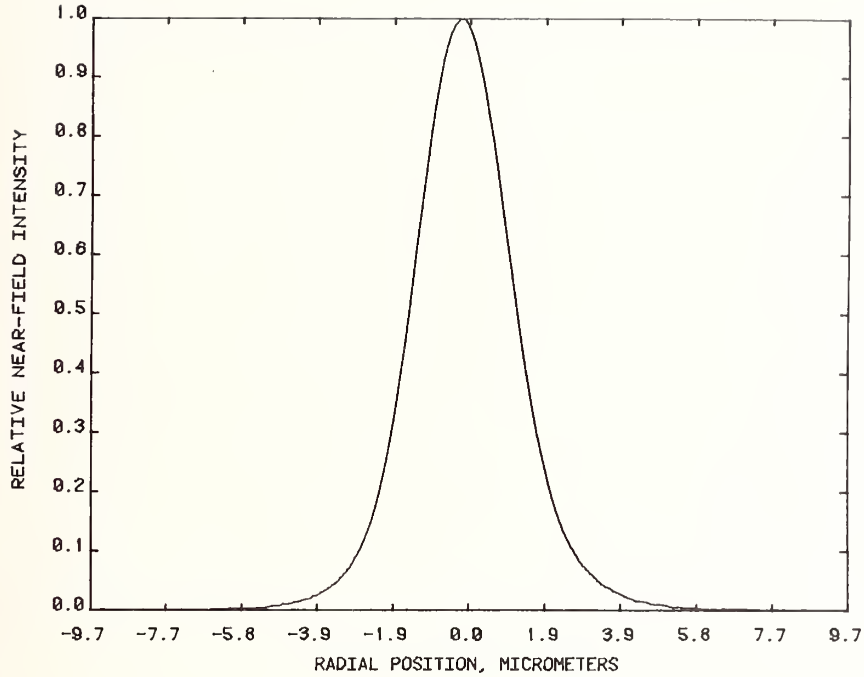

Figure 74. Single-mode fiber near-field pattern, fiber SMA.

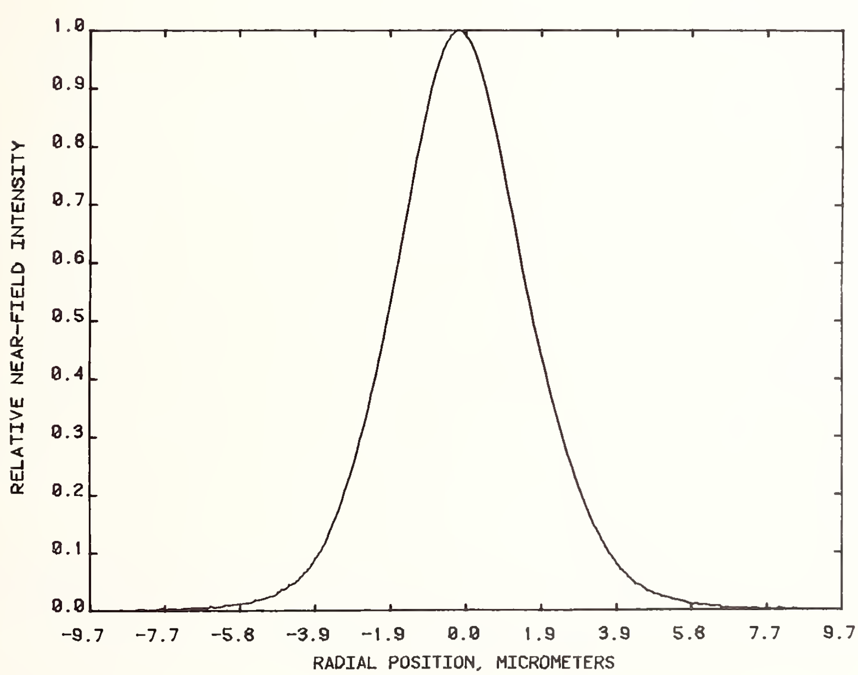

Figure 75. Single-mode fiber near-field pattern, fiber SMB.

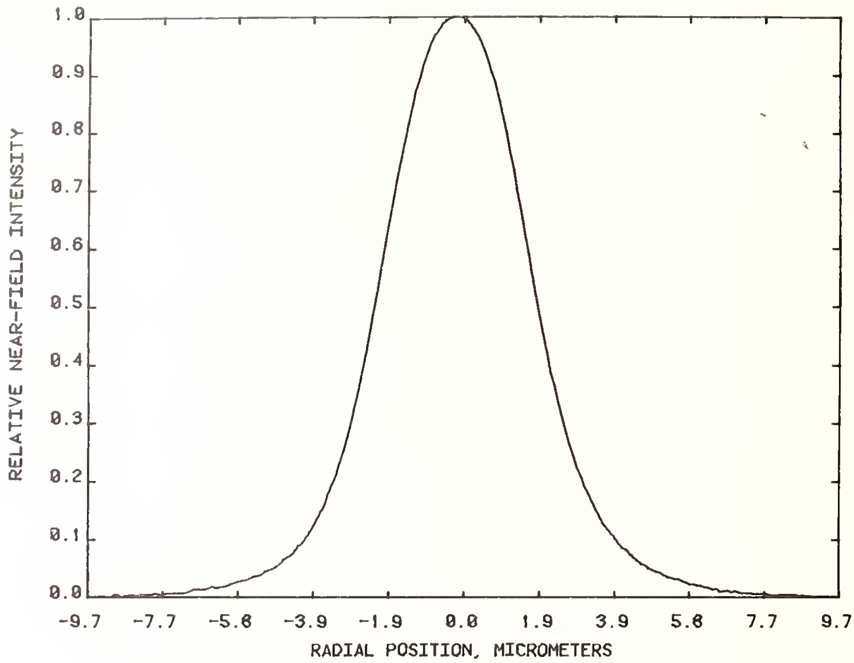

Figure 76. Single-mode fiber near-field pattern, fiber SMC.

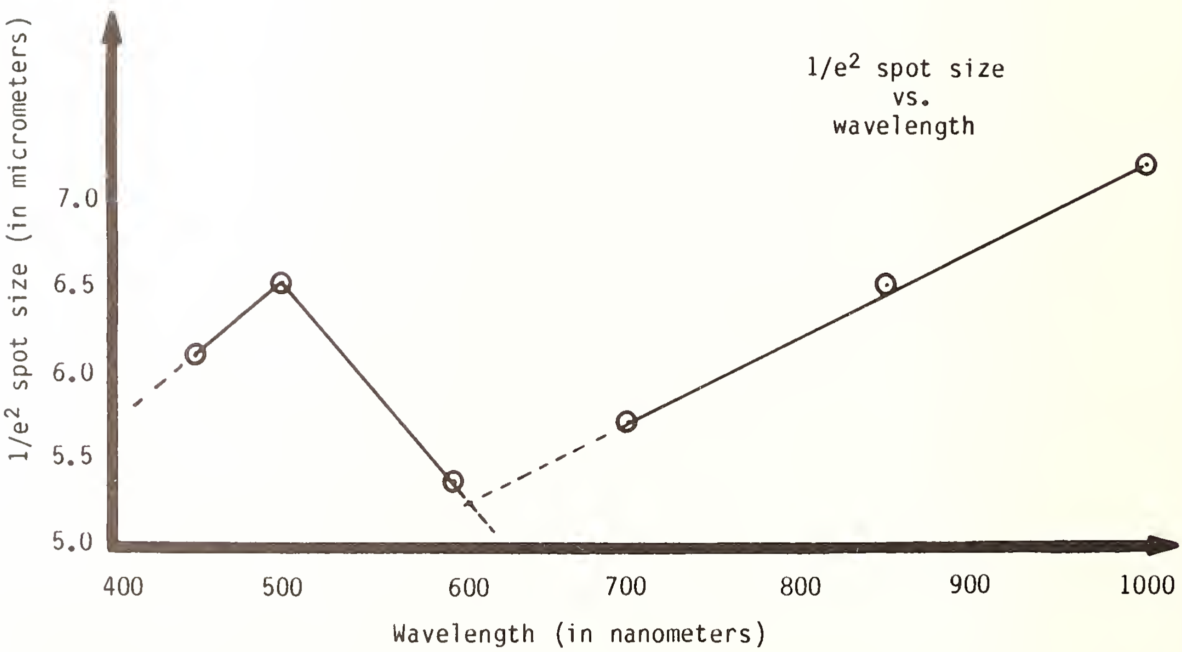

Figure 77. Graph of single-mode fiber spot size as a function of wavelength. The cutoff wavelength for the fiber is around 600 nm.

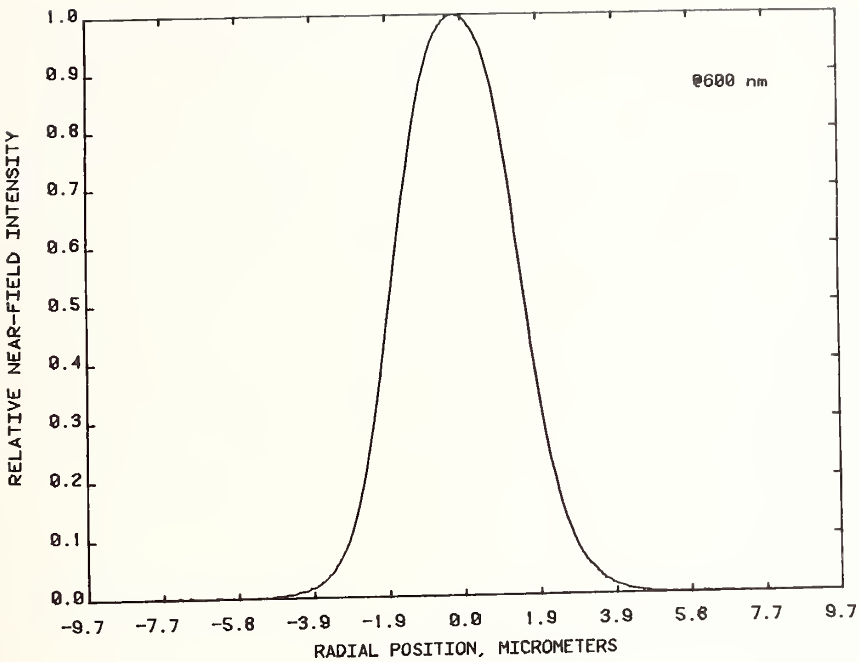

(a)

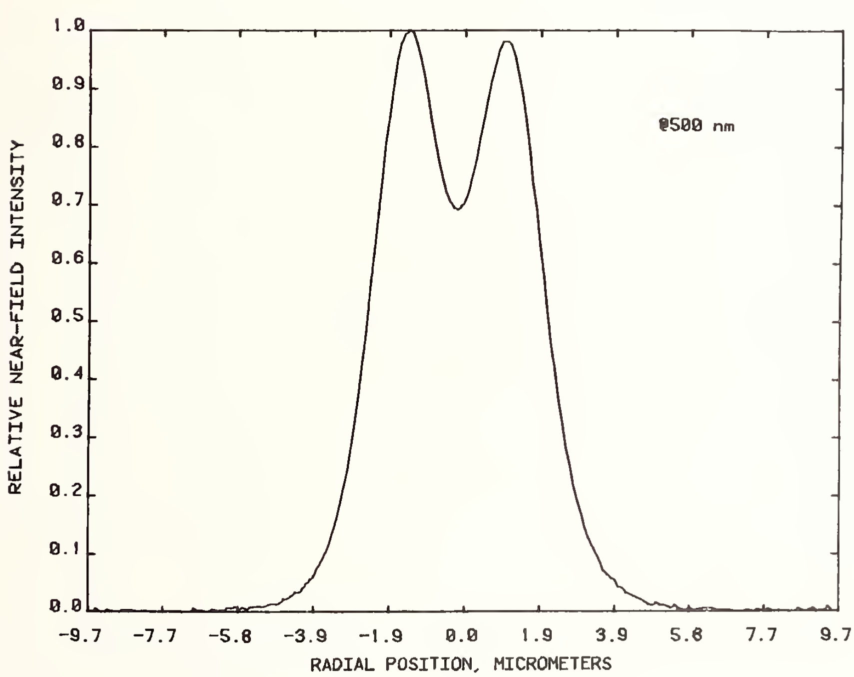

(b)

Figure 78. (a) Near-field profile of a single-mode fiber at 600 nm. The fiber is propagating a single mode. (b) Near-field profile of the same fiber at 500 nm. There is significant second order mode power present. Therefore the cutoff wavelength for this fiber is between 500 and 600 nm.

7.3 Cutoff Wavelength via Near-Field Dip

The cutoff wavelength of the second order mode may also be determined by observing the shape of the near-field pattern [20]. Figure 78 shows the near-field pattern from a fiber at two wavelengths on either side of cutoff. Near-field profile (a) is at a wavelength slightly longer than cutoff, and is the characteristic Gaussian shape. Near-field profile (b) is at a wavelength slightly less than cutoff and significant second order mode power is present to give an on-axis depression. The cutoff wavelength for this fiber would be between 500 and 600 nm. Curves (a) and (b) were obtained using two different interference filters. In practice, the source would be continuously variable, for example a monochrometer. Cutoff could then be defined as the wavelength where the depression just begins to appear. This method of determining cutoff can be made rapidly if the detector is a quantitative vidicon or array to display the two dimensional profile in real time.

7.4 Estimating Index Profiles of 1.3 μm Single Mode Fibers by Blue Near-Field Measurements†*

Single mode fibers can be characterized with different parameters and measurement techniques. In quality control, manufacturers frequently measure attenuation, spot size, cutoff wavelength, and minimum dispersion wavelength. The role of fiber index profile measurements in quality control is not yet clear. The most generally accepted index-profiling technique for single mode fibers is the refracted ray method sometimes referred to as the RNF (refracted near-field) [43,44,45,46]. While RNF yields high resolution with good accuracy, it is susceptible to contamination and requires a sophisticated apparatus with submicrometer positioning accuracy. In the case of 50 μm core diameter multimode fibers, the TNF method (transmitted near-field) gives an acceptable measure of the index profile and is used by many manufacturers to measure core diameter. This section investigates the feasibility of using TNF methods to determine the index profile of singlemode fibers designed for 1.3 μm. While TNF methods cannot achieve the resolution of RNF, they could be useful in some applications especially if high resolution index profiles are not routinely needed.

Early work by Sladen et al. showed that, for equal mode excitation (Lambertian source) on short lengths of multimode fiber, the TNF closely resembles the refractive index profile [2]. A large number of fiber modes are required to replicate an index profile with high resolution [23]. This means the measurements must be made at a sufficiently high value of the normalized frequency, V [47].

The effect of V value on near-field profiles was investigated theoretically by solving numerically the scalar wave equation to give the waveguide modes for commonly encountered index profiles [48]. The near-field intensity is then calculated by summing the intensities of all bound modes allowed for a given value of V. Assumptions in the calculation include

†RNF measurements for this study were contributed by M. Young of NBS.
*Theoretical TNF profiles were contributed by P. M. Rodhe, an NBS guest worker on leave from Sieverts Kabelverk, Sundyberg Sweden.

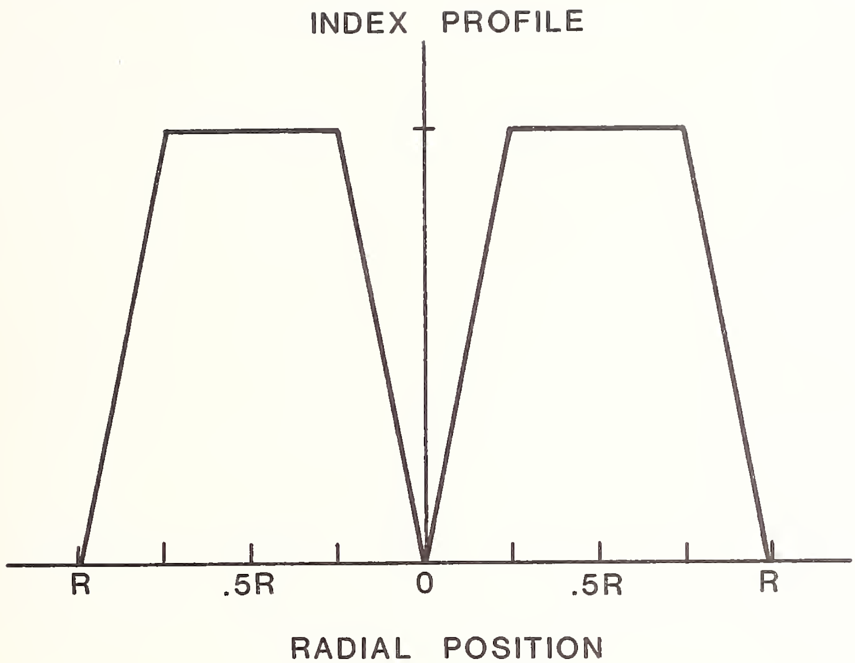

Figure 79. Model of a typical index profile exhibiting tapered core-clad boundary and a deep on-axis dip.

equal mode excitation, an unpolarized nearly incoherent source, and a weakly guiding approximation to the scalar wave equation. Many single mode fibers have step-like cores with a deep on-axis index depression. A model for this type of profile is given in figure 79. Here the on-axis dip goes completely to the cladding and recovers linearly to a step at 0.25 R, where R is the core radius. Instead of an abrupt core-cladding boundary, the profile starts to taper linearly to the cladding at 0.75 R. Calculated near-field intensities for this profile are given in figures 80(a) and 80(b) for V values of 2, 2.79, 8, and 40. When V equals 2, the fiber supports only a single mode, and the near field is Gaussian shaped with significant power propagating in the cladding. Two modes are present when V equals 2.79, and the near-field intensity exhibits an on-axis dip characteristic of the radial variation of the second order mode. With higher V, the near-field intensity begins to approach the index profile. When V equals 8, there is still significant mode ripple while at a V of 40 the near-field intensity is almost exactly the index profile. Mode ripple can be reduced somewhat by using a broad linewidth source which tends to average the fluctuations [23]. Near-field intensities in figure 80 were calculated assuming a single frequency source.

Telecommunication fibers that are single mode at 1.3 μm have cut-off wavelengths near 1.2 μm where V is approximately 2.4 (step-index fiber). With blue light (0.4 to 0.45 μm), measurements at a V of 7 are possible. It would not be advisable to increase V appreciably

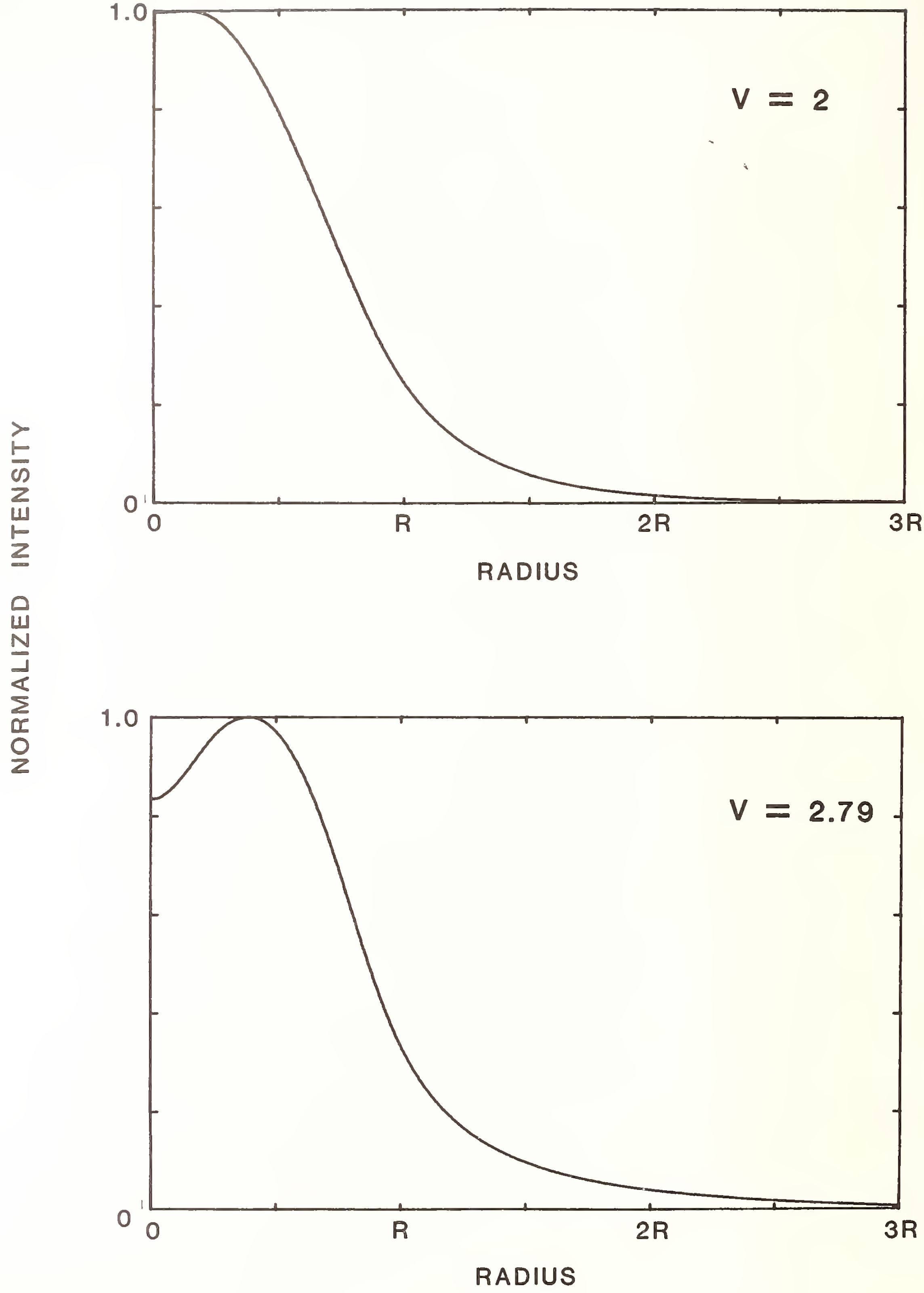

Figure 80a. Near-field radiation pattern for index profile of figure 1 at V = 2 (top) where there is a single mode, and at V = 2.79 (bottom) where there are two modes. Cutoff occurs at V = 2.76.

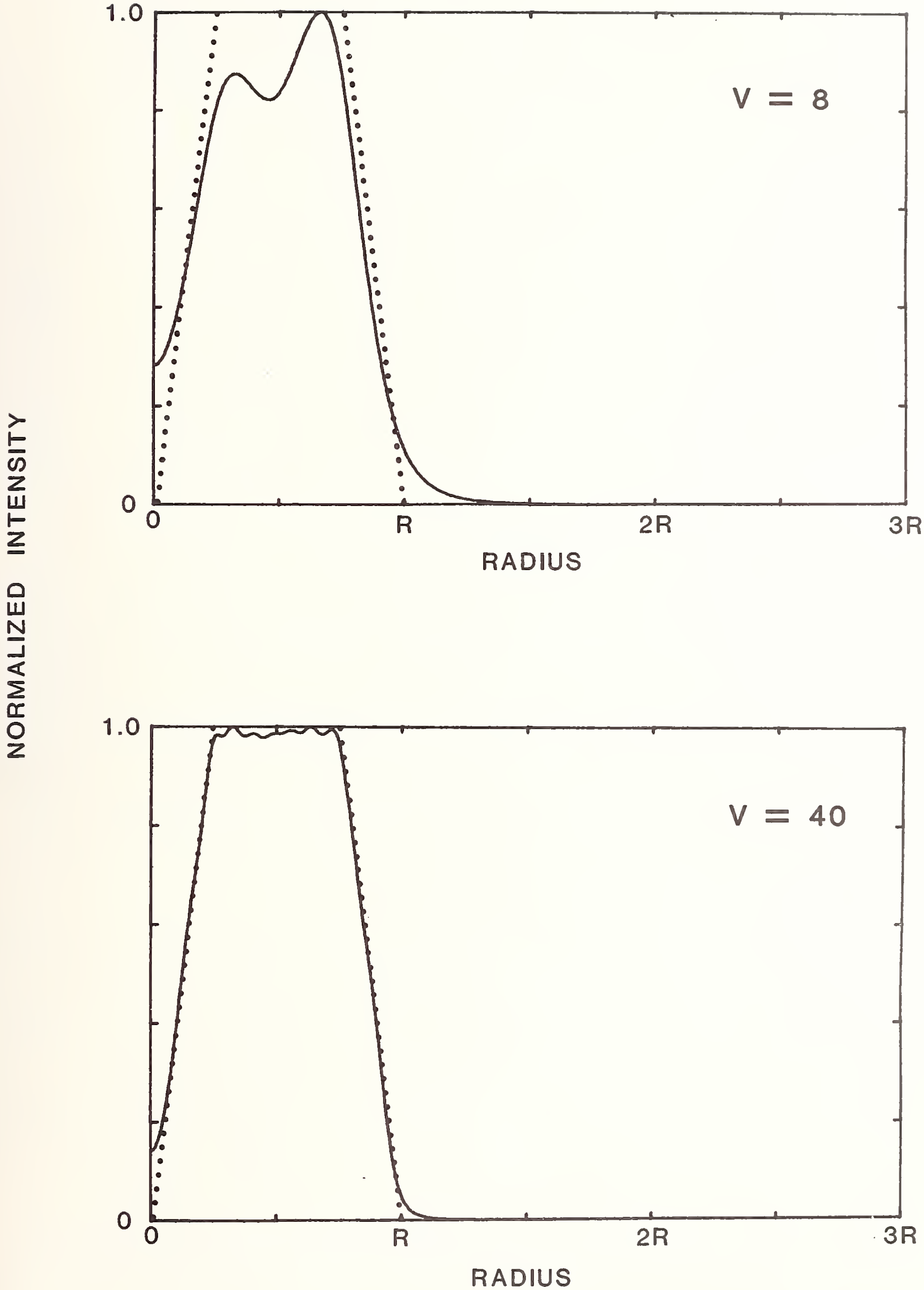

Figure 80b. Near-field radiation pattern for index profile of figure 1 at V = 8 (top) and V = 40 (bottom). Dotted line is the actual index profile.

by a further decrease in wavelength since germania silicate has absorption bands in the ultraviolet [49]. Near an absorption peak the index exhibits high dispersion, and profile shapes would be expected to change. To investigate the magnitude of this effect, measurements were made on 50 μm core, 0.2 NA (numerical aperture) multimode fibers at wavelengths of 0.45 and 0.85 μm. Over this wavelength range the near-field profiles were similar. As an example, for one fiber, the full widths at half maximum differed by only 3 percent.

Experimental TNF profiles for the 1.3 μm single mode fibers were obtained using a tungsten halogen source and optics to project a 100 μm diameter spot on the input fiber end. A broadband interference filter centered at 0.45 μm with a linewidth of 0.07 μm determined the source spectral characteristics. The output end of the typical 2 m long fiber sample was imaged by a 40x, 0.65 NA microscope objective. A silicon detector with a 30 μm diameter pinhole was used to scan the image. Referred to the fiber end face, the pinhole is equivalent to a 0.75 μm diameter collecting aperture. The pinhole-detector was scanned using a computer controlled stepper-motor translator to take data points every 0.1 μm as referred to the fiber end face. Dimensional calibration of the scan at 0.45 μm was accomplished using a previously described calibration reticle [50].

Near-field patterns can be influenced by contributions from leaky modes [2]. These contributions cause the near-field intensity to deviate from the actual index profile. In practice, it is not necessary to apply corrections to near-parabolic profile fibers [50,9]; however, for step index fibers the corrections can be significant. Fortunately for pure step index fibers, the leaky modes can be eliminated by launching with a NA which is close to that of the fiber. TNFs at 0.45 μm were obtained at launch NAs of 0.36 and 0.14 for the single mode fibers used in this study and little difference was observed in the profiles. Moreover, most of the near-field profiles did not exhibit the characteristic leaky mode "ears" observed for step index fibers. We therefore conclude that leaky modes are not a significant problem at least in the fibers tested.

TNF profiles were measured at a wavelength of 0.45 μm for six 1.3-μm single-mode fibers. Figures 81 and 82 give profiles at wavelengths of 1.0 and 0.45 μm for fibers SM1 and SM2, respectively. These results are in qualitative agreement with the theoretical trend predicted in figure 80. At 1.0 μm there are only a few modes and appreciable power extends into the cladding. The contribution from the second order mode results in a smooth central depression. At 0.45 μm there are approximately 25 modes ($V^2/2$), and the near-field power is more confined to the core. In the case of fiber SM2 the on-axis dip is narrower and deeper.

The most interesting results are the comparisons of TNF profiles to the actual index profiles as determined by RNF. These comparisons are given for four of the fibers in figures 83 through 86 and are representative of the six fibers measured. The height to

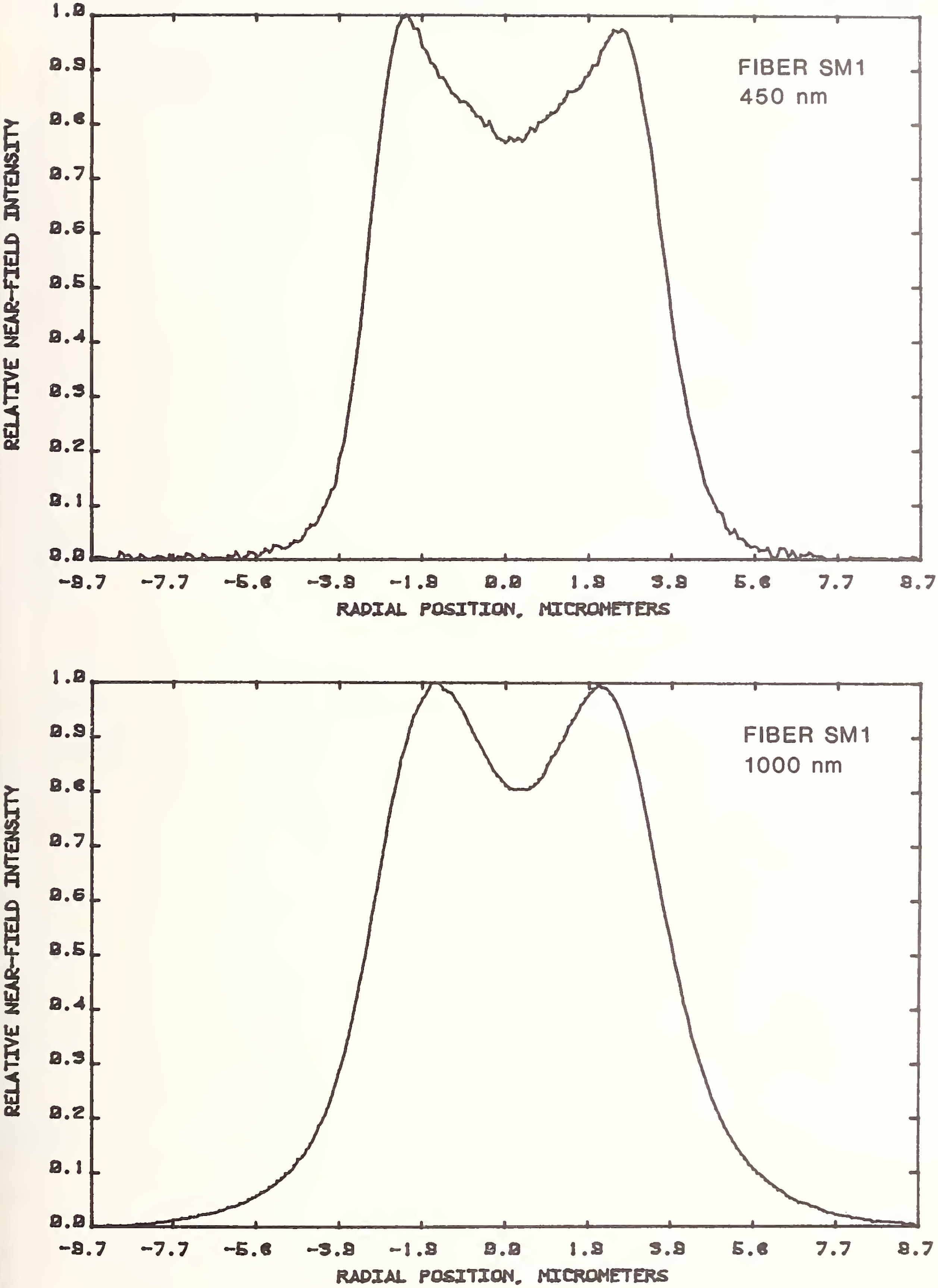

Figure 81. Near-field radiation pattern, fiber SM1, at 0.45 μm and 1.0 μm showing the effect of increased V.

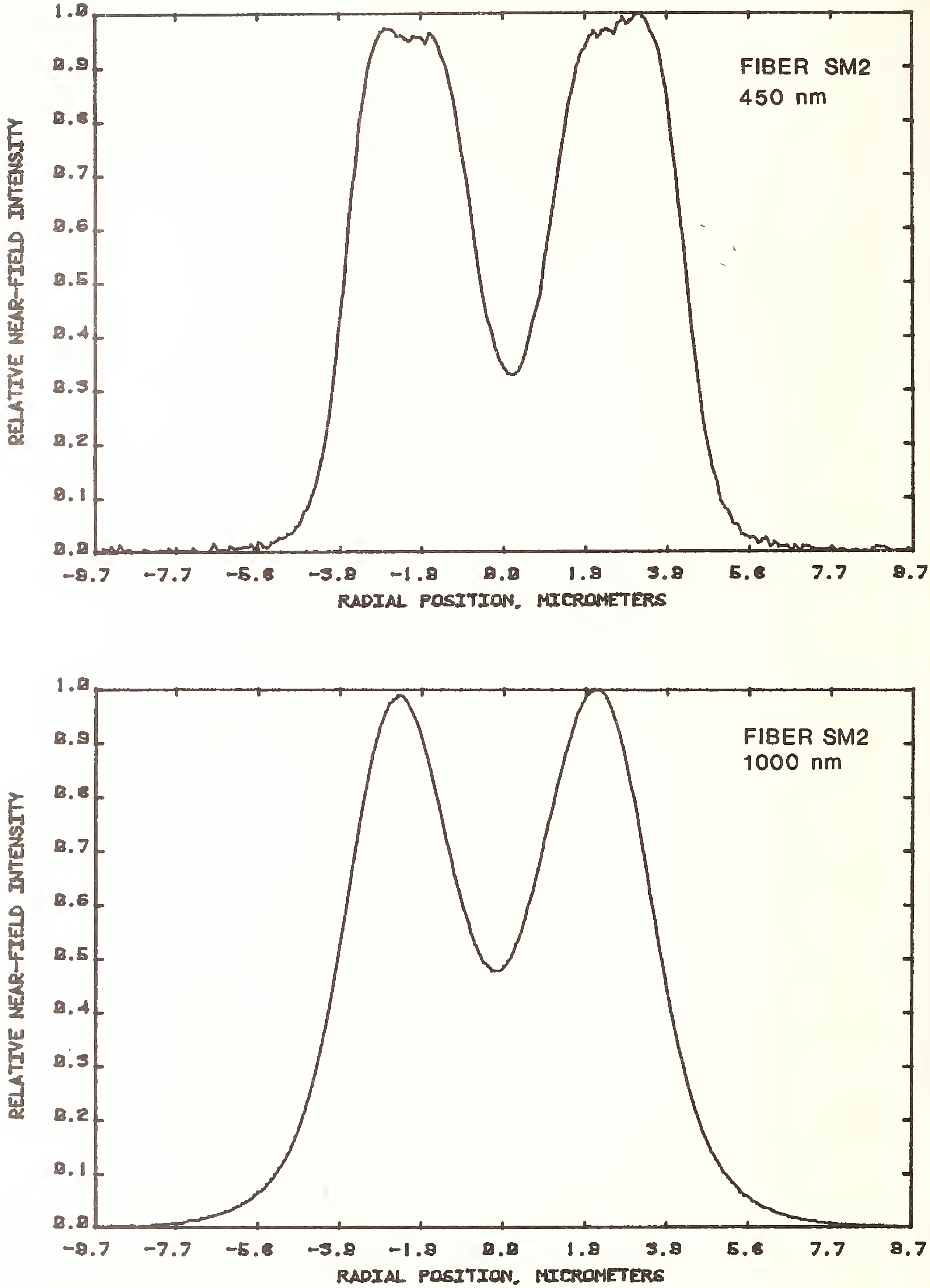

Figure 82. Near-field radiation pattern, fiber SM2, at 0.45 μm and 1.0 μm showing the effect of increased V.

FIBER SM1

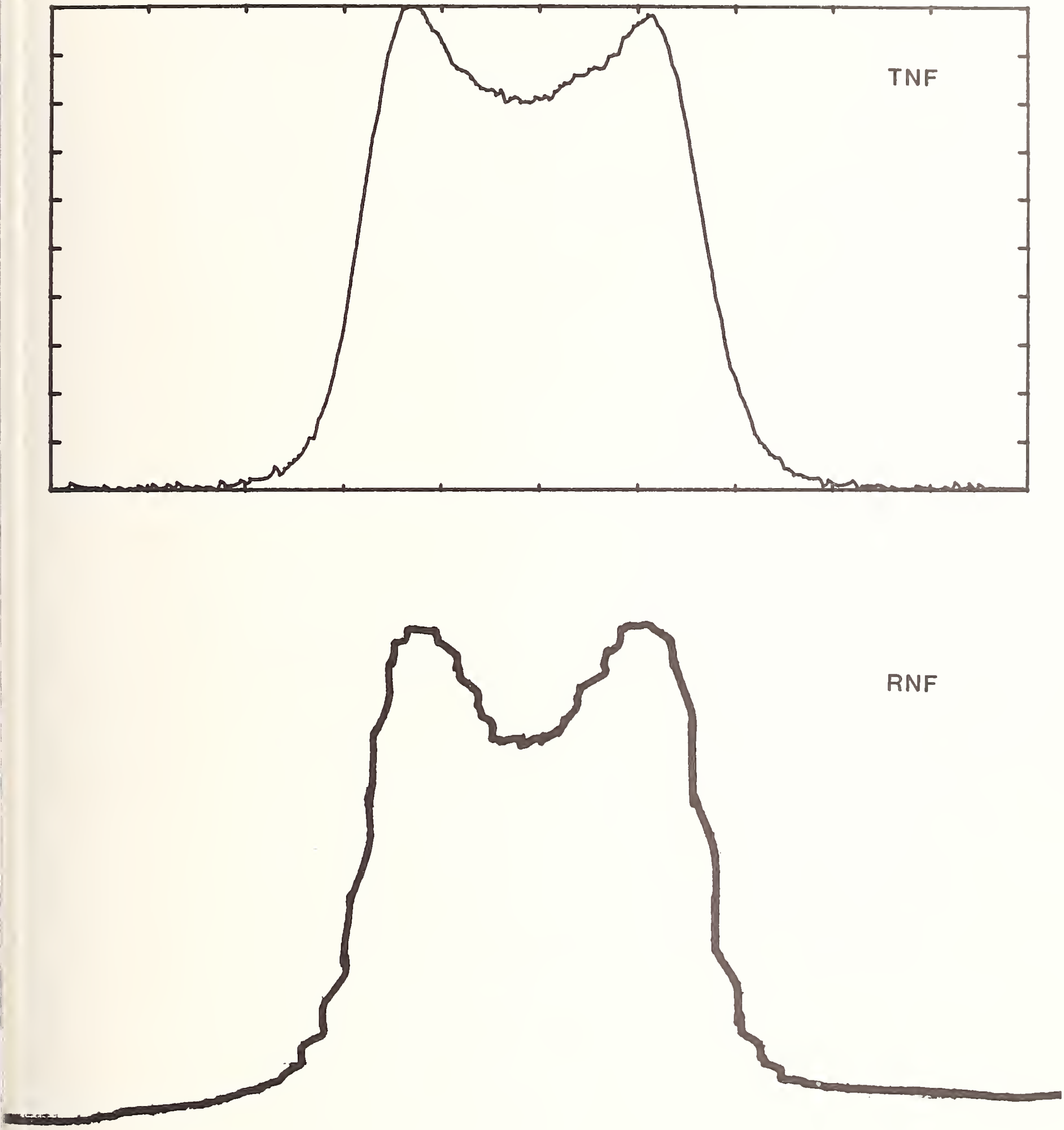

Figure 83. Comparison of 0.45 μm TNF and RNF, fiber SM1.

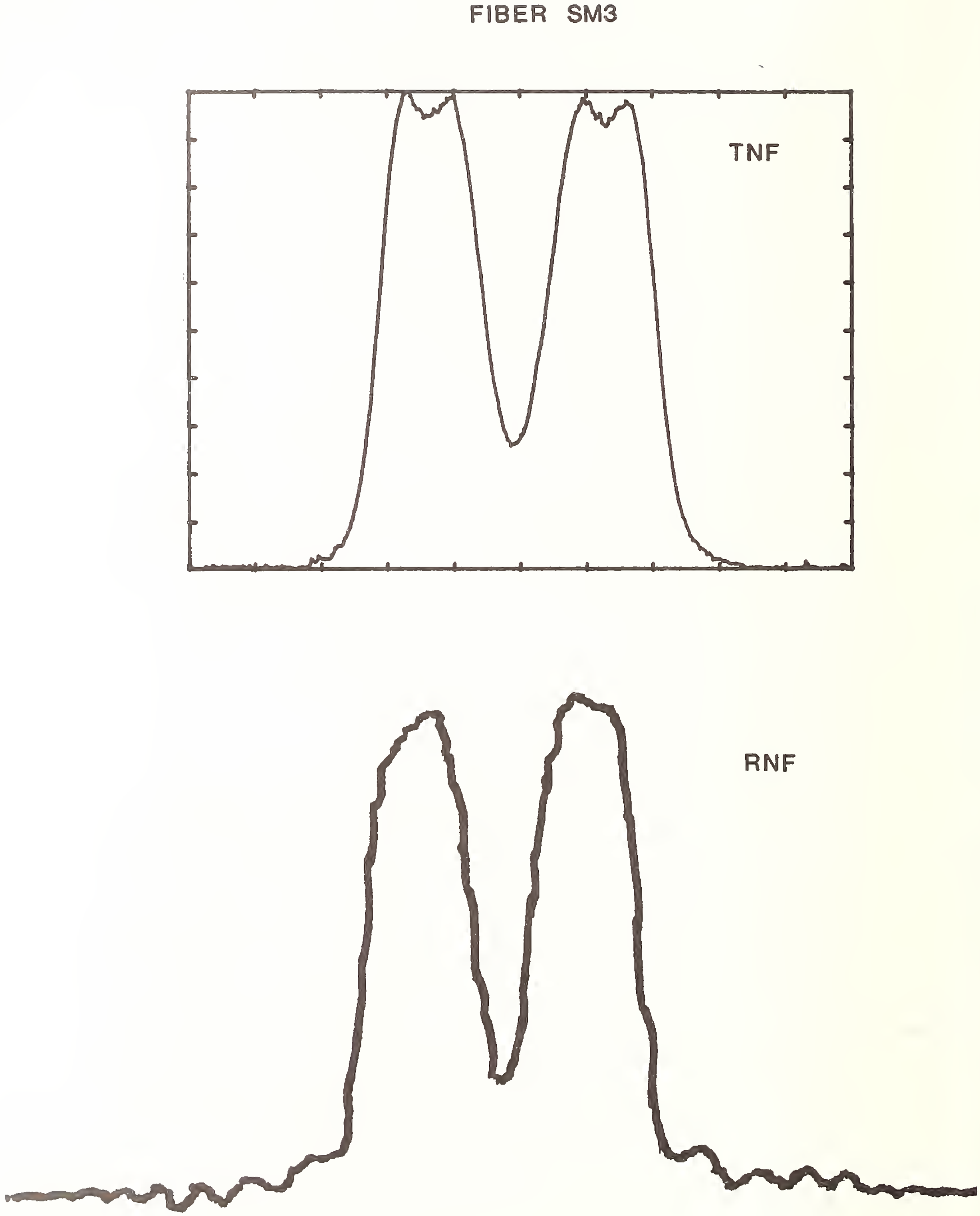

Figure 84. Comparison of 0.45 μm TNF and RNF, fiber SM3.

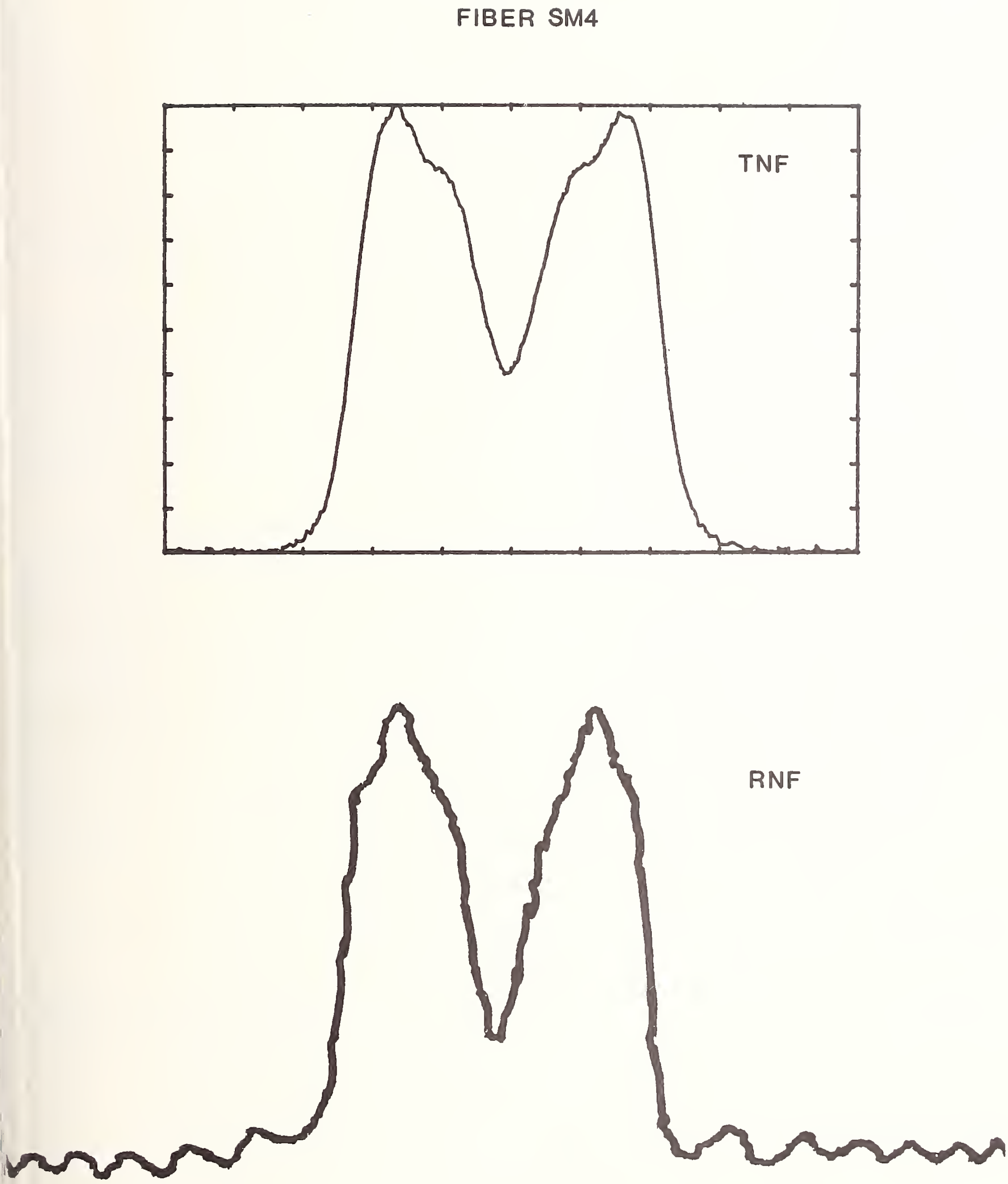

Figure 85. Comparison of 0.45 μm TNF and RNF, fiber SM4.

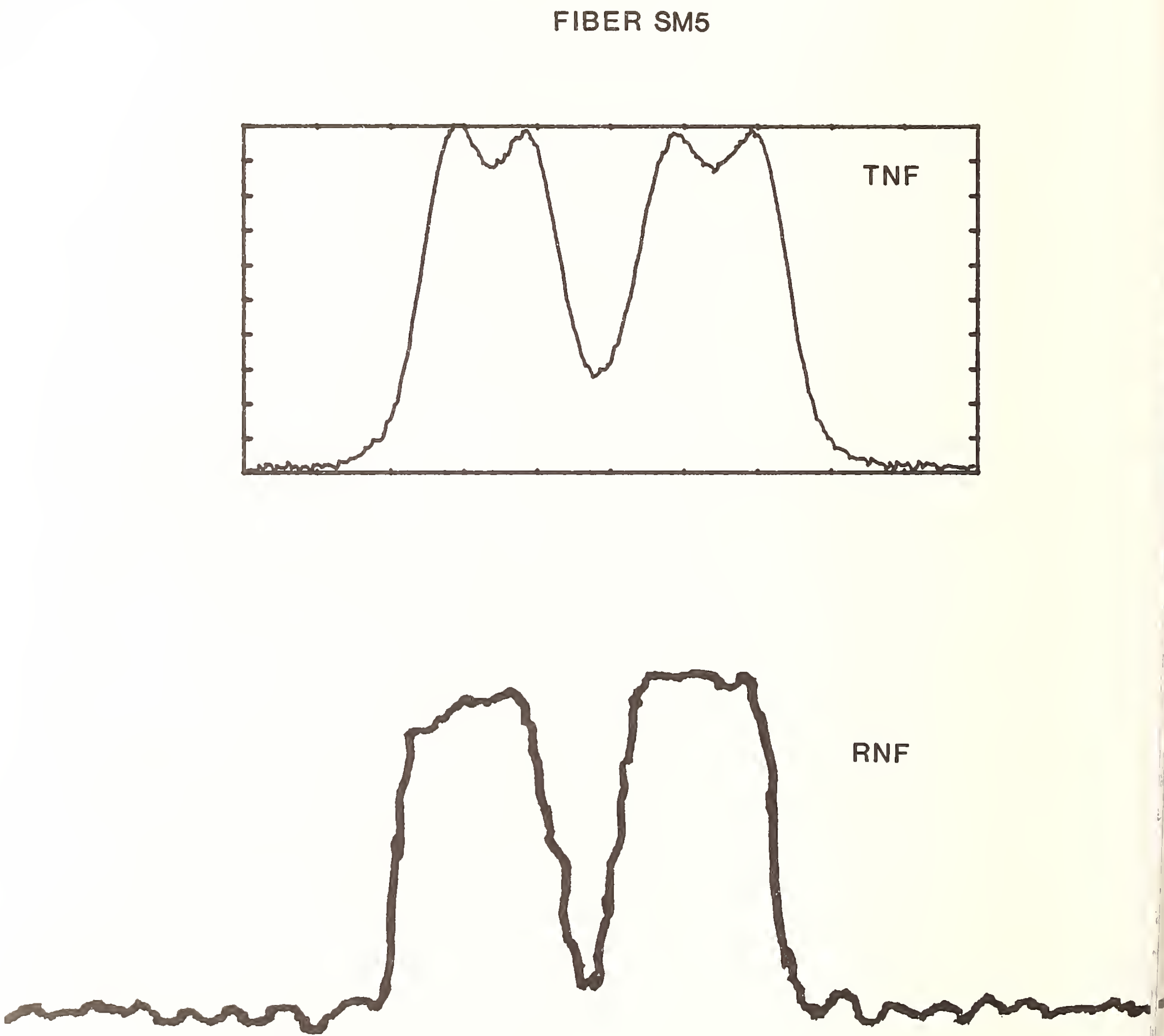

Figure 86. Comparison of 0.45 μm TNF and RNF, fiber SM5.

Table 9. 15 percent core diameters, μm.

Fiber	RNF	TNF	RNF-TNF
1	9.2	8.4	+0.8
2	9.6	9.2	+0.4
3	9.6	9.3	+0.3
4	10.4	9.8	+0.6
5	11.1	11.2	-0.1
6	9.6	9.1	+0.5
average			+0.4

width ratio of a given TNF profile was computer scaled to match the corresponding RNF profile approximately so that comparisons of shape can be more readily made. Actual dimensional information is given in table 9 for all six fibers. The RNF measurements were made at 0.6328 μm and have a resolution of 0.75 μm with a dimensional accuaracy of approximately ±0.5 μm.

Fiber SM1 has a shallow index depression and the TNF predicts the same shape and on-axis depth as the RNF. Fiber SM3 has a much deeper depression and again the TNF and RNF give about the same on-axis depth. The main differences are the two 5-percent depressions near the peaks of the TNF. Fiber SM4 has a funnel-shaped index depression which is also predicted by the TNF, but appears slightly exaggerated. Fiber SM5 is nearly a perfect step with a depression going almost to the cladding. The TNF does not completely resolve the dip and 10 percent depressions are apparent in the peaks. Table 9 compares the core diameters measured by the two methods. The comparisons are made at the 15 percent levels because there are ripples and fine structures near the baseline in the RNFs. The RNFs are larger by 0.4 μm on the average. This may not be significant since the RNF calibration accuracy was ±0.5 μm.

TNF profiles have less resolution than RNF and exhibit ripple in some cases. Index dips for the RNF profiles often appear deeper, core-cladding boundaries more perpendicular, and abrupt features more evident. However, the general TNF shapes are correct and relatively insensitive to end preparation, and ripple is less than 10 percent for all fibers tested. This level of ripple is less than theory predicts, probably because of broad source linewidth. Blue-ultraviolet TNFs on 1.3 μm single mode fibers could be useful in situations requiring experimental simplicity and two dimensional information. With sensitive photomultiplier detectors, it would be possible to scan cores in a matter of seconds. Also vidicons with computer image acquisition can rapidly obtain two dimensional information such as core size, core ovality, and concentricity.

8. REFERENCES

[1] Cathey, W. T. Optical information processing and holography. New York: John Wiley; 1974.

[2] Sladen, F. M. E.; Payne, D. N.; Adams, M. J. Determination of optical fiber refractive index profiles by a near-field scanning technique. Appl. Phys. Lett. 28(5):255-258; 1976 March.

[3] Adams, M. J.; Payne, D. N.; Sladen, F. M. E. Leaky rays on optical fibers of arbitrary (circularly symmetric) index profiles. Electron. Lett. 11(11):239-240; 1975 May.

[4] Holmes G. T. Propagation parameter measurements of optical waveguides. Proc. SPIE, Fiber Optics for Communication and Control, Vol. 224; 1980.

[5] Kitayama, K., Keikai, S.; Uchida, N. Impulse response prediction based on experimental mode coupling coefficient in a 10-km long graded-index fiber. IEEE J. Quant. Elect. QE-16(3):356-362; 1980 March.

[6] Streckert, J.; Brinkmeyer, E. Characteristic parameters of monomode fibers. Appl. Opt. 21(11):1910-1915; 1982 June.

[7] Adams, M. J.; Payne, D. N.; Sladen, F. M. E. Length dependent effects due to leaky modes on multimode graded-index optical fibres. Opt. Commun. 17(2):204-209; 1976 May.

[8] Franzen, D. L.; Kim, E. M. Interlaboratory comparison to determine the radiation angle (N.A.) of graded-index optical fibers. Appl. Opt. 20(7):1218-1220; 1981 April.

[9] Petermann, K. Uncertainties of the leaky mode correction for near-square law optical fibres. Electron. Lett. 13(17):513-514; 1977 August 18.

[10] Barrell, K. F.; Pask, C. Leaky ray correction factors for elliptical multimode fibres. Electron. Lett. 16(14):532-533; 1980 July.

[11] Hanson, A. G.; Bloom, L. R.; Cherin, A. H.; Day, G. W.; Gallawa, R. L.; Gray, E. M.; Kao, C.; Kapron, F. P.; Kawasaki, B. S.; Reitz, P.; Young, M. Optical waveguide communications glossary. NBS Handbook 140; Nat. Bur. Stand. (U.S.) Handb. 140; 1982 January.

[12] This definition for core diameter is under consideration by the International Electrotechnical Commission (IEC), International Telegraph and Telephone Consultative Committee (CCITT), and Electronic Industries Association (EIA).

[13] Hazan, J. P. Intensity profile distortion due to resolution limitation in fibre index profile determination by near-field. Electron. Lett. 14(5):158-160; 1978 March.

[14] Sabine, P. V. H.; Donaghy, F.; Irving, D. Fibre refractive-index profiling by modified near-field scanning. Electron. Lett. 16(23): 882-883; 1980 November.

[15] Holmes, G. T. Propagation parameter measurements of optical waveguides. Proc. SPIE, Fiber Optics for Communication and Control, Vol. 224; 1980.

[16] Miller, S. E.; Chynoweth, A. G. Optical fiber telecommunications. New York: Academic Press; 1979.

[17] Stewart, W. J.; Reid, D. C. J.; Rees, G. Spot size and concentricity measurements of monomode fibers: improved techniques. Technical Digest, Topical Meeting on Optical Fiber Communication, New Orleans; p. 24; 1983 February.

[18] Anderson, W. T.; Philen, D. L. Spot size measurements in single-mode fibers. Technical Digest, Topical Meeting on Optical Fiber Communication, New Orleans; p. 24; 1983 February.

[19] Millar, C. A. Direct method of determining equivalent-step-index profiles for monomode fibres. Electron. Lett. 17(11):458-460; 1981 June.

[20] Murakami, Y.; Kawana, A.; Tsuchiya, H. Cut-off wavelength measurements for single-mode optical fibers. Appl. Opt. 18(7):1101-1104; 1979 April.

[21] Wang, C. C.; Villarruel, C. A.; Burns, W. K. Comparison of cutoff wavelength measurements for single mode waveguides. Technical Digest, Symposium on Optical Fiber Measurements, Boulder, Nat. Bur. Stand. (U.S.) Special Publication 641:97-100; 1982 October.

[22] Arnaud, J. A.; Derosier, R. M. Novel technique for measuring the index profile of optical fibers. Bell Syst. Tech. J. 55(10):1489-1509; 1976 December.

[23] Adams, M. J.; Payne, D. N.; Sladen, F. M. E.; Hartog, A. Resolution limit of the near-field scanning technique. Proc. Third European Conf. Opt. Commun., Munich, p. 25-27; 1977.

[24] Born, M.; Wolf, E. Principles of optics, fifth edition. New York: Pergamon Press; 1975.

[25] PIN photodiodes with built-in operational amplifiers are available from a number of sources. A 22 MΩ feedback resistor is used with the operational amplifier.

[26] Kim, E. M.; Franzen, D. L. Calibration reticle for optical fiber near-field core diameter measurements. CPEM Digest; 1982.

[27] From documents of the CCITT, EIA, and IEC.

[28] Cornsweet, T. N. Visual perception. New York: Academic Press; 1970.

[29] Saekeang, C.; Chu, P. L.; Whitbread, T. W. Nondestructive measurement of refractive-index profile and cross-sectional geometry of optical fiber preforms. Appl. Opt. 19(12):2025-2030; 1980 June.

[30] Presby, H. M. Ellipticity measurement of optical fibers. Appl. Opt. 15(12):492-494; 1976 February.

[31] Abushagur, M. A. G.; George, N. Measurement of optical fiber diameter using the fast Fourier transforms. Appl. Opt. 19(12):2031-2033; 1980 June.

[32] Marcuse, D.; Presby, H. M. Automatic geometric measurements of single-mode and multimode optical fibers. Appl. Opt. 18(3):402-408; 1979 February.

[33] Sharma, A. B.; Haline, S. J.; Butusov, M. M. Optical fiber systems and their components--an introduction. New York: Springer-Verlag; 1981.

[34] Gonzalez, R. C.; Wintz, P. Digital image processing. Reading, MA: Addison-Wesley; 1977.

[35] Freeman, H. On the encoding of arbitrary geometric configurations. IEEE Trans. Electron. Comp. EC-10:260-268; 1961 June.

[36] Eickhoff, W.; Kurmpholtz, O. Pulse response and microbending losses of an optical glass-fibre waveguide with a bump in its index profile. Electron. Lett. 13(9): 256-257; 1977 April.

[37] Young, M. Refracted-ray scanning (refracted near-field scanning) for measuring index profiles of optical fibers. Nat. Bur. Stand. (U.S.) Tech. Note 1038; 1981 May.

[38] Cherin, A. H.; Rich, P. J.; Mettler, S. Measurement of the core diameter of multimode GRIN fibers: a comparison of transmitted near-field and index profiling techniques. Technical Digest, Topical Meeting on Optical Fiber Communication, New Orleans; p. 48; 1983 February.

[39] LaFara, R. L. Computer methods for science and engineering. Hayden Book Co.; 1973.

[40] Irving, D. H.; Sabine, P. V. H.; Donaghy, F. A. A tunnelling correction factor for the modified near-field technique. Opt. Quant. Electron. 14:17-24; 1982.

[41] Sabine, P. V. H.; Irving, D. H.; Donaghy, F. A. Modified near-field intensity scanning of step-index fibres. Opt. Quant. Electron. 14:73-76; 1982.

[42] Wang, C. C.; Villarruel, C. A.; Burns, W. K. Comparison of cutoff wavelength measurements for single-mode waveguides. Appl. Opt. 22(7):985-990; 1983 April.

[43] Stewart, W. J. A new technique for measuring the refractive index profiles of graded optical fibers. Proc. Conf. Integrated Optics and Optical Communication, Japan; 1977.

[44] White, K. I. Practical application of the refracted near-field technique for the measurement of optical fibre refractive index profiles. Opt. Quantum Electron., 11:185-196; 1979.

[45] Young, M. Optical fiber index profiles by the refracted-ray method (refracted near-field scanning). Appl. Opt. 20:3415-3422; 1981.

[46] Saunders, M. J. Optical fiber profiles using the refracted near-field technique: a comparison with other methods. Appl. Opt. 20:1645; 1981.

[47] The normalized frequency V is given by $2\pi a\sqrt{2n\Delta n}/\lambda$, where a is the core radius, n the fiber refractive index, λ the wavelength, and Δn the index difference between the core and cladding. For large V, the number of bound modes is approximately $V^2/2$.

[48] Rodhe, P. M. On transmission properties of optical fibres with disturbed geometry. Thesis, Royal Institute of Technology, Stockholm, Sweden; or Calculation of scalar modes of optical fibres with circular symmetric cross sections. Technical Report TR-117-1982-06-29 (Institute of Optical Research, Stockholm); 1982.

[49] Yuen, M. J. Studies of MCVD glass preform by UV spectroscopy: a probe into Ge(formation. Technical Digest, Third International Conf. IOOC, Washington, DC; 1981.

[50] Kim, E. M.; Franzen, D. L. Measurement of the core diameter of graded-index optica fibers: an interlaboratory comparison. Appl. Opt. 21: 3443-3450; 1982.

Chapter 4

Measurement of Far-Field Radiation Patterns from Optical Fibers

E. M. Kim
D. L. Franzen

A system is described for measuring far-field radiation patterns from optical fibers. Parameters which affect measurement precision, accuracy, resolution, and signal-to-noise ratio are discussed. Measurements utilizing radiation patterns are covered; this includes radiation angle (numerical aperture), attenuation using mode filters, and mode volume transfer function. Experimental examples are given in many instances.

CONTENTS

		Page
1.	INTRODUCTION: RADIATION PATTERN CONSIDERATIONS IN OPTICAL FIBERS	189
2.	MEASUREMENTS UTILIZING FAR-FIELD PATTERNS	192
	2.1 Radiation Angle (Numerical Aperture)	192
	2.2 Attenuation with Restricted Launch via a Mode Filter	193
	2.3 Mode Volume Transfer Function--A Measurement Utilizing Both Far- and Near-Field Patterns	193
3.	DESCRIPTION OF FAR-FIELD MEASUREMENT SYSTEM	194
	3.1 Source	194
	3.2 Detector	194
4.	PERFORMANCE OF FAR-FIELD SYSTEM	196
	4.1 Precision	196
	4.2 Accuracy	198
	4.3 Dynamic Range	199
5.	TYPICAL RESULTS FROM FAR-FIELD MEASUREMENTS	200
	5.1 Radiation Angle (Numerical Aperture)	200
	5.2 Attenuation with Restricted Launch via a Mode Filter	202
	5.3 Symmetry of Radiation Patterns	202
	5.4 Mode Dependence of OH^- Absorption	203
6.	CONCLUSION	205
7.	REFERENCES	205

1. INTRODUCTION: RADIATION PATTERN CONSIDERATIONS IN OPTICAL FIBERS

(This introduction is identical to the one presented in chapter 3. It is repeated here for completeness.)

The radiation propagating in an optical fiber can take on various spatial and angular distributions depending upon the relative excitation of fiber modes. Useful information about the fiber can be obtained by analyzing the radiation exiting an end. This analysis can take place in either the far- or near-field region of the end. A far-field measurement determines the angular dependence of intensity (irradiance) sufficiently far from the end of the fiber (fig. 1); whereas, a near-field measurement determines the spatial intensity distribution in the plane of the end face.

In the far-field, the normalized, angular intensity distribution no longer depends on distance from the fiber. While the intensity at any given angular coordinate decreases as the square of the distance from the fiber end, the normalized pattern remains constant. If the far-field pattern is circularly symmetric about the fiber axis, then a single angular coordinate is sufficient to describe the pattern.

The far-field, which is synonymous with the Fraunhoffer diffraction region, is usually said to start at a distance

$$z_0 = \frac{(2a)^2}{\lambda} \qquad (1)$$

from the fiber end, where λ is the wavelength of light and a the core radius [1]. When $z \gg z_0$, the amplitude (electric field) distribution in the far-field is closely related to the spatial Fourier transform of the amplitude distribution existing at $z = 0$, [1]. In practice, far-field measurements are made at distances greater than 10 z_0 from the fiber end. For the standard graded-index core diameter of 50 μm and a wavelength of 1 μm, 10 z_0 is 2.5 cm. For the standard step-index core diameter of 100 μm, the distance becomes 10 cm. Both of these lengths represent convenient laboratory working distances.

Radiation patterns are measured on either short or long lengths of fiber, depending upon the application. Frequently the short length is a 2 m cutback length left over from an attenuation or bandwidth measurement. In this chapter, a long length refers to the entire length of fiber under test and, for telecommunications fibers, generally exceeds 1 km.

Radiation patterns depend upon launching conditions and contain contributions from both guided and tunneling leaky modes of the fiber [2,3]. In short lengths, patterns result mainly from guided modes with a significant contribution from leaky modes. The relative

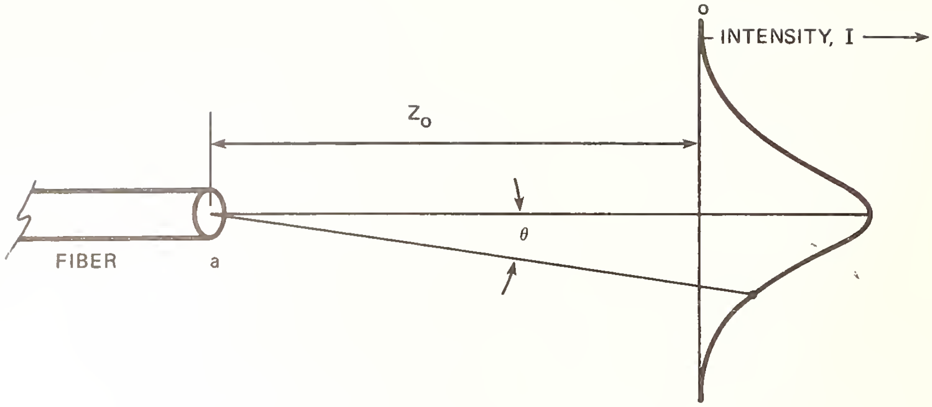

(a) FAR FIELD

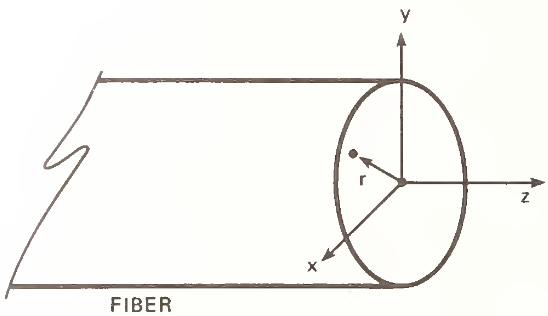

(b) NEAR FIELD

Figure 1. Radiation pattern measurements from optical fibers, (a) far field is given by $I(\theta)$ at $z >> z_o$, (b) near field is given by $I(r)$ in xy plane.

importance of the leaky mode contribution depends upon the index profile and launching conditions. In long lengths, leaky modes have generally decayed and the patterns result from guided modes modified by differential mode attenuation and mode coupling. Far- and near-field patterns resulting from overfilled launching conditions on graded-index fibers generally become restricted with further propagation along the fiber. This occurs because differential mode attenuation is generally higher for higher order modes. Eventually an equilibrium is reached between mode coupling and differential mode attenuation to yield a steady state pattern. However, steady state is seldom observed in practice since mode coupling lengths in good fibers are several kilometers [4] if not tens of kilometers [5].

The remainder of this section briefly discusses the measurement applications of far-field patterns. Various applications are summarized in table 1. For some of these measurements, procedures are pending before standards groups [6]. In general, more attention has been given to standardizing procedures for graded-index fibers than for step-index fibers.

Table 1. Measurement applications of radiation patterns from multimode fibers.

Application	Fiber length employed: short (2 m)	Fiber length employed: long	Radiation pattern: far field	Radiation pattern: near field	Launching condition	General comments
1 Radiation angle	X		X		Overfilled	Meridionally defined NA approximated for near parabolic graded-index fibers. Special considerations necessary for step index.
2 Attenuation using restricted launch via a mode filter	X	X	X		Overfilled	Used to qualify mode filters; applies to graded-index fibers over 1 km in length.
3 Index profile	X			X	Overfilled	Little or no leaky mode correction required for near parabolic graded-index fibers; large correction for step index. Limited resolution information on guiding regions of fiber only.
4 Core diameter	X			X	Overfilled	Possible uncertainty due to low index "barrier" layer, poor resolution near core-cladding boundary, is easy to implement.
5 Mode volume transfer function	X	X	X	X	Restricted	Applies to graded-index fibers; measurement system must have ability to control launch mode volume and therefore beam optics systems capable of independently variable launch spot and NA are usually required.

2. MEASUREMENTS UTILIZING FAR-FIELD PATTERNS

2.1 Radiation Angle (Numerical Aperture)

The cone of light rays accepted by a fiber is of practical importance. Launching efficiency of sources like LEDs and loss performance of joined sections of dissimilar fiber depend upon this parameter. "Radiation angle" is a measure of the cone angle transmitted by the fiber [7]. This measurement is usually made in the far field of a short, 2 m length excited at a specified wavelength using overfilled launching conditions; i.e., constant irradiance over the core with a launch angle greatly exceeding the fiber acceptance angle.

In early fiber work, the cone angle containing 90 percent of the transmitted power was determined by either integrating a far-field intensity pattern or by translating an aperture in the far field. The sine of the half angle of this cone was frequently termed "90 percent numerical aperture."

More recent procedures pending before standards groups define radiation angle directly from a far-field intensity pattern [8]. In this instance, radiation angle is defined as the half angle where the far-field intensity has decreased to 5 percent of the peak value. The sine of this angle, for near-parabolic index multimode fibers, is close to the index defined numerical aperture.

Historically, the term "numerical aperture" (NA) has been used to describe the largest angle meridional ray accepted by a fiber, figure 2, with

$$NA \equiv \sin \theta_o = \sqrt{n_1^2 - n_2^2} \qquad (2)$$

$$= n_1\sqrt{2\Delta} \text{ with } \Delta \approx \frac{n_1 - n_2}{n_1} \qquad (3)$$

where n_1 is the core index of refraction, n_2 the cladding index, and Δ is defined by the above equations. While figure 2 applies to step fibers, analysis shows that the numerical aperture of graded-index fibers is also given by eq (2) with n_1 being the on-axis index of refraction [9].

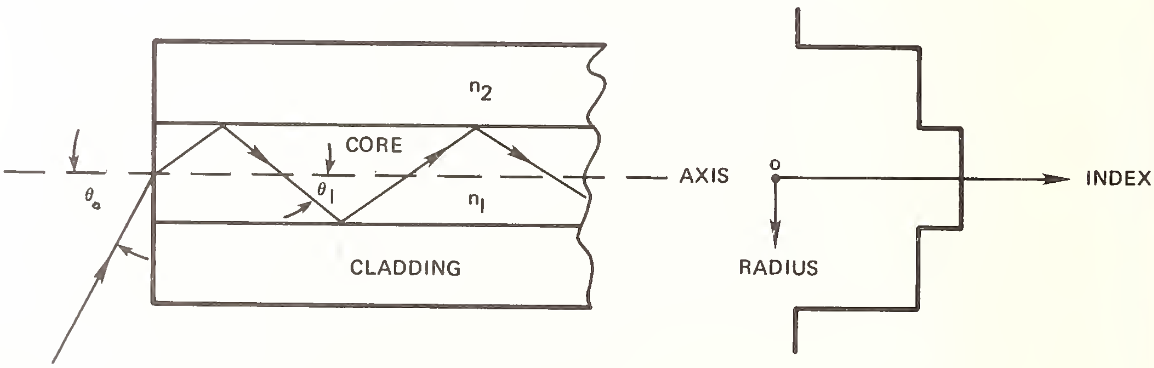

Figure 2. The meridional ray in a step-index fiber making the maximum possible angle, θ_1, with the fiber axis.

The sine of the radiation angle based on the 5 percent intensity points is close to the index defined NA of eq (2) for near-parabolic index fibers. Theoretical work shows the acceptance angle of skew rays is always less than that of meridional rays in near-parabolic index fibers [10]. Adams, et al., show that leaky modes in a near-parabolic index fiber are all contained within the meridionally defined numerical aperture [3]. Thus, when all modes are excited, the largest observed angle in a far-field pattern would be given by θ_0 in eq (2). At the 5 percent level, patterns are close to the maximum observable angle.

For step fibers, the situation is quite different. Here the acceptance angles for skew rays can exceed θ_0. When all modes are excited, radiation would appear at angles greater than θ_0. Thus, to obtain the numerical aperture based on eq (2) for short step-index fibers, special launching conditions would be necessary. This would probably mean launching only meridional rays. This could be accomplished by small spot excitation at core center.

2.2 Attenuation with Restricted Launch Via a Mode Filter

In measuring the attenuation of long telecommunications type fibers, it is useful to launch with a distribution which gives good concatenation predictions [11]. This is presently accomplished by restricting the launch to avoid the excitation of certain high loss modes which do not propagate far in the fiber. In general, this can be accomplished by one of two approaches. The beam optics approach avoids the initial excitation of certain high loss modes by restricting the launch spot size and numerical aperture at the fiber input end. (70 percent of the core diameter at 70 percent of the fiber NA is the choice pending before standards groups.) In the mode filter approach, the fiber is initially overfilled and a mode filter is applied to strip out certain high loss modes.

Far-field radiation pattern measurements on long and short fiber lengths are used to qualify a mode filter for an attenuation measurement. Current proposals call for overfilling the input of the fiber under test in both spot size and numerical aperture, then measuring the radiation angle (5 percent intensity) exiting the long length. An appropriate mode filter is applied so the radiation angle exiting a 2 m length is less than that of the long length by 3 ± 3 percent. Now the mode filter has stripped away enough of the high angle-high loss modes to simulate, in a 2 m cutback length, the radiation pattern resulting from a kilometer or more of propagation. Common mode filters include dummy fibers and mandrel wraps [12], [13].

2.3 Mode Volume Transfer Function--A Measurement Utilizing Both Far- and Near-Field Patterns

Holmes, et al., have introduced a concept describing the effect of propagation on spatial and angular intensity distributions in graded-index fibers [4]. They define an "EMV" (effective mode volume) based on far- and near-field intensity distributions. Specifically, the EMV at a given point along the fiber is the square of the product of the FWHM (full width at half maximum) of the near field and the sine of the HWHM (half width at half maximum) of the far field.

EMV is related to the number of modes excited in the fiber. This can be intuitively seen when applied to the expression for the total number of guided modes, N, in a fully excited graded-index fiber having a power law profile α [9].

$$N = \frac{\alpha\Delta}{2+\alpha} \left(\frac{2\pi n_1 a}{\lambda}\right)^2 \qquad (5)$$

where a is the core radius, λ the wavelength, and other terms have been previously defined. After arranging terms,

$$N = \frac{\alpha}{2+\alpha} \left(\frac{2\pi^2}{\lambda^2}\right) [(NA) \cdot a]^2 \qquad (6)$$

$$\approx \frac{\alpha}{2+\alpha} \left(\frac{2\pi^2}{\lambda^2}\right) \cdot EMV. \qquad (7)$$

Of interest is the EMV transfer characteristic for a fiber. This describes how various EMVs propagate in the fiber and is a plot of output EMV versus input EMV. By controlling launch spot and NA, various input EMVs can be generated. Input EMVs are determined from radiation patterns exiting a 2 m length at the input. The corresponding output EMVs are obtained from radiation patterns exiting the long length.

The EMV transfer characteristic gives information on mode coupling, differential mode attenuation, and quasi-steady state EMV. A fiber without mode coupling or differential mode attenuation appears as a 45° line on the transfer characteristic plot; i.e., the output EMV is equal to the input EMV.

A principle use of the EMV concept is in the prediction of concatenation. EMV transfer characteristics and attenuation versus EMV for all the fibers in the link allows one to predict accurately the concatenated attenuation for any input EMV [4].

3. DESCRIPTION OF FAR-FIELD MEASUREMENT SYSTEM

3.1 Source

The radiation source and launch optics are identical to the ones used in the near-field system. A detailed description is presented in chapter 3, section 4.

3.2 Detector

The far field may be scanned by a number of different techniques: (1) fixed fiber end, rotating detector, (2) fixed detector, rotating fiber end, (3) fixed fiber end, fixed detector, rotating mirror, and (4) fixed fiber end, detector array.

The system described in this chapter uses a fixed fiber end and a rotating detector (fig. 3). This approach represents perhaps the simplest construction of available choices.

The fiber first passes through a cladding mode stripper consisting of two 10 cm long felt pads wetted with index matching fluid. Buffer coatings are removed from the fiber where it contacts the mode stripper. Near-field scans show this type of mode stripper effectively removes light from the cladding.

A vee groove positions the fiber so the end is coincident with the axis of rotation. Some measurements, especially near fields, are affected by the amount of force used to hold the fiber in the vee groove. These distortion effects are eliminated when a small, felt padded weight holds the fiber in the groove. Before making a measurement, the fiber end is visually inspected for flatness and perpendicularity. The vee groove position can be slightly adjusted by a two dimensional translation stage to assure that the detector scan passes through the maximum intensity part of the pattern.

Scanning is accomplished with a stepper motor controlled rotary table which swings the detector through a 12 cm radius arc. At this distance the far-field criteria is satisfied for core diameters of 100 µm or less. Angular motion (1/2 arc min. per step) is fine enough to give smooth far-field curves.

Detector aperture size is chosen with a trade-off between resolution and signal-to-noise ratio. Presently, a 0.8 mm diameter aperture is used giving a resolution of 0.38°.

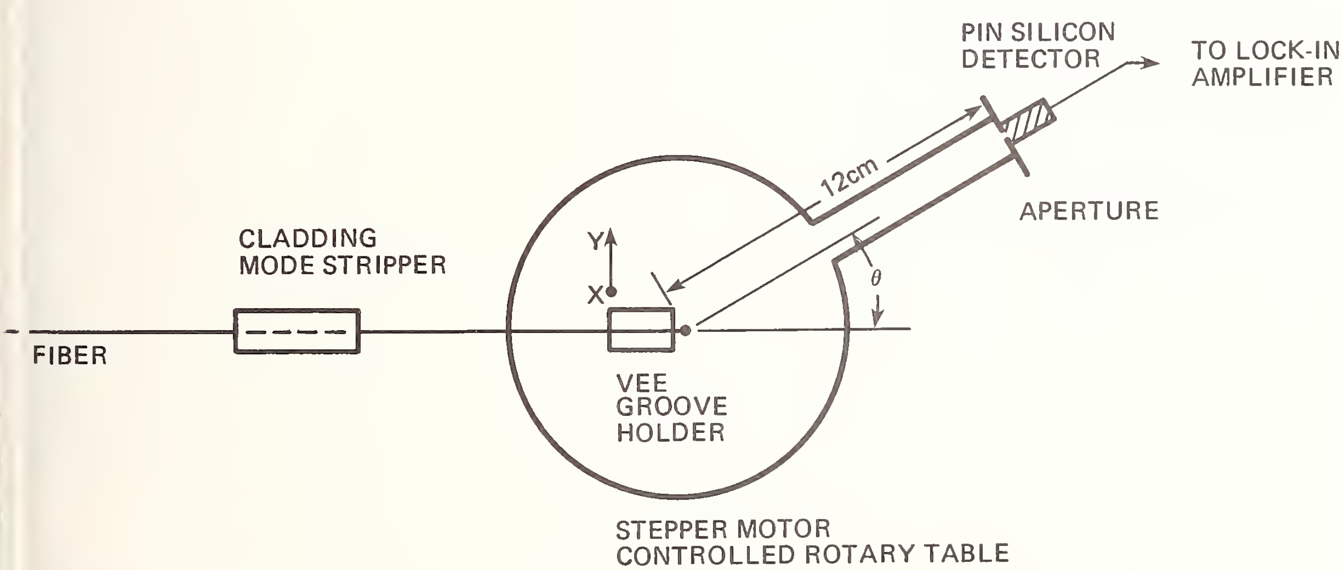

Figure 3. Far-field measurement system using a fixed fiber end and a rotating detector.

Reducing aperture size to improve resolution, and hence accuracy, would not be important for most measurements which are relative comparisons (Table 1). Radiation angle (NA) is the only far-field measurement which is absolute. A simple one-dimensional model based on a parabolic shaped far-field pattern with an NA of 0.2 predicts an error of 1.6 percent in the determination of radiation angle when the curve is acquired with 0.38° resolution. Measurement precision for determining radiation angle is in the range of 1 to 2 percent when a new output end is prepared and realigned (Sect. 4.1); therefore, a significant reduction in aperture size would not result in much improvement.

A silicon PIN diode operating in the photovoltaic mode is used as the detector [14]. This detector with an active area of 5.1 mm^2 has a built-in operational amplifier and is mounted directly behind the aperture. To improve signal-to-noise ratio, a time constant of 0.4 s is used on the lock-in amplifier. The scanning rate is chosen so a resolution element (0.38°) is scanned in approximately three time constants. At this rate a fiber far-field pattern is obtained in three to four minutes.

Data may be acquired by several methods. For most applications, a good, wide paper strip chart recorder is adequate. However, a digital acquisition system may be necessary to perform numerical analysis on the data. In that case, the computer data acquisition system used for the near-field measurements is used. A description of this system is given in chapter 3, section 4.

4. PERFORMANCE OF FAR-FIELD SYSTEM

4.1 Precision

Precision is a statement of measurement repeatability. It says nothing about a "systematic" error which is the offset of the average of a large number of measurements from the true value. Best precision is obtained when a measurement is repeated without disturbing any parameter. A typical example of this precision is given in figure 4. Here a far-field measurement was repeated seven times on graded-index fiber A using overfilled launching conditions at a wavelength of 860 nm. Standard deviations for determining the full widths at the 80, 50, 20, 10, and 5 percent intensity points are shown. Error bars represent ± one standard deviation (2 standard deviations in length) and are given as a percentage of the full width at that particular point. A typical value is in the 0.5 percent range. It should be noted that the width of an ink line is approximately 0.3 percent of the curve FWHM and therefore represents a limitation in determining actual precision. The main conclusion drawn from figure 4 is that the system has no appreciable dc drift problems.

For many measurements, the above precision is not applicable. In practice, new ends must be prepared and the system aligned. To determine this precision, far-field measurements were repeated seven times, for each measurement a new output end was prepared and the system slightly realigned to the maximum intensity point. Three different fibers representing two different manufacturers were measured, figures 5 and 6 [15]. Standard deviations

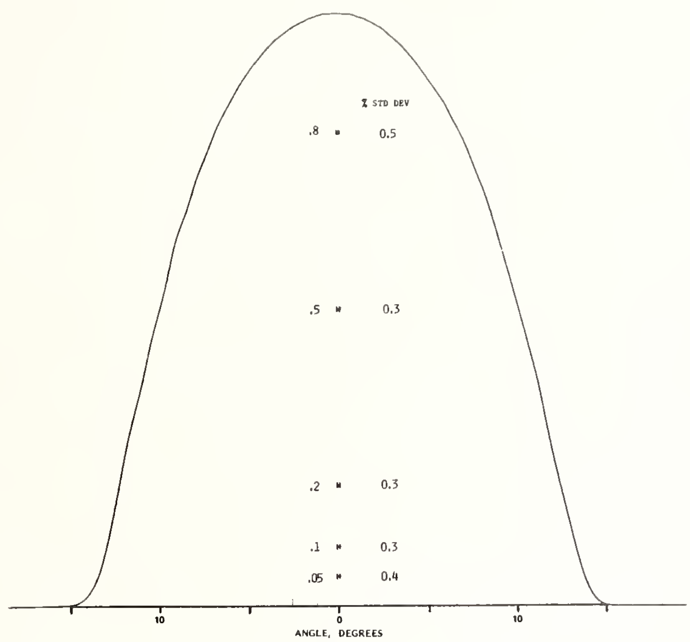

Figure 4. Far-field measurement precision when no parameters are changed. Fiber A, graded index, 1.1 km length, 5 dB/km, 0.23 NA, 860 nm; ± one standard deviation indicated along ordinate at 0.8, 0.5, 0.2, 0.1, and 0.05 of maximum as a percentage of full angular width at that point.

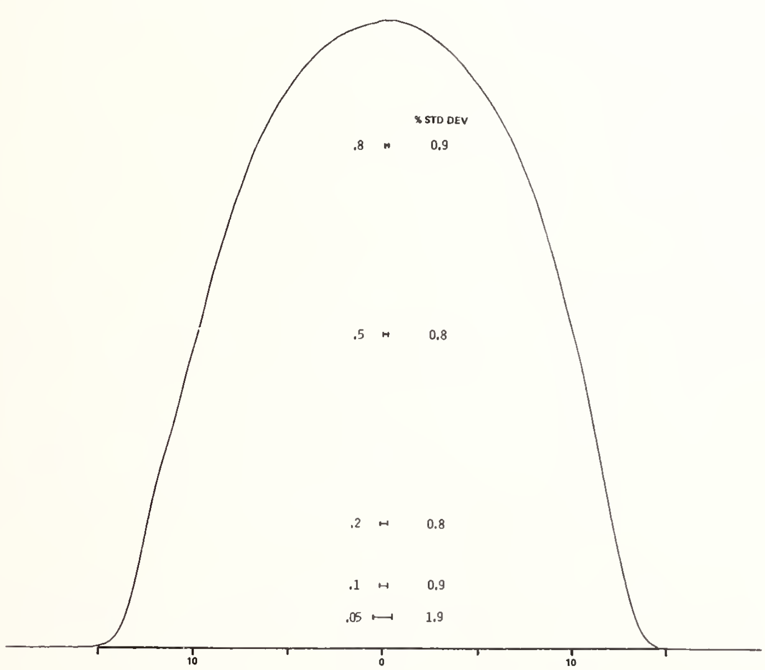

Figure 5. Far-field measurement precision with recleaved output end and realignment for each measurement. Graded-index fiber A; ± one standard deviation indicated along ordinate at 0.8, 0.5, 0.2, 0.1 and 0.05 of maximum.

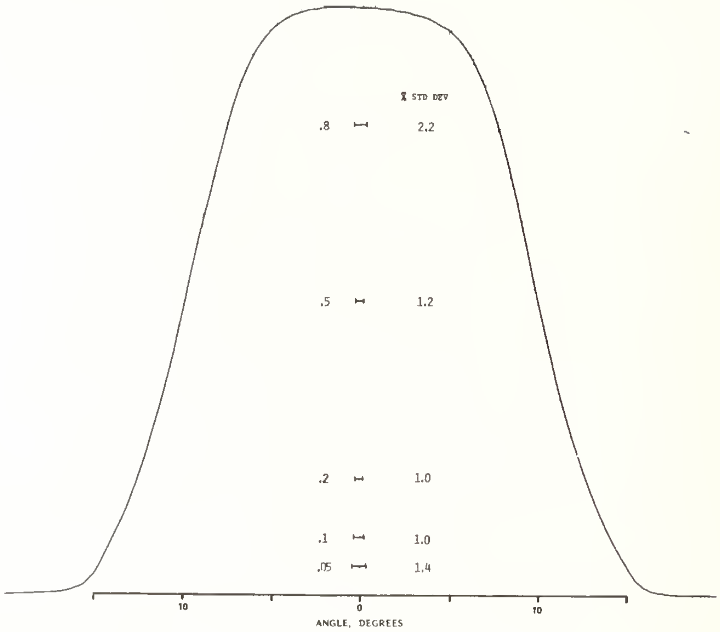

Figure 6. Far-field measurement precision with recleaved output end and realignment for each measurement. Fiber C, step index, 1.2 km length, 6 dB/km, 860 nm; ± one standard deviation indicated along ordinate at 0.8, 0.5, 0.2, 0.1, and 0.05 of maximum.

for graded-index fiber B (not shown) were about 1 percent on lower parts of the curve. For graded-index fiber A the corresponding values are a little higher--in the 1 to 2 percent range. Fiber C, with a step index, has a much flatter top in general agreement with theory [16]. Here the precision is also in the 1 to 2 percent range. From these tests, a precision of 1 to 2 percent is indicated for a radiation angle measurement.

4.2 Accuracy

Accuracy is determined by the absolute value of the angular calibration factor, angular resolution, and system linearity. The angular calibration factor was determined by reflecting a low divergence He-Ne laser beam off a mirror attached to the rotary table and onto the laboratory wall. The table was rotated through 360° and the beam returned, within the nearest step, to the original position. This procedure determines the angular rotation per step more accurately than is practically needed.

As previously mentioned, the finite angular resolution introduces an error when determining the radiation angle. This error is estimated to be less than 1.6 percent.

Detector non-linearity could affect the shape of the measured pattern. A calibrated neutral density filter was used to confirm detector linearity up to the highest power levels used with the system.

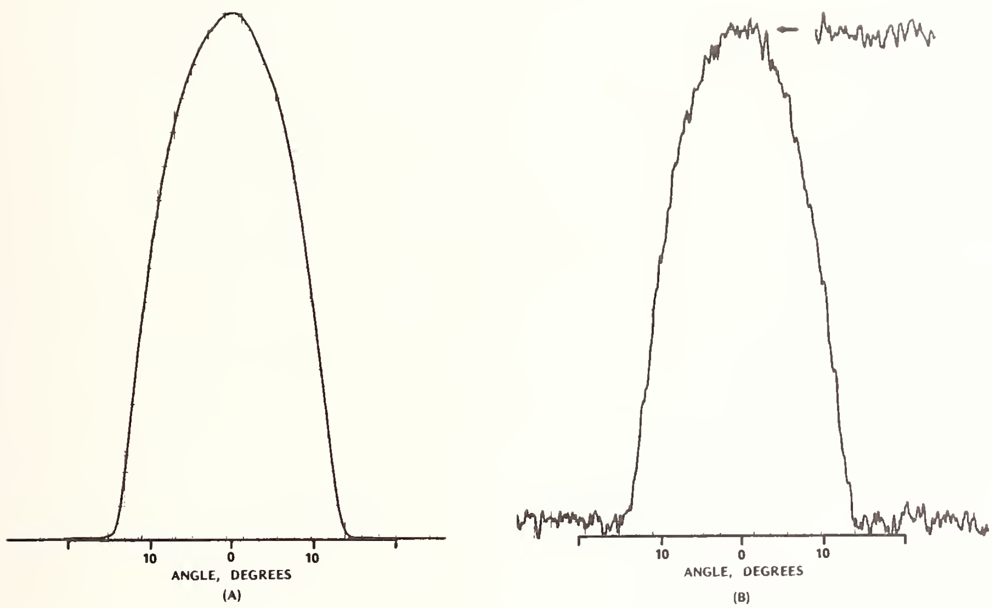

Figure 7. (A) Far field from graded-index fiber having a loss of 5 dB; (B) same as (A) but with source attenuated by 17 dB, signal-to-noise ratio of (B) is 12 dB.

4.3 Dynamic Range

Signal-to-noise ratio was determined by attenuating the source until the noise level was observed. Figure 7a shows the far field from a fiber having a loss of 5 dB when excited with overfilled launch conditions. In figure 7b, the source is attenuated by approximately 17 dB to display the noise level. Also shown is the noise level on the baseline and at the peak value; in both cases the noise is about 4 μV peak-to-peak. Signal-to-noise ratio for a short length of fiber, having negligible attenuation, is 34 dB at 860 nm using an 80 nm bandpass interference filter, overfilled launching conditions, and a time constant of 0.4 s on the lock-in amplifier. In figure 7b the signal-to-noise ratio is 12 dB and represents the lowest level for making a reasonable measurement. Based on this criteria, the system has a dynamic range of 22 dB. There are measurements, especially with very restricted launching conditions, where more signal-to-noise would be desirable. The easiest way to increase signal is to increase source linewidth. For some measurements this may be acceptable. An additional 7 dB improvement in signal can be obtained by replacing the broadband interference filter with a long pass filter having a cut-on wavelength of 0.78 μm. In this case the long wavelength cutoff, 1.1 μm, is determined by the spectral response of the silicon detector.

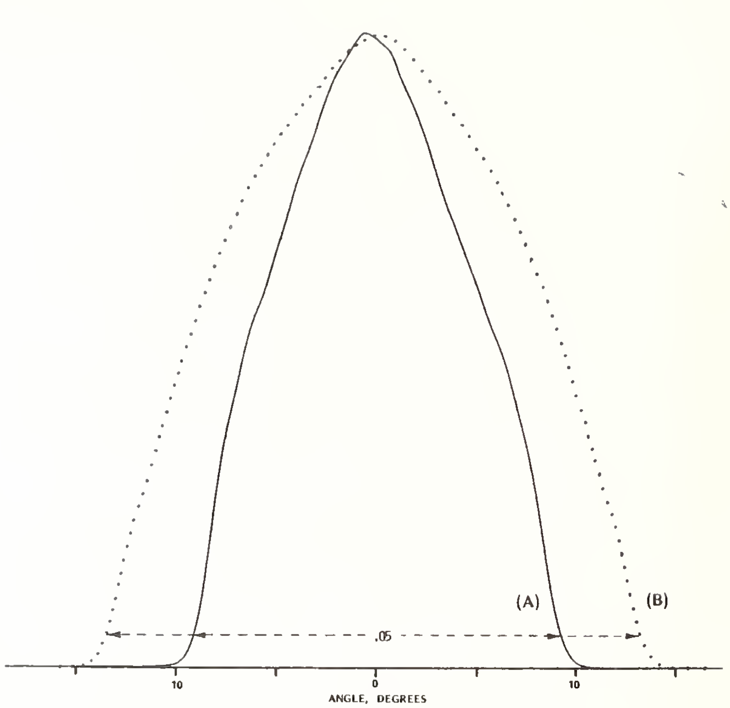

Figure 8. Examples of graded-index fibers with high and low radiation angles (5 percent intensity width). NA's of 0.16 and 0.23 are obtained from curves (A) and (B) respectively.

5. TYPICAL RESULTS FROM FAR-FIELD MEASUREMENTS

5.1 Radiation Angle (Numerical Aperture)

Radiation angle was determined for a number of commercially available multimode fibers. Measurement precision was consistent with the results of section 3.1. Figure 8a is a typical result from a graded-index fiber with a rather low NA of 0.16; while figure 8b shows a fiber with a rather high NA of 0.23. Results of figure 8 were obtained using overfilled launching conditions on a 2 m length of fiber. In almost all cases, far-field patterns from commercial graded-index fibers have been smooth, bell shaped, and exhibit a single central maximum.

Differences in radiation angle for two lengths of the same fiber with identical launch conditions is shown in figure 9. Note that the radiation angle for the 1 km length is smaller than that of the 2 m length. This is due to the attenuation of higher order (large angle) modes. These measurements were made with the computer data acquisition system.

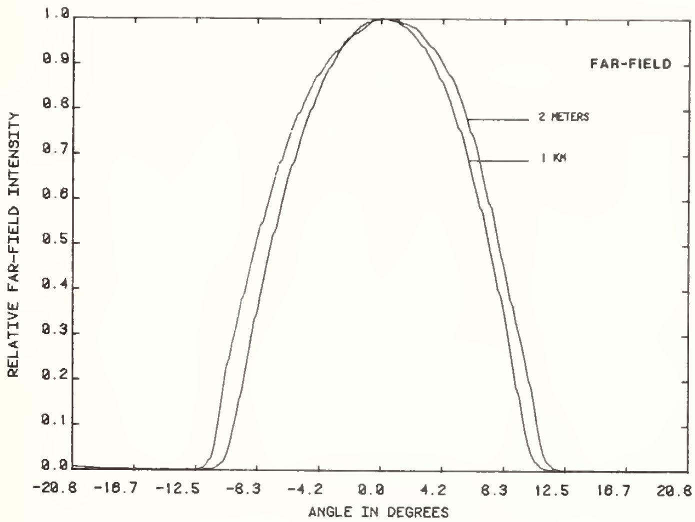

Figure 9. Measurement of the far-field pattern for 1 km and 2 m lengths of the same fiber. The computer data acquisition system was used.

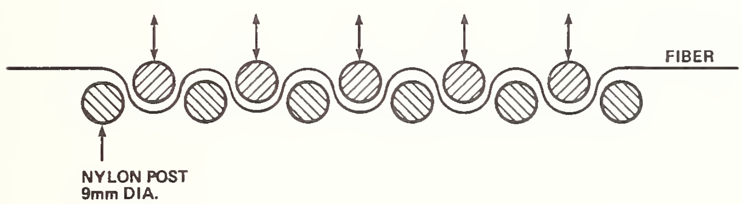

Figure 10. One type of mode filter consisting of a series of serpentine, macroscopic bends. Moveable posts can be translated into alignment with fixed adjacent posts.

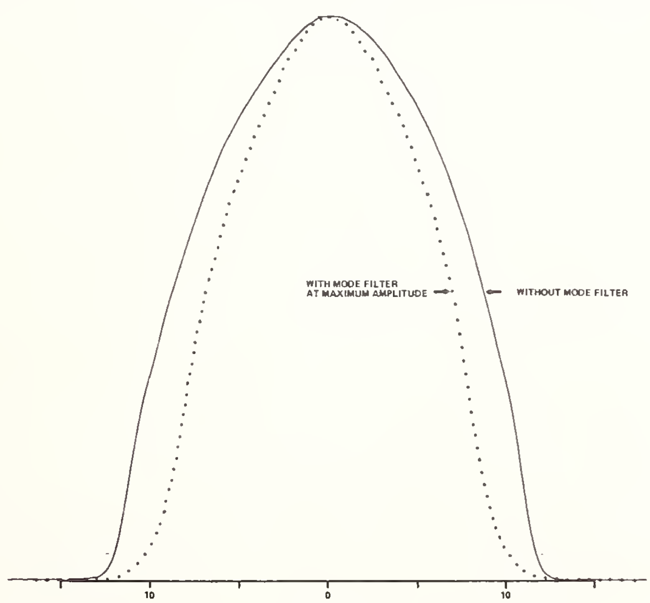

Figure 11. Effect of mode filter on 2 m length of graded-index fiber. Solid curve is without mode filter, dotted curve is with mode filter set at maximum amplitude.

5.2 Attenuation with Restricted Launch via a Mode Filter

Radiation pattern measurements on both long (1 km or more) and short (2 m) lengths of the same fiber are necessary to qualify mode filters for restricted launch attenuation measurements. A successful mode filter produces an output radiation angle from a 2 m length equivalent to the output radiation angle from the full test length excited by overfilled launching conditions. Restrictions in radiation angle, due to fiber propagation, are a function of differential mode attenuation and mode coupling. For many typical graded-index fibers, the radiation angle from an overfilled launch restricts by 4 to 8 percent after a kilometer of propagation.

One mode filter possibility is a series of serpentine, macroscopic bends, figure 10. This geometry in a step-index fiber has been previously used as a mode-scrambler for bandwidth measurements [17,18]. The specific geometry used here consists of eleven, 9 mm diameter nylon posts--six fixed and five moveable. A fiber is placed in the mode filter and the movable posts are translated to produce sinusoidal bends having a period of 22 mm with variable amplitude. Maximum far-field restrictions are obtained when the posts are evenly aligned (9 mm peak-to-peak amplitude).

The effect of this mode filter on the far-field pattern from a short length of graded-index fiber is shown in figure 11. The solid curve was obtained without the mode filter using overfilled launching conditions to the 2 m length. The dotted curve is the same but with the mode filter set to maximum amplitude. A restriction of 16 percent in radiation angle is achieved at maximum amplitude. This particular fiber, when excited by overfilled launching conditions, exhibits a 6 percent restriction in radiation angle after 0.9 km of propagation. Thus, the serpentine mode filter in this case would be more than adequate to achieve the necessary restriction (9 percent) for an attenuation measurement.

It should be emphasized that mode filters affect different fibers in different ways. The exact nature of the mode reduction is a function of: mode filter, buffer coating, cladding diameter, core diameter, numerical aperture, etc. Fibers have been found where the serpentine mode filter has produced significantly different results than figure 11. It is therefore necessary to "qualify" a mode filter for the particular class of fibers being measured.

5.3 Symmetry of Radiation Patterns

In general, far-field measurements on single core fibers give smooth, symmetric, bell shaped curves having a single maximum. Fine structure from the core would be diffracted into relatively large angles. For example, a plane wave illuminating a circular aperture of diameter d has a diffraction angle of $1.22\ \lambda/d$. This is 1.4° when applied to a 50 µm diameter core at a wavelength of 1 µm.

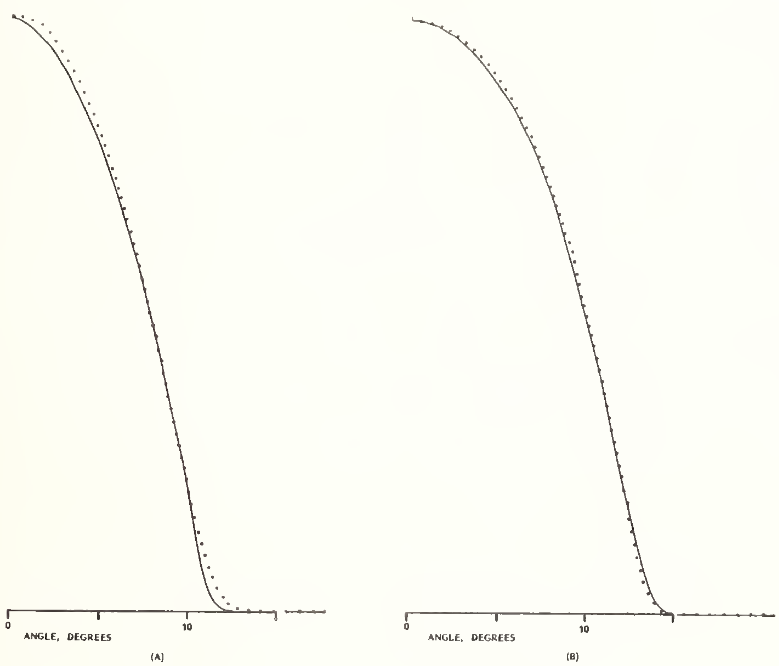

Figure 12. Typical symmetry of far-field patterns from graded-index fibers. Left part of pattern (dotted line) is folded about a vertical axis through mid-point of half maximum width to compare with right part of pattern (solid line). Far-field (B) exhibits better symmetry than far-field (A).

Pattern symmetry is indicated in figure 12. Here far-field patterns are folded about a vertical axis passing through the midpoint of the width at half maximum. These examples were selected from measurements on a large number of commercial fibers and are typical of good and poor symmetries. Even in the poor case, the symmetry is fairly good.

5.4 Mode Dependance of OH^- Absorption

The OH^- radical causes spectrally localized absorption in optical fibers. One of the stronger lines occurs near 950 nm. Previous backscatter measurements show that OH^- is not necessarily distributed uniformly along the fiber length [19]. This section describes far-field measurements to qualitatively determine the mode dependence of OH^- absorption in a particular fiber.

For these measurements, a 0.9 km fiber was chosen with a large OH^- absorption peak and little mode coupling. Spectral attenuation measurements indicate a loss of 5 dB/km at 850 nm which increases to 40 dB/km at 950 nm. By analyzing far-field patterns at 850 nm from overfilled and restricted mode volume launches, this fiber was found to have little mode coupling.

Qualitatively, if more OH^- were located near the core-cladding interface, higher order (large radius-large angle) modes would be attenuated more and a narrower pattern would result at the output from an overfilled input; the converse would be true if the OH^- were concentrated near the axis.

Figure 13 is the superposition of normalized far-field patterns at 857 nm and 957 nm using overfilled launching conditions and 70 nm bandpass filters. Precision in determining these differences should be quite good since only interference filters were changed between the two measurements. As shown, the presence of OH^- absorption at 957 nm does little to alter the shape from the pattern at 857 nm where no OH^- absorption is present. Therefore, the OH^- in this fiber appears to be uniformly distributed with a slight indication of more OH^- near the axis (957 nm curve is wider). The distribution of OH^- would depend upon the preform fabrication process so the above results apply only to the particular fiber.

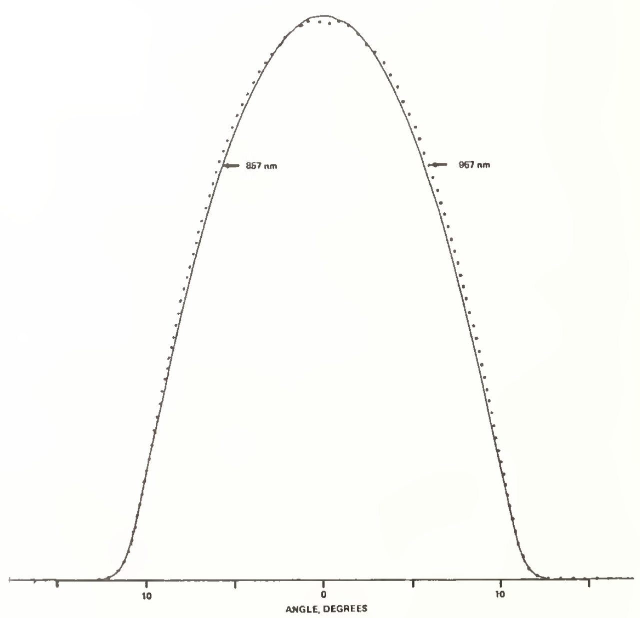

Figure 13. Experiment to qualitatively determine mode dependence of OH^- absorption. Little mode dependence is indicated for this particular fiber.

6. CONCLUSION

The determination of radiation angle (numerical aperture) from far-field data at the 5 percent intensity points should result in good measurement precision and accuracy when applied to near-parabolic, index fibers. In these fibers, leaky modes are contained within the meridionally defined numerical aperture so they should not affect the intensity at the largest observed angles. However, in step-index fibers the situation is different. Here leaky modes cause uncertainty if meridionally defined numerical aperture is desired. At present, standards groups have not made recommendations for step-index fibers.

A procedure for determining radiation angle (numerical aperture) of graded-index optical fibers was tested by an interlaboratory measurement comparison among six fiber manufacturers and NBS. Measurements on five fibers showed an average standard deviation (one σ) of 2.0 percent. Detailed discussion of the comparison can be found in chapter 4 of Optical Fiber Characterization, Volume 1, NBS Special Publication 637.

7. REFERENCES

[1] Cathey, W. T. Optical information processing and holography. New York:John Wiley; 1974.

[2] Sladen, F. M. E., et al. Determination of optical fiber refractive index profiles by a near-field scanning technique. A.P.L. 28(5):255-258; 1976 March.

[3] Adams, M. J., et al. Leaky rays on optical fibers of arbitrary (circularly symmetric) index profiles. Electronics Letters, 11(11):239-240; 1975 May.

[4] Holmes, G. T. Propagation parameter measurements of optical waveguides. Proceedings of the SPIE, Fiber Optics for Communication and Control, Vol. 224; 1980.

[5] Kitayama, K., et al. Impulse response prediction based on experimental mode coupling coefficient in a 10-km long graded-index fiber. IEEE J. Quant. Elect. QE-16(3):356-362; 1980 March.

[6] Procedures for determining radiation angle (numerical aperture) and core diameter from far and near-field patterns respectively are under consideration by Committee P6.6 of the Electronic Industries Association.

[7] Hanson, A. G., et al. Optical waveguide communications glossary. NTIA Special publication, NTIA-SP-79-4; 1979 September.

[8] Electronics Industries Association Committee P6.6 is currently recommending that radiation angle be based on the far-field pattern half width at the 5 percent intensity points.

[9] Miller, S. E.; Chynoweth, A. G. Optical Fiber Telecommunications. New York:Academic Press; 1979.

[10] Matsumura, H. The light acceptance angle of a graded index fibre. Optical and Quantum Electronics 7:81-86; 1975.

[11] Eriksrud, M., et al. Comparison between measured and predicted transmission characteristics of 12 km spliced graded-index fibres. Optical and Quantum Electronics. 11:517-523; 1979.

[12] Tateda, M. Optical loss measurements in graded-index fiber using a dummy fiber. Applied Optics. 18(19):3272-3275; 1979 October.

[13] Cherin, A. H.; Gardner, W. B. Standardization of optical fiber transmission measurements. Laser Focus. 16(8):60-65; 1980 August.

[14] PIN photodiodes with built-in operational amplifiers are available from a number of sources. A 22 megohm feedback resistor is used with the operational amplifier.

[15] The alphabetical fiber designations are consistent within this Technical Note but do not apply to any other NBS publications.

[16] Gloge, D.; Marcatili, E. A. J. Multimode theory of graded-core fibers. B.S.T.J. 52(9):1563-1578; 1973 November.

[17] Tokuda, M., et al. Measurement of baseband frequency response of multimode fibre by using a new type of mode scrambler. Electronic Letters. 13(5):146-147; 1977 March.

[18] Franzen, D. L.; Day, G. W. Measurement of optical fiber bandwidth in the time domain. Nat. Bur. Stand. (U.S.) Tech. Note 1019; 1980 February.

[19] Conduit, A. J., et al. Spectral and length-dependent losses in optical fibres investigated by a two-channel backscatter technique. Electronics Letters. 16(3): 77-78; 1980 January.

Appendix:

Optical Waveguide Communications Glossary

A. G. Hanson
L. R. Bloom
A. H. Cherin
G. W. Day
R. L. Gallawa
E. M. Gray
C. Kao
F. P. Kapron
B. S. Kawasaki
P. Reitz
M. Young

Absorption:
In an optical waveguide, that portion of attenuation resulting from conversion of optical power into heat.
Note. Intrinsic components consist of tails of the ultraviolet and infrared absorption bands. Extrinsic components include (a) impurities, e.g., the OH^- ion and transition metal ions and, (b) defects, e.g., results of thermal history and exposure to nuclear radiation. See also: Attenuation.

Acceptance angle:
Half the vertex angle of that cone within which optical power may be coupled into bound modes of an optical waveguide.
Note 1. Acceptance angle is a function of position on the entrance face of the core when the refractive index is a function of radius in the core. In that case, the local acceptance angle is

$$\arcsin \sqrt{n^2(r) - n_2^2}$$

where n(r) is the local refractive index and n_2 is the minimum refractive index of the cladding. The sine of the local acceptance angle is sometimes referred to as the local numerical aperture.
Note 2. Power may be coupled into leaky modes at angles exceeding the acceptance angle. See also: Launch numerical aperture; Power-law index profile.

Access coupler:
A device placed between two waveguide ends to allow signals to be withdrawn from or entered into one of the waveguides. See also: Optical waveguide coupler.

Acousto-optic effect:
A periodic variation of refractive index caused by an acoustic wave.
Note. The acousto-optic effect is used in devices that modulate and deflect light. See also: Modulation.

Active laser medium:
The material within a laser, such as crystal, gas, glass, liquid, or semiconductor, that emits coherent radiation (or exhibits gain) as the result of stimulated electronic or molecular transitions to lower energy states. Synonym: Laser medium. See also: Laser; Optical cavity.

Aligned bundle:
A bundle of optical fibers in which the relative spatial coordinates of each fiber are the same at the two ends of the bundle.
Note. The term "coherent bundle" is often employed as a synonym, and should not be confused with phase coherence or spatial coherence. Synonym: Coherent bundle. See also: Fiber bundle.

Alpha profile:
See Power-law index profile.

Angle of deviation:
In optics, the net angular deflection experienced by a light ray after one or more refractions or reflections.
Note. The term is generally used in reference to prisms, assuming air interfaces. The angle of deviation is then the angle between the incident ray and the emergent ray. See also: Reflection; Refraction.

Angle of incidence:
The angle between an incident ray and the normal to a reflecting or refracting surface. See also: Critical angle; Total internal reflection.

Angstrom (A):
A unit of optical wavelength (obsolete).
1 A $= 10^{-10}$ meters.
Note. The angstrom has been used historically in the field of optics, but it is not an SI (International System) unit.

Angular misalignment loss:
The optical power loss caused by angular deviation from the optimum alignment of source to optical waveguide, waveguide to waveguide, or waveguide to detector. See also: Extrinsic joint loss; Gap loss; Intrinsic joint loss; Lateral offset loss.

Anisotropic:
Pertaining to a material whose electrical or optical properties are different for different directions of propagation or different polarizations of a traveling wave. See also: Isotropic.

Antireflection coating:
A thin, dielectric or metallic film (or several such films) applied to an optical surface to reduce the reflectance and thereby increase the transmittance.
Note. The ideal value of the refractive index of single layered film is the square root of the product of the refractive indices on either side of the film, the ideal optical thickness being one quarter of a wavelength. See also: Dichroic filter; Fresnel reflection; Reflectance; Transmittance.

APD:
Abbreviation for Avalanche photodiode.

Note. apd and a.p.d. are also used.

Attenuation:
In an optical waveguide, the diminution of average optical power.
Note. In optical waveguides, attenuation results from absorption, scattering, and other radiation. Attenuation is generally expressed in dB. However, attenuation is often used as a synonym for attenuation coefficient, expressed in dB/km. This assumes the attenuation coefficient is invariant with length. See also: Attenuation coefficient; Coupling loss; Differential mode attenuation; Equilibrium mode distribution; Extrinsic joint loss; Insertion loss; Intrinsic joint loss; Leaky modes; Macrobend loss; Material scattering; Microbend loss; Rayleigh scattering; Spectral window; Transmission loss; Waveguide scattering.

Attenuation coefficient:
The rate of diminution of average optical power with respect to distance along the waveguide. Defined by the equation

$$P(z) = P(0)\ 10^{-(\alpha z/10)}$$

where P(z) is the power at distance z along the guide and P(0) is the power at z=0; α is the attenuation coefficient in dB/km if z is in km. From this equation,

$$\alpha z = -10 \log_{10}[P(z)/P(0)].$$

This assumes that α is independent of z; if otherwise, the definition must be given in terms of incremental attenuation as:

$$P(z) = P(0)10^{-\int_0^z \frac{\alpha(z)dz}{10}}$$

or, equivalently,

$$\alpha(z) = -10 \frac{d}{dz} \log_{10} [P(z)/P(0)]$$

See also: Attenuation; Attenuation constant; Axial propagation constant.

Attenuation constant:
For a particular mode, the real part of the axial propagation constant. The attenuation coefficient for the mode power is twice the attenuation constant. See also: Attenuation coefficient, Axial propagation constant; Propagation constant.

Attenuation-limited operation:
The condition prevailing when the received signal amplitude (rather than distortion) limits performance. See also: Bandwidth-limited operation; Distortion-limited operation.

Avalanche photodiode (APD):
A photodiode designed to take advantage of avalanche multiplication of photocurrent.
Note. As the reverse-bias voltage approaches the breakdown voltage, hole-electron pairs created by absorbed photons acquire sufficient energy to create additional hole-electron pairs when they collide with ions; thus a multiplication (signal gain) is achieved. See also: Photodiode; PIN photodiode.

Axial propagation constant:
The propagation constant evaluated along the axis of a waveguide (in the direction of transmission).
Note. The real part of the axial propagation constant is the attenuation constant while the imaginary part is the phase constant. Synonym: Axial propagation wave number. See also: Attenuation; Attenuation coefficient; Attenuation constant; Propagation constant.

Axial propagation wave number:
Synonym for Axial propagation constant.

Axial ray:
A light ray that travels along the optical axis. See also: Geometric optics; Fiber axis; Meridional ray; Paraxial ray; Skew ray.

Axial slab interferometry:
Synonym for Slab interferometry.

Backscattering:
The scattering of light into a direction generally reverse to the original one. See also: Rayleigh scattering; Reflectance; Reflection.

Bandpass filter:
See Optical filter.

Bandwidth:
See Fiber bandwidth.

Bandwidth-limited operation:
The condition prevailing when the system bandwidth, rather than the amplitude (or power) of the signal, limits performance. The condition is reached when the system distorts the shape of the waveform beyond specified limits. For linear systems, bandwidth-limited operation is equivalent to distortion-limited operation. See also: Attenuation-limited operation; Distortion-limited operation; Linear optical element.

Barrier layer:
In the fabrication of an optical fiber, a layer that can be used to create a boundary against OH^- ion diffusion into the core. See also: Core.

Baseband response function:
Synonym for Transfer function (of a device).

Beam diameter:
The distance between two diametrically opposed points at which the irradiance is a specified fraction of the beam's peak irradiance; most commonly applied to beams that are circular or nearly circular in cross section. Synonym: Beamwidth. See also: Beam divergence.

Beam divergence:
1. For beams that are circular or nearly circular in cross section, the angle subtended by the far-field beam diameter.
2. For beams that are not circular or nearly circular in cross section, the far-field angle subtended by two diametrically opposed points in a plane perpendicular to the optical axis, at which points the irradiance is a specified fraction of the beam's peak irradiance. Generally, only the maximum and minimum divergences (corresponding to the major and minor diameters of the far-field irradiance) need be specified. See also: Beam diameter; Collimation; Far-field region.

Beamsplitter:
A device for dividing an optical beam into two or more separate beams; often a partially reflecting mirror.

Beamwidth:
Synonym for Beam diameter.

Bidirectional transmission:
Signal transmission in both directions along an optical waveguide or other component.

Birefringence:
See Birefringent medium.

Birefringent medium:
A material that exhibits different indices of refraction for orthogonal linear polarizations of the light. The phase velocity of a wave in a birefringent medium thus depends on the polarization of the wave. Fibers may exhibit birefringence. See also: Refractive index (of a medium).

Blackbody:
A totally absorbing body (which reflects no radiation).
Note. In thermal equilibrium, a blackbody absorbs and radiates at the same rate; the radiation will just equal absorption when thermal equilibrium is maintained. See also: Emissivity.

Bolometer:
A device for measuring radiant energy by measuring the changes in resistance of a temperature-sensitive device exposed to radiation. See also: Radiant energy; Radiometry.

Boltzmann's constant:
The number k that relates the average energy of a molecule to the absolute temperature of the environment. k is approximately 1.38×10^{-23} joules/kelvin.

Bound mode:
In an optical waveguide, a mode whose field decays monotonically in the transverse direction everywhere external to the core and which does not lose power to radiation. Specifically, a mode for which

$$n(a)k \leq \beta \leq n(0)k$$

where β is the imaginary part (phase constant) of the axial propagation constant, n(a) is the refractive index at r=a, the core radius, n(0) is the refractive index at r=0, k is the free-space wavenumber, $2\pi/\lambda$, and λ is the wavelength. Bound modes correspond to guided rays in the terminology of geometric optics.
Note. Except in a monomode fiber, the power in bound modes is predominantly contained in the core of the fiber. Synonyms: Guided mode; Trapped mode. See also: Cladding mode; Guided ray; Leaky mode; Mode; Normalized frequency; Unbound mode.

Bound ray:
Synonym for Guided ray.

Brewster's angle:
For light incident on a plane boundary between two regions having different refractive indices, that angle of incidence at which the reflectance is zero for light that has its electric field vector in the plane defined by the direction of propagation and the normal to the surface. For propagation from medium 1 to medium 2, Brewster's angle is

$$\arctan (n_2/n_1)\ .$$

See also: Angle of incidence; Reflectance; Refractive index (of a medium).

Brightness:
An attribute of visual perception, in accordance with which a source appears to emit more or less light; obsolete.
Note 1. Usage should be restricted to nonquantitative reference to physiological sensations and perceptions of light.
Note 2. "Brightness" was formerly used as a synonym for the photometric term "luminance" and (incorrectly) for the radiometric term "radiance". See also: Radiance; Radiometry.

Buffer:
See Fiber buffer.

Bundle:
See Fiber bundle.

Cable:
See Optical cable.

Cable assembly:
See Multifiber cable; Optical cable assembly.

Cavity:
See Optical cavity.

Chemical vapor deposition (CVD) technique:
A process in which deposits are produced by heterogeneous gas-solid and gas-liquid chemical reactions at the surface of a substrate.
Note. The CVD method is often used in fabricating optical waveguide preforms by causing gaseous materials to react and deposit glass oxides. Typical starting chemicals include volatile compounds of silicon, germanium, phosphorous, and boron, which form corresponding oxides after heating with oxygen or other gases. Depending upon its type, the preform may be processed further in preparation for pulling into an optical fiber. See also: Preform.

Chirping:
A rapid change (as opposed to long-term drift) of the emission wavelength of an optical source. Chirping is most often observed in pulsed operation of a source.

Chromatic dispersion:
Redundant synonym for Dispersion.

Cladding:
The dielectric material surrounding the core of an optical waveguide. See also: Core; Normalized frequency; Optical waveguide; Tolerance field.

Cladding center:
The center of the circle that circumscribes the outer surface of the homogeneous cladding, as defined under Tolerance field. See also: Cladding; Tolerance field.

Cladding diameter:
The length of the longest chord that passes through the fiber axis and connects two points on the periphery of the homogeneous cladding. See also: Cladding; Core diameter; Tolerance field.

Cladding mode:
A mode that is confined by virtue of a lower index medium surrounding the cladding. Cladding modes correspond to cladding rays in the terminology of geometric optics. See also: Bound mode; Cladding ray; Leaky mode; Mode; Unbound mode.

Cladding mode stripper:
A device that encourages the conversion of cladding modes to radiation modes; as a result, the cladding modes are stripped from the fiber. Often a material having a refractive index equal to or greater than that of the waveguide cladding. See also: Cladding; Cladding mode.

Cladding ray:
In an optical waveguide, a ray that is confined to the core and cladding by virtue of reflection from the outer surface of the cladding. Cladding rays correspond to cladding modes in the terminology of mode descriptors. See also: Cladding mode; Guided ray; Leaky ray.

Coherence area:
The area in a plane perpendicular to the direction of propagation over which light may be considered highly coherent. Commonly the coherence area is the area over which the degree of coherence exceeds 0.88. See also: Coherent; Degree of Coherence.

Coherence length:
The propagation distance over which a light beam may be considered coherent. If the spectral linewidth of the source is $\Delta\lambda$ and the central wavelength is λ_0, the coherence length in a medium of refractive index n is approximately $\lambda_0^2/n\Delta\lambda$. See also: Degree of coherence; Spectral width.

Coherence time:
The time over which a propagating light beam may be considered coherent. It is equal to coherence length divided by the phase velocity of light in a medium; approximately given by $\lambda_0^2/c\Delta\lambda$, where λ_0 is the central wavelength, $\Delta\lambda$ is the spectral linewidth and c is the velocity of light in vacuum. See also: Coherence length; Phase velocity.

Coherent:
Characterized by a fixed phase relationship between points on an electromagnetic wave.
Note. A truly monochromatic wave would be perfectly coherent at all points in space. In practice, however, the region of high coherence may extend only a finite distance. The area on the surface of a wavefront over which the wave may be considered coherent is called the coherence area or coherence patch; if the wave has an appreciable coherence area, it is said to be spatially coherent over that area. The distance parallel to the wave vector along which the wave may be considered coherent is called the coherence length; if the wave has an appreciable coherence length, it is said to be phase or length coherent. The coherence length divided by the velocity of light in the medium is known as the coherence time; hence a phase coherent beam may also be called time (or temporally) coherent. See also: Coherence area; Coherence length; Coherence time; Degree of coherence; Monochromatic.

Coherent bundle:
Synonym for Aligned bundle.

Coherent radiation:
See Coherent.

Collimation:
The process by which a divergent or convergent beam of radiation is converted into a beam with the minimum divergence possible for that system (ideally, a parallel bundle of rays). See also: Beam divergence.

Concatenation (of optical waveguides):
The linking of optical waveguides, end to end.

Concentricity error:
When used in conjunction with a tolerance field to specify core/cladding geometry, the distance between the center of the two concentric circles specifying the cladding diameter and the center of the two concentric circles specifying the core diameter. See also: Cladding; Cladding diameter; Core; Core diameter; Tolerance field.

Connector:
See Optical waveguide connector.

Connector insertion loss:
See Insertion loss.

Conservation of radiance:
A basic principle stating that no passive optical system can increase the quantity Ln^{-2} where L is the radiance of a beam and n is the local refractive index. Formerly called "conservation of brightness" or the "brightness theorem." See also: Brightness; Radiance.

Core:
The central region of an optical waveguide through which light is transmitted. See also: Cladding; Normalized frequency; Optical waveguide.

Core area:
The cross sectional area enclosed by the curve that connects all points nearest the axis on the periphery of the core where the refractive index of the core exceeds that of the homogeneous cladding by k times the difference betwen the maximum refractive index in the core and the refractive index of the homogeneous cladding, where k is a specified positive or negative constant $|k|<1$. See also: Cladding; Core; Homogeneous cladding; Tolerance field.

Core center:
A point on the fiber axis. See also: Fiber axis; Optical axis.

Core diameter:
The diameter of the circle that circumscribes the core area. See also: Cladding; Core; Core area; Tolerance field.

Cosine emission law:
Synonym for Lambert's cosine law.

Coupled modes:
Modes whose energies are shared. See also: Mode.

Coupler:
See Optical waveguide coupler.

Coupling:
See Mode coupling.

Coupling efficiency:
The efficiency of optical power transfer between two optical components. See also: Coupling loss.

Coupling loss:
The power loss suffered when coupling light from one optical device to another. See also: Angular misalignment loss; Extrinsic joint loss; Gap loss; Insertion loss; Intrinsic joint loss; Lateral offset loss.

Critical angle:
When light propagates in a homogeneous medium of relatively high refractive index (n_{high}) onto a planar interface with a homogeneous material of lower index (n_{low}), the critical angle is defined by

$$\arcsin (n_{low} / n_{high}).$$

Note. When the angle of incidence exceeds the critical angle, the light is totally reflected by the interface. This is termed total internal reflection. See also: Acceptance angle; Angle of incidence; Reflection; Refractive index (of a medium); Step index profile; Total internal reflection.

Curvature loss:
Synonym for Macrobend loss.

Cutback technique:
A technique for measuring fiber attenuation or distortion by performing two transmission measurements. One is at the output end of the full length of the fiber. The other is within 1 to 3 meters of the input end, access being had by "cutting back" the test fiber. See also: Attenuation.

Cutoff wavelength:
That wavelength greater than which a particular waveguide mode ceases to be a bound mode.
Note. In a single mode waveguide, concern is with the cutoff wavelength of the second order mode. See also: Mode.

CVD:
Abbreviation for Chemical vapor deposition.

D* (pronounced "D-star"):
A figure of merit often used to characterize detector performance, defined as the reciprocal of noise equivalent power (NEP), normalized to unit area and unit bandwidth.

$$D^* = \sqrt{A(\Delta f)} / NEP,$$

where A is the area of the photosensitive region of the detector and (Δf) is the effective noise bandwidth. Synonym: Specific detectivity. See also: Detectivity; Noise equivalent power.

Dark current:

The external current that, under specified biasing conditions, flows in a photosensitive detector when there is no incident radiation.

Degree of coherence:

A measure of the coherence of a light source; the magnitude of the degree of coherence is equal to the visibility, V, of the fringes of a two-beam interference experiment, where

$$V = \frac{I_{max} - I_{min}}{I_{max} + I_{min}},$$

I_{max} is the intensity at a maximum of the interference pattern, and I_{min} is the intensity at a minimum.

Note. Light is considered highly coherent when the degree of coherence exceeds 0.88, partially coherent for values less than 0.88, and incoherent for "very small" values. See also: Coherence area; Coherence length; Coherent; Interference.

Density:

See Optical density.

Detectivity:

The reciprocal of noise equivalent power (NEP). See also: Noise equivalent power (NEP).

Dichroic filter:

An optical filter designed to transmit light selectively according to wavelength (most often, a high-pass or low-pass filter). See also: Optical filter.

Dichroic mirror:

A mirror designed to reflect light selectively according to wavelength. See also: Dichroic filter.

Dielectric filter:

See Interference filter.

Differential mode attenuation:

The variation in attenuation among the propagating modes of an optical fiber.

Differential mode delay:

The variation in propagation delay that occurs because of the different group velocities of the modes of an optical fiber. Synonym: Multimode group delay. See also: Group velocity; Mode; Multimode distortion.

Differential quantum efficiency:

In an optical source or detector, the slope of the curve relating output quanta to input quanta.

Diffraction:

The deviation of a wavefront from the path predicted by geometric optics when a wavefront is restricted by an opening or an edge of an object.

Note. Diffraction is usually most noticeable for openings of the order of a wavelength. However, diffraction may still be important for apertures many orders of magnitude larger than the wavelength. See also: Far-field diffraction pattern; Near-field diffraction pattern.

Diffraction grating:

An array of fine, parallel, equally spaced reflecting or transmitting lines that mutually enhance the effects of diffraction to concentrate the diffracted light in a few directions determined by the spacing of the lines and the wavelength of the light. See also: Diffraction.

Diffraction limited:

A beam of light is diffraction limited if: a) the far-field beam divergence is equal to that predicted by diffraction theory, or b) in focusing optics, the impulse response or resolution limit is equal to that predicted by diffraction theory. See also: Beam divergence angle; Diffraction.

Diffuse reflection:

See Reflection.

Diode laser:

Synonym for Injection laser diode (ILD).

Directional coupler:

See Tee coupler.

Dispersion:

A term used to describe the chromatic or wavelength dependence of a parameter as opposed to the temporal dependence which is referred to as distortion. The term is used, for example, to describe the process by which an electromagnetic signal is distorted because the various wavelength components of that signal have different propagation characteristics. The term is also used to describe the relationship between refractive index and wavelength.

Note. Signal distortion in an optical waveguide is caused by several dispersive mechanisms: waveguide dispersion, material dispersion, and profile dispersion. In addition, the signal suffers degradation from multimode "distortion," which is often (erroneously) referred to as multimode "dispersion." See also: Distortion; Intramodal distortion; Material dispersion; Material dispersion parameter; Multimode distortion; Profile dispersion; Profile dispersion parameter; Waveguide dispersion.

Distortion:

A change of signal waveform shape.

Note. In a multimode fiber, the signal can suffer degradation from multimode distortion. In addition, several dispersive mechanisms can cause signal distortion in an optical waveguide: waveguide dispersion, material dispersion, and profile dispersion. See also: Dispersion; Profile dispersion.

Distortion-limited operation:
The condition prevailing when the distortion of the received signal, rather than its amplitude (or power), limits performance. The condition is reached when the system distorts the shape of the waveform beyond specified limits. For linear systems, distortion-limited operation is equivalent to bandwidth-limited operation. See also: Attenuation-limited operation; Bandwidth-limited operation; Distortion; Multimode distortion.

Divergence:
See Beam divergence.

Double crucible method:
A method of fabricating an optical waveguide by melting core and clad glasses in two suitably joined concentric crucibles and then drawing a fiber from the combined melted glass. See also: Chemical vapor deposition technique.

D-star:
See D*.

Effective mode volume:
The square of the product of the diameter of the near-field pattern and the sine of the radiation angle of the far-field pattern. The diameter of the near-field radiation pattern is defined here as the full width at half maximum and the radiation angle at half maximum intensity.
Note. Effective mode volume is proportional to the breadth of the relative distribution of power amongst modes in a multimode fiber. It is not truly a spatial volume but rather an "optical volume" equal to the product of area and solid angle. See also: Mode volume; Radiation pattern.

Electroluminescence:
Nonthermal conversion of electrical energy into light. One example is the photon emission resulting from electron-hole recombination in a pn junction such as in a light emitting diode. See also: Injection laser diode.

Electro-optic effect:
A change in the refractive index of a material under the influence of an electric field.
Note 1. Pockels and Kerr effects are electro-optic effects that are respectively linear and quadratic in the electric field strength.
Note 2. Electro-optic is often erroneously used as a synonym for optoelectronic. See also: Optoelectronic.

Emissivity:
The ratio of power radiated by a substance to the power radiated by a blackbody at the same temperature. Emissivity is a function of wavelength and temperature. See also: Blackbody.

Equilibrium coupling length:
Synonym for Equilibrium length.

Equilibrium length:
For a specific excitation condition, the length of multimode optical waveguide necessary to attain equilibrium mode distribution.
Note. The term is sometimes used to refer to the longest such length, as would result from a worst-case, but undefined excitation. Synonyms: Equilibrium coupling length; Equilibrium mode distribution length. See also: Equilibrium mode distribution; Mode coupling.

Equilibrium mode distribution:
The condition in a multimode optical waveguide in which the relative power distribution among the propagating modes is independent of length. Synomym: Steady-state condition. See also: Equilibrium length; Mode; Mode coupling.

Equilibrium mode distribution length:
Synonym for Equilibrium length.

Equilibrium mode simulator:
A device or optical system used to create an approximation of the equilibrium mode distribution. See also: Equilibrium mode distribution; Mode filter.

Evanescent field:
A time varying electromagnetic field whose amplitude decreases monotonically, but without an accompanying phase shift, in a particular direction is said to be evanescent in that direction.

Excess insertion loss:
In an optical waveguide coupler, the optical loss associated with that portion of the light which does not emerge from the nominally operational ports of the device. See also; Optical waveguide coupler.

Extrinsic joint loss:
That portion of joint loss that is not intrinsic to the fibers (i.e., loss caused by imperfect jointing). See also: Angular misalignment loss; Gap loss; Intrinsic joint loss; Lateral offset loss.

Far-field diffraction pattern:
The diffraction pattern of a source (such as an LED, ILD, or the output end of an optical waveguide) observed at an infinite distance from the source. Theoretically, a far-field pattern exists at distances that are large compared with s^2/λ, where s is a characteristic dimension of the source and λ is the wavelength. Example: If the source is a uniformly illuminated circle, then s is the radius of the circle.

Note. The far-field diffraction pattern of a source may be observed at infinity or (except for scale) in the focal plane of a well-corrected lens. The far-field pattern of a diffracting screen illuminated by a point source may be observed in the image plane of the source. Synonym: Fraunhofer diffraction pattern. See also: Diffraction; Diffraction limited.

Far-field pattern:
Synonym for Far-field radiation pattern.

Far-field radiation pattern:
See Radiation pattern.

Far-field region:
The region, far from a source, where the diffraction pattern is substantially the same as that at infinity. See also: Far-field diffraction pattern.

FDHM:
Abbreviation for full duration at half maximum. See also: Full width (duration) half maximum.

Ferrule:
A mechanical fixture, generally a rigid tube, used to confine the stripped end of a fiber bundle or a fiber. See also: Fiber bundle.
Note 1. Typically, individual fibers of a bundle are cemented together within a ferrule of a diameter designed to yield a maximum packing fraction. See also: Packing fraction.
Note 2. Nonrigid materials such as shrink tubing may also be used for ferrules for special applications. See also: Reference surface.

FET photodetector:
A photodetector employing photogeneration of carriers in the channel region of an FET structure to provide photodetection with current gain. See also: Photocurrent; Photodiode.

Fiber:
See Optical fiber.

Fiber axis:
The line connecting the centers of the circles that circumscribe the core, as defined under Tolerance field. Synonym: Optical axis. See also: Tolerance field.

Fiber bandwidth:
The lowest frequency at which the magnitude of the fiber transfer function decreases to a specified fraction of the zero frequency value. Often, the specified value is one-half the optical power at zero frequency. See also: Transfer function.

Fiber buffer:
A material that may be used to protect an optical fiber waveguide from physical damage, providing mechanical isolation and/or protection.
Note. Cable fabrication techniques vary, some resulting in firm contact between fiber and protective buffering, others resulting in a loose fit, permitting the fiber to slide in the buffer tube. Multiple buffer layers may be used for added fiber protection. See also: Fiber bundle.

Fiber bundle:
An assembly of unbuffered optical fibers. Usually used as a single transmission channel, as opposed to multifiber cables, which contain optically and mechanically isolated fibers, each of which provides a separate channel.
Note 1. Bundles used only to transmit light, as in optical communications, are flexible and are typically unaligned.
Note 2. Bundles used to transmit optical images may be either flexible or rigid, but must contain aligned fibers. See also: Aligned bundle; Ferrule; Fiber optics; Multifiber cable; Optical cable; Optical fiber; Packing fraction.

Fiber optics (FO):
The branch of optical technology concerned with the transmission of radiant power through fibers made of transparent materials such as glass, fused silica, or plastic.
Note 1. Telecommunication applications of fiber optics employ flexible fibers. Either a single discrete fiber or a nonspatially aligned fiber bundle may be used for each information channel. Such fibers are often referred to as "optical waveguides" to differentiate from fibers employed in noncommunications applications.
Note 2. Various industrial and medical applications employ (typically high-loss) flexible fiber bundles in which individual fibers are spatially aligned, permitting optical relay of an image. An example is the endoscope.
Note 3. Some specialized industrial applications employ rigid (fused) aligned fiber bundles for image transfer. An example is the fiber optics faceplate used on some high-speed oscilloscopes.

Flux:
Obsolete synonym for Radiant power.

Fraunhofer diffraction pattern:
Synonym for Far-field diffraction pattern.

Frequency response:
Synonym for Transfer function (of a device).

Fresnel diffraction pattern:
Synonym for Near-field diffraction pattern.

Fresnel reflection:
The reflection of a portion of the light incident on a planar interface between two homogeneous media having different refractive indices.

Note 1. Fresnel reflection occurs at the air-glass interfaces at entrance and exit ends of an optical waveguide. Resultant transmission losses (on the order of 4% per interface) can be virtually eliminated by use of antireflection coatings or index matching materials.
Note 2. Fresnel reflection depends upon the index difference and the angle of incidence; it is zero at Brewster's angle for one polarization. In optical elements, a thin transparent film is sometimes used to give an additional Fresnel reflection that cancels the original one by interference. This is called an antireflection coating. See also: Antireflection coating; Brewster's angle; Index matching material; Reflectance; Reflection; Refractive index.

Fresnel reflection method:
The method for measuring the index profile of an optical fiber by measuring the reflectance as a function of position on the end face. See also: Fresnel reflection; Index profile; Reflectance.

Full width (duration) half maximum:
A measure of the extent of a function. Given by the difference between the two extreme values of the independent variable at which the dependent variable is equal to half of its maximum value. The term "duration" is preferred when the independent variable is time.
Note. Commonly applied to the duration of pulse waveforms, the spectral extent of emission or absorption lines, and the angular or spatial extent of radiation patterns.

Fundamental mode:
The lowest order mode of a waveguide. In fibers, the mode designated LP_{01} or HE_{11}. See also: Mode.

Fused quartz:
Glass made by melting natural quartz crystals; not as pure as vitreous silica. See also: Vitreous silica.

Fused silica:
Synonym for Vitreous silica. See also: Fused quartz.

Fusion splice:
A splice accomplished by the application of localized heat sufficient to fuse or melt the ends of two lengths of optical fiber, forming a continuous, single fiber.

FWHM:
Abbreviation for full width at half maximum. See also: Full width (duration) half maximum.

Gap loss:
That optical power loss caused by a space between axially aligned fibers.
Note. For waveguide-to-waveguide coupling, it is commonly called "longitudinal offset loss." See also: Coupling loss.

Gaussian beam:
A beam of light whose electric field amplitude distribution is gaussian. When such a beam is circular in cross section, the amplitude is

$$E(r) = E(0) \exp[-(r/w)^2],$$

where r is the distance from beam center and w is the radius at which the amplitude is 1/e of its value on the axis; w is called the beamwidth. See also: Beam diameter.

Gaussian pulse:
A pulse that has the waveform of a gaussian distribution. In the time domain, the waveform is

$$f(t) = A \exp[-(t/a)^2],$$

where A is a constant, and a is the pulse half duration at the 1/e points. See also: Full width (duration) half maximum.

Geometric optics:
The treatment of propagation of light as rays.
Note. Rays are bent at the interface between two dissimilar media or may be curved in a medium in which refractive index is a function of position. See also: Axial ray; Meridional ray; Optical axis; Paraxial ray; Physical optics; Skew ray.

Graded index optical waveguide:
A waveguide having a graded index profile in the core. See also: Graded index profile; Step index optical waveguide.

Graded index profile:
Any refractive index profile that varies with radius in the core. Distinguished from a step index profile. See also: Dispersion; Mode volume; Multimode optical waveguide; Normalized frequency; Optical waveguide; Parabolic profile; Profile dispersion; Profile parameter; Refractive index; Step index profile; Power-law index profile.

Group index (Denoted N):
For a given mode propagating in a medium of refractive index n, the velocity of light in vacuum, c, divided by the group velocity of the mode. For a plane wave of wavelength λ, it is related thus to the refractive index:

$$N = n - \lambda (dn/d\lambda)$$

See also: Group velocity; Material dispersion parameter.

Group velocity:
1. For a particular mode, the reciprocal of the rate of change of the phase constant with respect to angular frequency.

Note. The group velocity equals the phase velocity if the phase constant is a linear function of the angular frequency.

2. Velocity of the signal modulating a propagating electromagnetic wave. See also: Differential mode delay; Group index; Phase velocity.

Guided mode:
Synonym for Bound mode.

Guided ray:
In an optical waveguide, a ray that is completely confined to the core. Specifically, a ray at radial position r having direction such that

$$0 \leq \sin \theta(r) \leq [n^2(r) - n^2(a)]^{1/2}$$

where $\theta(r)$ is the angle the ray makes with the waveguide axis, n(r) is the refractive index, and n(a) is the refractive index at the core radius. Guided rays correspond to bound (or guided) modes in the terminology of mode descriptors. Synonyms: Bound ray; Trapped ray. See also: Bound mode; Leaky ray.

HE_{11} mode:
Designation for the fundamental mode of an optical fiber. See Fundamental mode.

Heterojunction:
A junction between semiconductors that differ in their doping level conductivities, and also in their atomic or alloy compositions. See also: Homojunction.

Homogeneous cladding:
That part of the cladding wherein the refractive index is constant within a specified tolerance, as a function of radius. See also: Cladding; Tolerance field.

Homojunction:
A junction between semiconductors that differ in their doping level conductivities but not in their atomic or alloy compositions. See also: Heterojunction.

Hybrid mode:
A mode possessing components of both electric and magnetic field vectors in the direction of propagation.
Note. Such modes correspond to skew (nonmeridional) rays. See also: Mode; Skew ray; Transverse electric mode; Transverse magnetic mode.

ILD:
Abbreviation for Injection laser diode.

Impulse response:
The function h(t) describing the response of an initially relaxed system to an impulse (Dirac-delta) function applied at time t = 0. The root-mean-square (rms) duration, σ_{rms}, of the impulse response is often used to characterize a component or system through a single parameter rather than a function:

$$\sigma_{rms} = [1/M_0 \int_{-\infty}^{\infty} (T-t)^2 h(t) dt]^{1/2}$$

$$\text{where } M_0 = \int_{-\infty}^{\infty} h(t)\, dt$$

$$T = 1/M_0 \int_{-\infty}^{\infty} t h(t)\, dt.$$

Note. The impulse response may be obtained by deconvolving the input waveform from the output waveform, or as the inverse Fourier transform of the transfer function. See also: Root-mean-square (rms) pulse duration; Transfer function.

Inclusion:
Denoting the presence of extraneous or foreign material.

Incoherent:
Characterized by a degree of coherence significantly less than 0.88. See also: Coherent; Degree of coherence.

Index dip:
A decrease in the refractive index at the center of the core, caused by certain fabrication techniques. Sometimes called profile dip. See also: Refractive index profile.

Index matching material:
A material, often a liquid or cement, whose refractive index is nearly equal to the core index, used to reduce Fresnel reflections from a fiber end face. See also: Fresnel reflection; Mechanical splice; Refractive index.

Index of refraction:
Synonym for Refractive index (of a medium).

Index profile:
In an optical waveguide, the refractive index as a function of radius. See also: Graded index profile; Parabolic profile; Power-law index profile; Profile dispersion; Profile dispersion parameter; Profile parameter; Step index profile.

Infrared (IR):
The region of the electromagnetic spectrum between the long-wavelength extreme of the visible spectrum (about 0.7 μm) and the shortest microwaves (about 1 mm).

Injection fiber:
Synonym for Launching fiber.

Injection laser diode (ILD):
A laser employing a forward-biased semiconductor junction as the active medium. Synonyms: Diode laser; Semiconductor laser. See also: Active laser medium; Chirping; Laser; Superradiance.

Insertion loss:
The total optical power loss caused by the insertion of an optical component such as a connector, splice, or coupler.

Integrated optical circuit (IOC):
An optical circuit, either monolithic or hybrid, composed of active and passive components, used for coupling between optoelectronic devices and providing signal processing functions.

Intensity:
The square of the electric field amplitude of a light wave. Intensity is proportional to irradiance and may be used in place of the term "irradiance" when only relative values are important. See also: Irradiance; Radiant intensity; Radiometry.

Interference:
In optics, the interaction of two or more beams of coherent or partially coherent light. See also: Coherent; Degree of coherence; Diffraction.

Interference filter:
An optical filter consisting of one or more thin layers of dielectric or metallic material. See also: Dichroic filter; Interference; Optical filter.

Interferometer:
An instrument that employs the interference of light waves for purposes of measurement. See also: Interference.

Intermodal distortion:
Synonym for Multimode distortion.

Intramodal distortion:
That distortion resulting from dispersion of group velocity of a propagating mode. It is the only distortion occurring in single mode waveguides. See also: Dispersion; Distortion.

Intrinsic joint loss:
That loss, intrinsic to the fiber, caused by fiber parameter (e.g., core dimensions, profile parameter) mismatches when two nonidentical fibers are joined. See also: Angular misalignment loss; Extrinsic joint loss; Gap loss; Lateral offset loss.

IOC:
Abbreviation for Integrated optical circuit.

Ion exchange technique:
A method of fabricating a graded index optical waveguide by an ion exchange process. See also: Chemical vapor deposition technique; Double crucible method; Graded index profile.

IR:
Abbreviation for Infrared.

Irradiance:
Radiant power incident per unit area upon a surface, expressed in watts per square meter. "Power density" is colloquially used as a synonym. See also: Radiometry.

Isolator:
A device intended to prevent return reflections along a transmission path.
Note. The Faraday isolator uses the magneto-optic effect.

Isotropic:
Pertaining to a material whose electrical or optical properties are independent of direction of propagation and of polarization of a traveling wave. See also: Anisotropic; Birefringent medium.

Lambert's cosine law:
The statement that the radiance of certain idealized surfaces, known as Lambertian radiators, Lambertian sources, or Lambertian reflectors, is independent of the angle from which the surface is viewed.
Note. The radiant intensity of such a surface is maximum normal to the surface and decreases in proportion to the cosine of the angle from the normal. Synonym: Cosine emission law.

Lambertian radiator:
See Lambert's cosine law.

Lambertian reflector:
See Lambert's cosine law.

Lambertian source:
See Lambert's cosine law.

Laser:
A device that produces optical radiation using a population inversion to provide Light Amplification by Stimulated Emission of Radiation and (generally) an optical resonant cavity to provide positive feedback. Laser radiation may be highly coherent temporally, or spatially, or both. See also: Active laser medium; Injection laser diode; Optical cavity.

Laser diode:
Synonym for Injection laser diode.

Laser medium:
Synonym for Active laser medium.

Lasing threshold:
The lowest excitation level at which a laser's output is dominated by stimulated emission rather than spontaneous emission. See also: Laser; Spontaneous emission; Stimulated emission.

Lateral offset loss:
A power loss caused by transverse or lateral deviation from optimum alignment of source to optical waveguide, waveguide to waveguide, or waveguide to detector. Synonym: Transverse offset loss.

Launch angle:
The angle between the light input propagation vector and the optical axis of an optical fiber or fiber bundle. See also: Launch numerical aperture.

Launch numerical aperture (LNA):
The numerical aperture of an optical system used to couple (launch) power into an optical waveguide.
Note 1. LNA may differ from the stated NA of a final focusing element if, for example, that element is underfilled or the focus is other than that for which the element is specified.
Note 2. LNA is one of the parameters that determine the initial distribution of power among the modes of an optical waveguide. See also: Acceptance angle; Launch angle.

Launching fiber:
A fiber used in conjunction with a source to excite the modes of another fiber in a particular fashion.
Note. Launching fibers are most often used in test systems to improve the precision of measurements. Synonym: Injection fiber. See also: Mode; Pigtail.

Leaky mode:
In an optical waveguide, a mode whose field decays monotonically for a finite distance in the transverse direction but which becomes oscillatory everywhere beyond that finite distance. Specifically, a mode for which

$$[n^2(a)k^2 - (\ell/a)^2]^{1/2} \leq \beta \leq n(a)k$$

where β is the imaginary part (phase term) of the axial propagation constant, ℓ is the azimuthal index of the mode, n(a) is the refractive index at r=a, the core radius, and k is the free-space wavenumber, $2\pi/\lambda$, and λ is the wavelength. Leaky modes correspond to leaky rays in the terminology of geometric optics.
Note. Leaky modes experience attenuation, even if the waveguide is perfect in every respect. Synonym: Tunnelling mode. See also: Bound mode; Cladding mode; Leaky ray; Mode; Unbound mode.

Leaky ray:
In an optical waveguide, a ray for which geometric optics would predict total internal reflection at the core boundary, but which suffers loss by virtue of the curved core boundary. Specifically, a ray at radial position r having direction such that

$$n^2(r) - n^2(a) \leq \sin^2\theta(r)$$

and

$$\sin^2\theta(r) \leq [n^2(r)-n^2(a)] \;/\; [1-(r/a)^2\cos^2\phi(r)]$$

where $\theta(r)$ is the angle the ray makes with the waveguide axis, n(r) is the refractive index, a is the core radius, and $\phi(r)$ is the azimuthal angle of the projection of the ray on the transverse plane. Leaky rays correspond to leaky (or tunnelling) modes in the terminology of mode descriptors. Synonym: Tunnelling ray. See also: Bound mode; Cladding ray; Guided ray; Leaky mode.

LED:
Abbreviation for Light emitting diode.

Light:
1. In a strict sense, the region of the electromagnetic spectrum that can be perceived by human vision, designated the visible spectrum and nominally covering the wavelength range of 0.4μm to 0.7μm.
2. In the laser and optical communication fields, custom and practice have extended usage of the term to include the much broader portion of the electromagnetic spectrum that can be handled by the basic optical techniques used for the visible spectrum. This region has not been clearly defined but, as employed by most workers in the field, may be considered to extend from the near-ultraviolet region of approximately 0.3μm, through the visible region, and into the mid-infrared region to 30μm. See also: Infrared (IR); Optical spectrum; Ultraviolet (UV).

Light current:
See Photocurrent.

Light emitting diode (LED):
A pn junction semiconductor device that emits incoherent optical radiation when biased in the forward direction. See also: Incoherent.

Light ray:
The path of a point on a wavefront. The direction of a light ray is generally normal to the wavefront. See also: Geometric optics.

Lightguide:
Synonym for Optical waveguide.

Line source:
1. In the spectral sense, an optical source that emits one or more spectrally narrow lines as opposed to a continuous spectrum. See also: Monochromatic.
2. In the geometric sense, an optical source whose active (emitting) area forms a spatially narrow line.

Line spectrum:
An emission or absorption spectrum consisting of one or more narrow spectral lines, as opposed to

a continuous spectrum. See also: Monochromatic; Spectral line; Spectral width.

Linear element:
A device for which the output electric field is linearly proportional to the input electric field and no new wavelengths or modulation frequencies are generated. A linear element can be described in terms of a transfer function or an impulse response function.

Linearly polarized (LP) mode:
A mode for which the field components in the direction of propagation are small compared to components perpendicular to that direction.
Note. The LP description is an approximation which is valid for weakly guiding waveguides, including typical telecommunication grade fibers. See also: Mode; Weakly guiding fiber.

Linewidth:
See Spectral width.

LNA:
Abbreviation for Launch numerical aperture.

Longitudinal offset loss:
See Gap loss.

Loss:
See Absorption; Angular misalignment loss; Attenuation; Backscattering; Differential mode attenuation; Extrinsic joint loss; Gap loss; Insertion loss; Intrinsic joint loss; Lateral offset loss; Macrobend loss; Material scattering; Microbend loss; Nonlinear scattering; Rayleigh scattering; Reflection; Transmission loss; Waveguide scattering.

LP mode:
Abbreviation for Linearly polarized mode.

LP_{01} mode:
Designation of the fundamental LP mode. See Fundamental mode.

Macrobend loss:
In an optical waveguide, that loss attributable to macrobending. Macrobending usually causes little or no radiative loss. Synonym: Curvature loss. See also: Macrobending; Microbend loss.

Macrobending:
In an optical waveguide, all macroscopic deviations of the axis from a straight line; distinguished from microbending. See also: Macrobend loss; Microbend loss; Microbending.

Magneto-optic:
Pertaining to a change in a material's refractive index under the influence of a magnetic field. Magneto-optic materials generally are used to rotate the plane of polarization.

Material absorption:
See Absorption.

Material dispersion:
That dispersion attributable to the wavelength dependence of the refractive index of material used to form the waveguide. Material dispersion is characterized by the material dispersion parameter M. See also: Dispersion; Distortion; Material dispersion parameter; Profile dispersion parameter; Waveguide dispersion.

Material dispersion parameter (M):

$$M(\lambda) = -1/c\ (dN/d\lambda) = \lambda/c\ (d^2n/d\lambda^2)$$

where n is the refractive index,
N is the group index: $N = n - \lambda(dn/d\lambda)$,
λ is the wavelength, and
c is the velocity of light in vacuum.
Note 1. For many optical waveguide materials, M is zero at a specific wavelength λ_0, usually found in the 1.2 to 1.5μm range. The sign convention is such that M is positive for wavelengths shorter than λ_0 and negative for wavelengths longer than λ_0.
Note 2. Pulse broadening caused by material dispersion in a unit length of optical fiber is given by M times spectral linewidth ($\Delta\lambda$), except at $\lambda = \lambda_0$, where terms proportional to $(\Delta\lambda)^2$ are important. (See Note 1.) See also: Group index; Material dispersion.

Material scattering:
In an optical waveguide, that part of the total scattering attributable to the properties of the materials used for waveguide fabrication. See also: Rayleigh scattering; Scattering; Waveguide scattering.

Mechanical splice:
A fiber splice accomplished by fixtures or materials, rather than by thermal fusion. Index matching material may be applied between the two fiber ends. See also: Fusion splice; Index matching material; Optical waveguide splice.

Meridional ray:
A ray that passes through the optical axis of an optical waveguide (in contrast with a skew ray which does not). See also: Axial ray; Geometric optics; Numerical aperture; Optical axis; Paraxial ray; Skew ray.

Microbend loss:
In an optical waveguide, that loss attributable to microbending. See also: Macrobend loss.

Microbending:
In an optical waveguide, sharp curvatures involving local axial displacements of a few micrometers and spatial wavelengths of a few millimeters. Such bends may result from waveguide coating, cabling, packaging, installation, etc.
Note. Microbending can cause significant radiative losses and mode coupling. See also: Macrobending.

Misalignment loss:
See Angular misalignment loss; Gap loss; Lateral offset loss.

Modal noise:
Noise generated in an optical fiber system by the combination of mode dependent optical losses and fluctuation in the distribution of optical energy among the guided modes or in the relative phases of the guided modes. Synonym: Speckle noise. See also: Mode.

Mode:
In any cavity or transmission line, one of those electromagnetic field distributions that satisfies Maxwell's equations and the boundary conditions. The field pattern of a mode depends on the wavelength, refractive index, and cavity or waveguide geometry. See also: Bound mode; Cladding mode; Differential mode attenuation; Differential mode delay; Equilibrium mode distribution; Equilibrium mode simulator; Fundamental mode; Hybrid mode; Leaky modes; Linearly polarized mode; Mode volume; Multimode distortion; Multimode laser; Multimode optical waveguide; Single mode optical waveguide; Transverse electric mode; Transverse magnetic mode; Unbound mode.

Mode coupling:
In an optical waveguide, the exchange of power among modes. The exchange of power may reach statistical equilibrium after propagation over a finite distance that is designated the equilibrium length. See also: Equilibrium length; Equilibrium mode distribution; Mode; Mode scrambler.

Mode dispersion:
Often erroneously used as a synonym for Multimode distortion.

Mode (or modal) distortion:
Synonym for Multimode distortion.

Mode filter:
A device used to select, reject, or attenuate a certain mode or modes.

Mode mixer:
Synonym for Mode scrambler.

Mode scrambler:
1. A device for inducing mode coupling in an optical fiber.
2. A device composed of one or more optical fibers in which strong mode coupling occurs.
Note. Frequently used to provide a mode distribution that is independent of source characteristics or that meets other specifications. Synonym: Mode mixer. See also: Mode coupling.

Mode stripper:
See Cladding mode stripper.

Mode volume:
The number of bound modes that an optical waveguide is capable of supporting; for $V>5$, approximately given by $V^2/2$ and $(V^2/2)[g/(g+2)]$, respectively, for step index and power-law profile waveguides, where g is the profile parameter, and V is normalized frequency. See also: Effective mode volume; Mode; Normalized frequency; Power-law index profile; Step index profile; V number.

Modulation:
A controlled variation with time of any property of a wave for the purpose of transferring information.

Monochromatic:
Consisting of a single wavelength or color. In practice, radiation is never perfectly monochromatic but, at best, displays a narrow band of wavelengths. See also: Coherent; Line source; Spectral width.

Monochromator:
An instrument for isolating narrow portions of the spectrum.

Monomode optical waveguide:
Synonym for Single mode optical waveguide.

Multifiber cable:
An optical cable that contains two or more fibers, each of which provides a separate information channel. See also: Fiber bundle; Optical cable assembly.

Multifiber joint:
An optical splice or connector designed to mate two multifiber cables, providing simultaneous optical alignment of all individual waveguides.
Note: Optical coupling between aligned waveguides may be achieved by various techniques including proximity butting (with or without index matching materials), and the use of lenses.

Multilayer filter:
See Interference filter.

Multimode distortion:
In an optical waveguide, that distortion resulting from differential mode delay.

Note. The term "multimode dispersion" is often used as a synonym; such usage, however, is erroneous since the mechanism is not dispersive in nature. Synonyms: Intermodal distortion; Mode (or modal) distortion. See also: Distortion.

Multimode group delay:
Synonym for Differential mode delay.

Multimode laser:
A laser that produces emission in two or more transverse or longitudinal modes. See also: Laser; Mode.

Multimode optical waveguide:
An optical waveguide that will allow more than one bound mode to propagate.
Note. May be either a graded index or step index waveguide. See also: Bound mode; Mode; Mode volume; Multimode distortion; Normalized frequency; Power-law index profile; Single mode optical waveguide; Step index optical waveguide.

NA:
Abbreviation for Numerical aperture.

Near-field diffraction pattern:
The diffraction pattern observed close to a source or aperture, as distinguished from far-field diffraction pattern.
Note. The pattern in the output plane of a fiber is called the near-field radiation pattern. Synonym: Fresnel diffraction pattern. See also: Diffraction; Far-field diffraction pattern; Far-field region.

Near-field pattern:
Synonym for Near-field radiation pattern. See Radiation pattern.

Near-field region:
The region close to a source, or aperture. The diffraction pattern in this region typically differs significantly from that observed at infinity and varies with distance from the source. See also: Far-field diffraction pattern; Far-field region.

Near-field radiation pattern:
See Radiation pattern.

Near-field scanning:
The technique for measuring the index profile of an optical fiber by illuminating the entrance face with an extended source and measuring the point-by-point radiance of the exit face. See also: Refracted ray method.

Noise equivalent power (NEP):
At a given modulation frequency, wavelength, and for a given effective noise bandwidth, the radiant power that produces a signal-to-noise ratio of 1 at the output of a given detector.
Note 1. Some manufacturers and authors define NEP as the minimum detectable power per root unit bandwidth; when defined in this way, NEP has the units of watts/(hertz)$^{1/2}$. Therefore, the term is a misnomer, because the units of power are watts. See also: D*; Detectivity.
Note 2. Some manufacturers define NEP as the radiant power that produces a signal-to-dark-current noise ratio of unity. This is misleading when dark-current noise does not dominate, as is often true in fiber systems.

Nonlinear scattering:
Direct conversion of a photon from one wavelength to one or more other wavelengths. In an optical waveguide, nonlinear scattering is usually not important below the threshold irradiance for stimulated nonlinear scattering.
Note. Examples are Raman and Brillouin scattering. See also: Photon.

Normalized frequency:
A dimensionless quantity (denoted by V), given by

$$V = \frac{2\pi a}{\lambda} \sqrt{n_1^2 - n_2^2}$$

where a is waveguide core radius, λ is wavelength in vacuum, and n_1 and n_2 are the maximum refractive index in the core and refractive index of the homogeneous cladding, respectively. In a fiber having a power-law profile, the approximate number of bound modes is $(V^2/2)[g/(g+2)]$, where g is the profile parameter. Synonym: V number. See also: Bound mode; Mode volume; Parabolic profile; Power-law index profile; Single mode optical waveguide.

Numerical aperture (NA):
1. The sine of the vertex angle of the largest cone of meridional rays that can enter or leave an optical system or element, multiplied by the refractive index of the medium in which the vertex of the cone is located. Generally measured with respect to an object or image point and will vary as that point is moved.
2. For an optical fiber in which the refractive index decreases monotonically from n_1 on axis to n_2 in the cladding the numerical aperture is given by

$$NA = \sqrt{n_1^2 - n_2^2}$$

3. Colloquially, the sine of the radiation or acceptance angle of an optical fiber, multiplied by the refractive index of the material in contact with the exit or entrance face. This usage is approximate and imprecise, but is often encountered. See also: Acceptance angle; Launch numerical aperture; Meridional ray; Radiation angle; Radiation pattern.

Optic axis:
In an anisotropic medium, a direction of propagation in which orthogonal polarizations have the same phase velocity. Distinguished from "optical axis." See also: Anisotropic.

Optical axis:
In an optical waveguide, synonymous with "fiber axis."

Optical blank:
A casting consisting of an optical material molded into the desired geometry for grinding, polishing, or (in the case of optical waveguides) drawing to the final optical/mechanical specifications. See also: Preform.

Optical cable:
A fiber, multiple fibers, or fiber bundle in a structure fabricated to meet optical, mechanical, and environmental specifications. Synonym: Optical fiber cable. See also: Fiber bundle; Optical cable assembly.

Optical cable assembly:
An optical cable that is connector terminated. Generally, an optical cable that has been terminated by a manufacturer and is ready for installation. See also: Fiber bundle; Optical cable.

Optical cavity:
A region bounded by two or more reflecting surfaces, referred to as mirrors, end mirrors, or cavity mirrors, whose elements are aligned to provide multiple reflections. The resonator in a laser is an optical cavity. Synonym: Resonant cavity. See also: Active laser medium; Laser.

Optical combiner:
A passive device in which power from several input fibers is distributed among a smaller number (one or more) of input fibers. See also: Star coupler.

Optical conductor:
Deprecated synonym for Optical waveguide.

Optical connector:
See Optical waveguide connector.

Optical coupler:
See Optical waveguide coupler.

Optical data bus:
An optical fiber network, interconnecting terminals, in which any terminal can communicate with any other terminal. See also: Optical link.

Optical density:
A measure of the transmittance of an optical element expressed by: $\log_{10}(1/T)$ or $-\log_{10}T$, where T is transmittance. The analogous term $\log_{10}(1/R)$ is called reflection density.
Note. The higher the optical density, the lower the transmittance. Optical density times 10 is equal to transmission loss expressed in decibels; for example, an optical density of 0.3 corresponds to a transmission loss of 3 dB. See also: Transmission loss; Transmittance.

Optical detector:
A transducer that generates an output signal when irradiated with optical power. See also: Optoelectronic.

Optical fiber:
Any filament or fiber, made of dielectric materials, that guides light, whether or not it is used to transmit signals. See also: Fiber bundle; Fiber optics; Optical waveguide.

Optical fiber cable:
Synonym for Optical cable.

Optical fiber waveguide:
Synonym for Optical waveguide.

Optical filter:
An element that selectively transmits or blocks a range of wavelengths.

Optical link:
Any optical transmission channel designed to connect two end terminals or to be connected in series with other channels.
Note. Sometimes terminal hardware (e.g., transmitter/receiver modules) is included in the definition. See also: Optical data bus.

Optical path length:
In a medium of constant refractive index n, the product of the geometrical distance and the refractive index. If n is a function of position,

$$\text{optical path length} = \int n ds,$$

where ds is an element of length along the path.
Note. Optical path length is proportional to the phase shift a light wave undergoes along a path. See also: Optical thickness.

Optical power:
Colloquial synonym for Radiant power.

Optical repeater:
In an optical waveguide communication system, an optoelectronic device or module that receives a signal, amplifies it (or, in the case of a digital signal, reshapes, retimes, or otherwise reconstructs it) and retransmits it. See also: Modulation.

Optical spectrum:
Generally, the electromagnetic spectrum within the wavelength region extending from the vacuum ultraviolet at 40 nm to the far infrared at 1 mm. See also: Infrared; Light.

Optical thickness:
The physical thickness of an isotropic optical element, times its refractive index. See also: Optical path length.

Optical time domain reflectometry:
A method for characterizing a fiber wherein an optical pulse is transmitted through the fiber and the resulting light scattered and reflected back to the input is measured as a function of time. Useful in estimating attenuation coefficient as a function of distance and identifying defects and other localized losses. See also: Rayleigh scattering; Scattering.

Optical waveguide:
1. Any structure capable of guiding optical power.
2. In optical communications, generally a fiber designed to transmit optical signals. Synonyms: Lightguide; Optical conductor (deprecated); Optical fiber waveguide. See also: Cladding; Core; Fiber bundle; Fiber optics; Multimode optical waveguide; Optical fiber; Single mode waveguide; Tapered fiber waveguide.

Optical waveguide connector:
A device whose purpose is to transfer optical power between two optical waveguides or bundles, and that is designed to be connected and disconnected repeatedly. See also: Multifiber joint; Optical waveguide coupler.

Optical waveguide coupler:
1. A device whose purpose is to distribute optical power among two or more ports. See also: Star coupler; Tee coupler.
2. A device whose purpose is to couple optical power between a waveguide and a source or detector.

Optical waveguide preform:
See Preform.

Optical waveguide splice:
A permanent joint whose purpose is to couple optical power between two waveguides.

Optical waveguide termination:
A configuration or a device mounted at the end of a fiber or cable which is intended to prevent reflection. See also: Index matching material.

Optically active material:
A material that can rotate the polarization of light that passes through it.
Note. An optically active material exhibits different refractive indices for left and right circular polarizations (circular birefringence). See also: Birefringent medium.

Optoelectronic:
Pertaining to a device that responds to optical power, emits or modifies optical radiation, or utilizes optical radiation for its internal operation. Any device that functions as an electrical-to-optical or optical-to-electrical transducer.
Note 1. Photodiodes, LEDs, injection lasers and integrated optical elements are examples of optoelectronic devices commonly used in optical waveguide communications.
Note 2. "Electro-optical" is often erroneously used as a synonym. See also: Electro-optic effect; Optical detector.

Output angle:
Synonym for Radiation angle.

Packing fraction:
In a fiber bundle, the ratio of the aggregate fiber cross-sectional core area to the total cross-sectional area (usually within the ferrule) including cladding and interstitial areas. See also: Ferrule; Fiber bundle.

Parabolic profile:
A power-law index profile with the profile parameter, g, equal to 2. Synonym: Quadratic profile. See also: Graded index profile; Multimode optical waveguide; Power-law index profile; Profile parameter.

Paraxial ray:
A ray that is close to and nearly parallel with the optical axis.
Note. For purposes of computation, the angle, θ, between the ray and the optical axis is small enough for $\sin\theta$ or $\tan\theta$ to be replaced by θ (radians). See also: Light ray.

PCS:
Abbreviation for Plastic clad silica.

Peak wavelength:
The wavelength at which the radiant intensity of a source is maximum. See also: Spectral line; Spectral width.

Phase coherence:
See Coherent.

Phase constant:
The imaginary part of the axial propagation constant for a particular mode, usually expressed in radians per unit length. See also: Axial propagation constant.

Phase velocity:
For a particular mode, the ratio of the angular frequency to the phase constant. See also: Axial propagation constant; Coherence time; Group velocity.

Photoconductivity:
The conductivity increase exhibited by some nonmetallic materials, resulting from the free carriers generated when photon energy is absorbed in electronic transitions. The rate at which free carriers are generated, the mobility of the carriers,

and the length of time they persist in conducting states (their lifetime) are some of the factors that determine the amount of conductivity change. See also: Photoelectric effect.

Photocurrent:
The current that flows through a photosensitive device (such as a photodiode) as the result of exposure to radiant power. Internal gain, such as that in an avalanche photodiode, may enhance or increase the current flow but is a distinct mechanism. See also: Dark current; Photodiode.

Photodiode:
A diode designed to produce photocurrent by absorbing light. Photodiodes are used for the detection of optical power and for the conversion of optical power to electrical power. See also: Avalanche photodiode (APD); Photocurrent; PIN photodiode.

Photoelectric effect:
1. External photoelectric effect: The emission of electrons from the irradiated surface of a material. Synonym: Photoemissive effect.
2. Internal photoelectric effect: Photoconductivity.

Photoemissive effect:
Synonym for (external) Photoelectric effect.

Photon:
A quantum of electromagnetic energy. The energy of a photon is $h\nu$ where h is Planck's constant and ν is the optical frequency. See also: Nonlinear scattering; Planck's constant.

Photon noise:
Synonym for Quantum noise.

Photovoltaic effect:
The production of a voltage difference across a pn junction resulting from the absorption of photon energy. The voltage difference is caused by the internal drift of holes and electrons. See also: Photon.

Physical optics:
The branch of optics that treats light propagation as a wave phenomenon rather than a ray phenomenon, as in geometric optics.

Pigtail:
A short length of optical fiber, permanently fixed to a component, used to couple power between it and the transmission fiber. See also: Launching fiber.

PIN photodiode:
A diode with a large intrinsic region sandwiched between p- and n-doped semiconducting regions. Photons absorbed in this region create electron-hole pairs that are then separated by an electric field, thus generating an electric current in a load circuit.

Planck's constant:
The number h that relates the energy E of a photon with the frequency ν of the associated wave through the relation $E = h\nu$. $h = 6.626 \times 10^{-34}$ joule second. See also: Photon.

Plane wave:
A wave whose surfaces of constant phase are infinite parallel planes normal to the direction of propagation.

Plastic clad silica fiber:
An optical waveguide having silica core and plastic cladding.

Power:
See Irradiance; Radiant intensity; Radiant power.

Power density:
Colloquial synonym for Irradiance.

Power-law index profile:
A class of graded index profiles characterized by the following equations:

$$n(r) = n_1(1-2\Delta(r/a)^g)^{1/2} \quad r \leq a$$

$$n(r) = n_2 = n_1(1-2\Delta)^{1/2} \quad r \geq a$$

$$\text{where } \Delta = \frac{n_1^2 - n_2^2}{2n_1^2}$$

where n(r) is the refractive index as a function of radius, n_1 is the refractive index on axis, n_2 is the refractive index of the homogeneous cladding, a is the core radius, and g is a parameter that defines the shape of the profile.
Note 1. α is often used in place of g. Hence, this is sometimes called an alpha profile.
Note 2. For this class of profiles, multimode distortion is smallest when g takes a particular value depending on the material used. For most materials, this optimum value is around 2. When g increases without limit, the profile tends to a step index profile. See also: Graded index profile; Mode volume; Profile parameter; Step index profile.

Preform:
A glass structure from which an optical fiber waveguide may be drawn. See also: Chemical vapor deposition technique; Ion exchange technique; Optical blank.

Primary coating:
The material in intimate contact with the cladding surface, applied to preserve the integrity of that surface. See also: Cladding.

Profile:
See Graded index profile; Index profile; Parabolic profile; Power-law index profile; Step index profile.

Profile dispersion:
1. In an optical waveguide, that dispersion attributable to the variation of refractive index contrast with wavelength, where contrast refers to the difference between the maximum refractive index in the core and the refractive index of the homogeneous cladding. Profile dispersion is usually characterized by the profile dispersion parameter, defined by the following entry.
2. In an optical waveguide, that dispersion attributable to the variation of refractive index profile with wavelength. The profile variation has two contributors: (a) variation in refractive index contrast, and (b) variation in profile parameter. See also: Dispersion; Distortion; Refractive index profile.

Profile dispersion parameter (P):

$$P(\lambda) = \frac{n_1}{N_1} \frac{\lambda}{\Delta} \frac{d\Delta}{d\lambda}$$

where n_1, N_1 are, respectively, the refractive and group indices of the core, and $n_1\sqrt{1-2\Delta}$ is the refractive index of the homogeneous cladding, $N_1 = n_1 - \lambda(dn_1/d\lambda)$, and Δ is the refractive index constant. Sometimes it is defined with the factor (-2) in the numerator. See also: Dispersion.

Profile parameter:
The shape-defining parameter, g, for a power-law index profile. See also: Power-law index profile; Refractive index profile.

Propagation constant:
For an electromagnetic field mode varying sinusoidally with time at a given frequency, the logarithmic rate of change, with respect to distance in a given direction, of the complex amplitude of any field component.
Note. The propagation constant is a complex quantity.

Pulse broadening:
An increase in pulse duration.
Note. Pulse broadening may be specified by the impulse response, the root-mean-square pulse broadening, or the full-duration-half-maximum pulse broadening. See also: Impulse response; Root-mean-square pulse broadening; Full width (duration) half maximum.

Pulse distortion:
See Distortion.

Pulse duration:
The time between a specified reference point on the first transition of a pulse waveform and a similarly specified point on the last transition. The time between the 10%, 50%, or 1/e points is commonly used, as is the rms pulse duration. See also: Root-mean-square pulse duration.

Pulse length:
Often erroneously used as a synonym for Pulse duration.

Pulse width:
Often erroneously used as a synonym for Pulse duration.

Quadratic profile:
Synonym for Parabolic profile.

Quantum efficiency:
In an optical source or detector, the ratio of output quanta to input quanta. Input and output quanta need not both be photons.

Quantum noise:
Noise attributable to the discrete or particle nature of light. Synonym: Photon noise.

Quantum-noise-limited operation:
Operation wherein the minimum detectable signal is limited by quantum noise. See also: Quantum noise.

Radiance:
Radiant power, in a given direction, per unit solid angle per unit of projected area of the source, as viewed from that given direction. Radiance is expressed in watts per steradian per square meter. See also: Brightness; Conservation of radiance; Radiometry.

Radiant emittance:
Radiant power emitted into a full sphere (4π steradians) by a unit area of a source; expressed in watts per square meter. Synonym: Radiant exitance. See also: Radiometry.

Radiant energy:
Energy that is transferred via electromagnetic waves, i.e., the time integral of radiant power; expressed in joules. See also: Radiometry.

Radiant exitance:
Synonym for Radiant emittance.

Radiant flux:
Synonym for Radiant power (obsolete).

Radiant incidance:
See Irradiance.

Radiant intensity:
Radiant power per unit solid angle, expressed in watts per steradian. See also: Intensity; Radiometry.

Radiant power:
The time rate of flow of radiant energy, expressed in watts. The prefix is often dropped and the term

"power" is used. Colloquial synonyms: Flux; Optical power; Power; Radiant flux. See also: Radiometry.

Radiation angle:

Half the vertex angle of the cone of light emitted by a fiber.

Note. The cone is usually defined by the angle at which the far-field irradiance has decreased to a specified fraction of its maximum value or as the cone within which can be found a specified fraction of the total radiated power at any point in the far field. Synonym: Output angle. See also: Acceptance angle; Far-field region; Numerical aperture.

Radiation mode:

In an optical waveguide, a mode whose fields are transversely oscillatory everywhere external to the waveguide, and which exists even in the limit of zero wavelength. Specifically, a mode for which

$$\beta \leq [n^2(a)k^2-(\ell/a)^2]^{1/2}$$

where β is the imaginary part (phase term) of the axial propagation constant, ℓ is the azimuthal index of the mode, n(a) is the refractive index at r=a, the core radius, and k is the free-space wavenumber, $2\pi/\lambda$, where λ is the wavelength. Radiation modes correspond to refracted rays in the terminology of geometric optics. Synonym: Unbound mode. See also: Bound mode; Leaky mode; Mode; Refracted ray.

Radiation pattern:

Relative power distribution as a function of position or angle.

Note 1. Near-field radiation pattern describes the radiant emittance ($W \cdot m^{-2}$) as a function of position in the plane of the exit face of an optical fiber.

Note 2. Far-field radiation pattern describes the irradiance as a function of angle in the far field region of the exit face of an optical fiber.

Note 3. Radiation pattern may be a function of the length of the waveguide, the manner in which it is excited, and the wavelength. See also: Far-field region; Near-field region.

Radiometry:

The science of radiation measurement. The basic quantities of radiometry are listed below.

RADIOMETRIC TERMS

TERM NAME	SYMBOL	QUANTITY	UNIT
Radiant energy	Q	Energy	joule (J)
Radiant power Synonym: Optical power	ϕ	Power	watt (W)
Irradiance	E	Power incident per unit area (irrespective of angle)	$W \cdot m^{-2}$
Spectral irradiance	E_λ	Irradiance per unit wavelength interval at a given wavelength	$W \cdot m^{-2} \cdot nm^{-1}$
Radiant emittance Synonym: Radiant excitance	W	Power emitted (into a full sphere) per unit area	$W \cdot m^{-2}$
Radiant intensity	I	Power per unit solid angle	$W \cdot sr^{-1}$
Radiance	L	Power per unit angle per unit projected area	$W \cdot sr^{-1} \cdot m^{-2}$
Spectral radiance	L_λ	Radiance per unit wavelength interval at a given wavelength	$W \cdot sr^{-1} \cdot m^{-2} \cdot nm^{-1}$

Ray:
See Light ray.

Rayleigh scattering:
Light scattering by refractive index fluctuations (inhomogeneities in material density or composition) that are small with respect to wavelength. The scattered field is inversely proportional to the fourth power of the wavelength. See also: Material scattering; Scattering; Waveguide scattering.

Reference surface:
That surface of an optical fiber which is used to contact the transverse-alignment elements of a component such as a connector. For various fiber types, the reference surface might be the fiber core, cladding, or buffer layer surface.
Note. In certain cases the reference surface may not be an integral part of the fiber. See also: Ferrule; Optical waveguide connector.

Reflectance:
The ratio of reflected power to incident power.
Note. In optics, frequently expressed as optical density or as a percent; in communication applications, generally expressed in dB. Reflectance may be defined as specular or diffuse, depending on the nature of the reflecting surface. Formerly: "reflection." See also: Reflection.

Reflection:
The abrupt change in direction of a light beam at an interface between two dissimilar media so that the light beam returns into the medium from which it originated. Reflection from a smooth surface is termed specular, whereas reflection from a rough surface is termed diffuse. See also: Critical angle; Reflectance; Reflectivity; Total internal reflection.

Reflectivity:
The reflectance of the surface of a material so thick that the reflectance does not change with increasing thickness; the intrinsic reflectance of the surface, irrespective of other parameters such as the reflectance of the rear surface. No longer in common usage. See also: Reflectance.

Refracted near-field scanning method:
See Refracted ray method.

Refracted ray:
In an optical waveguide, a ray that is refracted from the core into the cladding. Specifically a ray at radial position r having direction such that

$$\frac{n^2(r) - n^2(a)}{1 - (r/a)^2\cos^2\phi(r)} \leq \sin^2\theta(r)$$

where $\phi(r)$ is the azimuthal angle of projection of the ray on the transverse plane, $\theta(r)$ is the angle the ray makes with the waveguide axis, n(r) is the refractive index, n(a) is the refractive index at the core radius, and a is the core radius. Refracted rays correspond to radiation modes in the terminology of mode descriptors. See also: Cladding ray; Guided ray; Leaky ray; Radiation mode.

Refracted ray method:
The technique for measuring the index profile of an optical fiber by scanning the entrance face with the vertex of a high numerical aperture cone and measuring the change in power of refracted (unguided) rays. Synonym: Refracted near-field scanning method. See also: Refraction; Refracted ray.

Refraction:
The bending of a beam of light in transmission through an interface between two dissimilar media or in a medium whose refractive index is a continuous function of position (graded index medium). See also: Angle of deviation; Refractive index (of a medium).

Refractive index (of a medium):
Denoted by n, the ratio of the velocity of light in vacuum to the phase velocity in the medium. Synonym: Index of refraction. See also: Cladding; Core; Critical angle; Dispersion; Fresnel reflection; Fused silica; Graded index optical waveguide; Group index; Index matching material; Index profile; Linearly polarized mode; Material dispersion; Mode; Normalized frequency; Numerical aperture; Optical path length; Power-law index profile; Profile dispersion; Scattering; Step index optical waveguide; Weakly guiding fiber.

Refractive index contrast:
Denoted by Δ, a measure of the relative difference in refractive index of the core and cladding of a fiber, given by

$$\Delta = (n_1^2 - n_2^2) / 2n_1^2$$

where n_1 and n_2 are, respectively, the maximum refractive index in the core and the refractive index of the homogeneous cladding.

Refractive index profile:
The description of the refractive index along a fiber diameter. See also: Graded index profile; Parabolic profile; Power-law index profile; Profile dispersion; Profile dispersion parameter; Profile parameter; Step index profile.

Regenerative repeater:
A repeater that is designed for digital transmission. Synonym: Regenerator. See also: Optical repeater.

Regenerator:
Synonym for Regenerative repeater.

Repeater:
See Optical repeater.

Resonant cavity:
See Optical cavity.

Responsivity:
The ratio of an optical detector's electrical output to its optical input, the precise definition depending on the detector type; generally expressed in amperes per watt or volts per watt of incident radiant power.
Note. "Sensitivity" is often incorrectly used as a synonym.

rms pulse duration:
See Root-mean-square (rms) pulse duration.

Root-mean-square (rms) deviation:
A single quantity characterizing a function given, for f(x), by

$$\sigma_{\mathrm{rms}} = [1/M_0 \int_{-\infty}^{\infty} (x-M_1)^2 f(x)\, dx]^{1/2}$$

$$\text{where } M_0 = \int_{-\infty}^{\infty} f(x)dx$$

$$M_1 = 1/M_0 \int_{-\infty}^{\infty} xf(x)dx$$

Note. The term rms deviation is also used in probability and statistics, where the normalization, M_0, is unity. Here, the term is used in a more general sense. See also: Impulse response; Root-mean-square (rms) pulse broadening; Root-mean-square (rms) pulse duration; Spectral width.

Root-mean-square (rms) pulse broadening:
The temporal rms deviation of the impulse response of a system. See also: Root-mean-square (rms) deviation; Root-mean-square (rms) pulse duration.

Root-mean-square (rms) pulse duration:
A special case of root-mean-square deviation where the independent variable is time and f(t) is pulse waveform. See also: Root-mean-square deviation.

Scattering:
The change in direction of light rays or photons after striking a small particle or particles. It may also be regarded as the diffusion of a light beam caused by the inhomogeneity of the transmitting medium. See also: Leaky modes; Material scattering; Mode; Nonlinear scattering; Rayleigh scattering; Refractive index (of a medium); Unbound mode; Waveguide scattering.

Semiconductor laser:
Synonym for Injection laser diode (ILD).

Sensitivity:
Imprecise synonym for Responsivity. In optical system receivers, the minimum power required to achieve a specified quality of performance in terms of output signal-to-noise ratio or other measure.

Shot noise:
Noise caused by current fluctuations due to the discrete nature of charge carriers and random and/or unpredictable emission of charged particles from an emitter.
Note. There is often a (minor) inconsistency in referring to shot noise in an optical system: many authors refer to shot noise loosely when speaking of the mean square shot noise current (amp^2) rather than noise power (watts). See also: Quantum noise.

Single mode optical waveguide:
An optical waveguide in which only the lowest order bound mode (which may consist of a pair of orthogonally polarized fields) can propagate at the wavelength of interest. In step index guides, this occurs when the normalized frequency, V, is less than 2.405. For power-law profiles, single mode operation occurs for normalized frequency, V, less than approximately $2.405\sqrt{(g+2)/g}$, where g is the profile parameter.
Note. In practice, the orthogonal polarizations may not be associated with degenerate modes. Synonym: Monomode optical waveguide. See also: Bound mode; Mode; Multimode optical waveguide; Normalized frequency; Power-law index profile; Profile parameter; Step index optical waveguide.

Skew ray:
A ray that does not intersect the optical axis of a system (in contrast with a meridional ray). See also: Axial ray; Geometric optics; Hybrid mode; Meridional ray; Optical axis; Paraxial ray.

Slab interferometry:
The method for measuring the index profile of an optical fiber by preparing a thin sample that has its faces perpendicular to the axis of the fiber, and measuring its index profile by interferometry. Synonym: Axial slab interferometry. See also: Interferometer.

Source efficiency:
The ratio of emitted optical power of a source to the input electrical power.

Spatial coherence:
See Coherent.

Spatially aligned bundle:
See Aligned bundle.

Spatially coherent radiation:
See Coherent.

Specific detectivity:
Synonym for D*.

Speckle noise:
Synonym for Modal noise.

Speckle pattern:
A power intensity pattern produced by the mutual interference of partially coherent beams that are subject to minute temporal and spatial fluctuations.
Note. In a multimode fiber, a speckle pattern results from a superposition of mode field patterns. If the relative modal group velocities change with time, the speckle pattern will also change with time. If, in addition, differential mode attenuation is experienced, modal noise results. See also: Modal noise.

Spectral irradiance:
Irradiance per unit wavelength interval at a given wavelength, expressed in watts per unit area per unit wavelength interval. See also: Irradiance; Radiometry.

Spectral line:
A narrow range of emitted or absorbed wavelengths. See also: Line source; Line spectrum; Monochromatic; Spectral width.

Spectral radiance:
Radiance per unit wavelength interval at a given wavelength, expressed in watts per steradian per unit area per wavelength interval. See also: Radiance; Radiometry.

Spectral responsivity:
Responsivity per unit wavelength interval at a given wavelength. See also: Responsivity.

Spectral width:
A measure of the wavelength extent of a spectrum.
Note 1. One method of specifying the spectral linewidth is the full width at half maximum (FWHM), specifically the difference between the wavelengths at which the magnitude drops to one-half of its maximum value. This method may be difficult to apply when the line has a complex shape.
Note 2. Another method of specifying spectral width is a special case of root-mean-square deviation where the independent variable is wavelength (λ), and $f(\lambda)$ is a suitable radiometric quantity. See also: Root-mean-square (rms) deviation.
Note 3. The relative spectral width $(\Delta\lambda)/\lambda$ is frequently used, where $\Delta\lambda$ is obtained according to Note 1 or Note 2. See also: Coherence length; Line spectrum; Material dispersion;

Spectral window:
A wavelength region of relatively high transmittance, surrounded by regions of low transmittance. Synonym: Transmission window.

Spectrum:
See Optical spectrum.

Specular reflection:
See Reflection.

Splice:
See Optical waveguide splice.

Splice loss:
See Insertion loss.

Spontaneous emission:
Radiation emitted when the internal energy of a quantum mechanical system drops from an excited level to a lower level without regard to the simultaneous presence of similar radiation.
Note. Examples of spontaneous emission include: 1) radiation from an LED, and 2) radiation from an injection laser below the lasing threshold. See also: Injection laser diode; Light emitting diode; Stimulated emission; Superradiance.

Star coupler:
A passive device in which power from one or several input waveguides is distributed amongst a larger number of output optical waveguides. See also: Optical combiner; Tee coupler.

Steady-state condition:
Synonym for Equilibrium mode distribution.

Step index optical waveguide:
An optical waveguide having a step index profile. See also: Step index profile.

Step index profile:
A refractive index profile characterized by a uniform refractive index within the core and a sharp decrease in refractive index at the core-cladding interface.
Note. This corresponds to a power-law profile with profile parameter, g, approaching infinity. See also: Critical angle; Dispersion; Graded index profile; Mode volume; Multimode optical waveguide; Normalized frequency; Optical waveguide; Refractive index (of a medium); Total internal reflection.

Stimulated emission:
Radiation emitted when the internal energy of a quantum mechanical system drops from an excit-

ed level to a lower level when induced by the presence of radiant energy at the same frequency. An example is the radiation from an injection laser diode above lasing threshold. See also: Spontaneous emission.

Superluminescent LED:
An emitter based on stimulated emission with amplification but insufficient feedback for oscillation to build up. See also: Spontaneous emission; Stimulated emission.

Superradiance:
Amplification of spontaneously emitted radiation in a gain medium, characterized by moderate line narrowing and moderate directionality.
Note. This process is generally distinguished from lasing action by the absence of positive feedback and hence the absence of well-defined modes of oscillation. See also: Laser; Spontaneous emission; Stimulated emission.

Surface wave:
A wave that is guided by the interface between two different media or by a refractive index gradient in the medium. The field components of the wave may exist (in principle) throughout space (even to infinity) but become negligibly small within a finite distance from the interface.
Note. All guided modes, but not radiation modes, in an optical waveguide belong to a class known in electromagnetic theory as surface waves.

Tap:
A device for extracting a portion of the optical signal from a fiber.

Tapered fiber waveguide:
An optical waveguide whose transverse dimensions vary monotonically with length. Synonym: Tapered transmission line.

Tapered transmission line:
Synonym for Tapered fiber waveguide.

TE mode:
Abbreviation for Transverse electric mode.

Tee coupler:
A passive coupler that connects three ports. See also: Star coupler.

TEM mode:
Abbreviation for Transverse electromagnetic mode.

Temporal coherence:
See Coherent.

Temporally coherent radiation:
See Coherent.

Thin film waveguide:
A transparent dielectric film, bounded by lower index materials, capable of guiding light. See also: Optical waveguide.

Threshold current:
The driving current corresponding to lasing threshold. See also: Lasing threshold.

Time coherence:
See Coherent.

TM mode:
Abbrevation for Transverse magnetic mode.

Tolerance field:
1. In general, the region between two curves (frequently two circles) used to specify the tolerance on component size.
2. When used to specify fiber cladding size, the annular region between the two concentric circles of diameter $D+\Delta D$ and $D-\Delta D$. The first circumscribes the outer surface of the homogeneous cladding; the second (smaller) circle is the largest circle that fits within the outer surface of the homogeneous cladding.
3. When used to specify the core size, the annular region between the two concentric circles of diameter $d+\Delta d$ and $d-\Delta d$. The first circumscribes the core area; the second (smaller) circle is the largest circle that fits within the core area.

Note. The circles of definition 2 need not be concentric with the circles of definition 3. See also: Cladding; Core; Concentricity error; Homogeneous cladding.

Total internal reflection:
The total reflection that occurs when light strikes an interface at angles of incidence (with respect to the normal) greater than the critical angle. See also: Critical angle; Step index optical waveguide.

Transfer function (of a device):
The complex function, H(f), equal to the ratio of the output to input of the device as a function of frequency. The amplitude and phase responses are, respectively, the magnitude of H(f) and the phase of H(f).
Note 1. For an optical fiber, H(f) is taken to be the ratio of output optical *power* to input optical *power* as a function of modulation frequency.
Note 2. For a linear system, the transfer function and the impulse response h(t) are related through the Fourier transform pair, a common form of which is given by

$$H(f) = \int_{-\infty}^{\infty} h(t)\, \exp(i2\pi ft)\, dt$$

and

$$h(t) = \int_{-\infty}^{\infty} H(f) \exp(-2\pi ft)\, df$$

where f is frequency. Often H(f) is normalized to H(0) and h(t) to

$\int_{-\infty}^{\infty} h(t)dt$, which by definition is H(0). Synonyms:

Baseband response function; Frequency response. See also: Impulse response.

Transmission loss:
Total loss encountered in transmission through a system. See also: Attenuation; Optical density; Reflection; Transmittance.

Transmission window:
Synonym for Spectral window.

Transmissivity:
The transmittance of a unit length of material, at a given wavelength, excluding the reflectance of the surfaces of the material; the intrinsic transmittance of the material, irrespective of other parameters such as the reflectances of the surfaces. No longer in common use. See also: Transmittance.

Transmittance:
The ratio of transmitted power to incident power. *Note.* In optics, frequently expressed as optical density or percent; in communications applications, generally expressed in dB. Formerly called "transmission." See also: Antireflection coating; Optical density; Transmission loss.

Transverse electric (TE) mode:
A mode whose electric field vector is normal to the direction of propagation.
Note. In an optical fiber, TE and TM modes correspond to meridional rays. See also: Meridional ray; Mode.

Transverse electromagnetic (TEM) mode:
A mode whose electric and magnetic field vectors are both normal to the direction of propagation. See also: Mode.

Transverse interferometry:
The method used to measure the index profile of an optical fiber by placing it in an interferometer and illuminating the fiber transversely to its axis. Generally, a computer is required to interpret the interference pattern. See also: Interferometer.

Transverse magnetic (TM) mode:
A mode whose magnetic field vector is normal to the direction of propagation.
Note. In a planar dielectric waveguide (as within an injection laser diode), the field direction is parallel to the core-cladding interface. In an optical waveguide, TE and TM modes correspond to meridional rays. See also: Meridional ray; Mode.

Transverse offset loss:
Synonym for Lateral offset loss.

Transverse propagation constant:
The propagation constant evaluated along a direction perpendicular to the waveguide axis.
Note. The transverse propagation constant for a given mode can vary with the transverse coordinates. See also: Propagation constant.

Transverse scattering:
The method for measuring the index profile of an optical fiber or preform by illuminating the fiber or preform coherently and transversely to its axis, and examining the far-field irradiance pattern. A computer is required to interpret the pattern of the scattered light. See also: Scattering.

Trapped mode:
See Bound mode.

Trapped ray:
Synonym for Guided ray.

Tunnelling mode:
Synonym for Leaky mode.

Tunnelling ray:
Synonym for Leaky ray.

Ultraviolet (UV):
The region of the electromagnetic spectrum between the short wavelength extreme of the visible spectrum (about 0.4 μm) and 0.04 μm. See also: Infrared; Light.

Unbound mode:
Any mode that is not a bound mode; a leaky or radiation mode of the waveguide. Synonym: Radiative mode. See also: Bound mode; Cladding mode; Leaky mode.

V number:
Synonym for Normalized frequency.

Visible spectrum:
See Light.

Vitreous silica:
Glass consisting of almost pure silicon dioxide (SiO_2). Synonym: Fused silica. See also: Fused quartz.

Wavefront:

The locus of points having the same phase at the same time.

Waveguide dispersion:

For each mode in an optical waveguide, the term used to describe the process by which an electromagnetic signal is distorted by virtue of the dependence of the phase and group velocities on wavelength as a consequence of the geometric properties of the waveguide. In particular, for circular waveguides, the dependence is on the ratio (a/λ), where a is core radius and λ is wavelength. See also: Dispersion; Distortion; Material dispersion; Multimode distortion; Profile dispersion.

Waveguide scattering:

Scattering (other than material scattering) that is attributable to variations of geometry and index profile of the waveguide. See also: Material scattering; Nonlinear scattering; Rayleigh scattering; Scattering.

Wavelength division multiplexing (WDM):

The provision of two or more channels over a common optical waveguide, the channels being differentiated by optical wavelength.

Weakly guiding fiber:

A fiber for which the difference between the maximum and the minimum refractive index is small (usually less than 1%).

Window:

See Spectral window.

NBS-114A (REV. 2-80)

U.S. DEPT. OF COMM. BIBLIOGRAPHIC DATA SHEET (See instructions)	1. PUBLICATION OR REPORT NO. NBS SP 637 Vol.2	2. Performing Organ. Report No.	3. Publication Date October 1983

4. TITLE AND SUBTITLE

Optical Fiber Characterization

Attenuation, Frequency Domain Bandwidth, and Radiation Patterns

5. AUTHOR(S)

G.E. Chamberlain, G.W. Day, D.L. Franzen, R.L. Gallawa, E.M. Kim, M. Young

6. PERFORMING ORGANIZATION (If joint or other than NBS, see instructions)

NATIONAL BUREAU OF STANDARDS
DEPARTMENT OF COMMERCE
WASHINGTON, D.C. 20234

7. Contract/Grant No.

8. Type of Report & Period Covered

9. SPONSORING ORGANIZATION NAME AND COMPLETE ADDRESS (Street, City, State, ZIP)

Same as Item No. 6, with partial support from the Department of Defense, Calibration Coordination Group (CCG).

10. SUPPLEMENTARY NOTES

Library of Congress Catalog Card Number: 82-600563

☐ Document describes a computer program; SF-185, FIPS Software Summary, is attached.

11. ABSTRACT (A 200-word or less factual summary of most significant information. If document includes a significant bibliography or literature survey, mention it here)

This is the second volume of a series intended to describe optical fiber measurement systems developed at the National Bureau of Standards. The topics covered in this volume are attenuation, bandwidth (frequency domain), and far-field near-field radiation patterns. Each chapter includes a tutorial section and a detailed description of the apparatus. The volume concludes with a glossary of optical communications terms.

12. KEY WORDS (Six to twelve entries; alphabetical order; capitalize only proper names; and separate key words by semicolons)

attenuation; bandwidth; core diameter; far field; measurements; near field; optical fiber

13. AVAILABILITY

[X] Unlimited
☐ For Official Distribution. Do Not Release to NTIS
☐ Order From Superintendent of Documents, U.S. Government Printing Office, Washington, D.C. 20402.
[X] Order From National Technical Information Service (NTIS), Springfield, VA. 22161

14. NO. OF PRINTED PAGES

239

15. Price

USCOMM-DC 6043-P80

☆ U.S. GOVERNMENT PRINTING OFFICE : 1983 O - 417-234

NBS TECHNICAL PUBLICATIONS

PERIODICALS

JOURNAL OF RESEARCH—The Journal of Research of the National Bureau of Standards reports NBS research and development in those disciplines of the physical and engineering sciences in which the Bureau is active. These include physics, chemistry, engineering, mathematics, and computer sciences. Papers cover a broad range of subjects, with major emphasis on measurement methodology and the basic technology underlying standardization. Also included from time to time are survey articles on topics closely related to the Bureau's technical and scientific programs. As a special service to subscribers each issue contains complete citations to all recent Bureau publications in both NBS and non-NBS media. Issued six times a year. Annual subscription: domestic $18; foreign $22.50. Single copy, $5.50 domestic; $6.90 foreign.

NONPERIODICALS

Monographs—Major contributions to the technical literature on various subjects related to the Bureau's scientific and technical activities.

Handbooks—Recommended codes of engineering and industrial practice (including safety codes) developed in cooperation with interested industries, professional organizations, and regulatory bodies.

Special Publications—Include proceedings of conferences sponsored by NBS, NBS annual reports, and other special publications appropriate to this grouping such as wall charts, pocket cards, and bibliographies.

Applied Mathematics Series—Mathematical tables, manuals, and studies of special interest to physicists, engineers, chemists, biologists, mathematicians, computer programmers, and others engaged in scientific and technical work.

National Standard Reference Data Series—Provides quantitative data on the physical and chemical properties of materials, compiled from the world's literature and critically evaluated. Developed under a worldwide program coordinated by NBS under the authority of the National Standard Data Act (Public Law 90-396).

NOTE: The principal publication outlet for the foregoing data is the Journal of Physical and Chemical Reference Data (JPCRD) published quarterly for NBS by the American Chemical Society (ACS) and the American Institute of Physics (AIP). Subscriptions, reprints, and supplements available from ACS, 1155 Sixteenth St., NW, Washington, DC 20056.

Building Science Series—Disseminates technical information developed at the Bureau on building materials, components, systems, and whole structures. The series presents research results, test methods, and performance criteria related to the structural and environmental functions and the durability and safety characteristics of building elements and systems.

Technical Notes—Studies or reports which are complete in themselves but restrictive in their treatment of a subject. Analogous to monographs but not so comprehensive in scope or definitive in treatment of the subject area. Often serve as a vehicle for final reports of work performed at NBS under the sponsorship of other government agencies.

Voluntary Product Standards—Developed under procedures published by the Department of Commerce in Part 10, Title 15, of the Code of Federal Regulations. The standards establish nationally recognized requirements for products, and provide all concerned interests with a basis for common understanding of the characteristics of the products. NBS administers this program as a supplement to the activities of the private sector standardizing organizations.

Consumer Information Series—Practical information, based on NBS research and experience, covering areas of interest to the consumer. Easily understandable language and illustrations provide useful background knowledge for shopping in today's technological marketplace.

Order the **above** *NBS publications from: Superintendent of Documents, Government Printing Office, Washington, DC 20402.*

Order the **following** *NBS publications—FIPS and NBSIR's—from the National Technical Information Service, Springfield, VA 22161.*

Federal Information Processing Standards Publications (FIPS PUB)—Publications in this series collectively constitute the Federal Information Processing Standards Register. The Register serves as the official source of information in the Federal Government regarding standards issued by NBS pursuant to the Federal Property and Administrative Services Act of 1949 as amended, Public Law 89-306 (79 Stat. 1127), and as implemented by Executive Order 11717 (38 FR 12315, dated May 11, 1973) and Part 6 of Title 15 CFR (Code of Federal Regulations).

NBS Interagency Reports (NBSIR)—A special series of interim or final reports on work performed by NBS for outside sponsors (both government and non-government). In general, initial distribution is handled by the sponsor; public distribution is by the National Technical Information Service, Springfield, VA 22161, in paper copy or microfiche form.

U.S. Department of Commerce
National Bureau of Standards

Washington, D.C. 20234
Official Business